Imperial College London

Avian influenza virus as an oncolytic therapy for pancreatic cancer

Department of Medicine

Division of Infectious Diseases

Submitted for degree of

Doctor of Philosophy

Matteo Samuele Pizzuto

Supervised by

Prof. Wendy S. Barclay

(Imperial College London)

Dr. Ilaria Capua

(IZSVe)

September 2015

Author's Declaration

I confirm that all work presented here is my own and that the use of all material from other sources has been properly and fully acknowledged.

Matteo Samuele Pizzuto

Copyright Declaration

'The copyright of this thesis rests with the author and is made available under a Creative Commons Attribution Non-Commercial No Derivatives licence. Researchers are free to copy, distribute or transmit the thesis on the condition that they attribute it, that they do not use it for commercial purposes and that they do not alter, transform or build upon it. For any reuse or redistribution, researchers must make clear to others the licence terms of this work'.

Acknowledgments

First of all I would like to thank my supervisor Professor Wendy Barclay who accepted me as a part-time PhD student in her lab at Imperial College London and has always been a source of advice, support and inspiration. I would also like to express my sincere gratitude to my advisor at the Istituto Zooprofilattico delle Venezie (IZSVe, Padua - Italy), Dr. Ilaria Capua, for having believed in my capacity and sponsored my PhD, an opportunity which has made me grow both as a scientist and as a person.

I am extremely grateful to all the past and current members of the Flu lab who made me feel at home every time I was in London and never spared to provide me with logistical and technical help, scientific advice, knowledge and fun. In particular, I would like to thank Olivier, who would be the world champion of table football if he were not an even better scientist; Ruth, for her availability and help while I was writing my thesis; Dan, Deena, Jason, Anna, Rebecca, Pete, Jon, Neeltje, David, Matt, Holly…

My thanks also to Dr. Samantha Kasloff (IZSVe) and Dr. Micol Silic-Benussi (Istituto Oncologico Veneto - IOV, Padua - Italy), who contributed to generate the preliminary data on which the present project has been built up.

Thanks to my parents for supporting me throughout my life in general and for their efforts to understand what my PhD project was about. Finally, a special thought goes to my wife Angela, who has never ceased to believe in me in good times and bad times, and to my son Cesare ("Cece"), who has helped me to clarify important issues of my project with interesting mono-vocal conversations at dawn.

Abstract

Pancreatic ductal adenocarcinoma (PDA) is one of the leading causes of cancer-related deaths worldwide and the development of new treatment strategies for patients suffering from PDA is of crucial importance.

Virotherapy uses natural or engineered oncolytic viruses (OVs) to selectively kill tumour cells. Although various OVs are being investigated as agents for pancreatic cancer treatment, due to the genetic heterogeneity of PDA cells and their consequent mixed permissiveness to viruses, virotherapy should not rely on a short list of possible candidates. As such, preliminary data from our group demonstrating the potent pro-apoptotic effect of the low pathogenicity avian influenza virus (LPAIV) H7N3 A/turkey/Italy/2962/03 in PDA cells, previously established to be resistant to other OVs, suggested that this virus might be effective against specific sub-classes of pancreatic cancer. Therefore, in the present studies, the avian isolate was selected for further development.

Preferential replication of the H7N3 virus in IFN-deficient cells, a trait of the majority of PDA cell lines, was improved by the truncation of the viral NS1 protein (NS1-77), which compromised the virus' ability to counteract the IFN-mediated antiviral response and, as bystander effect, enhanced the killing of uninfected cancer cells by stimulating IFN expression from healthy cells.

Introduction of L75H mutation within the mitochondrial targeting sequence (MTS) of the viral protein PB1-F2 increased virus replication in permissive IFN deficient cells and also lessened PB1-F2's ability to counter the IFN response induced by overexpression of mitochondrial antiviral signalling protein (MAVS), further enhancing selectivity for PDA cells.

Substitution of the genes expressing avian surface antigens haemagglutinin (HA) and neuraminidase (NA) with those of the well characterized human H1N1 A/Puerto Rico/8/1934 virus eliminated the potential risk of reassortment of the H7N3 virus with circulating human influenza strains that might result in a new pandemic virus, nonetheless, preserving the oncolytic properties of the parental isolate.

Finally, to promote anti-tumour immunity, the newly generated PR8 H1/N1-2962 NS1-77 virus was "armed" to express the human granulocyte-macrophage colony-stimulating factor (GM-CSF) gene during infection.

Taken together our data demonstrate the possibility to select an IAV from the avian reservoir on the basis of its strain-specific oncolytic skills in PDA cells and, through engineering, improve its selectivity, safety and tumour debulking activity.

List of acronyms and abbreviations used in this project

5’ppp	5’-triphosphate
BLI	Bioluminescence imaging
bp	Base pairs
CDKN2A	Cyclin-dependent kinase inhibitor 2A gene
Cis	Cisplatin
CLU	Clusterin
CPSF30	Cleavage and Polyadenylation Specificity Factor 30
cRNA	Complementary RNA
CTD	C-terminal regulatory domain
Cyt c	Cytochrome C
DC	Dendritic Cell
DPC4/SMAD4	Deleted in pancreatic carcinoma locus 4 gene
ECE	Embryonated chicken eggs
ED	Effector domain
EE	Early endosome
FACS	Fluorescence-Activated Cell Sorting
FMDV	Foot and mouth disease virus
Gem	Gemcitabine
GFP	Green Fluorescent Protein
GM-CSF	Granulocyte macrophage colony stimulating factor
HA	Hemagglutinin
HPAI	Highly Pathogenic Avian Influenza
hpi	Hours post-infection
IAV	Influenza A virus
ICC	Immunocytochemistry
IFN-α/β	Interferon alpha and beta
IOV	Istituto Oncologico Veneto
IZSVe	Istituto Zooprofilattico Sperimetale delle Venezie
KDa	kilodalton
KRAS	Kirsten rat sarcoma viral oncogene homolog gene
LE	Late endosome

LPAI	Low Pathogenic Avian Influenza
LR	Linker region
M.O.I.	Multiplicity Of Infection
MAVS	Mitochondrial antiviral signalling protein
MM	Mitochondrial membrane
mRNA	Messenger RNA
MTS	Mitochondrial targeting sequence
Mx	Myxovirus-resistance protein
NA	Neuraminidase
NDV	Newcastle Disease virus
NEP	Nuclear Export Protein
NLS	Nuclear localization signal
NP	Nucleoprotein
NPC	Nuclear Pore Complex
NS1	Non-Structural protein 1
OAS	2'-5'-oligodenylate synthetases
OV	Oncolytic virus
PA	Polymerase Acidic protein
PAMP	Pathogen associated molecular pattern
PB1	Polymerase Basic protein 1
PB1-F2	Polymerase Basic protein 1-Frame 2
PB2	Polymerase Basic protein 2
PDA	Pancreatic ductal adenocarcinoma
Pfu	Plaque forming unit
pH1N1-09	Human 2009 pandemic H1N1 virus
PKR	Protein Kinase RNA-activated
PR8	A/Puerto Rico/8/34 (H1N1)
PRR	Pattern recognition receptor
RBD	dsRNA binding domain
rg	Reverse genetics
RIG-I	Retinoic acid inducible gene 1
RLU	Relative Light Units
RT-PCR	Reverse Transcriptase - Polymerase Chain Reaction

SA	Sialic acid
SCID	Severe combined immunodeficiency
TP53	Tumour suppressor protein p53 gene
URT	Upper respiratory tract
UTR	Un-translated region
V5	Simian virus 5 epitope
vRNA	Viral RNA
vRNP	Viral ribonucleoprotein
VSV	Vesicular stomatitis virus

Table of Contents

List of figures

List of tables

Chapter 1. Introduction

1.1 The Pancreas.

1.1.1 Gross anatomy.

The pancreas is an elongated, tapered retroperitoneal organ located behind the stomach, which can be subdivided in four main regions: the head, the neck, the body and the tail (Figure 1). The head lies in the curve of the second and third portion of the duodenum, while the remaining left side consisting of the neck and the body of the pancreas extends slightly upward and ends in the tail adjacent to the spleen.

The distal end of the common bile duct passes through the head of the pancreas and joins the pancreatic duct entering the duodenum. The blood supply to the pancreas is from two major arteries supplying the abdominal organs, the celiac and superior mesenteric arteries. Venous drainage is via the splenic vein, which runs along the body of the pancreas, and the superior mesenteric vein draining into the portal vein (Pandol, 2010).

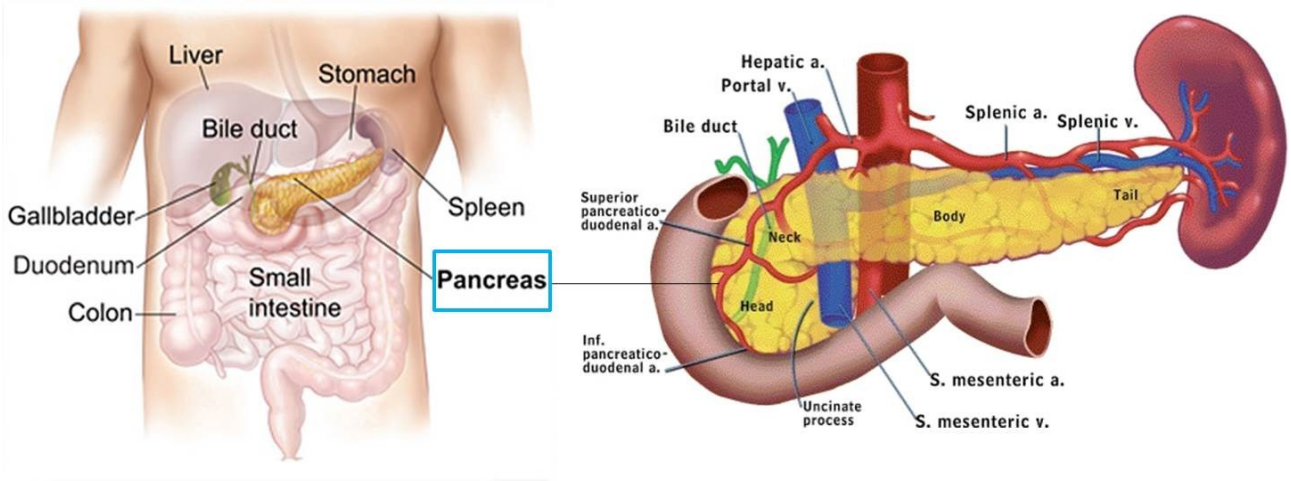

*Figure 1. **Pancreas: gross anatomy and vascular system.** Adapted from* (Pandol, 2010).

1.1.2 Functional anatomy.

The pancreas is a dual-function gland, which presents both endocrine and exocrine features and regulates two major physiological processes: glucose metabolism and digestion.

The endocrine portion of the pancreas controls the homeostasis of glucose in the bloodstream. Blood glucose levels must be maintained within certain limits so that there is a constant supply of glucose to feed the cells of the body but not so much as to damage the kidneys and other organs.

The part of the pancreas with endocrine function is made up of cell clusters, called islets of Langerhans, crisscrossed by a dense network of capillaries with which they are in direct contact (Figure 2). Their name was coined by Edouard Laguesse (1861-1927), a histologist working at the University of Lille, who deduced that they were involved in endocrine secretion and named them after Paul Langerhans (1849-1888), who in 1869 first described these clusters but was unable to attribute them with a specific function (Laguesse, 1893).

Four main cell types exist in the islets and can be classified based on their secretions. Alpha (α) cells make up 30-45% of the human islet cells and are responsible for synthesizing and secreting the peptide hormone glucagon, which causes the liver to convert stored glycogen into glucose, thereby increasing the glucose level into the bloodstream (Baum et al., 1962). To counteract spikes in blood glucose concentrations beta (β) cells (55-70%) store and release the insulin hormone which reduces the glucose concentration in the blood by stimulating its uptake from skeletal muscles and fat tissue (Orci, 1986). Alpha and beta cell activity is finely regulated by somatostatin hormone which is produced by delta cells (Δ) and can inhibit or suppress the release of pancreatic hormones (Luft et al., 1974). Lastly, Γ (gamma) cells or (PP cells) secrete pancreatic polypeptide, which also contributes to self-regulate pancreatic endocrine and exocrine secretion activities.

The pancreas as an exocrine gland is involved in the digestive process secreting a pancreatic fluid which contains digestive enzymes that reach the small intestine to further break down the carbohydrates, proteins and lipids in the chime (the semifluid mass of partly digested food expelled

by the stomach into the duodenum). The exocrine component of the pancreas comprises around 85% of the total mass of the organ and its functional unit is composed of an acinus (from the Latin term meaning “berry in a cluster”) and its draining ductule (Figure 2).

The acinar cells are specialized to synthesize, store, and secrete precursor form (or zymogen) of digestive enzymes. The major proteases secreted by the pancreas are trypsinogen and chymotrypsinogen and to a lesser degree pancreatic lipase and pancreatic amylase. In normal pancreas, the precursor enzymes are inactive in order to avoid autodegradation, which might lead to pancreatitis. However, once released in the intestine, the enzyme enteropeptidase (also called enterokinase) present in the intestinal mucosa activates trypsinogen by cleaving it to form trypsin (Kunitz, 1939). The free trypsin then cleaves the rest of the trypsinogen, as well as chymotrypsinogen to its active forms (Dreyer and Neurath, 1955).

Control of the exocrine function of the pancreas is exerted via hormones gastrin, cholecystokinin and secretin, which are produced by cells in the stomach and duodenum, in response to distension and/or food and cause secretion of pancreatic juices (Williams, 2001).

The basal region of the acinar cell contains the nucleus as well as abundant rough endoplasmic reticulum for protein synthesis, while the apical region contains zymogen granules and a store of digestive enzymes. Secretion of digestive enzymes occurs into the lumen of the acinus, which is directly connected to the ductal system. A ductule from the acinus drains the enzymes into the interlobular ducts, which in turn deliver them into the main pancreatic duct to finally reach the duodenum.

Although, ductal cells represent a minor cell type in the adult pancreas (around 10% number and 4% volume) they have two essential functions (i) forming a network that delivers enzymes from the acini into the digestive tract and (ii) producing bicarbonate ions ($HCO3^-$), in response to the hormone secretin, to neutralize the acidic chime entering the duodenum from the stomach

(Githens, 1988). Because of the latter function their epithelium consists of cells that are cuboidal to pyramidal and contain abundant mitochondria necessary to produce energy for ion transport.

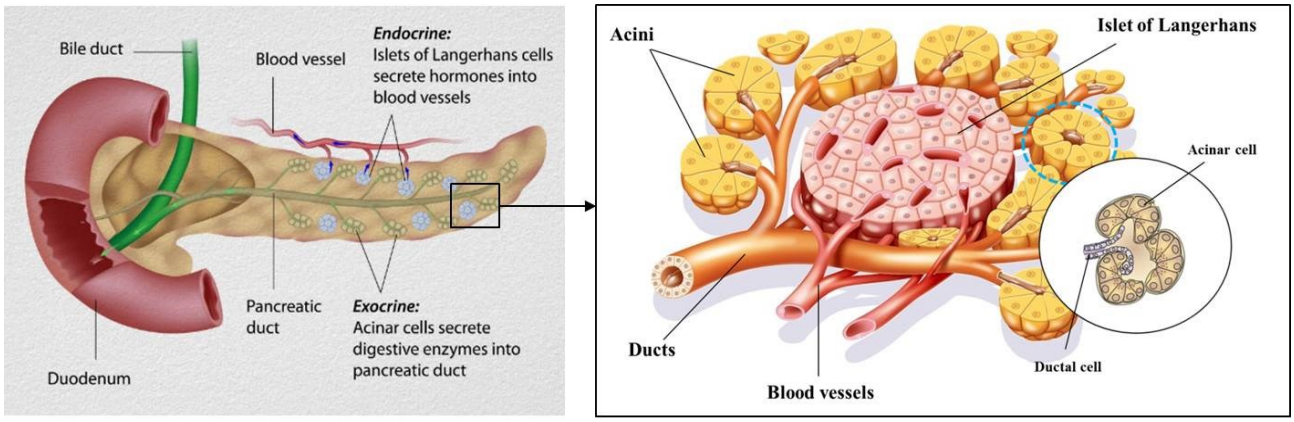

Figure 2. ***Representation of the endocrine and exocrine components of the pancreas.*** *A islet of Langerhans (clusters of pink cells) with endocrine function is surrounded by pancreatic acini producing digestive enzymes which are drain to the duodenum via a system of ducts. Adapted from* (Bardeesy and DePinho, 2002) *and* (Logsdon and Ji, 2013).

1.2 Pancreatic Cancer.

1.2.1 Pancreatic ductal adenocarcinoma (PDA).

Endocrine and exocrine cells form completely different types of tumours with distinct risk factors, symptoms, diagnostic tests, treatment, and survival rates (American Cancer Society, 2013).

Endocrine tumours, also called islet cell tumours or pancreatic neuroendocrine tumours (PNETs or PanNETs), are less common than exocrine tumours, making up about 1% of pancreatic cancers. A pancreatic neuroendocrine tumour can be functioning, meaning it still makes hormones, or non-functioning. A functioning neuroendocrine tumour is named based on the hormone the cells normally make such as for example insulinoma, glucagonoma and somatostatinoma (Yao et al., 2007; Zhang et al., 2013). Non-functional tumours account for 85% of PanNETs and have a statistically significantly worse prognosis compared to functioning PanNETs, wherein a specific syndrome from hormone oversecretion is seen (Franko et al., 2010; Halfdanarson et al., 2008).

Exocrine tumours are the most common type of pancreatic cancer. About 95% of people with pancreatic cancer have adenocarcinoma (*adeno* "gland", *karkínos* "cancerous" and *oma* "tumor") arising from the exocrine component. Pancreatic ductal adenocarcinoma (PDA), derived from the ductal cells lining the ducts, is the most common primary malignancy of the pancreas, representing 85-90% of all pancreatic neoplasms (Cubilla and Fitzgerald, 1984). Ductal adenocarcinomas are composed of infiltrating glands surrounded by dense, reactive fibrous connective tissue, which makes them highly invasive hard tumours with aggressive local growth and rapid metastases to surrounding tissues (Figure 3). PDA cells appear pleomorphic with variation in shape, lack of polarity, irregular nuclei and prominent nucleoli (Stathis and Moore, 2010). Because PDA are representative of the vast majority of tumours of the pancreas, the next part of the thesis will be focused on this type of neoplasm and within the text the acronym PDA will be used as synonym of pancreatic cancer.

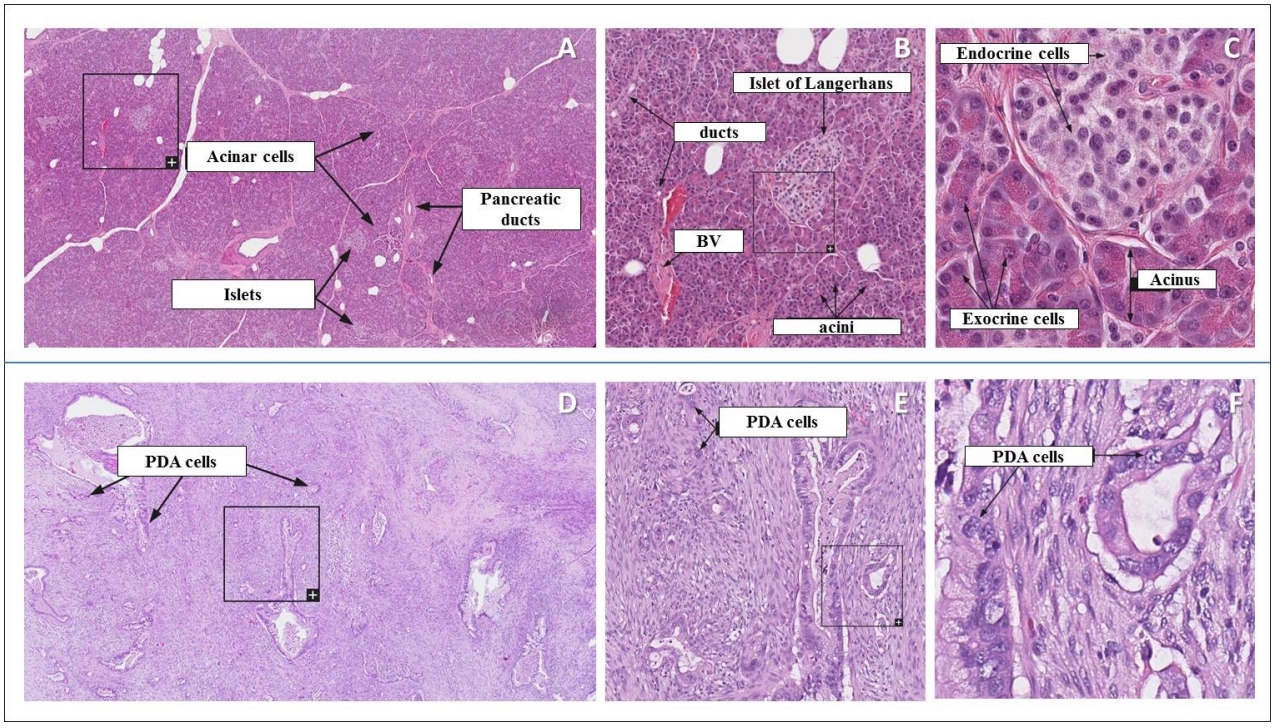

Figure 3. Histology of normal pancreas (A-B-C) and pancreatic ductal adenocarcinoma (PDA) (D-E-F) at different magnifications. Adapted from (The Human Protein Atlas).

1.2.2 PDA Risk Factors.

Different factors affect the incidence and death rates of PDA, including sex, age and racial/ethnic group (Silverman et al., 2003). Although the exact etiopathogenesis remains unknown, many risk factors have been associated with PDA.

Risk factors that a person can control are called **modifiable risk factors**. Among these, tobacco **smoking** is the most important known factor for pancreatic ductal adenocarcinoma. Approximately 20% of PDA are attributable to cigarette smoking (Iodice et al., 2008) and the risk of developing pancreatic cancer is about twice as high among smokers as among those who have never been smokers. Mutations in carcinogen-metabolizing genes, such as glutathione-S-transferase, N-acetyl-transferase, cytochrome P450 and DNA-repair genes (XRCC1, OGG1) may be genetic modifiers for smoking-related pancreatic cancer (Duell et al., 2002; Li et al., 2006).

Obesity has also been fairly consistently linked to increased risk of PDA. Obese individuals have a 20% higher risk of developing pancreatic cancer than those who are normal weight (Berrington de Gonzalez et al., 2003; Michaud et al., 2001). Enhanced risk in overweight patients has been linked to a positive association of Fat mass and obesity-associated (FTO) and Adiponectin (ADIPOQ) gene variants (Tang et al., 2011). Obesity during early adulthood may be associated with an even greater risk of pancreatic cancer and a younger age of disease onset (Li et al., 2009).

Whether **alcoho**l use causes PDA remains to be determined, since a positive association was found in several but not all studies (Genkinger et al., 2009). Accumulating evidence suggests that a moderate increased risk is limited to heavy alcohol users (Tramacere et al., 2010).

Conversely to modifiable risk factors, **non-modifiable risk factors** are not dependent on the lifestyle of an individual and cannot be controlled or limited by his or her behaviour.

Although rare in the human population, several **hereditary syndromes** linked to gene mutations represent non-modifiable risk factors associated with general increased risk of cancer, including pancreatic cancer. **Hereditary breast ovarian cancer syndrome** is associated with germ line mutation

in the breast cancer, early onset genes BRCA2 and BRCA1. BRCA2 and BRCA1 are tumour suppressor genes normally expressed in the cells of breast and other tissue, which are involved in a number of cellular pathways that maintain genomic stability and regulate transcription and apoptosis (Schlacher et al., 2011; Wu et al., 2010). Mutations in the BRCA2 gene are associated with an increased risk of pancreatic cancer and account for the highest proportion of known causes of inherited pancreatic cancer (Couch et al., 2007; Hahn et al., 2003).

Patients with **Peutz-Jeghers Syndrome (PJS)**, usually associated to mutations in the STK11 tumour suppressor gene (Jenne et al., 1998), also have a 11% to 36% chance of developing PDA during their lifetime (Giardiello et al., 2000); while the risk for those with **hereditary pancreatitis** linked to PRSS1 mutations increase approximately to 40%-50% (Raimondi et al., 2010; Whitcomb et al., 1996). Moreover, **Familial Atypical Multiple Mole Melanoma (FAMMM) syndrome**, a rare hereditary syndrome characterized by multiple atypical nevi and an increased risk of melanoma due to mutations within the cyclin-dependent kinase inhibitor 2A (CDKN2A) tumour suppressor gene, has also been associated with a 13- to 22-fold increased risk of PDA (Lynch et al., 2008).

A number of studies have linked family history to an increased risk of pancreatic cancer. Generally, individuals with a **family history of pancreatic cancer** have a nearly 2-fold increased risk for developing pancreatic cancer, compared to those without such a history (Permuth-Wey and Egan, 2009). Families with only one relative with pancreatic cancer or with multiple pancreatic cancers in more distant relatives are considered as sporadic. However, the risk increases to 7- to 9-fold for individuals with at least 1 first-degree relative (a parent or sibling) with pancreatic cancer and 17- to 32-fold for individuals with 3 or more first degree relatives with pancreatic cancer (Klein et al., 2004).

Oncogenic transformation in the pancreas is currently understood to be a multistage process that involves the accumulation of inherited and acquired mutations of specific cancer-associated genes in **premalignant lesions**. The literature describes two main types of PDA precursor lesions:

pancreatic intraepithelial neoplasia (PanIN) and intraductal papillary mucinous neoplasm (IPMN). PanIN is by far the most common lesion in the small ducts and ductules in the pancreas, which growing evidence suggests that are the precursors to infiltrating ductal adenocarcinomas (Hruban et al., 2000b; McCarthy et al., 2001). Based on a number of studies that have correlated microscopic findings with genetic alterations, three grades of PanIN have been described as cells progress from low grade dysplasia (PanIN-1) to high grade dysplasia (PanIN-3) (Hruban et al., 2001) (Figure 4).

Accumulating evidence suggests that also long-standing chronic pancreatitis is a strong risk factor for PDA, though pancreatitis may also be an early indicator of pancreatic cancer (Lowenfels et al., 1993; Malka et al., 2002; Raimondi et al., 2010). Pancreatic cancer risk is almost threefold higher in people with chronic pancreatitis, compared with healthy controls (Duell et al., 2012). In addition, PDA risk is 40-120% higher in diabetics compared to non-diabetics since the diabetes itself may be the cause or an early manifestation of pancreatic cancer (Batabyal et al., 2014; Ben et al., 2011; Elena et al., 2013; Starup-Linde et al., 2013; Stevens et al., 2007).

1.2.3 The genetics of PDA.

Different mutations occur in PDA cells that mediate escape from the apoptotic pathway which will otherwise remove unwanted or damaged cells from multicellular organisms in an orderly, non-inflammatory manner. The identification of signature gene mutations in pancreatic adenocarcinoma was recognized as a valuable starting point to study the progression of the disease. Alteration in the Kirsten rat sarcoma viral oncogene homolog gene (*KRAS*), cyclin-dependent kinase inhibitor 2A gene (*CDKN2A*), Tumour suppressor protein p53 gene (*TP53*), and deleted in pancreatic carcinoma locus 4 gene (*DPC4*), also known as SMAD4, are considered hallmarks of PDA (Figure 4).

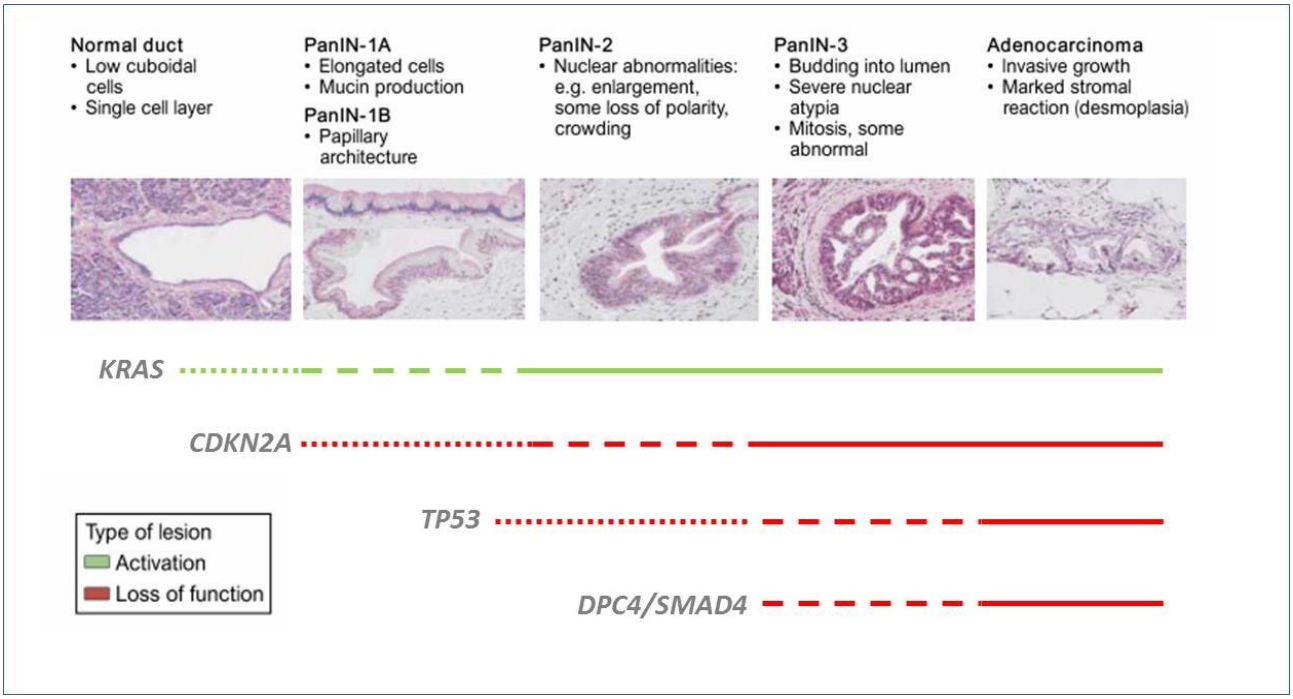

Figure 4. **Genetic progression model of PDA.** *Pancreatic intraepithelial neoplasias (PanINs) seem to represent progressive stages of neoplastic growth that are precursors to pancreatic adenocarcinomas. The genetic alterations documented in adenocarcinomas also occur in PanIN in what seems to be a temporal sequence. The stage of onset of these lesions is depicted. Adapted from* (Bardeesy and DePinho, 2002).

Mutations in *KRAS* constitute the earliest genetic abnormalities underlying the development of pancreatic neoplasms (Feldmann et al., 2007; Maitra et al., 2006) (Figure 4). RAS protein produced by wild-type *KRAS* is important in normal growth, proliferation, and differentiation of cells, acting as a molecular switch, which is functionally characterized by the change from an inactive GDP-binding state to an active GTP-binding state. GTP-bound RAS can interact with more than 20 effector proteins to regulate various cellular responses including proliferation, survival and differentiation (Normanno et al., 2009). *KRAS* oncogene on human chromosome 12p12.1 is activated by point mutations in approximately 90% of PDA (Almoguera et al., 1988; Griffin et al., 1995; Grunewald et al., 1989; Shibata et al., 1990).

Through the use of shared coding regions and alternative reading frames, cyclin-dependent kinase inhibitor 2A gene (*CDKN2A*), on chromosome 9p21, encodes two major proteins (p16 or INK4 and

p14 or ARF) involved in the control of the retinoblastoma (RB) and the p53 (TP53) cell cycle regulatory pathways (Robertson and Jones, 1999; Schutte et al., 1997). Like *KRAS* mutation, loss of function of the *CDKN2A* gene, brought by mutation, homozygous deletion or promoter hypermethylation, occurs in 80-95% of sporadic pancreatic adenocarcinomas (Rozenblum et al., 1997) and is considered an early event in the progression of pancreatic neoplasm (Figure 4).

In addition, homozygous deletions of the genetic material within chromosome arm 9p21, which lead to the *CDKN2A* gene inactivation, can also delete both copies of interferon alpha and beta (IFN-α/β) genes located in the same locus. This loss is responsible for the lack of IFN expression in nearly 80% of PDA cells (Chen et al., 1996; Ghadimi et al., 1999; Hruban et al., 2000a; Vitale et al., 2007), although responsiveness to exogenous IFN is maintained in several cases (Booy et al., 2014; Murphy et al., 2012; Vitale et al., 2007).

In approximately 50–75% of PDAs also the tumour suppressor gene *TP53,* on chromosome 17p13.1, has undergone bi-allelic inactivation generally by missense alterations of the DNA-binding domain (Rozenblum et al., 1997). The transcription factor p53, produced by *TP53*, responds to diverse cellular stresses formulated to regulate target genes participating in G1-S cell cycle checkpoint, cell cycle arrest, apoptosis, senescence and DNA repair (Redston et al., 1994). Studies suggest that loss of p53 function contribute to the genomic instability observed in pancreatic cancers (Hingorani et al., 2005) and that *TP53* gene mutations constitute late events in pancreatic cancer progression (Maitra et al., 2003) (Figure 4).

About 55% of human somatic pancreatic carcinomas show also allelic loss at chromosome locus 18q21.1, where the *DPC4* (also known as *SMAD4*) tumour suppressor gene is located (Schutte et al., 1996). The loss of *DPC4/SMAD4,* infrequently in non-pancreatic cancers, interferes with the intracellular signalling cascades downstream from transforming growth factor beta (TGF-B), resulting in uncontrolled cell proliferation due to the loss of pro-apoptotic signalling or inappropriate G1/S transition (Massague et al., 2000). Like *TP53*, loss of *DPC4/SMAD4* expression is

a late genetic event in pancreatic neoplasm progression and is considered a predictor of decreased survival for PDA patients (Feldmann et al., 2007).

Interestingly, although a characteristic pattern of genetic lesions (KRAS, CDKN2A, TP53 and SMAD4/DPC4) plays a pivotal role in PDA progression (Bardeesy and DePinho, 2002), molecular research together with advances in sequencing technologies have identified many secondary genetic alterations in patients with pancreatic cancer revealing a marked genetic heterogeneity of individual tumours (Biankin et al., 2012; Yachida and Iacobuzio-Donahue, 2013). This heterogeneity can lead to various PDA sub-classes, as shown by various cancer-derived cell lines (Deer et al., 2010), and appears to have substantial implications for differing responses to therapy (Biankin et al., 2012; Collisson et al., 2011).

1.2.4 PDA prognosis and current treatments.

Pancreatic ductal adenocarcinoma (PDA) is considered one of the most lethal malignancies with a 5-year survival rate of merely 6% (American Cancer Society, 2013). The prognosis of PDA is largely determined by the stage of disease at diagnosis, which is based on the tumour's size, lymph node involvement and the extent of spread locally and to distant organs.

Whether the poor prognosis of patients with pancreatic cancer compared to others with different type of cancers is due to late diagnosis or early dissemination to distant organs is still debated. Previous studies split tumour progression in three intervals associated with (i) the time between tumour initiation to establishment of the founder parental clone (average 10 years, T1); (ii) the time between the appearance of the parental clone and the arise of subclones with metastatic potential (average 6.8 years, T2); and (iii) the time from metastatic dissemination to patient's death (average 2.7 years, T3) (Luebeck, 2010; Yachida et al., 2010). Unfortunately, the vast majority of PDA patients are diagnosed within the last two years of tumour development.

At present, surgery provides the best chance of prolonged survival for PDA patients, but due to the asymptomatic form of the early stage disease together with the lack of early detection methods only about 15% to 20% of diagnosed pancreatic cancer cases are eligible for surgery and even for patients with a tumour that has been surgically removed the 5-year survival is only about 20 to 25% (American Cancer Society, 2013).

For advanced disease, chemotherapy is often offered and may lengthen survival. Nevertheless, in spite of numerous efforts, the 5-year survival rate for pancreatic cancer has not improved much for last few decades. One reason contributing to this is the lack of chemotherapeutic agents which would effectively improve the survival of patients (American Cancer Society, 2014).

5-fluorouracil (5-FU), a pyrimidine analog which works as suicide inhibitor through irreversible inhibition of thymidylate synthase, has been used for half a century in advanced PDA. However, as a single agent, objective responses rates have typically been less than 10% and responses were usually for less than six months. In 1997, a randomized trial found Gemcitabine to have superior clinical effect when compared to 5-fluorouracil (Burris et al., 1997).

Gemcitabine (2', 2'- difluorodeoxycytidine or dFdC) is a difluoro analog of deoxycytidine and, at the time of this writing, is the first line chemotherapeutic agent used in the treatment of PDA. Gemcitabine enters the cell via human equillibrative nucleotide transporter 1 (hENT1) (Mackey et al., 1998) and therefore patients with detectable expression of hENT had significantly longer survival than patients with low levels or absence of this protein (Spratlin et al., 2004).

In its triphosphate form (dFdCTP) Gemcitabine competes with deoxycytidine triphosphate (dCTP) to get incorporated into the DNA strand during replication blocking elongation and triggering apoptosis. In addition, the diphosphate metabolite (dFdCDP) inhibits the enzyme ribonucleotide reductase (RNR), responsible for the production of the deoxyribonucleotides, further preventing the formation of triphosphate nucleotide required for DNA replication and repair (Huang et al., 1991).

Gemcitabine has been used either alone or in combination with other agents to inhibit the growth of cancer cells by interfering with specific molecules involved in tumor progression. In November 2005, the FDA approved in combination with Gemcitabine the use of Erlotinib hydrochloride (trade name Tarceva), previously shown to be effective in lung cancer patients with epidermal growth factor receptor (EGFR) mutations (Kobayashi and Hagiwara, 2013), for treatment of locally advanced, unresectable, or metastatic pancreatic cancer. However, so far Erlotinib has failed to demonstrate a marked improvement in the treatment of advanced pancreatic cancer survival (American Cancer Society, 2014).

Cisplatin, a platinum-based anti-neoplastic drug which binds to DNA causing cross-linkage and ultimately triggering apoptosis, has been also administered in combination with gemcitabine to treat advanced pancreatic cancer. However, although median overall survival was more favorable in the combination arm as compared with gemcitabine alone, the difference did not reach statistical significance (Heinemann et al., 2006).

Drug resistance is one of the pivotal factors responsible for low survival rate of PDA patients. Cancer cells can acquire resistance against a drug through various mechanisms: (i) blocking the drug's entry into the cell, (ii) increasing its exit from the cell, and/or (iii) enhancing its degradation or preventing its activation once inside the cell (Gottesman, 2002). Numerous studies over the past decades have suggested that PDAs are associated with various genetic alterations which contribute to its resistant characteristics (Shi et al., 2002; Tamburrino et al., 2013).

Radiotherapy (RT) is commonly used together with chemotherapy for locally advanced pancreatic cancer. RT uses ionizing radiation that works by damaging the DNA of cancerous tissue leading to cellular death. However, normal cells around the cancer or where the radiation beams pass through the body can also be damaged, sometimes causing side effects. Radiotherapy, like chemotherapy, does not cure the cancer, but may help to control it and slow down its growth.

Because cancer therapies proven successful in other tumour types have shown little efficacy in treating pancreatic cancer, the development of new treatment strategies for patients suffering from PDA is of crucial importance.

1.3 Virotherapy

1.3.1 Oncolytic Viruses.

Viruses began to be employed for cancer therapy at the end of the nineteenth century, but their use was not based on a particular theory of alternative treatment, rather it was the result of the observation that, occasionally, cancer patients who contracted an infectious disease went into brief periods of clinical remission. In the case of leukemia, it was well recognized that contraction of influenza sometimes produced beneficial effects as shown by an example dated 1896, in which a woman was reported to recover from “myelogenous leukemia” following a presumed influenza infection (Dock, 1904). The report was made 35 years before the etiological cause of influenza was first discovered in pigs by Richard Shope (Shope, 1931) and 37 years before the first isolation of the virus from humans by a group headed by Patrick Laidlaw (Smith et al., 1933). However, in 1912 the Italian physician Nicola De Pace presented findings that one of his female patients suffering from cervical carcinoma had undergone a complete spontaneous remission after receiving an inoculation of the live attenuated Pasteur-Roux rabies virus vaccine following a dog bite (De Pace, 1912). This was the first documented case of a tumour remission that was attributed to the lytic effects of a virus and began the field of oncolytic virotherapy.

Oncolytic virotherapy is a treatment that uses natural or engineered oncolytic viruses (OVs) to selectively kill tumour cells. OVs exploit cancer-associated genetic aberrations to replicate and propagate selectively in tumour cells, thus leading to their lysis, while not affecting or displaying limited effect on surrounding normal cells. This behaviour may be attributed to the fact that many

of the hallmarks of cancer, such as blocks of apoptosis, deregulation of the cell cycle control and immune evasion, are also optimal cellular condition for successful viral replication. Tumour cells are therefore more susceptible to viral infection that normal cells.

Virotherapy offers several advantages over the use of conventional small drugs as cancer therapeutics, including selectivity, potency and mechanism of cell killing. Cancer cell death through apoptosis triggered by OVs has been increasingly recognized as a promising therapeutic approach for many cancers as, differently from necrosis, the typical constituents of dying cells are not released into the extracellular environment (Brown and Attardi, 2005; Call et al., 2008; Guo et al., 2008; Noteborn, 2009).

Various naturally occurring or genetically engineered viruses are being investigated as oncolytic agents for cancer treatment (Table 1). The translational impact of this technique was strengthened by the approval of the first genetically-modified tumour killing adenovirus H101 for the treatment of head and neck cancer patients in China (Garber, 2006) and by the successful progression of other DNA viruses in advanced clinical trials, including the engineered herpes simplex virus Talimogene laherparepvec (T-Vec) for melanoma and the engineered vaccinia-vaccine-derived JX-594 (Pexa-Vec) for colorectal carcinoma and liver cancer (Donnelly et al., 2013; Goins et al., 2014; Heo et al., 2013). Beside DNA viruses, several RNA viruses have also entered the clinic displaying promising results. Reolysin, an unmodified reovirus type 3 Dearing strain, has probably been the most extensively studied among the oncolytic RNA viruses due to its natural replication preference in tumour cells and spontaneously transformed cells with overactive Ras pathway (Kelly et al., 2009). During the last decade more than 30 clinical trials have evaluated the oncolytic potential of locally or systemic administered Reolysin against different types of neoplasm. Multi-dose intravenous administration of Reolysin to patients with advanced cancers resulted in intratumoural localisation of reovirus with little toxicity (Vidal et al., 2008). Recently, Reolysin has completed a phase III clinical study in patients with metastatic or recurrent squamous cell carcinoma of the head and neck

designed to compare response rates following its intravenous administration in combination with paclitaxel and carboplatin versus the chemotherapy treatment alone (Table 1).

The diversity and abundance of viruses available in nature has provided a constant basin from which to choose new oncolytic candidates, including viruses derived from the animal reservoir. Newcastle disease virus (NDV), a negative-sense single-stranded RNA virus with a natural avian host range, has been thoroughly investigated as oncolytic candidate for human disease (Elankumaran et al., 2010; Freeman et al., 2006; Hotte et al., 2007). Although, NDV can cause severe and lethal disease in poultry, infection is mostly asymptomatic in humans due to limited replication capacity in the cytoplasm of normal mammalian cells. Conversely, NDV displays selective replication in and lysis of tumour cells presumably because of their defective interferon (IFN) signalling pathways (Reichard et al., 1992; Wilden et al., 2009). In 2006 Freeman et al. presented the first clinical evaluation of a attenuated lentogenic isolate of NDV (HUJ) administered systemically and the first evaluation of any NDV strain in glioblastoma patients (Freeman et al., 2006) demonstrating good tolerability and encouraging responses.

Another example of a non-human virus is represented by Vesicular Stomatitis Virus (VSV), a non-segmented negative-strand RNA virus that can infect insects, cattle, horses and pigs. VSV is also able to selectively infect and kill human tumour cells defective in type-I IFN production and responses (Barber, 2004; Lichty et al., 2004). At the time of this writing a Phase I clinical trial to evaluate the safety of intra-tumoural injections of an engineered VSV expressing human IFN-β in patients with liver cancer is recruiting (Table1).

Virus Family	Phase and type of clinical trial	Virus name	Genetic changes	Route/ Combination therapy	NCT or PMID number
DNA viruses					
Herpesviridae	Phase III complete; melanoma, primary end point met.	Talimogene laherparepvec (T-Vec)	• Armed with GM-CSF • Tumour-specific replication; ICP 34.5 deleted, US11 altered • Enabled antigen presentation: ICP47 deleted	IT/ None	NCT00769704
Adenoviridae	Phase II and III; Bladder cancer	CG0070	• Armed with GM-CSF • Preferential replication in Rb-deficient tumours	IT/ None	NCT01438112
	Approved therapeutic (China); SCCHN	Oncorine (H101)	• Preferential replication in tumours: E1B-55K deleted	IT/ Cisplatin	PMID15601557
Poxviridae	Phase IIB; hepatocellular carcinoma	JX-594 (Pexa-Vec)	• Armed with GM-CSF • Preferential replication in tumours: thymidine kinase deleted	IT/ Cisplatin	NCT01387555 PMID23396206
RNA viruses					
Paramyxoviridae	Phase I; myeloma	MV-NIS	• Armed with human NIS • Preferential replication in tumours incompetent to block STAT1 and MDA5	IV/ Cyclophosphamide	NCT02192775 NCT00450814
	Phase I/II; glioma	NDV-HUJ	None	IV/ None	PMID16257582 NCT01174537
Rhabdoviridae	Phase I; hepatocellular carcinoma	VSV-hIFNβ	• Armed with human IFNβ	IT/ None	NCT01628640
Retroviridae	Phase I and II; glioma	Toca 511	• Armed with cytosine deaminase	IT; IV; into resection cavity/ 5-flurocytosine	NCT01156584 NCT01470794 NCT01985256
Reoviridae	Phase III; SCCHN	Reolysin	None	IV/ Carboplatin paclitaxel	NCT01166542

Table 1. ***Selected examples of current clinical trials involving oncolytic viruses from different families.*** *GM-CSF Granulocyte-macrophage colony stimulating factor; hIFNβ, human interferon β, ICP, infected cell protein; IT, intratumoural; IV, intravenous; MDA5, melanoma differentiation-associated protein 5; MV, measles virus ; NCT, national clinical trial; NIS, sodium-iodide symporter; PMID, PubMed identifier; Rb, retinoblastoma protein; SCCHN, squamous cell carcinoma of the head and neck; STAT1, signal transducer and activator of transcription 1; US, unique sequence; VSV, vesicular stomatitis virus. Adapted from* (Miest and Cattaneo, 2014).

Whether or not an oncolytic virus reaches the clinic, its development is constantly subject to improvement. The most important technical challenges for a successful oncolytic virus are the optimization and enhancement of (i) systemic virus delivery, (ii) tumour targeting, (iii) intra-tumoural virus spread and (iv) anti-cancer immune response.

1.3.1.1 Systemic virus delivery.

When an oncolytic virus is delivered systemically through intravenous administration it can be rapidly cleared from the circulation due to neutralization by serum factors such as antibodies accumulated to a previous infection or administration and/or to sequestration by the mononuclear phagocytic system (MPS) in the liver and spleen (Underhill and Ozinsky, 2002) (Figure 5). Thus, different studies are focused on minimizing the impact of these barriers by changing or physically hiding the epitopes that are recognized by antibodies.

Although several papers demonstrated the superior performances obtained by hiding oncolytic viruses inside carrier cells or through chemical modification of viral coat proteins by conjugation of biocompatible polymers (Croyle et al., 2004; Doronin et al., 2009; Ilett et al., 2009; Morrison et al., 2008; Power and Bell, 2008), the most basic method of genetic shielding oncolytic viruses from pre-existing immunity is serotype exchange, where a different serotype of the same virus species is engineered onto the core of an established virus. This strategy requires the availability of multiple serotypes for a given virus or of serotypes that humans have not previously encountered, with low homology between their surface-exposed glycoproteins or capsid proteins. Multiple engineering strategies that differ in the type and magnitude of modification have been applied to different virus families, but the result is always a chimeric virus with an engineered serotype that is not recognized by the pre-existing antibodies present in the target patient population (Kaufmann and Nettelbeck, 2012; Miest et al., 2011; Roberts et al., 2006; Sarkioja et al., 2008).

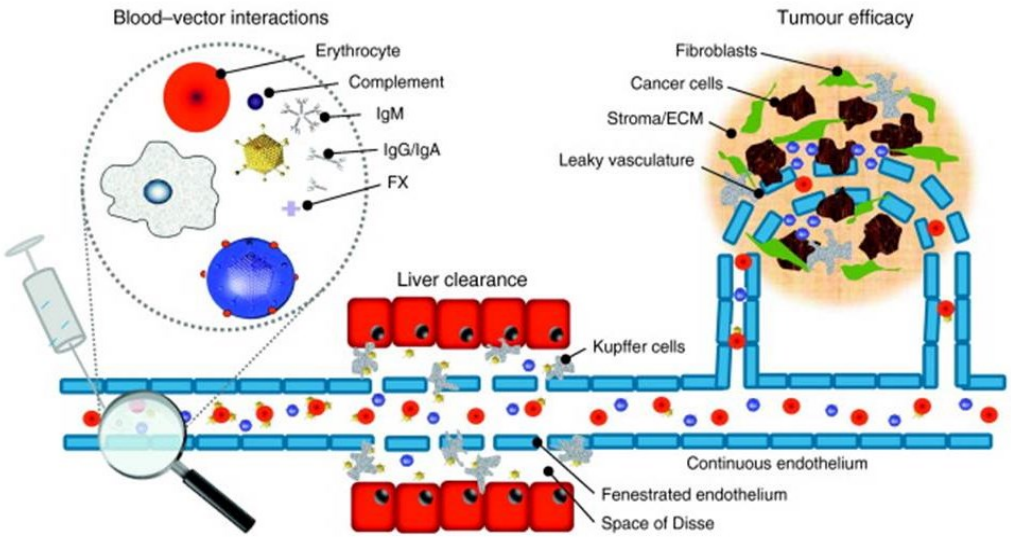

Figure 5. ***Barriers to systemic delivery of oncolytic viruses.*** *There are three main areas that must be addressed to enable systemic delivery of virus particles, namely (i) avoiding neutralisation by components of the bloodstream, (ii) avoiding premature scavenging by phagocytes, such as hepatic Kupffer cells, (iii) maximising extravasation within tumour vasculature and penetration to infect all viable tumour cells whilst avoiding other components of the interstitium. Adapted from* (Tedcastle et al., 2012).

1.3.1.2 Tumour targeting.

Tumour selectivity can be enhanced either at the stage of virus entry in the target cells or post-entry during replication.

Virus retargeting can be achieved through different approaches; for example by making virus binding/entry dependent on proteases specifically secreted by tumour cells (Springfeld et al., 2006). Another common strategy involves fusion to the virus attachment protein of a single-chain antibody or a peptide known to bind a tumour-associated cell surface marker overexpressed in a wide variety of neoplasms (Coughlan et al., 2009; Jing et al., 2009; Nakamura et al., 2005) or specifically expressed by a particular type of malignancy (Grandi et al., 2010; Hasegawa et al., 2006; Liu et al., 2009; Menotti et al., 2006).

Post-entry targeting can be obtained by placing essential viral gene under the regulation of a specific promoter overactive in cancer cells (Doloff et al., 2011; Hardcastle et al., 2007; Kambara et

al., 2005; Lee et al., 2010), or by inserting in the viral genome sequences complementary to tissue specific miRNA which are downregulated in tumour cells (Hikichi et al., 2011; Ylosmaki et al., 2008). Oncolytic viruses can also be made tumour replication selective by mutating viral genes required for virus survival in normal cells but not in malignant cells. Deletion of adenovirus (Ad) E1A and E1B genes or vaccinia virus (VV) thymidine kinase (TK) genes restricts virus replication to cells with defects in retinoblastoma (Rb) and p53-controlled tumour suppressor pathways or in active proliferation, respectively (Fukuda et al., 2003; McCart et al., 2001). In the same manner impairment of influenza A virus NS1 gene limits virus growth in IFN competent cells, but does not affect viral replication in most cancer cells characterized by defective IFN expression or signalling pathway (Muster et al., 2004).

1.3.1.3 Improving virus spread in tumours.

Enhancement of intratumoural spreading also requires improvement, as the movement of viruses through tumour cells can be reduced or even blocked by dense intratumoural connective tissue (Sauthoff et al., 2003; Yun, 2008). Some oncolytic viruses are naturally well equipped to spread within and between tumours (Kirn et al., 2008; Patel et al., 2011), others require further engineering or synergy with drugs capable of enhancing the fluidity of the environment surrounding the tumour cell. Injection of hyaluronidase, an enzyme that catalyses the hydrolysis of hyaluronan, a key component of the tumour extracellular matrix (ECM), lowers the viscosity of the tumour environment, thereby increasing tissue permeability and enhancing the spread and efficacy of oncolytic adenoviruses (Ganesh et al., 2008). In the wake of this approach a hyaluronidase-expressing oncolytic adenovirus was generated and displayed improved spread and activity in a human melanoma xenograft model (Guedan et al., 2010). More recently, Losartan (Cozaar), an angiotensin II receptor antagonist and antihypertensive agent, has been used to improve the

intratumoral spreading of HSV by disrupting transforming growth factor-β1 (TGF-β1) signalling, which decreases collagen production (Diop-Frimpong et al., 2011).

1.3.1.4 Enhancing antitumor immunity.

Immune evasion is one of the hallmarks of cancer. Tumours produce immunosuppressive cytokines and recruit immune inhibitory cells paralyzing any antitumor immune response (Melcher et al., 2011; Yang et al., 2010). If stimulation of immune responses against oncolytic viruses represents a barrier to clinical success, immune response against cancer cells could help to achieve tumour destruction and potentially to prevent disease relapse. Oncolytic viruses may constitute a strategy for combining tumour lytic activity with a potent activation of adaptive and innate immune responses. Targeted infection of the tumour can lead to a localized inflammatory response, stimulating an immune storm directly within the malignancy, thereby facilitating immune recognition of cancer-specific antigens (Melcher et al., 2011). The understanding of the importance of the immune response stimulation in the final clinical outcomes has driven the design of new class of oncolytic viruses combining lytic infection and immunostimulatory transgene expression. To date the most successful strategy uses the expression by OVs of the granulocyte-macrophage colony-stimulating factor (GM-CSF), a cytokine associated with the recruitment and differentiation of activating dendritic cells (DC) in the tumour microenvironment, which boosts adaptive immunity against tumour-associated antigens (Figure 6). Herpes simplex virus (HSV T-Vec), adenoviruses (Ad CG0070) and vaccinia viruses (VV JX-594) expressing GM-CSF have reached advanced clinical trials, repeatedly displaying efficacy, especially for malignancies that are sensitive to immune-therapy (Andtbacka et al., 2015; Breitbach et al., 2012; Burke et al., 2012; Cripe et al., 2014; Heo et al., 2013). Another immune-modulatory gene often engineered within different OV scaffolds is the interferon-β (IFN-β) gene (Kirn et al., 2007; Li et al., 2010; Willmon et al., 2009). Interestingly, the initial aim of IFN-β expression by OVs was to restrict viral replication in normal tissue, thus

increasing direct oncolysis and the therapeutic index; further studies showed that the viruses worked via an enhanced immune response rather than via virus-mediated tumour lysis.

OVs expressing other immune-modulatory signalling molecules (including IL-12, IL-24, IL-4, RANTES, CD80, IL-18, and IFN-α), which act on different immune pathways, have also been generated and tested for their oncolytic activity (Kaur et al., 2009). The success of current oncolytic viruses that express immunostimulatory transgenes, even in the absence of robust intratumoral proliferation, highlights the potential of new viruses characterized by high transcription rate and consequent high transgene expression to stimulate the immune response against the tumour microenvironment (Miest and Cattaneo, 2014).

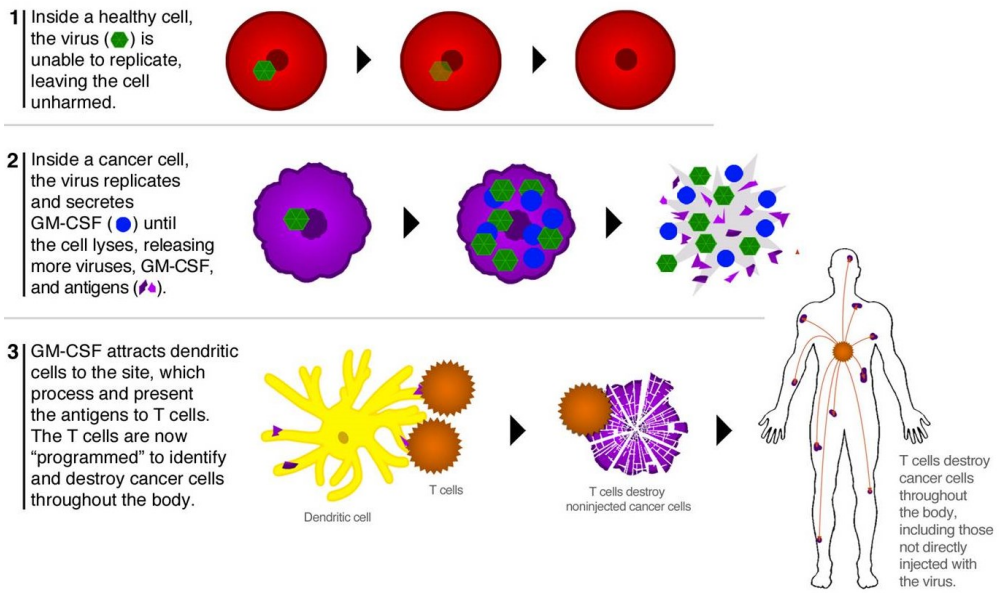

*Figure 6. **Mechanism of action of GM-CSF armed oncolytic viruses*** (Talimogene laherparepvec MOA).

1.3.2 Virotherapy for PDA.

Based on the promising results obtained for other type of malignancies, oncolytic virus therapy might be a feasible treatment for pancreatic cancer. Indeed, within the past decade, many OVs have been intensively studied as potential treatments for PDA and some of these, such as adenoviruses, herpesviruses and reoviruses, are currently under clinical trials.

At the time of this writing a phase I dose escalation study using a tumour-selective replication-competent VCN-01 adenovirus, alone or in combination with Gemcitabine, in patients with advanced pancreatic cancer is currently recruiting (NCT02045589). VCN-01 virus harbours a T1 mutation and expresses PH20 hyaluronidase. The T1 mutation consists of a single Adenine truncating insertion in the endoplasmic reticulum retention domain of the E3/19K protein (445A mutation), which relocates the protein to the plasma membrane and is responsible for enhanced virus release and virus anti-tumour activity when injected intra-tumorally or systemically *in vivo* (Gros et al., 2008). As previously discussed (see paragraph 1.3.1.3), the hyaluronidase technology improves intratumoral spread of oncolytic viruses increasing their debulking activity (Guedan et al., 2010).

Since *KRAS* is one of the most frequent mutations in PDA cells (80-95%) (Almoguera et al., 1988; Griffin et al., 1995; Grunewald et al., 1989; Shibata et al., 1990) reovirus has also been extensively studied for the treatment of pancreatic cancer and currently a clinical trial testing the use of Reolysin in combination with Gemcitabine in patients with advanced PDA is ongoing (NCT00998322).

Besides agents that already have reached clinical trial stage, many different oncolytic candidates have been tested in preclinical studies for the treatment of PDA. For example, the oncolytic potential of attenuated VSV-ΔM51-GFP and VSV-p1-GFP (Wollmann et al., 2010) was analyzed in a panel of 13 clinically relevant human PDA cell lines *in vitro* and in a xenograft model in comparison to conditionally replicative adenoviruses (CRAds), Sendai virus (SeV) and respiratory syncytial virus (RSV) (Murphy et al., 2012). Different NDV lentogenic strains were also evaluated for their oncolytic potential against PDA cells *in vitro* (Buijs et al., 2014; Walter et al., 2012).

1.4 Influenza A viruses.

1.4.1 Classification.

The word “virus” derives from Latin, for poison and other noxious substances. It was used in English for the first time in 1392 as a meaning of "agent that causes infectious disease" and then recorded in reference to venereal disease in 1728, a long time before the description of a non-bacterial pathogen infecting tobacco plants by Dimitri Ivanovsky in 1892 which led to the discovery the tobacco mosaic virus by Martinus Beijerinck in 1898.

Influenza, commonly referred to as “flu”, is caused by a RNA viruses belonging to the *Orthomixoviridae* (ορθός, orthos, Greek for "straight"; μυξα, myxa, Greek for "mucus") family, which at the present consists of six genera: Influenza virus A, influenza virus B, Influenza virus C, Thogotovirus, Isavirus and Quaranjavirus (International Committee on Taxonomy of Viruses, 2014).

The three genera of Influenza virus (A, B and C), which are identified by antigenic variations in their nucleoprotein (NP) and matrix protein (M1), show different tropism for vertebrates. While influenza B and C circulate almost exclusively in humans, influenza A viruses are established also in different animal species including horses, swine, and a wide variety of domesticated and wild birds. In humans influenza A and B viruses are the predominant cause of significant disease, whereas Influenza C virus infects primarily young children usually resulting in a mild respiratory illness (Gatherer, 2010; O'Callaghan et al., 1980) and is not included in the seasonal influenza vaccine.

Genome organization and structural features suggest that influenza A, B, and C viruses had a common ancestor, which is distinct from those of other negative sense RNA viruses (Desselberger et al., 1980; Webster et al., 1992). Based on the same features, influenza A and B viruses appear to share more similarities than they do to influenza C, suggesting that the latter diverged before the split between influenza A and B viruses. Nevertheless, during the long human adaptation process, influenza B viruses accumulated increasing differences compared to influenza A viruses which

prevent potential intertypic reassortment. While Influenza B viruses can be further broken down only into lineages and strains, type A influenza viruses are divided into different subtypes based on the antigenic relationship of the surface glycoproteins, haemagglutinin (HA) and neuraminidase (NA).

1.4.2 Morphology

Influenza A virus (IAV) particles are pleomorphic, since many strains bud as spherical particles (approximately 100 nm in diameter) while others produce long filaments (up to 20 µm in length), depending on the virus strain, cell origin, passage history and Matrix protein (M1-M2) features (Elleman and Barclay, 2004; Roberts et al., 2013; Roberts et al., 1998) (Figure 7). Although it is unclear whether one morphology has advantages over the other, it is well established that serial passage of a filamentous strain in embryonated chicken eggs (ECE) results in selection of spherical particles (CHOPPIN et al., 1960), whereas the dominant morphology of viruses isolated from the upper respiratory tract (URT) of human patients is filamentous (CHU et al., 1949; KILBOURNE and MURPHY, 1960), suggesting that the latter phenotype might be clinically more relevant and may have a selective advantage in circulating strains.

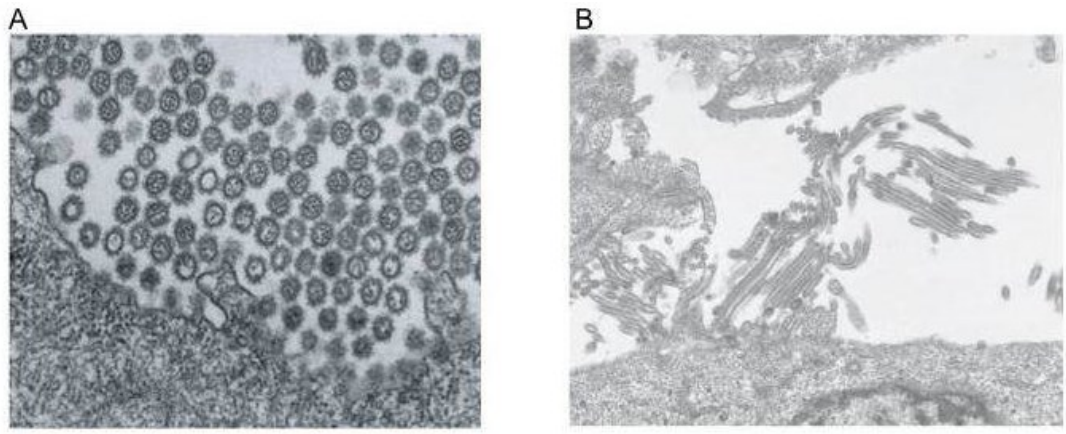

*Figure 7. **Different shapes of influenza A viruses**. Spherical (A)* (Noda et al., 2006) *and filamentous (B) structures* (Neumann et al., 2009).

1.4.3 Genome and structure.

Influenza A virus (IAV) genome is composed of eight negative-sense single stranded RNA gene segments (-ssRNA) that encode 11 major proteins and several auxiliary peptides (Table 2). Production of infectious progeny virions requires incorporation of all eight vRNA segments and occurs at the apical membrane of infected cells (Wise et al., 2009). The eight vRNA molecules of varying sizes are individually packed and stabilized by wrapping around multiple copies of nucleoprotein (NP; ~56 kDa) (Compans et al., 1972; Ortega et al., 2000) (Figure 8A). The ends of each genomic segment are short complementary elements that form the viral promoter and are recognized by the viral RNA dependent RNA polymerase (RdRp), which is composed of the three subunits PB2, PB1 and PA (Fodor et al., 1994; Hagen et al., 1994; Hsu et al., 1987; Huang et al., 1990; Lee et al., 2002). The polymerase complex together with the nucleoproteins (NP) and the RNA segment form the viral ribonucleoprotein complex (vRNP), which is responsible for virus mRNA synthesis and genome replication (Figure 8A). The eight vRNPs are located inside a shell of M1 protein, that lines the viral lipid membrane derived from the plasma membrane of the infected cells during the budding process. Embedded in the membrane there are two surface glycoproteins the hemagglutinin (HA) and the neuraminidase (NA) and a membrane ion-channel (M2) (K.G. Nicholson, R.G. Webster & A.J. Hay, 1998) (Figure 8B).

The HA is a glycosylated type I integral membrane protein which functions as both receptor-binding protein and fusion protein. NA is a type II integral membrane glycoprotein exerting the sialidase enzymatic activity required for cleavage of both host cell receptors and receptors on the virion surface to allow the release of the nascent virions preventing their aggregation.

IAVs are subdivided by antigenic characterization of the HA and NA surface glycoproteins which are the major antigenic targets of the host humoral immune response. At the time of this writing eighteen HA (H1-H18) and eleven NA (N1-N11) subtypes are known and can be found in numerous

different combinations (eg. H1N1, H3N2 H7N3, H7N1, H18N11, etcc) depending on the host (Fouchier et al., 2005; Tong et al., 2013).

Table 2. Influenza A virus genomic segments and major proteins.

Segment	Protein	Functions
1	Polymerase basic protein 2 (**PB2**)	PB2 subunit is part of the viral RNA-dependent RNA polymerase (Fodor et al., 1994; Hagen et al., 1994; Hsu et al., 1987; Huang et al., 1990; Lee et al., 2002) and is involved in the recognition and binding of 5'-capped host pre-mRNAs (cap snatching) (Guilligay et al., 2008; Huang et al., 1990).
2	Polymerase basic protein 1 (**PB1**)	PB1 subunit is part of the viral RNA-dependent RNA polymerase (Fodor et al., 1994; Hagen et al., 1994; Hsu et al., 1987; Huang et al., 1990; Lee et al., 2002).
	PB1-F2	PB1-F2 induces mitochondria-associated apoptosis (Henkel et al., 2010; Zamarin et al., 2005), exerts IFN atagonist properties by inhibing the activity of Mitochondrial antiviral signaling protein (MAVS) (Varga et al., 2011) and interacts with PB1 influencing the polymerase activity (Mazur et al., 2008).
	N40	N40 maintains the balance between PB1 and PB1-F2 expression
3	Polymerase acidic protein (**PA**)	PA subunit is part of the viral RNA-dependent RNA polymerase (Fodor et al., 1994; Hagen et al., 1994; Hsu et al., 1987; Huang et al., 1990; Lee et al., 2002) and is involved in the snatching of 5'-capped host pre-mRNAs providing RNA endonuclease activity (Dias et al., 2009).
	PA-X	PA-X modulates the host response and viral virulence (Jagger et al., 2012).
4	Haemagglutinin (**HA**)	HA is responsible for binding to sialic acid receptors on the cell surface and fusion with endosomal membrane (Skehel and Wiley, 2000).
5	Nucleoprotein (**NP**)	NP is the major component of the viral ribonucleoprotein (RNP) complex and controls the nuclear transport of vRNPs (Portela and Digard, 2002).
6	Neuraminidase (**NA**)	NA cleaves off sialic acid from cellular receptors of HA to enable progeny escape from infected cells and avoid virus aggregation (Palese et al., 1974).
7	Matrix protein (**M1**)	M1 is the main component of the viral membrane; it underlies the viral envelope and plays multiple roles in virion assembly and infection (Ali et al., 2000; Rossman and Lamb, 2011). M1 is also involved in apoptosis by sequestrating cellular Hsp70 protein (Halder et al., 2011).
	Matrix protein (**M2**)	M2 is a membrane protein that forms a proton channel activated under endosomal pH conditions and has a pivotal role in virus uncoating and genome release in the cytoplasm of the infected cells (Helenius, 1992).
8	Non-structural protein (**NS1**)	NS1 is a multifunctional protein that is involved in numerous virus – host interactions, but the major role ascribed to this protein is to antagonize the host IFN-mediated antiviral response (Hale et al., 2008).
	Nuclear Export Protein (**NEP**)	NEP is a structural component of the viral particle and mediates vRNP export from the nucleus to the cytoplasm (Paterson and Fodor, 2012). NEP accumulation has been associated with the switch between transcription and replication of vRNAs (Robb et al., 2009).

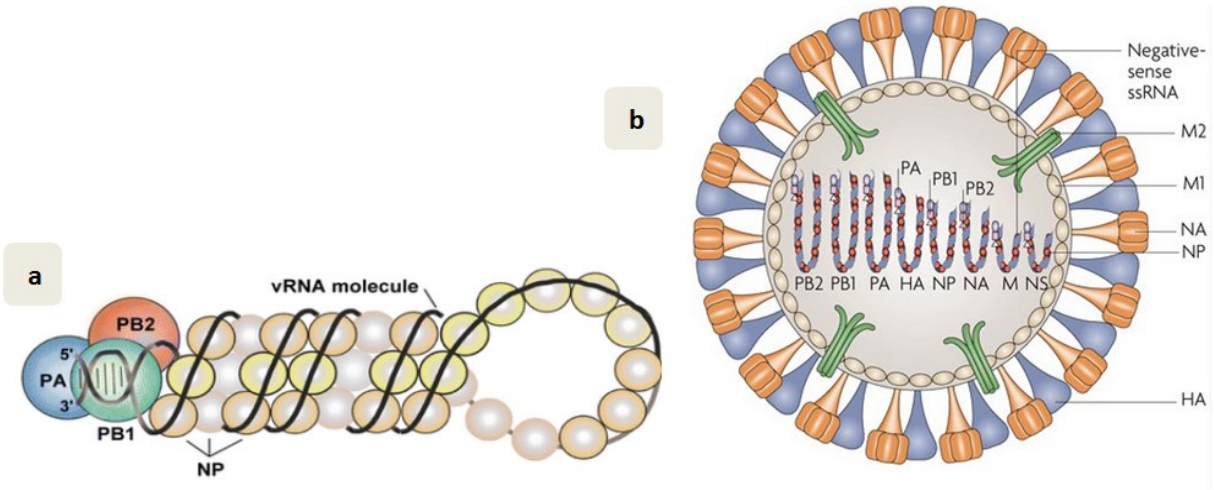

Figure 8. ***IAV genome and structure.*** *A) Structural organization of influenza virus ribonucleoproteins (RNPs). The single-stranded viral RNA (vRNA) molecule (black line) is coiled into a hairpin structure associated with nucleoprotein (NP) (yellow spheres). A short region of duplex vRNA (formed between the 5′ and 3′ ends) constitutes the binding site for the heterotrimeric RNA-dependent RNA polymerase. B) Schematic representation of IAV structure. Adapted from* (Naffakh et al., 2008) *and* (Nelson and Holmes, 2007).

1.4.4 Host Range.

1.4.4.1 Birds.

Although IAVs infect humans causing annual epidemics, economic loss and, occasionally, serious pandemics, the primary reservoir of the virus are wild aquatic birds (Figure 9). However, probably due to the asymptomatic form of most infections in birds, it was not until the mid-1970s that systematic investigations of IAVs in feral birds were undertaken. These studies revealed enormous genetic pools of the virus in the wild bird population (Alexander, 2007) from which subsequently sixteen HA (H1-16) and nine NA (N1-N9) subtypes were isolated (Fouchier et al., 2005).

In addition to the classification based on HA and NA antigenic types, avian IAV can be further classified on the basis of their pathogenic properties. The proteolytic cleavage that is exerted by host proteases on the viral HA protein activates virus infectivity and has been shown to be an important determinant of influenza virus pathogenicity (Klenk and Garten, 1994; Steinhauer, 1999). The main characteristic of HA that determines its sensitivity to host proteases is the cleavage site,

which consists of either a single arginine (monobasic site) or an R-X-K/R-R motif (multibasic site) (Klenk and Garten, 1994). HAs containing monobasic cleavage sites are activated by trypsin or trypsin-like proteases (Klenk et al., 1975; Lazarowitz and Choppin, 1975) and thus IAVs bearing these glycoproteins are restricted to replication at sites in the host where these enzymes are found, such as the respiratory and intestinal tracts of birds (Steinhauer, 1999). Such viruses (Klenk and Garten, 1994; Steinhauer, 1999) display limited virulence and hence are called "low pathogenicity avian influenza" (LPAI) viruses. The introduction of basic amino acids into the hemagglutinin cleavage site allows HA activation in the trans-Golgi network by ubiquitous furin or related proprotein convertases (Morsy et al., 1994; Stieneke-Grober et al., 1992) resulting in virus spreading beyond the respiratory or gastrointestinal tract and causing an acute generalized disease. IAVs having multibasic cleavage sites, called "highly pathogenic avian influenza" (HPAI) virus, are highly virulent and induce systemic infection in their avian hosts with mortality rate as high as 100% (Webster and Rott, 1987).

The highly pathogenic form of IAV, has been known since the end of the 19th century, when an Italian scientist, Edoardo Perroncito, reported what is believed to be the first documented evidence of "fowl plague" as a distinct disease (Perroncito, 1878). In August 2006, the Food and Agricultural Organization (FAO) estimated that, since a chain of outbreaks in late 2003, the HPAI H5N1 virus led to the death or destruction of more than 200 million birds worldwide, resulting in economic losses of over 20 billion dollars (Harris, August 2006).

Interestingly, the HPAI viruses are found only in some H5 and H7 strains, whereas all the other avian influenza strains, including the H5 and H7 influenza A viruses with monobasic cleavage site, are LPAI viruses. It appears that most of the HPAI viruses arose by mutations after LPAI viruses were introduced into domestic poultry from the wild bird reservoir. Several mechanisms might be responsible for this mutation including duplications of purine triplets due to polymerase slippage (Garcia et al., 1996; Perdue et al., 1997) and recombination with cellular or viral RNAs (Maurer-

Stroh et al., 2013). Nevertheless, the factors that determine mutation from LPAI to HPAI are still largely unknown. In some cases, the mutation seems to have taken place rapidly after introduction from wild birds; in others, the LPAI virus progenitor circulated in poultry for months before the mutation occurred. Although it is not possible to predict whether and when this mutation will happen, it is likely to assume that the longer the circulation of LPAI among poultry and domestic birds the higher the chance of the mutation to HPAI (Monne et al., 2014; Senne et al., 2006; Senne, 2007). Thus the screening of the wild bird population and the monitoring of the domestic bird farms are essential condition to control the highly pathogenic form of the disease.

1.4.4.2 Humans.

Avian IAVs may, on occasion, be transmitted directly or indirectly to other host species such as domestic birds, pigs, horses, mink, marine mammals, and humans and either cause transient or endemic circulation of influenza A viruses in these new host populations (Webster et al., 1992). Zoonotic infections, in which a pathogen adapted to another animal species can cause disease in humans, may be sporadic, dead-end infections without adaptation to humans (eg. West Nile Virus). Other zoonotic infections can stably adapt to humans, leading to sustained person-to-person transmission (e.g. HIV and SARS). Influenza A viruses fall into both categories, displaying in the majority of the cases dead-end infections (eg. H5N1), but sporadically resulting in stable host switch events following adaptive mutations (eg. H1N1 “Spanish Flu”). Although 16 HA subtypes have been identified in wild birds, only H1, H2 and H3 subtypes have emerged in human population as a result of stable introduction of virus or viral genes from the avian reservoir following adaptive mutations (Neumann et al., 2009). The different subtypes showed cyclical appearance in humans: H3 viruses emerged around 1890, H1 in 1918, then H2 in 1957, H3 in 1968, and H1 in 2009 (Smith et al., 2009; Webster et al., 1992). Since these subtypes do not contain viruses with a multibasic cleavage site their infections in human usually result in localized replication within the respiratory tract and mild

symptoms, which include fever, cough, sore throat, muscle aches and conjunctivitis. Most people recover within a week without requiring medical attention, but influenza sometimes can cause severe illness or death especially in people at high risk, such as the elderly, immunocompromised subjects, children, pregnant women and patients with chronic medical conditions.

Seasonal influenza occurs globally in humans with an annual attack rate estimated between 5%–10% in adults and 20%–30% in children. Worldwide, these annual epidemics are estimated to result in about 3 to 5 million cases of severe illness, and about 250,000 to 500,000 deaths (World Health Organization (WHO), March 2014). In temperate regions influenza epidemics show a marked wintertime seasonality, with circulation detected over a 2- to 3-month period between November and March in the Northern Hemisphere and between May and September in the Southern Hemisphere (Tamerius et al., 2013). Different factors are proposed to synergistically drive the flu epidemic seasonality. These include fluctuations in host immune competence mediated by seasonal factors, such as lower levels of vitamin D, an important activator of the innate immune response (antimicrobial activity and antigen presentation), due to reduced exposure to UV light during the winter (Cannell et al., 2006; Hewison, 2011). Seasonal changes in host behavior, such as school attendance or crowding indoors, have also been associated with enhanced virus spreading during inclement weather in winter. Moreover, winter environmental factors, such as typical low temperature and low humidity, have been shown to enhance the stability of infectious bioaerosols (Lofgren et al., 2007; Tamerius et al., 2011), allowing more transmission of influenza virus by the respiratory droplet or aerosol route (Lowen and Steel, 2014).

1.4.4.3 Pigs.

Three influenza A subtypes have become established in pigs: H1N1, H3N2, and H1N2 viruses. These swine viruses are antigenically and genetically different from their counterparts circulating in humans. Nevertheless, signs of disease in pigs are similar those observed in humans and include

nasal discharge, coughing, fever, breathing difficulties and conjunctivitis. Due to their susceptibility to infection by both human and avian IAVs, pigs are considered a mixing vessels for avian and human influenza A virus genes (Myers et al., 2007; Van Reeth, 2007) (Figure 9). Thus pigs can contribute to mammalian adaptation of avian influenza viruses or to the generation of new reassortant viruses between avian and human influenza strains that have the potential to cause pandemics (Brown, 2000).

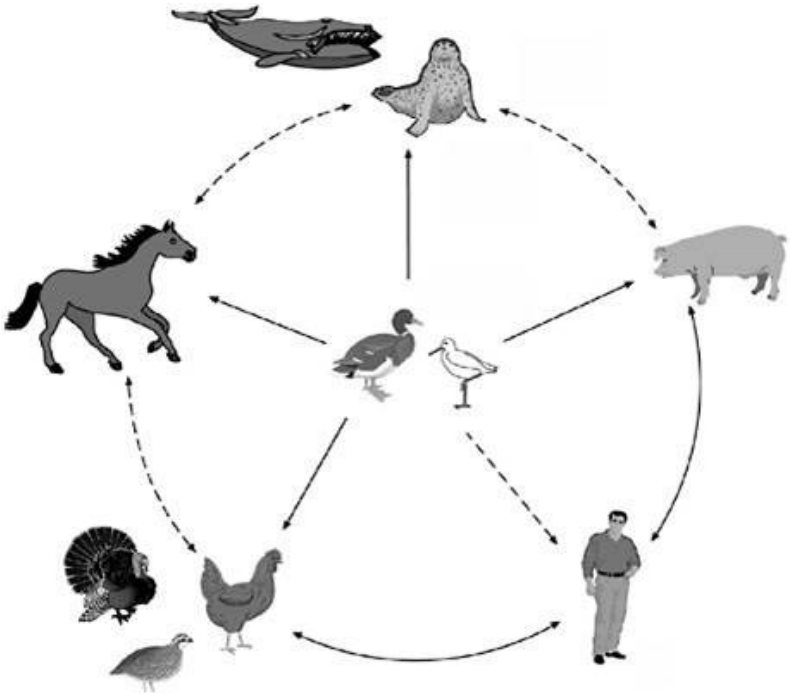

Figure 9. The reservoir of influenza A viruses (Institute of Medicine (US) Forum on Microbial Threats, 2005). *Wild aquatic birds are the reservoir of influenza viruses for avian and mammalian species. Transmission of influenza has been demonstrated between pigs and humans and between chickens and humans (solid lines) but not between wild birds and humans (dotted lines).*

1.4.5 Replication cycle.

1.4.5.1 Cell binding, entry and uncoating.

Hemagglutinin (HA) is the major viral glycoprotein that exerts two main functions: (i) receptor binding and (ii) host membrane fusion. HA is a trimeric transmembrane glycoprotein (three 84-KDa subunits), in which each subunit consists of two disulfide-linked glycopolypeptides, HA1 (58 kDa)

and HA2 (26 KDa) (Doms and Helenius, 1986). The two subunits, HA1 and HA2, are generated from the precursor HA0 by proteolytic cleavage, which is exerted during the replication cycle by different host proteases depending on the amino acid composition of the cleavage site (see paragraph 1.4.4.1).

The cleavage of HA0 is required to allow the structural rearrangement of HA1 and HA2 subunits activating both the binding and fusion functions. Most of the HA1, involved in the binding process, folds into a globular domain containing the receptor binding site (RBS) at the top of the molecule; while the HA2, bearing the fusion peptide at its N-terminus, forms the stalk that projects the glycoprotein outward from the surface of the virus (Figure 10).

IAV infection is initiated via viral attachment mediated by HA proteins binding to sialic acid (SA) (N-acetylneuraminic acid) linked to sugars on the tips of host cell glycoproteins. The binding interactions are very weak, and high avidity is achieved by multiple bonds between HA molecules on the virus and SA receptors on the target cell (Matrosovich et al., 2009). After the binding, IAV entry and uncoating within the cells occurs exploiting the endocytic pathway (Figure 10). To achieve delivery of the viral genome into the cytoplasm, vRNPs must disconnect from the M1 layer and the viral shell must open up to the cytoplasm via membrane fusion (Bui et al., 2000; Martin and Helenius, 1991; Skehel and Wiley, 2000). Both membrane fusion and uncoating of influenza virus are driven by the low endosomal pH through two distinct steps involving different endosomal intermediates (Li et al., 2014). The first step, in early endosomes (EE), depends on the activity of the influenza virus M2 protein, which is a proton-selective ion channel protein present within the viral envelope (Schnell and Chou, 2008; Sugrue and Hay, 1991). In the EE (pH ~5.5–6.0), M2 begins to pump ions into the viral lumen acidifying the virus interior and allowing disruption of the M1-vRNP interaction and weakening of the M1 layer (Li et al., 2014). The dissociation of matrix proteins from the vRNPs has been shown to be important since otherwise M1 would down-regulate the nuclear import of vRNPs by directly inhibiting their binding to the nuclear pore complexes (NPCs) (Babcock

et al., 2004; Martin and Helenius, 1991). As the pH is further lowered in the late endosome (LE) (pH ~5.0–5.5), the dissociation of M1 from the viral bilayer permits conformational change of HA and, eventually, membrane fusion (Li et al., 2014). Indeed, in the LE the pH decrease leads the HA2 subunit, in which the N-terminus was hidden in the structure derived from the HA0 cleavage, to undergo a conformational change and to expose the fusion peptide. Once the fusion peptide is anchored in the endosome membrane the whole HA molecule can fold back allowing the merging of the two bilayers (Figure 10).

After fusion the viral genome, consisting of the eight vRNPs, is released in the cytoplasm by diffusion (Babcock et al., 2004). The vRNPs gain access to the nucleus through the nuclear pore complexes (NPCs) by interacting with soluble nuclear import receptors (importin α/β transport system), which mainly recognize nuclear localization signals (NLSs) on the viral nucleoprotein NP (Cros et al., 2005; O'Neill et al., 1995; Wang et al., 1997).

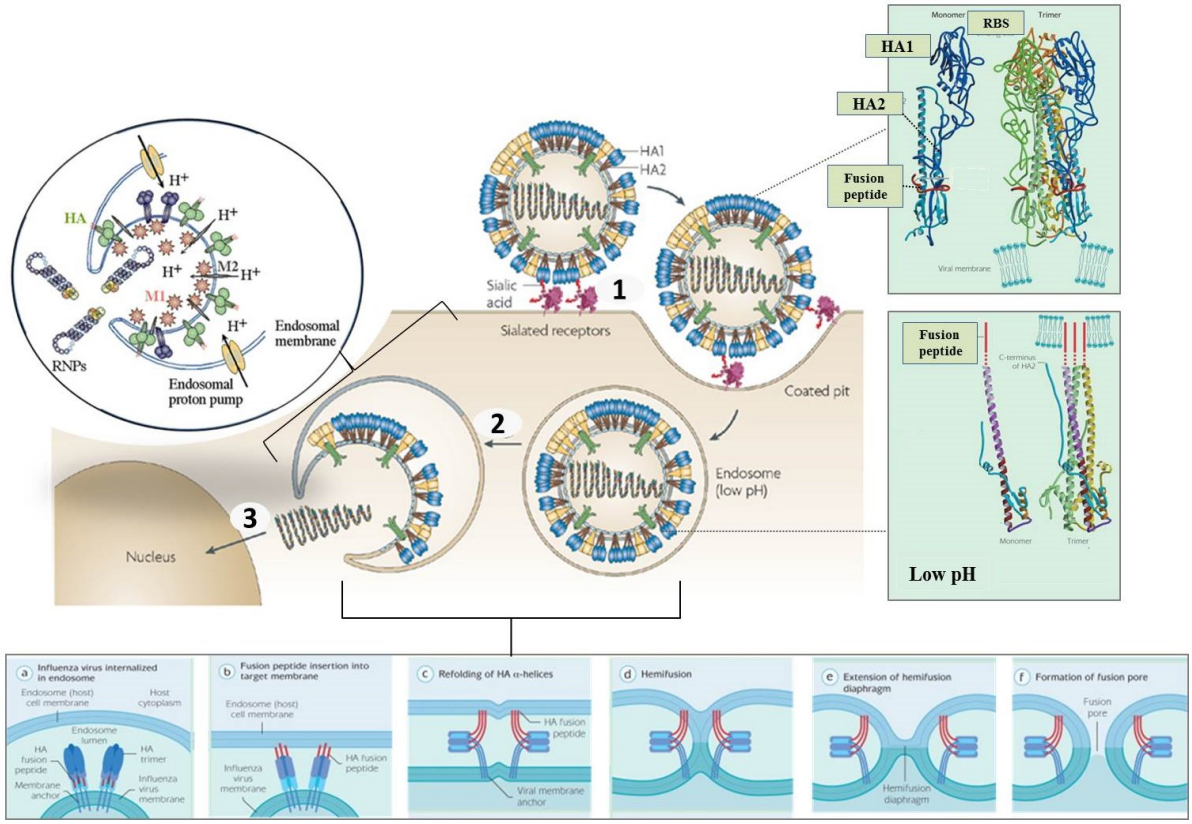

Figure 10. ***Influenza A virus binding, entry and uncoating.*** *IAV binds via haemagglutinin 1 (HA1) to terminal sialic acids present on glycoproteins or on glycolipids (step* ***1****). The virus is subsequently internalized by receptor-mediated*

*endocytosis into a low pH compartment (endosome). M2 ion-channel allows entry of H+ into the viral lumen decreasing the pH within the virion and triggering the dissociation of vRNPs from the Matrix protein (M1). As the pH is further decreased, HA2 undergoes a conformational changes that expose the viral fusion peptide and allow the fusion of the virus envelope with the endosomal membrane (step **2**). Subsequently, the genomic ribonucleoprotein complex is transported to the nucleus to initiate transcription and replication of the viral genome (step **3**). Adapted from* (Bullough et al., 1994; Cross et al., 2001; Karlsson Hedestam et al., 2008; Weis et al., 1990).

1.4.5.2 Genome transcription and replication.

IAV transcription is initiated with the synthesis of positive-sense viral mRNAs(+) from the negative-sense viral genome (vRNAs-) (Figure 11A). As for cellular mRNAs, IAV transcripts require a 7-methylguanylate cap (m^7G) at the 5' terminus to promote nuclear export, to avoid degradation and to bind the ribosome for protein translation. Thus, viral mRNAs synthesis is primed using stolen fragments of cellular capped pre-mRNAs which are bound by the viral PB2 subunit (Guilligay et al., 2008; Ulmanen et al., 1983) and then cleaved by the endonucleolytic domain of the polymerase subunit PA (Dias et al., 2009; Yuan et al., 2009) in a process called "cap snatching". Conversely, polyadenylation of IAV mRNAs is independent of cellular 3'-end processing factors (Hay and Skehel, 1979; Plotch and Krug, 1977) as all eight vRNA segments contain a stretch of uridines (U's) near the 5' end which correspond to the polyadenylation site in viral mRNAs (Li and Palese, 1994; Robertson et al., 1981).

The mature mRNAs generated from virus genome transcription exit the nucleus by recruiting the cellular nuclear export factor 1 (NXF1) through factors binding to the 5' cap structure or the 3' poly(A) tail (York and Fodor, 2013) and then undergo translation using the host cell machinery. Once expressed, the proteins are sorted based on their localization signals. While HA and NA signal peptides guide these glycoproteins to the plasma membrane, several of the viral proteins are targeted back into the nucleus by cellular NLS-mediated pathways. Nuclear import is observed for the three polymerase proteins (PB2, PB1 and PA) and NP, as well as for the matrix M1 protein, the non-structural NS1 protein and the nuclear export protein NEP (Smith et al., 1987) (Figure 11A).

The replication of the negative-sense IAV genome is a two-step process: (i) first a complementary positive-sense copy (cRNA+) of the vRNA- is produced and then (ii) the cRNA associates with NP and the polymerase complex to form a complementary ribonucleoprotein (cRNP) which directs the synthesis of a new vRNA- (Figure 11A). Although viral cRNAs and mRNAs are both positive strands derived from the same template, the fact that cRNAs do not present 5'cap and are full-length copies (including untranslated regions UTR) of the vRNA molecules (Park et al., 2003) suggests the existence of two distinct mechanisms to produce these RNAs (Jorba et al., 2009). Therefore, a proper timing between transcription and replication is of paramount importance for efficient virus production. To this end a major role in the regulation of the polymerase activity has been ascribed to the influenza nuclear export protein (NEP) (Bullido et al., 2001; Manz et al., 2012; Robb et al., 2009). Previous publications showed that the expression of NEP during the replication cycle can regulate the accumulation of viral RNA species, leading to a switch from viral transcription during early viral replication to production of new vRNPs (Manz et al., 2012; Robb et al., 2009) (Figure 11A). The importance of NEP in the regulation of viral replication was also emphasized by the observation that adaptive mutations within its N-terminus enhance the polymerase activity of avian polymerases in mammalian cell cultures (Manz et al., 2012). Beside NEP, the presence of 22 to 27 nucleotides long small viral RNAs (svRNAs), synthesized from the 3' end of cRNAs and corresponding to the 5' ends of genomic vRNAs, has been associated with the switch from mRNA transcription to genome replication (Perez et al., 2010). Functional characterization indicates that svRNAs directly interact with the PA subunit and could provide a segment-specific guide for the viral polymerase to the cRNA templates, thereby promoting synthesis of genomic vRNAs which in turn will generate new vRNPs (Perez et al., 2012).

The newly synthesized viral ribonucleoprotein complex (vRNP) is exported from the nucleus at late stage of infection. The current model of vRNP nuclear export implicates both the viral matrix protein M1 and the viral nuclear export protein NEP as crucial co-factors (Martin and Helenius,

1991; O'Neill et al., 1998). In this so called ‘‘daisy-chain’’ model the C-terminus of matrix protein (M1) binds strongly to the vRNP through interaction with NP (Baudin et al., 2001). Next the C-terminus of NEP binds to the nuclear localization signal (NLS) on the N-terminal domain of the viral matrix protein M1 (Akarsu et al., 2003; Shimizu et al., 2011; Yasuda et al., 1993). Finally, the β-importin Crm1 (chromosome region maintenance 1, also referred to as exportin1 or Xpo1) binds the N-terminal domain of NEP, and together with its cofactor GTPase Ran (Neumann et al., 2000) mediates nuclear export of the vRNP though the nuclear pore complex (NPC) (Figure 11B).

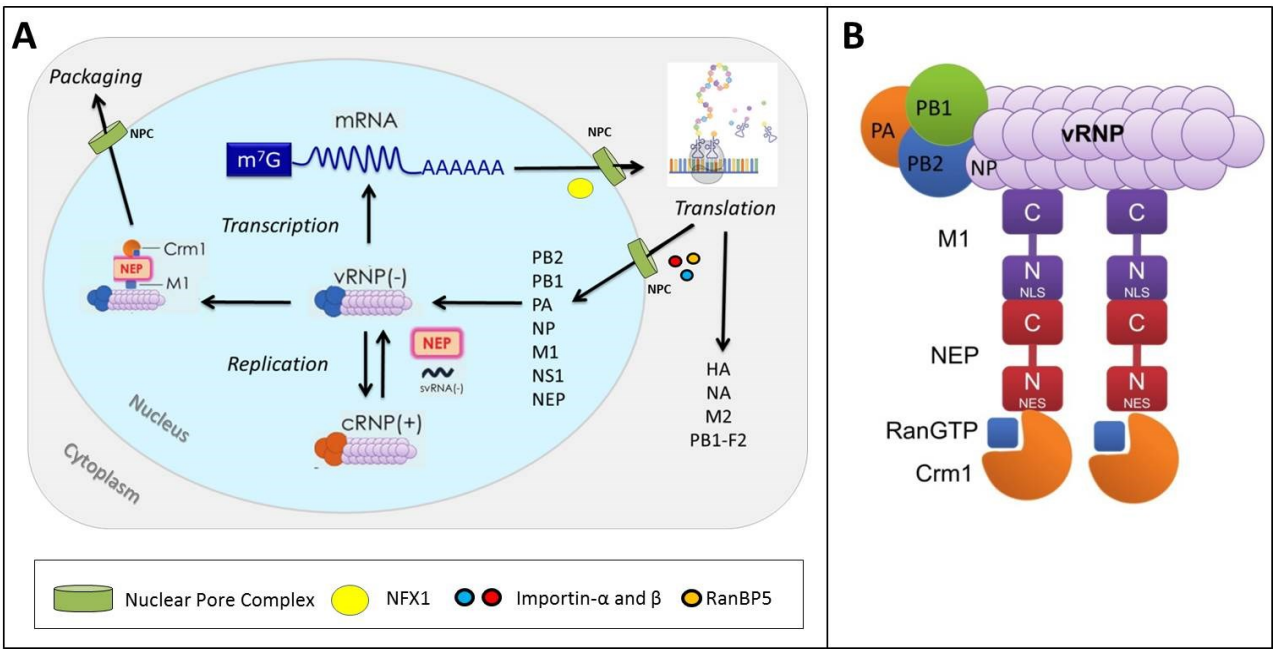

Figure 11. ***Influenza A virus genome transcription, replication and nuclear export.*** *A) The transcription and replication of influenza vRNPs. B) The daisy chain model for NEP-mediated nuclear export of influenza virus vRNPs. Crm1 mediates nuclear export of the vRNP complex by binding to the N-terminal domain of NEP, as well as to its cofactor, the small GTPase Ran. The C-terminus of NEP binds to the nuclear localisation signal (NLS) on the N-terminal domain of the viral matrix protein M1. The C-terminus of M1 in turn binds strongly to the vRNP through interaction with NP. Adapted from* (Paterson and Fodor, 2012).

1.4.5.3 Virus packaging and budding.

Two models were originally proposed for the incorporation of the eight vRNPs into infectious IAV particles: the random incorporation model and the selective incorporation model (Hutchinson et

al., 2010) (Figure 12A). The random incorporation model, where the virus discriminates the vRNAs against cRNAs and other cellular RNAs but does not selectively incorporate one copy of each of eight segments into the new virion, implies the existence of a common feature in all the vRNAs. However, recent publications support the selective packaging model of the IAV segmented genome, which, beside common features, predicts also the existence of segment-specific signatures in each vRNA (Hutchinson et al., 2010).

In the selective model, the packaging machinery must: (i) discriminate vRNAs embedded in vRNPs from positive-sense RNAs, which include viral cRNAs also packed into complementary RNPs (cRNPs), viral mRNAs and cellular RNAs; and (ii) discriminate between the eight vRNAs to ensure packaging of a complete and functional set of viral segments (Gerber et al., 2014).

To discriminate vRNAs from all the other nonviral RNAs, signals that are common to all influenza A vRNAs are required. Sequences that match this criterion are the conserved U12 and U13 sequences, which are located at the extreme termini respectively of 3' and 5' non coding regions (NCRs) of each vRNA segment and are selectively recognized by the viral polymerase (Arranz et al., 2012; Moeller et al., 2012). U12 and U13 sequences has been shown to permit incorporation of the vRNAs into virus-like particles (VLPs) (Luytjes et al., 1989; Muramoto et al., 2006).

Nuclear export might also represent an important step in discriminating vRNAs as, unlike 5' capped cellular RNAs and viral mRNAs, vRNPs are exported from the nucleus via a Crm1-dependent pathway (Hutchinson and Fodor, 2013). Discrimination between vRNAs and their positive-sense copy cRNAs may also rely on nuclear export since cRNPs are not exported from the nucleus due to a single bulged nucleotide in the cRNA termini, which determines differential recognition from viral polymerase and consequent variation in its conformation while bound to them (Tchatalbachev et al., 2001). Therefore, nuclear export together with U12 and U13, and possibly with the polymerase complex, could achieve the first level of selectivity.

The second level of recognition in the selective packaging appears to be carried out by both specific vRNA segment signatures and cytoplasmic trafficking. The transport of influenza vRNPs from the perinuclear region to the apical plasma membrane involves the Rab-11 positive recycling endosome system (van Ijzendoorn, 2006) together with an intact microtubule-organising centre (MTOC) for membrane targeting (Amorim et al., 2011; Avilov et al., 2012; Eisfeld et al., 2011; Momose et al., 2011) (Figure 12B). Recent publications propose that, during late stage of infection, Rab-11 positive vesicles could serve as platforms for the vRNAs travelling in the cytoplasm to gather in close proximity, allowing segment-specific packaging regions, spanning from the 3' and 5' NCRs to part of the coding regions, to interact and form a core of vRNPs (Chou et al., 2013; Goto et al., 2013). The core complex might be constituted by a limited number of vRNPs in a virus strain-dependent combination as suggested by recent data confirming that vRNAs are exported neither individually nor all together from the nucleus. Viral RNA subcomplexes then would be further assembled on their way to the plasma membrane (Lakdawala et al., 2014).

Influenza A viruses, like several other enveloped viruses, assemble and bud in the ''budozone'' (Schmitt and Lamb, 2004; Simons and Ikonen, 1997; Takeda et al., 2003; Zhang et al., 2000), which is a large, stabilized, liquid ordered, cholesterol-/sphingolipid-enriched domain in the plasma membrane normally implicated in membrane traffic and signal transduction. These microdomains, commonly called "lipid rafts" or "detergent-insoluble glycolipid-enriched complexes" (DIGs) (Rossman and Lamb, 2011; Schmitt and Lamb, 2005; Veit and Thaa, 2011), are targeted by influenza HA and NA glycoproteins via their transmembrane domains (TMD) (Barman and Nayak, 2000; Kundu et al., 1996; Scheiffele et al., 1997; Zhang et al., 2000). Lipid raft targeting appears a strategy to concentrate sufficient HA and NA proteins on the virus' surface to guarantee efficient receptor binding, viral fusion and spread (Takeda et al., 2003).

The viral M2 proton channel, the third viral transmembrane protein, is present in lower amount on the virion's surface compared to HA and NA as it does not associate with lipid rafts when expressed

in the absence of other viral proteins (Thaa et al., 2010; Zhang et al., 2000). Nevertheless, M2 has been shown to cluster with HA in the plasma membrane independently of other virus proteins (Thaa et al., 2010) resulting in localization at the periphery of lipid raft which in turn will constitute the edge of the viral budding site (Thaa et al., 2011).

The localization of the vRNA segments at the budozone level on the plasma membrane is driven by association of the viral matrix protein M1, bound to the newly synthesized vRNP (see paragraph 1.4.5.2), to the cytoplasmic tails (CT) of HA, NA (Barman et al., 2001; Jin et al., 1997), and M2 (Chen et al., 2008; Wang et al., 2010).

Upon assembly of all viral components in the budozone, budding proceeds by membrane bending and ultimately scission of the nascent virus particle is mediated by the viral transmembrane protein M2, which localizes to the base of growing filamentous viruses (Rossman et al., 2010a; Rossman et al., 2010b) and inserts its amphiphilic helix into the membrane to modify membrane curvature (Rossman et al., 2010b).

Finally, influenza NA glycoprotein removes sialic acid from host cell glycol-conjugates and newly synthesized viral proteins allowing the release of the virions from the cell surface and preventing aggregation of the virus particles (Liu et al., 1995).

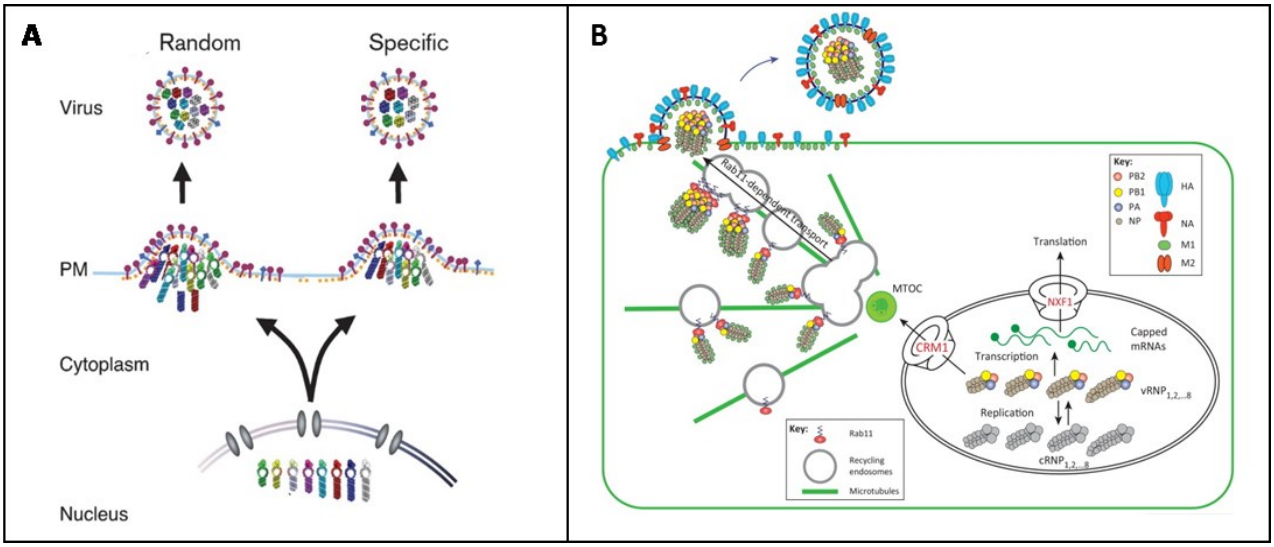

Figure 12. ***Influenza A virus packaging and budding.*** *A) Influenza virus random and selective models for genome packaging. B) Transport, selection, and packaging of vRNPs. Unlike viral and cellular mRNAs, vRNPs are exported via a*

CRM1-dependent pathway; cRNAs are incorporated into cRNPs that are not exported out of the nucleus. In the cytoplasm, vRNPs concentrate close to the microtubule organizing centre (MTOC). They bind recycling endosomes via Rab11 and migrate along the microtubule network. Several vRNP species migrate together, and this process might favour the formation of a supramolecular complex held together by base pairing between vRNAs. Adapted from (Gerber et al., 2014; Hutchinson et al., 2010).

1.5 Host defense mechanisms and influenza A virus countermeasures.

1.5.1 The RIG-I like receptor (RLR) pathway.

The innate immune system is a first line of defence against pathogen infection. The response to infection by the innate immune system of mammals is initiated with the detection of pathogen associated molecular patterns (PAMPs) by host pattern recognition receptors (PRRs). Viral RNA can be recognized on the cell surface and in the endosome by membrane-bound Toll-like receptors (TLRs) or in the cytoplasm by the cytosolic RIG-I-like receptors (RLRs). The latter group of receptors includes the retinoic acid inducible gene 1 (RIG-I, also known as DDX58) and the melanoma differentiation associated antigen 5 (MDA5, also known as IFIH1 or Helicard) (Kawai and Akira, 2006; Seth et al., 2006). RIG-I and MDA5, which belong to the superfamily 2 (SF2) helicases or ATPases (Gorbalenya et al., 1988; Hopfner and Michaelis, 2007), display a unique domain structure, consisting of two N-terminal caspase activation and recruitment domains (CARDs), a central SF2 type DECH box ATPase domain, and a C-terminal regulatory domain (CTD or RD) (Cui et al., 2008). Despite similarity in their structure, the two helicases sense different viruses (Kato et al., 2006; Schlee, 2013) as they recognize diverse viral RNA patterns. Indeed, while MDA5 detects long double-stranded RNAs (more than 2 kb), RIG-I recognizes short 5′ triphosphate (5′-ppp) dsRNAs (up to 1 kb) (Kato et al., 2008; Schlee et al., 2009; Schmidt et al., 2009) including those belonging to influenza A viruses. Although the partially complementary 5′- and 3′-ends of influenza virus ssvRNA form a short double stranded structure, called the “panhandle” (Hsu et al., 1987), the major PAMP detected by RIG-I is the 5′-ppp (Hornung et al., 2006; Pichlmair et al., 2006) which arises during

replication and is absent in cellular cytosolic RNAs due to cleavage or capping modifications (Fromont-Racine et al., 2003; Shatkin and Manley, 2000; Singh and Reddy, 1989).

The exact mechanism at the basis of RIG-I/vRNA recognition and signal transduction is still debated; however different studies involving crystal structure analysis and NMR identified a basic binding cleft within the CTD of RIG-I (amino acids 802–925) as the crucial 5'-pppRNA binding structure that determines ligand specificity. Based on these studies, the binding of the 5'ppp-dsRNA to the CTD would induces a conformational change in the enzyme which would allow the displacement of the N-terminal auto-inactivated CARDs from binding to the DECH box domain (Cui et al., 2008; Kolakofsky et al., 2012; Takahasi et al., 2008).

Once exposed the amino-terminal CARDs of RIG-I undergo robust Lys63-linked ubiquitination on Lys172 by tripartite motif 25 (TRIM25) ubiquitin E3 ligase (Gack et al., 2007) (Figure 13). The ubiquitination of CARDs activates RIG-I, which then rapidly binds the N-terminal CARD-like domain of the mitochondrial antiviral signalling protein MAVS (also called IPS-1, Cardif or VISA) on the mitochondrial membrane (MM). This interaction induces MAVS to recruit other MAVS molecules on the mitochondrial surface to form larger polymers (Hou et al., 2011). MAVS-mediated antiviral signalling is propagated through assembly of a MAVS "signalosome" containing TRAF3, TRAF6, TRAF family member-associated nuclear factor κB (NF-κB) activator (TANK), and TNFR1-associated death domain protein (TRADD). The formation of a MAVS signalling complex results in the phosphorylation and nuclear translocation of interferon regulatory factor 3 and 7 (IRF3 and IRF7) by TANK binding kinase 1 (TBK1) and/or IKKε, as well as activation of NF-κB to induce expression of type I interferons (IFNs) and pro-inflammatory cytokines (West et al., 2011).

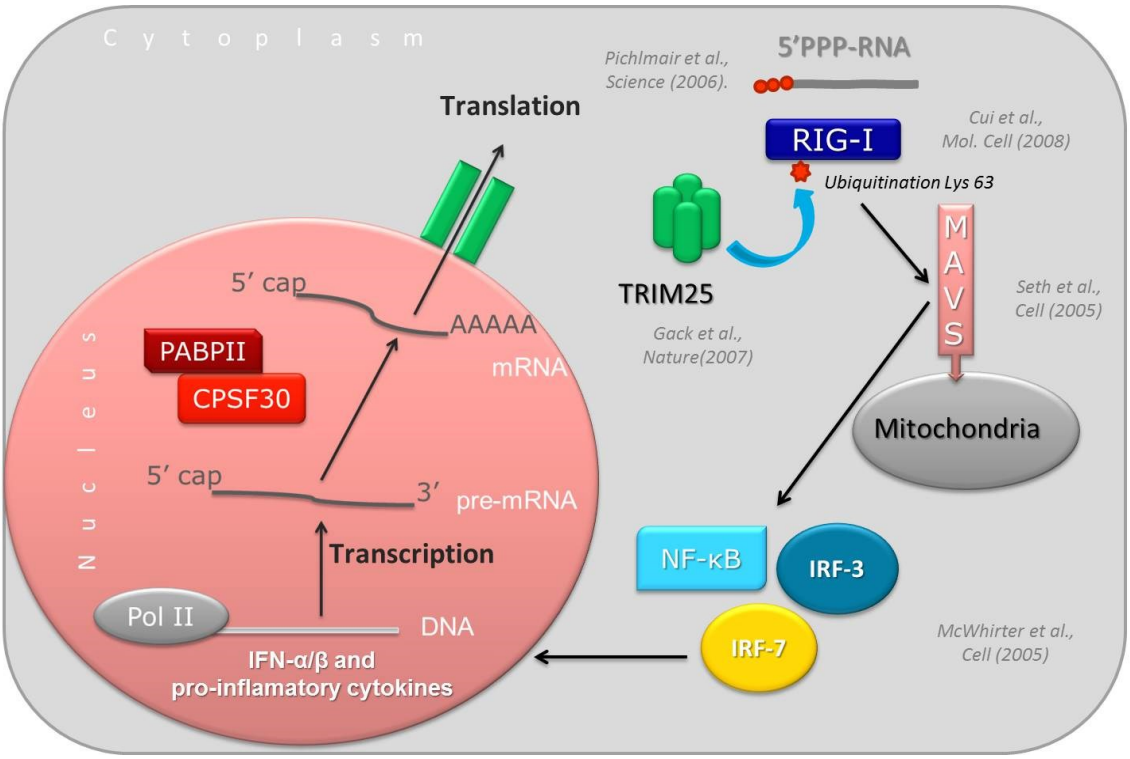

Figure 13. Schematic representation of RIG-I receptor pathway.

1.5.2 Interferon-stimulated genes (ISGs).

IFN-α or IFN-β, induced by the RLR pathway, are soluble cytokines that can act in both autocrine and paracrine manner to up-regulate the expression of more than 300 IFN-stimulated antiviral genes (ISGs) (Randall and Goodbourn, 2008a).

A key regulator of antiviral activities induced by IFN is the **Protein kinase RNA-activated** (**PKR**). In non-stimulated cells, PKR is present at a basal level that can vary depending on the tissue type and the degree of differentiation. However, IFN expression up-regulates the levels of PKR, allowing a robust response to a viral infection (Kuhen and Samuel, 1999). Human PKR is a latent serine/threonine kinase of 551 amino acids with two consecutive *N*-terminal dsRNA-binding motifs, a linker domain, and a *C*-terminal kinase domain (Meurs et al., 1990). Activation of PKR requires binding to dsRNA (Gabel et al., 2006) or, alternatively, to ssRNA molecules presenting internal dsRNA structure (Dauber et al., 2009; Katze et al., 1987) (Figure 14A). The binding to dsRNA leads to auto-phosphorylation of PKR on multiple sites (Galabru and Hovanessian, 1987; Samuel, 2001) and

its subsequent dimerization. PKR dimer blocks cellular and viral protein synthesis by phosphorylating the α subunit of the Eukaryotic Initiation Factor 2 (eIF2α) (Farrell et al., 1977) required for the initiation of translation (Samuel, 1993); thus playing a central role in host defence against viral infection (Gale and Katze, 1998).

Other key ISGs important in the antiviral state stimulated by IFN expression include the **human 2'-5'-oligoadenylate synthetases (OAS)** family, consisting of *OAS1*, *OAS2*, *OAS3*, and *OASL* (Baglioni et al., 1978). OAS proteins are synthesized in an inactive form and binding to viral dsRNA triggers their allosteric activation (Figure 14B). Active OAS oligomerizes ATP through an unusual 2'-5' phosphodiester linkage, generating 2'- 5'-oligoadenylates [2-5A or pppA(2'p5'A)n] which in turn binds to and activates the Latent RNase (RNase L). Upon activation, RNase L dimerizes and begins to degrade all RNAs within infected cells, both viral and cellular (Clemens and Williams, 1978; Dong and Silverman, 1997), thus preventing protein translation and shutting down viral replication.

Among the many antiviral factors upregulated by IFNs, the dynamin-like large GTPase Mx proteins expressed from the ***myxovirus resistance gene*** **(MX1)** are key effector molecules inhibiting different RNA viruses in many species (Haller et al., 1980; Haller et al., 2010; Haller and Kochs, 2011). With respect to IAV the murine Mx1 protein, present in the majority of wild type mice but mutated and functionally absent in most inbred laboratory strains (Haller et al., 1987; Staeheli et al., 1988), accumulates in the cell nucleus and inhibits virus primary transcription by targeting the viral ribonucleoprotein complex to degradation pathways (Haller and Kochs, 2002). In contrast to the murine counterpart, human MxA protein localizes in the cell cytoplasm in association with the smooth endoplasmic reticulum (ER) (Figure 14C). This localization has been shown to confer MxA the ability to exert its antiviral effect before virus primary transcription by preventing the input vRNPs from being transported into the nucleus (Matzinger et al., 2013; Xiao et al., 2013). A current model proposes that, upon viral infection, MxA recognizes the incoming vRNPs and starts to self-

assemble into rings around the viral nucleocapsid structure, resulting in a higher-order oligomeric complex that prevents vRNPs from entering the nucleus (Gao et al., 2011).

The identification and functional characterization of other ISGs that control influenza virus replication such as the recently described IFITM3 gene (Everitt et al., 2012), are a matter of current research in several laboratories.

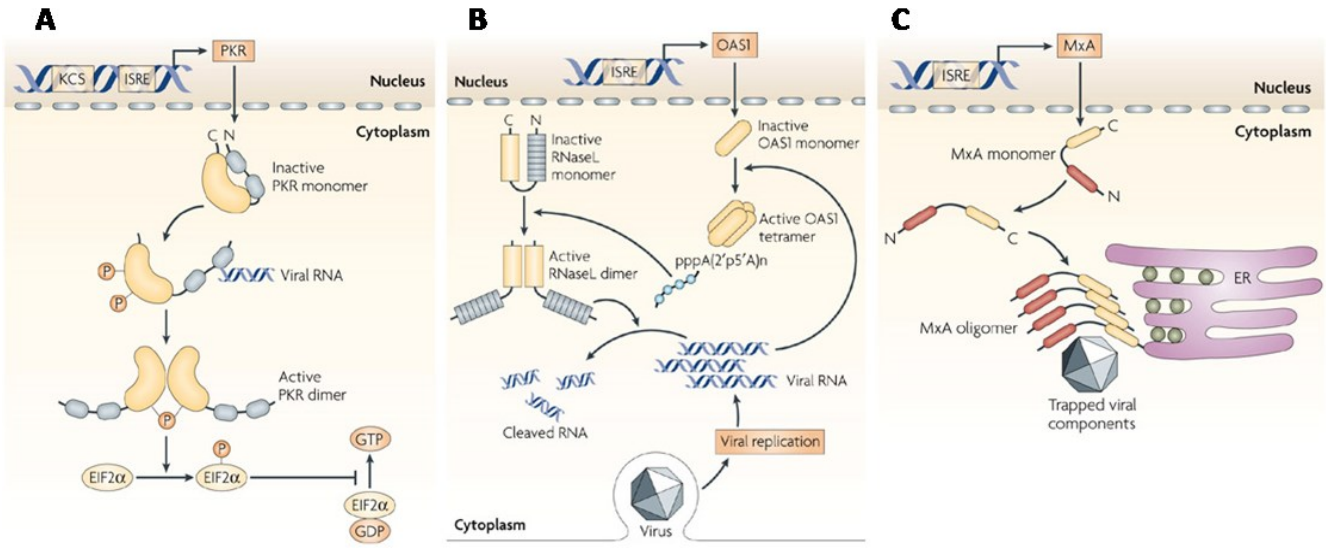

Figure 14. ***Activity of selected interferon stimulated antiviral genes (ISGs).*** *A) Protein kinase RNA-activated (PKR), B) 2',5'-oligoadenylate synthetase 1 (OAS1), C) MxA protein. Adapted from* (Sadler and Williams, 2008).

1.5.3 Apoptosis.

Apoptosis or programmed cell death is a highly regulated natural process of eliminating unwanted, redundant, or damaged cells from an organism without eliciting a major host inflammatory and/or immune response. Morphologically, cells are subject to cytoplasmic shrinkage, plasma membrane blebbing, DNA fragmentation, and chromatin condensation. Finally, the cells form cell fragments, termed apoptotic bodies, and are removed by phagocytic cells. The main difference from necrosis is the absence in the extracellular environment of constituents of the dying cells, which can induce unwanted inflammatory response (Raff, 1998).

Apoptosis is triggered through two signalling pathways: the intrinsic pathway (also known as the mitochondrial pathway) and the extrinsic pathway (also known as the death receptor pathway) (Figure 15).

The intrinsic pathway can be triggered by any stimulus that causes oxidative stress, DNA damage or mitochondrial disturbances. The involvement of the mitochondria in apoptosis first came to light when it was discovered that one of the critical factors required for the activation of programmed cell death was cytochrome *c* (cyt *c*) (Li et al., 1997). Indeed, mitochondrial damage can cause permeabilization of the outer mitochondrial membrane which facilitates cyt *c* release into the cytoplasm (Figure 15). Once released, cyt *c* binds the caspase adaptor protein Apaf-1 (apoptotic protease-activating factor-1), which then activates procaspase 9 forming a complex termed the "apoptosome". This complex in turn activates several downstream effector caspases, such as caspases 3, 6 and 7, leading to DNA fragmentation and cell death (Iannolo et al., 2008; Oliver and Vallette, 2005).

In contrast to the intrinsic pathway, the extrinsic pathway is induced by ligand binding to death receptors (Figure 15). The ligand-death receptor system includes different receptors such as the tumour necrosis factor receptor 1 (TNF-R1), the Fas ligand-Fas receptor (also known as CD95) (Mollinedo and Gajate, 2006) or TRAIL-TRAIL receptor (including TRAIL-R1, also termed DR4, and TRAIL-R2, also termed DR5). Binding of respective ligands leads to receptor oligomerization and recruitment of death signal adaptor proteins. Fas ligand (Fas-L) binding on the outer cellular membrane, for example, leads to Fas receptor oligomerization and a subsequent conformational change which activates its cytoplasmic death domains to recruit FADD protein (Fas-associated protein with death domain) (Iannolo et al., 2008) (Figure 15). Recruitment determines activation of FADD N-terminal death effector domain (DED) and consequent enrolment and activation of procaspase 8. The oligomerized receptors together with the recruited FADD and the initiator active

caspases 8 form a complex termed DISC (death-inducing signalling complex) which propagates the signal by activating effector caspases 3 and 7, hence leading to apoptotic events.

During the last decade it has become clear that, besides playing an important role in the development and maintenance of tissue homeostasis, apoptosis is also important for preventing or limiting viral replication during infections. Two types of virus-host interactions should be considered in this respect. First, apoptosis may be induced in infected cells by the endocrine or intrinsic pathway. Second, infected cells may trigger paracrine or extrinsic apoptosis in non-infected neighbouring cells through release of signalling molecules, such as IFNs (Zhirnov and Klenk, 2007). Indeed, another important function of IFNs is to establish a pro-apoptotic state in target cells, which can help to restrain the infection. Both IFN-α and IFN-β have been shown to be capable to induce apoptosis in various systems, although whether their effect is mainly exerted via extrinsic or intrinsic pathway is still unclear (Barber, 2001; Clemens, 2003; Randall and Goodbourn, 2008b). Probably it would involve both, as suggested by the different mechanisms proposed for PKR (Balachandran et al., 1998) and OAS (Ghosh et al., 2001) triggered cell death in response to viral infections.

Regardless of the pathway involved, the central players in the unfolding of apoptotic events are the caspases. These cysteine-dependent, aspartate-specific family of proteases, which are normally expressed as inactive precursors (zymogens) in the cytoplasm, are activated by proteolytic cleavage immediately downstream the two independent initiator pathways (Taylor et al., 2008). Activation of the effector caspases triggers different events, which can vary in the timeline depending on cell line or tissue examined, apoptosis-inducing agent, stimulus intensity and/or exposure time, but eventually they will determine an orderly cell death.

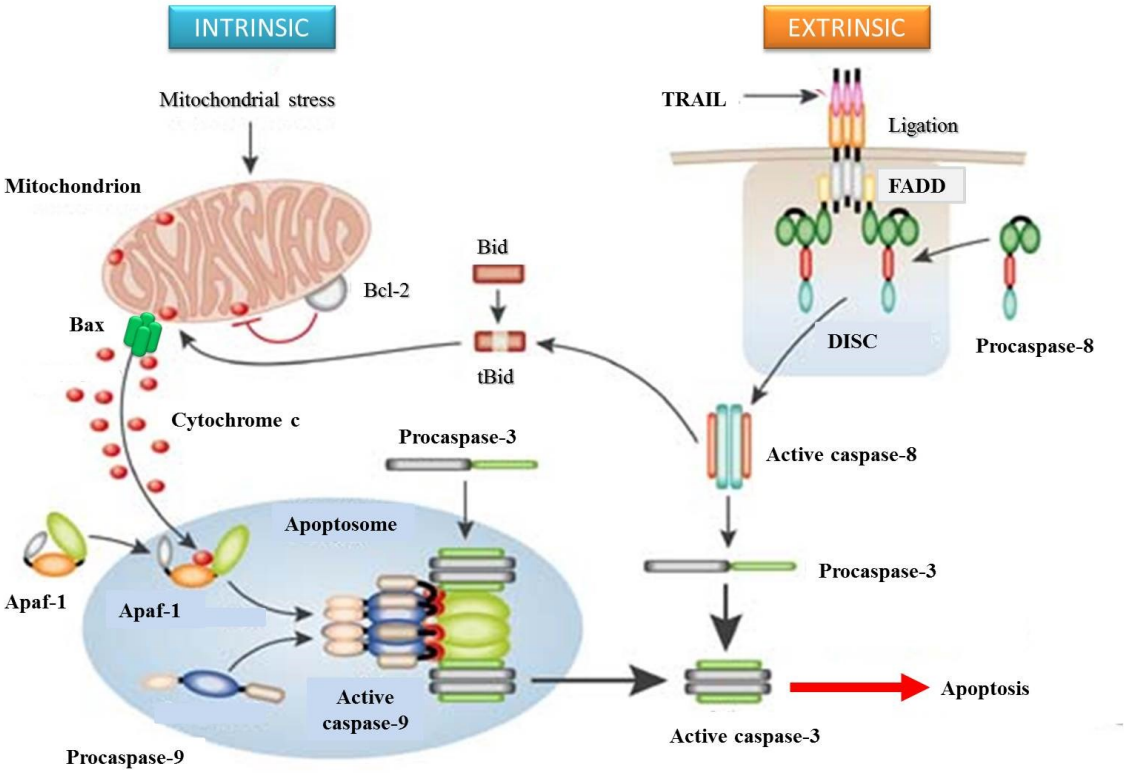

Figure 15. Schematic representation of the intrinsic (mitochondrial) and extrinsic (death receptor) apoptotic pathways. Adapted from (MacFarlane and Williams, 2004).

Different assays are available to detect and to study the biochemical changes that occur during apoptosis. The annexin V assay is based on morphological changes that occur in apoptotic cells. Under normal physiological conditions, a cell displays an asymmetric distribution of phospholipids in the two leaflets of the cellular membranes with phosphatidylserine (PS) facing the cytosolic side (Higgins, 1994). However, during the early stages of apoptosis this membrane asymmetry is rapidly lost, without concomitant loss of membrane integrity, resulting in externalization and exposure of PS on the outer leaflet of the plasma membrane, which serves as a label for recognition and subsequent removal of the dying cell by phagocytosis (van Engeland et al., 1998).

Annexin V is a 35-36 KDa phospholipid-binding protein, which was initially discovered for its strong anticoagulant properties (Reutelingsperger et al., 1985). This protein binds to phospholipids in a Ca^{2+} dependent manner (Raynal and Pollard, 1994), presenting higher preference for phospholipid

species such as PS, (Andree et al., 1990), while displaying minimal binding to phospholipid species such as phosphatidylcholine and sphingomyeline constitutively present in the outer leaflet of plasma membrane. Thus, fluorescein labelled annexin V represents a powerful probe to detect early apoptosis, characterized by PS externalization, in dying cells (Vermes et al., 1995).

DNA fragmentation is another key feature of apoptosis. The enzyme responsible for this fragmentation is the Caspase-Activated DNase (CAD), which is normally inhibited by another protein, the Inhibitor of Caspase Activated DNase (ICAD), in non-apoptotic growing cells. However, during apoptosis, the effector caspase 3 cleaves ICAD causing CAD activation (Enari et al., 1998). Because the double-stranded DNA of the nucleosomes is tightly complexed with the core histones and is thus protected from cleavage by CAD, the active endonuclease can only exert its activity at the most accessible internucleosomal linker region, generating mono- and oligonucleosomes bearing DNA fragments which are roughly discrete multiples of 180-bp (360, 540 etc.) (Skalka et al., 1976). This effect can be used to reveal apoptosis either via DNA laddering (Wyllie, 1980) on agarose gels or via enzymatic immunoassay detection of cytoplasmic histone-associated DNA fragments several hours before plasma membrane breakdown (Duke and Cohen, 1986; Terui et al., 1995).

Poly [ADP-ribose] polymerase 1 (PARP-1) cleavage is also a hallmark of caspase-dependent apoptosis (Aredia and Scovassi, 2014). Since apoptosis is an energy-dependent process (Wyllie et al., 1980), intracellular level of ATP is considered the crucial discriminant for activating the apoptotic pathway or dying through less regulated mechanisms, i.e. necrosis (Nicotera et al., 1998). In normal cells, genome integrity is assured in response to DNA damage/cellular stress by activation of PARP-1, which allows DNA repair by synthesizing poly(ADP-ribose) (PAR) through NAD consumption (Aredia and Scovassi, 2014). However, in cells undergoing apoptosis, PARP-1 activity would dramatically increase in the attempt to repair the damage caused by caspase-triggered DNA fragmentation. This would have a deleterious impact on cell metabolism, depleting the intracellular energy pool (Herceg

and Wang, 1999; Nicotera et al., 1998) required to support the ATP-consuming sequential steps of programmed cell death. Thus, during apoptosis caspase 3 and 7 inactivate PARP-1 by proteolytic cleavage. These proteases recognize and cleave a motif in the nuclear localization signal of PARP-1 separating a 24 KDa fragment (p24) zinc finger domain required for DNA binding from a 89 kDa fragment (p89), which includes the auto-modification domain and catalytic domain (Chaitanya et al., 2010; Lazebnik et al., 1994; Nicholson et al., 1995).

Cleaved PARP-1 protein fragments also inhibit any remaining functional PARPs by binding irreversibly to damaged DNA. The existence of this feed-back loop in caspase-mediated PARP-1 inactivation suggests that blocking PARP-1 activity is pivotal for the proper function of the apoptotic machinery.

1.5.4 Influenza A virus NS1-protein: antagonizing IFN-mediated antiviral response.

Influenza A virus NS1 protein is encoded on a collinear mRNA derived from vRNA segment eight, which upon splicing results in the synthesis of the nuclear export protein (NEP) mRNA (Lamb and Choppin, 1979). Both NS1 and NEP mRNA species share 56 nucleotides at the 5' end, resulting in NS1 and NEP proteins sharing 10 N-terminal amino acids (Lamb and Lai, 1980). In infected cells, the amount of spliced NEP mRNA was found to be only approximately 10% that of unspliced NS1 mRNA but this may vary depending on the strain (Lamb et al., 1980).

The NS1 protein has a strain-specific length of 219–237 aa (Hale et al., 2008), an approximate molecular mass of 26 kDa and it is notionally divided into two distinct functional domains: an N-terminal double-stranded RNA (dsRNA)-binding domain (RBD; aa 1-73) and a C-terminal effector domain (ED; aa 88-C teminus), which are connected via a short inter-domain linker region (LR) (Bornholdt and Prasad, 2008; Hale, 2014). Unlike NEP, NS1 protein is not considered a structural component of the virion, although recent proteomics analysis suggest it may in fact be present (Hutchinson et al., 2014). Nevertheless, NS1 is expressed at high levels in infected cells (Krug and

Etkind, 1973) where it exerts a plethora of different activities involved in regulation of viral RNA replication, viral protein synthesis, and general host-cell interaction (Hale et al., 2008). Despite its multiple activities, the major role ascribed to NS1 is to antagonize the host IFN-mediated antiviral responses at different levels. Although the IFN-antagonistic properties of NS1 proteins are strain-specific (Geiss et al., 2002; Hayman et al., 2006; Kochs et al., 2007), different studies demonstrated NS1 can limit IFN-β induction by pre-transcriptional and/or post-transcriptional mechanisms (Figure 16) .

Pre-transcriptional limitation of IFN induction occurs in the cytoplasm of infected cells and is performed by sequestrating viral RNAs from the cellular cytoplasmic pattern recognition receptor RIG-I (Donelan et al., 2003; Talon et al., 2000) and by blocking the multimerization of TRIM25, which is required for the ubiquitination and activation of RIG-I (see paragraph 1.5.1). Residues Arg-38 and Lys-41 within the NS1 RBD are mainly involved in pre-transcriptional limitation of IFN induction since a R38A/K41A mutant results defective both in sequestering viral RNA from molecular sensors and in suppressing TRIM25-mediated RIG-I ubiquitination (Donelan et al., 2003; Gack et al., 2009). However, a contribution in blocking TRIM25-triggered antiviral response has been also reported for residues E96 and E97 within the NS1 ED (Gack et al., 2009) (Figure 16). Interestingly in mouse cells, NS1 inhibited the activation of murine RIG-I in a TRIM25-independent manner by binding another ubiquitin E3 ligase called Riplet, which has also been shown important for RIG-I ubiquitination (Oshiumi et al., 2010; Rajsbaum et al., 2012).

Post-transcriptional limitation of IFN-β induction occurs in the nucleus and involves the C-terminal ED that binds directly to two zinc-finger regions in the 30 kDa subunit of Cleavage and Polyadenylation Specificity Factor (CPSF30) (Nemeroff et al., 1998; Noah et al., 2003; Twu et al., 2006) and interacts with Poly(A)-Binding Protein II (PABPII) (Chen et al., 1999). The NS1–CPSF30 complex prevents CPSF30 from binding cellular pre-mRNAs, thereby inhibiting normal cleavage and polyadenylation of the 3'- end of host-cell mRNAs (Nemeroff et al., 1998). Binding to CPSF30

appears to require Phe-103 and Met-106 as the influenza virus strain H1N1 A/Puerto Rico/8/34 (PR8) is unable to interact with CPSF30 due to amino acid substitutions in these positions (Kochs et al., 2007). Polyadenylation of influenza A virus mRNAs is independent of cellular 3'-end processing factors (see paragraph 1.4.5.2), therefore viral mRNAs are not affected by CPSF30 inhibition (Figure 16).

Besides limiting IFN expression in infected cells, NS1 can also directly block the functions of the cytoplasmic ISG antiviral proteins 2'-5'-oligoadenylate synthetase (OAS) (Min and Krug, 2006) and PKR (Li et al., 2006), which, as previously discussed (see paragraph 1.5.2), are key regulators of viral transcription/translation processes and play additional roles in other innate defences such as IFN induction and apoptosis (Garcia et al., 2006; Silverman, 2007). The RBD of NS1 protein out-competes OAS for interaction with dsRNA, thereby inhibiting this host antiviral strategy (Min and Krug, 2006), while NS1 interaction with PKR is suggested to occur in a RBD-independent manner, via residues 123–127 within the ED (Li et al., 2006; Min et al., 2007). In addition, the ED also interacts with other cellular proteins such as PI3K/Akt (Shin et al., 2007b) and Scribble (Liu et al., 2010) implicated in the apoptotic pathway.

Influenza A virus is a cytolytic virus that induces cell death in most cell types by apoptosis (Fesq et al., 1994; Hinshaw et al., 1994; Mori et al., 1995) and, only in certain cells, by necrosis (Arndt et al., 2002; Zhirnov and Klenk, 2003). Different publications suggest that the role of apoptosis in influenza virus replication can be seen from two perspectives. From one point of view apoptosis is seen as a host defence mechanism, which aims to limit virus replication (Barber, 2001; Kurokawa et al., 1999), on the other hand, apoptotic factors, such as caspase 3 and NF-kB/ Fas/Trail, promote influenza virus replication (Stray and Air, 2001; Wurzer et al., 2003; Wurzer et al., 2004). Therefore, a proper timing in apoptosis might be of paramount importance for virus replication. Accordingly, NS1 has been reported to have both anti and pro-apoptotic functions (Ehrhardt et al., 2007; Lam et al., 2008; Schultz-Cherry et al., 2001; Shin et al., 2007a; Stasakova et al., 2005; Zhirnov et al., 2002).

Indeed, the activation of the anti-apoptotic program early during infection eliminates an important defence mechanism of the host and, thus, provides conditions for efficient virus replication. Once this has been accomplished, apoptosis is up-regulated at the final stage of the viral life cycle to promote nuclear release of vRNPs and phagocytic clearance of infected cells, which might otherwise stimulate cell-mediated cytotoxic responses (Zhirnov and Klenk, 2007).

To interact with so many different host proteins and exert its multifunctional activity, NS1 has been suggested to adopt different quaternary conformations in infected cells on a concentration and spatial-dependent basis (Hale, 2014). Various papers report that at low concentrations NS1 protein is present as a dimer, which formation is likely mediated by the stable self-association between RBDs (Aramini et al., 2011; Kerry et al., 2011). However, at later time-post infection following increasing protein concentration, higher-order multimerization of NS1 can be observed (Aramini et al., 2011; Bornholdt and Prasad, 2008; Carrillo et al., 2014). Cell-based assays indicate that such multimerization is dependent upon the ED (Nemeroff et al., 1995) with the highly conserved tryptophan-187 (W187) exerting a crucial role (Aramini et al., 2014). This mutimerization have been proposed to enhance the NS1 affinity to dsRNA via cooperative binding of different monomers linked to one another by alternating stable RBD–RBD and ED–ED 'helix–helix' interactions (Hale, 2014). In line with spatial importance of dsRNA binding activity and concentration progression of NS1 protein, while dimers are mainly localized in the nucleus, higher-order multimerization occurs in the cytoplasm (Hale, 2014).

In addition to different quaternary structures, NS1 has also been shown to undergo post-translational modifications commonly occurring for different cellular proteins, such as phosphorylation and sumoylation of specific residues, which can affect in a strain-dependent manner protein interaction, protein activity and/or protein stability (Hsiang et al., 2012; Santos et al., 2013; Xu et al., 2011).

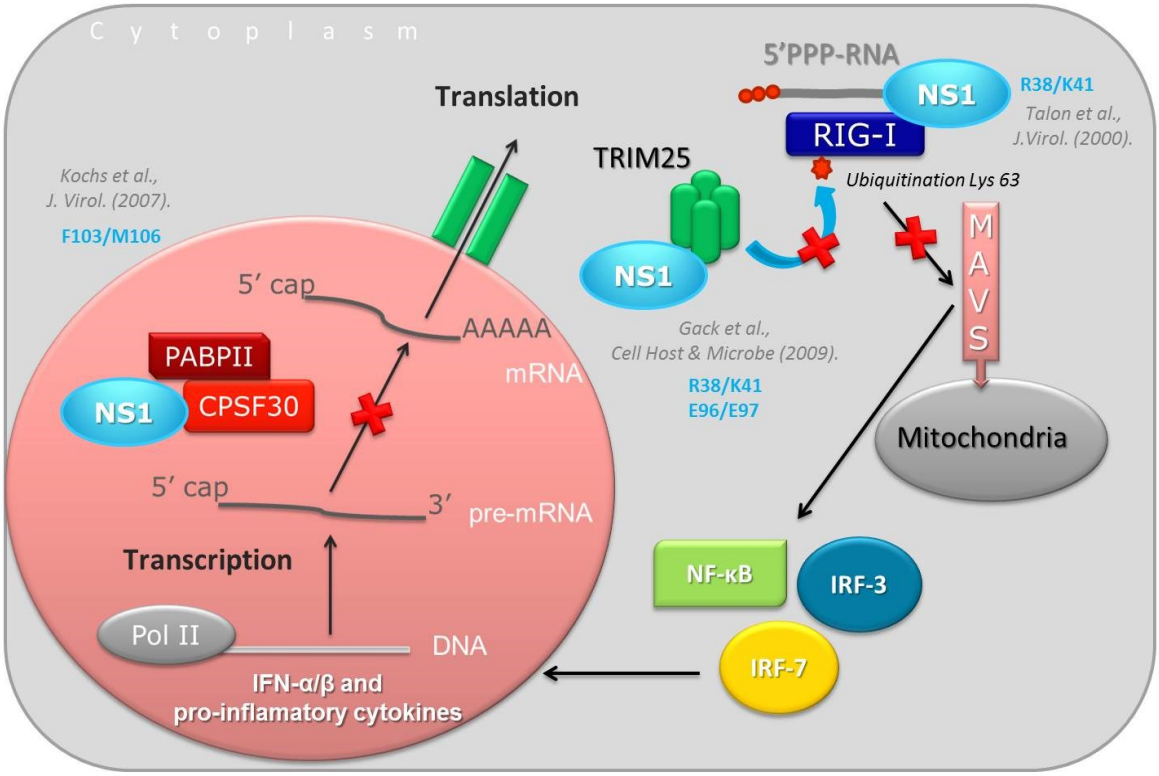

Figure 16. Influenza virus NS1 protein: pre- and post-transcriptional limitation of IFN expression in infected cells.

1.5.5 Influenza A virus PB1-F2 protein: apoptosis inducer.

As discussed in the previous paragraph, temporal regulation of both anti- and pro-apoptotic mechanisms is critical for the virus during its normal replication cycle. To counteract apoptosis during early infection, NS1 protein has been shown to modulate anti-apoptotic proteins (Liu et al., 2010; Shin et al., 2007b). However, in a later stage of infection, expression and localization of PB1-F2 viral protein, encoded by the +1 alternative ORF in the PB1 gene, at the mitochondrial membrane (MM) results in dissipation of membrane potential (ΔΨm), release of cytochrome c (cyt c) and activation of caspase-9-mediated intrinsic apoptotic pathway (Gibbs et al., 2003; Henkel et al., 2010; Zamarin et al., 2005) (Figure 17). A region near the C-terminus of PB1-F2 called Mitochondrial Targeting Sequence (MTS) (aa 65-87) is necessary and sufficient for its inner MM localization (Gibbs et al., 2003). PB1-F2 MTS mimics the most common type of mitochondrial targeting signal in cellular proteins, consisting of a terminal extension termed the presequence,

characterized by enriched positively charged, hydroxylated and hydrophobic residues, which have the potential to form an amphiphilic α helix (Pfanner, 2000). In a helical wheel projection, the positively charged residues localize to one side of the helix, while the opposite side is uncharged and hydrophobic (Roise and Schatz, 1988; von Heijne et al., 1989). Inside the MTS specific amino acids bearing hydrophobic side chains, such as Leucine (Leu or L) residues, appear crucial for mitochondrial targeting (Chen et al., 2010; Gibbs et al., 2003), which involves direct recognition and subsequent translocation into the intermembrane space (IMS) via the translocase of outer membrane 40 (TOM 40) (Melin et al., 2014; Yoshizumi et al., 2014). Following translocation, PB1-F2 assembles into a highly ordered oligomer (Yoshizumi et al., 2014) and triggers permeabilization of the MM likely by forming a nonselective ion channel (Henkel et al., 2010) or through interaction with proteins constituting the permeability transition pore complex (PTPC), such as the adenine nucleotide translocator 3 (ANT3) in the inner mitochondrial membrane and the voltage-dependent anion channel 1 (VDAC1) in the outer mitochondrial membrane (Zamarin et al., 2005). Although the exact mechanism of MM permeabilization is still debated, the final outcome consists in depolarization of membrane potential (ΔΨm) and release of cyt c which in turn activates the intrinsic apoptotic pathway.

In addition to its role in inducing apoptosis, localization at mitochondrial level of PB1-F2 was shown to exert IFN antagonist function by impairing the activity of the mitochondria antiviral signalling protein (MAVS), which, as a downstream adaptor protein for RIG-I, plays a central role in virus-triggered IFN-β induction (see paragraph 1.5.1). Different mechanisms can modulate MAVS expression and signalling. These include protein–protein interactions, alterations in mitochondrial dynamics, and/or post-translational modifications as previously reviewed by Jacobs and Coyne (Jacobs and Coyne, 2013). Among the alterations in mitochondrial dynamics, the membrane potential (ΔΨm) is essential for MAVS-mediated IFN-α/β induction (Koshiba et al., 2011). As such, PB1-F2 exerts its IFN antagonist function, at mitochondrial level, through the dissipation of the

membrane potential (ΔΨm) (Varga et al., 2012), which in turn results in inhibition of MAVS activity and consequent decrease of IFN expression (Varga et al., 2011) (Figure 17). Thus, PB1-F2 protein enhances influenza virus replication in two different ways: (i) it increases virion release by promoting apoptosis at late stage of infection, and (ii) it contributes to the inhibition of IFN expression therefore blocking the activation of paracrine IFN-mediated antiviral response.

Interestingly, beside mitochondria localization, PB1-F2 has also been found in the cytoplasm and in the nucleus of infected cells (Chen et al., 2010; Gibbs et al., 2003). The presence of the protein in the nucleus may allow for its proposed interaction with PB1, affecting viral polymerase activity (Mazur et al., 2008).

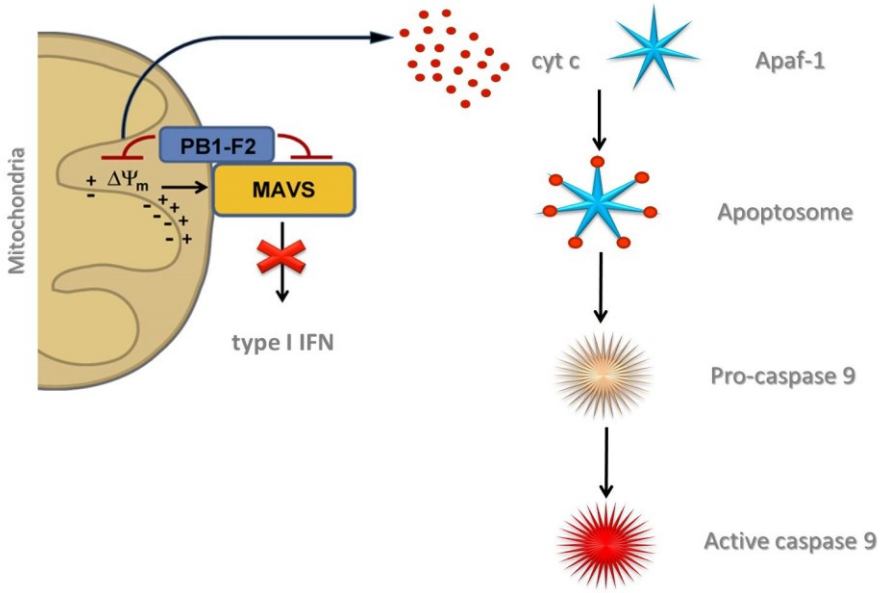

*Figure 17. **Pro-apoptotic and IFN-antagonist activities of influenza virus PB1-F2 protein at late stage of infection.** Adapted from* (Varga et al., 2012).

1.6 Influenza A virus evolution.

1.6.1 Antigenic Drift and Antigenic Shift.

Change is *a conditio sine qua non* for a virus since it allows escape from the host pre-existing immunity, enhancement of viral fitness during infection and adaptation to new host species. IAVs

are constantly changing through two different mechanisms called antigenic drift and antigenic shift (Figure 18).

“Antigenic drift” consists of selective amino acidic mutations in the antigenic portions of the surface glycoproteins HA and NA. These mutations are the results of small changes in viral genes that happen continually over time during virus replication. As in all RNA viruses, mutations in influenza occur frequently because the virus' RNA polymerase lacks exonuclease proofreading capability, resulting in an error rate between 1×10^{-3} and 8×10^{-3} substitutions per site per year during viral genome replication (Chen and Holmes, 2006). Random mutations can be rapidly selected from a viral population depending on the evolutionary pressures applied, (Murphy and Clements, 1989) and can accumulate over time resulting in antigenically different viruses, leading to immune response evasion (Smith et al., 2004) and/or drug resistance (Ong and Hayden, 2007). The numbers and locations of mutations in the surface proteins, allowing the virus to elude host immunity, have been characterized by different studies (Bush et al., 1999; Fitch et al., 1997; Smith et al., 2004) since these genetic changes are the main reason why people can get the flu more than one time during their lifetime and why the flu vaccine composition must be reviewed each year, and updated as needed to keep up with evolving viruses.

The other type of change consists in an abrupt, major variation in the IAV genetic constellation. Because the IAV genome consists of eight distinct RNA segments, co-infection of one host cell with two different IAVs can result in progeny viruses containing a mix of gene segments from both parental viruses (Figure 18). When this process of genetic reassortment involves the gene segments encoding the HA and/or NA surface glycoproteins it has been termed “antigenic shift”. While IAVs are changing by antigenic drift all the time, antigenic shift happens only occasionally; nevertheless reassortment has been shown to be both common and important in IAV evolution (Holmes et al., 2005) and host switch events (Garten et al., 2009; Scholtissek et al., 1978). Because antigenic shift results in a new influenza A subtype or a virus with a hemagglutinin or a

hemagglutinin/neuraminidase combination that has emerged from an animal population that is so different from the same subtype in humans, most people are completely naïve to the new virus, which can then rapidly spread and in some cases cause pandemics.

In 1957, an H2N2 “Asian” strain emerged bearing HA, NA, and PB1 genes from an avian IAV and the remaining five genes from the human H1N1 strain circulating at the time (Kawaoka et al., 1989). Because the human population had not previously experienced infection with H2 antigenic type, the entire world was susceptible to infection and the virus spread rapidly. The Asian flu virus killed between 1 million and 4 million people becoming the most frequent subtype circulating among humans until a new H3N2 subtype was introduced in 1968. This latter virus, called “Hong Kong” pandemic virus, was also the result of antigenic shift comprising H3 and PB1 gene segments of avian origin and the remaining six segments from previously circulating human H2N2 strain (Scholtissek et al., 1978). The H3N2 pandemic virus replaced the H2N2 subtype, claiming around 2 million human lives.

In 2009 a new pandemic H1N1 virus, characterized by a novel H1, was stably introduced into human population. The pH1N1-09 virus, also called “swine flu”, because the origin of the virus was initially thought to be in pig farms in Mexico, arose through a multiple-reassortment process combining avian-origin PB2 and PA, human PB1, classical swine HA, NP and NS and Eurasian swine NA and M segments (Garten et al., 2009; Novel Swine-Origin Influenza A (H1N1) Virus Investigation Team et al., 2009; Smith et al., 2009). The virus exhibited a remarkable transmissibility between humans most of whom had very little pre-existing immunity against this novel strain. Age distribution of morbidity during 2009 H1N1 pandemic was different from that of the two seasonal influenza epidemic viruses (H1N1 and H3N2) as the proportion of under-60s among influenza deaths was markedly higher (Lemaitre and Carrat, 2010). pH1N1-09 became the most frequent H1 subtype among humans and since then has been included in the seasonal trivalent and quadrivalent

vaccine formulations together with the drifted version of the previous H3N2 virus and influenza B viruses (World Health Organization (WHO), 20 February 2014).

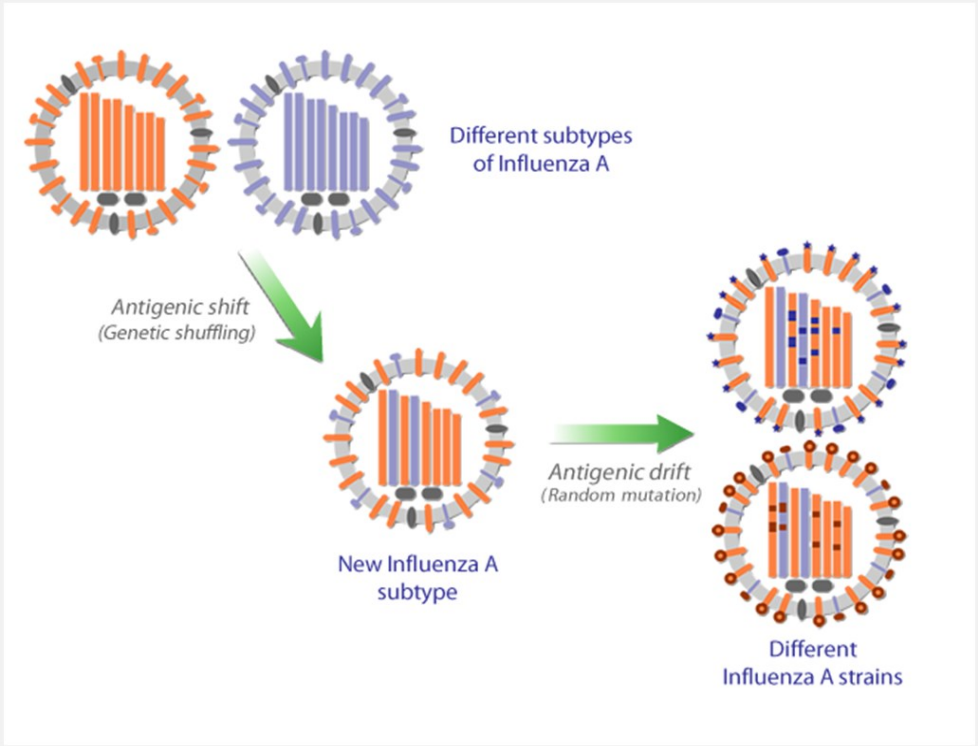

Figure 18. Influenza virus antigenic shift and antigenic drift.

1.6.2 Adaptation

Although wild birds are the natural reservoir of IAVs, mammals are often infected with influenza viruses of avian origin. The zoonotic transmissions can result in severe disease in different mammals including cats, dogs, horses, pigs and humans due to the lack of pre-existing immunity to the new influenza strain. In most of the cases the results are dead-end infections and are not further transmitted within the new host. However, on rare occasions, IAVs can pass the species barrier and establish an entirely new virus lineage in a mammalian species, as shown by the 1918 pandemic when the introduction into human population of an H1N1 subtype (called “Spanish flu”) directly from the avian reservoir, following a small number of adaptive mutations (Reid et al., 2004; Taubenberger et al., 2005), caused between 20-50 million deaths worldwide. Although the death

toll was very likely increased by historical and environmental factors such as the gathering of troops to the frontline, poor hygienic conditions and the lack of antibiotics available, the spillover of avian IAVs into human population represents a constant threat for the global health. Fortunately, different adaptive mutations are required for avian viruses to stably spread among humans, including those involved in the HA SA receptors binding and fusion activities, the polymerase efficiency and the ability of the virus to overcome cellular restriction factors.

1.6.2.1 Receptor binding and endosomal membrane fusion.

The HA protein has been widely associated with a major role in the host-range restriction of influenza A virus (Matrosovich et al., 2000; Rogers and Paulson, 1983). Indeed, one of the primary barriers to adaptation is the rather poor binding avidity of avian influenza virus HA for the predominant human receptors. IAVs have HAs with different specificities for the disaccharide consisting of SAs and the penultimate sugar (galactose or N-Acetylgalactosamine [GalNAc]) with different glycosidic bond isomerization. Avian IAVs have an HA receptor-binding specificity for α-2,3 SA mainly expressed on avian respiratory and enteric cells, while HAs from IAVs adapted to humans have higher specificity for α-2,6 SA abundantly present on the surface of the cells of the human upper respiratory tract (URT) (Figure 19). Therefore, a pre-requisite for an avian IAV to be stably transmitted from human-to human is adaptive mutations in the HA receptor-binding domain (RBD) to enhance or shift the binding preference to α-2,6 SA receptors. In line with this consideration, while the RBD is quite conserved in avian IAV HAs, those belonging to IAVs adapted to humans have mutations in several key residues, which have been linked to increased binding specificity to α-2,6 SA (Herfst et al., 2012; Imai et al., 2012).

However, enhanced binding to α-2,6 SA is not a requirement for human infections since the majority of H5N1 virus dead-end infections have occurred in viruses with RBD specificity for α-2,3

(Taubenberger and Kash, 2010). Moreover the receptor binding switch is sometime insufficient alone for a stable host switch of an avian IAV to humans,

Endosomal membrane fusion at the optimal pH is also crucial for efficient transmission between mammals (Imai et al., 2012). After binding to cellular receptors, influenza viruses are internalized by endocytosis. As the pH is progressively decreased from early endosome to late endosome, a threshold is reached at which the HA surface protein undergoes irreversible structural changes that facilitate fusion of the viral envelope with the endosomal membrane (see paragraph 1.4.5.1). Threshold pH values differ among influenza viruses, and a change in the pH of fusion of the HA protein can help influenza viruses to adapt to different cell lines (Lin et al., 1997) and host species (Giannecchini et al., 2006). In general, a high pH of HA protein activation could result in influenza virus inactivation in the environment or during transport to the cell surface. On the other hand, a low pH of HA protein activation could result in late uncoating or even degradation in the lysosome as the pH of the endocytic pathway decreases from early endosomes to late endosomes to lysosomes (Reed et al., 2010). Experimental infection in ducks and chickens infected with H5N1 influenza viruses, demonstrated that the highest levels of virus replication and pathogenesis correlated with HA activation at pH values that range between 5.6 and 6.0, while HA activation at pH values lower than 5.6 attenuated replication and pathogenesis. In contrast, replication of attenuated or reassorted H5 viruses in the URT of mice and ferrets was enhanced by mutations that decreased the H5 protein pH activation values to 5.6 or lower (Zaraket et al., 2013). Therefore, for efficient propagation within a biological host, an IAV should also have an optimal range of pHs of activation for the HA protein (Imai et al., 2012).

1.6.2.2 Temperature and polymerase activity.

In addition to the switch in receptor specificity, efficient virus production from the cell of the respiratory tract is also required for stable transmission of an avian-origin IAV in the human

population. One of the major barriers for the replication of avian IAVs in human cells consists in the different temperature at which replication occurs. Avian IAVs, which replicate at temperatures around 41°C in the intestinal tract of birds, need to adapt their polymerase activity at the much lower temperature of the human URT (33°C). To this end amino acid substitutions in the polymerase proteins have been shown to be of paramount importance to determine host range and transmission (Mehle and Doudna, 2009; Van Hoeven et al., 2009) (Figure 19).

The amino acid substitution Glu627→Lys627 (E627K) in the polymerase complex protein PB2 has been widely studied for its association with increased virus replication in mammalian cells at lower temperatures (de Wit et al., 2008; Subbarao et al., 1993). More recently, also PB2 residues S590 and R591 have been reported as responsible for efficient activity of the pH1N1-09 virus polymerase in human cells, which retains the avian signature 627E (Mehle and Doudna, 2009). Due to the proximity displayed by residues 590-591 to position 627 in the structural model (Tarendeau et al., 2008), it is likely that they contact the same human co-factor. However, cellular factors involved in PB2 627K mediated host adaptation and pathogenicity still remain poorly understood and 627 amino acid specific binding of any cellular component has yet to be demonstrated.

In several H5N1 viruses isolated from humans or other mammals, the PB2 gene does not contain E627K substitution but displayed a D701N mutation within the PB2 nuclear localization signal (NLS), which has been shown to enhance nuclear import of PB2 by importin-α in mammalian cells but not in avian cells (Gabriel et al., 2008; Gabriel et al., 2011). Mutation D701N can compensate for the absence of 627K signature, enhancing transmission from birds to mammals and between mammals (Gao et al., 2009; Steel et al., 2009). Another mammalian adaptive mutation at the level of PB2 is T271A, which is found in many human influenza viruses compared to the avian counterparts. This mutation, increases viral growth in human cells and is in part responsible for the pH1N1-09 high levels of polymerase activity (Bussey et al., 2010).

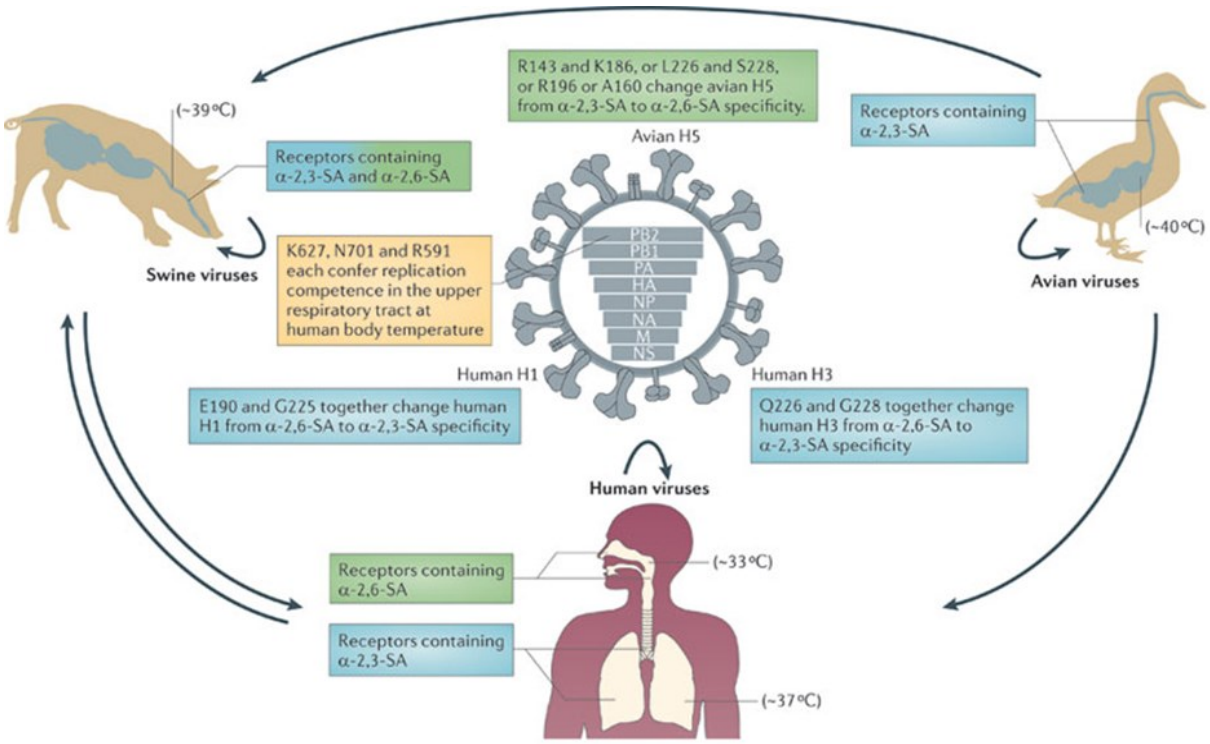

Figure 19. ***Influenza A viruses tropism and adaptation.*** *Avian IAVs bind preferentially to α-2,3-SA, which is found on receptors in the gut and respiratory tract of birds. By contrast, human-adapted IAVs have a higher affinity for α-2,6-SAs, which are expressed in the upper respiratory tract of humans. The swine trachea contains receptors with α-2,3-linked and α-2,6-linked sialic acid (α-2,3-SA and α-2,6-SA) moieties that allow for binding of both avian and human viruses, leading to the idea that pigs can serve as the 'mixing vessel' in which reassortment of human and avian viruses can occur. Beside the HA binding site, also the activity of the viral RNA-dependent RNA polymerase needs to adapt to the different temperature of the new hosts, to this end mutation within the PB2 protein has been widely characterized.* (Medina and Garcia-Sastre, 2011).

1.6.2.3 vRNPs nuclear import and the cellular restriction factor MxA.

Besides mutations that enhance interaction with positive cellular factors, and promote viral replication, other adaptive mutations allow IAVs to escape cellular restriction factors that otherwise would inhibit virus replication in the new hosts. The human interferon (IFN) system represents a major innate defence against zoonotic viruses. As previously described (see paragraph 1.5.2), among the many IFN-induced antiviral factors capable of inhibiting influenza A virus replication, the human *Myxovirus resistance gene A* (*MxA*) has been thoroughly characterized. The influenza virus nucleoprotein (NP) has been shown to be the viral target of MxA protein (Manz et al., 2013;

Zimmermann et al., 2011) and a direct interaction between human MxA and influenza NP has been observed (Turan et al., 2004). In line with these findings, MxA protein has been reported to exert its antiviral function in the cytoplasm of infected cells by binding NPs associated within the vRNPs, blocking influenza A virus replication before primary transcription, and preventing also newly translated NPs from entering the nucleus to participate in secondary transcription (Matzinger et al., 2013; Pavlovic et al., 1992; Xiao et al., 2013). Because MxA antiviral activity depends on appropriate binding sites on the viral NP, IAV strains differ in their sensitivity to MxA depending on the origin of the NP protein (Dittmann et al., 2008). In general, avian IAVs are more sensitive to MxA than human strains (Dittmann et al., 2008). This is likely the result of the absence of selective pressure exerted by Mx gene in avian species, where this ISG was previously shown to lack antiviral activity against different strains of IAVs (Schusser et al., 2011). Therefore, MxA contributes to a natural barrier to transmission of IAVs from avian reservoirs and avian IAVs stably introduced in mammals often acquire adaptive mutations on the NP protein to allow them to escape this restriction factor (Dittmann et al., 2008; Manz et al., 2013; Zimmermann et al., 2011). Among these mutations isoleucine at position 100 (100I), proline at position 283 (283P) and tyrosine at position 313 (313Y) have been reported to be essential for reduced Mx sensitivity in mammalian cell culture and *in vivo*, while asparagine at position 52 (52N) has been shown to partially compensate the absence of some of the previous amino acids (Riegger et al., 2015).

1.6.3 Reverse Genetics

The use of reverse genetics, to facilitate the generation of virus entirely from cloned cDNA, is a common practice nowadays to study IAV in laboratories worldwide. However, it took almost 20 years to set up this tool since the advent of recombinant DNA technology opened the door for conversion of viral RNA genomes into cDNA clones back in the late 1970s.

The *de novo* synthesis of a positive-sense RNA virus, in which naked RNA is infectious, was first reported for the bacteriophage Qβ (Taniguchi et al., 1978) in 1978 and then followed by many other positive-sense RNA viruses (Boyer and Haenni, 1994).

However, it took many years to adapt the techniques for the recovery from cDNAs of negative-sense RNA viruses, which possess genomes complementary to mRNA in their orientation and therefore rely on viral RNA-dependent RNA polymerases for transcription. In fact the generation of a nonsegmented negative-sense RNA virus entirely from cloned cDNA was not achieved until 1994, when Schnell et al. (Schnell et al., 1994) produced a recombinant rabies virus. In this system a plasmid containing full length copy of the viral antigenome, controlled by bacteriophage T7 RNA polymerase promoter, was transfected into cells that expressed T7 RNA polymerase. The components of the viral polymerase complex and NP protein were provided from protein expression plasmids, all controlled by generation of T7 RNA polymerase promoter. Although this work was soon followed by the generation of other nonsegmented negative-sense RNA viruses belonging to different families, the production of segmented negative-sense RNA viruses from cloned cDNA was even more challenging because it required the transfection of more than one genomic RNA at the same time. Only in 1996 did Bridgen and Elliot manage to generate a member of the Bunyaviridae family, characterized by a genome consisting of a three segments of negative-sense viral RNA, entirely from cloned cDNA (Bridgen and Elliott, 1996).

Influenza A virus was finally generated entirely from plasmids in 1999 by two different groups using a similar approach (Fodor et al., 1999; Neumann et al., 1999). Neumann et al. cloned cDNA encoding all eight segments of IAV in negative orientation between RNA polymerase I promoter and terminator sequences, which after transfection of human embryonic kidney (HEK 293T) cells, transcribed negative-sense vRNAs. The proteins required for transcription and replication of the vRNAs (PB2, PB1, PA and NP) were provided from co-transfected protein expression plasmids, controlled by chicken β-actin promoter (Figure 20A). Fodor et al. 1999 reported a similar system,

where all eight vRNAs were synthesized from plasmids containing the RNA polymerase I promoter and hepatitis delta ribozyme following transfection of African green monkey kidney (Vero) cells; while the NP and polymerase proteins were generated from expression constructs. Hence both approaches required 12 plasmids (Neumann and Kawaoka, 2004).

Later, Hoffmann et al. (Hoffmann et al., 2000) devised a modified RNA polymerase I system that reduced the number of plasmids required for influenza virus generation from 12 to 8. In this approach, cDNAs encoding viral RNAs were inserted in positive-sense orientation between an RNA polymerase II promoter and a polyadenylation signal. This cassette was then inserted in negative sense orientation between the RNA polymerase I promoter and the terminator sequence. Hence, capped and polyadenylated mRNAs for the expression of proteins and negative-sense vRNAs were generated from the same template. Although the RNA polymerase I/II system may be proved advantageous for virus generation in cell lines that cannot be efficiently transfected with 12 plasmids, the flexibility of virus generation is reduced, because both protein expression and vRNA synthesis are achieved from the same template. Nevertheless, regardless of the reverse genetics systems employed, the ability to alter the genomes of segmented negative-sense RNA viruses had a dramatic impact on the understanding of viral replication steps and on the virulence factors associated with viral fitness, transmission and host adaptation, and also facilitating the production of reassortant viruses, which can now be used as inactivated or live attenuated vaccines.

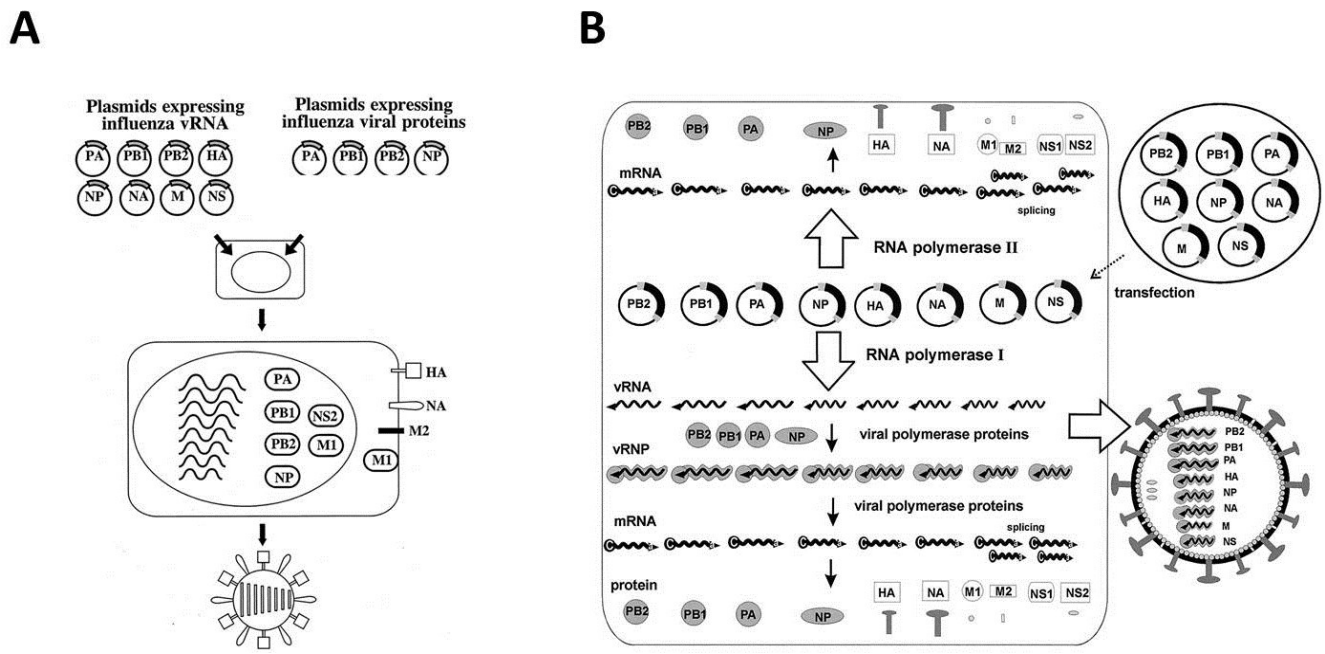

Figure 20. The 12 (A) and 8 (B) plasmids reverse-genetics methods for generating segmented negative-sense RNA influenza A viruses. Adapted from Neumann et al., 1999 and Hoffmann et al., 2000.

1.7 Rationale and scope of the thesis

Observational studies and pathological findings in animals naturally and experimentally infected with avian-origin IAVs revealed extensive replication of the virus in the pancreas, implying an enhanced tropism for this organ. The predilection of both highly pathogenic and low pathogenicity IAVs for the pancreas was previously reported in domesticated avian species and migratory waterfowl following experimental or natural infection (Bertran et al., 2011; Kwon et al., 2010; Mutinelli et al., 2003; Shinya et al., 1995). In mammals, spread of the infection through the pancreas was reported in ferrets following exposure of digestive system to highly pathogenic IAVs (Lipatov et al., 2009), while pancreatic post-mortem lesions ranging from inflammation to necrosis were observed in infected cats (Reperant et al., 2009; Rimmelzwaan et al., 2006; Yingst et al., 2006). In addition, in the wake of the 2009 pandemic, different publications reported pancreatic damage in humans cases associated with pH1N1-09 IAV infection (Blum et al., 2010; Cano et al., 2010; Nenna et al., 2011; Watanabe, 2011) and in a more recent study, using *in vitro* and *ex vivo*

models, human-origin pancreatic cells were shown sensitive to both IAV infection and induced cell death (Capua et al., 2013). Therefore, although the pancreas is not considered a typical site of replication after standard infection, IAV seems to be capable of infecting and damaging pancreatic cells in severe infections.

Although IAV infections are well studied because they represent a considerable health burden, the oncolytic potential of this virus has not been investigated as thoroughly as for some other viruses. However, IAVs present some features compatible with those required for OVs: (i) they induce apoptosis in numerous cell types *in vitro* (Fesq et al., 1994; Lowy, 2003; Takizawa et al., 1993) and *in vivo* (Ito et al., 2002; Mori et al., 1995; Mori and Kimura, 2000); (ii) they present different serotypes with typically low homology between their surface-exposed glycoproteins, which can be exploited to avoid host pre-existing immunity (Fouchier et al., 2005; Hay et al., 2001) (see paragraphs 1.3.1.1 and 1.4.3) and (iii) they have a genome structure that can be easily manipulated, since the introduction of reverse genetics (see paragraph 1.6.3), in order to modulate virus selectivity and pathogenicity.

Based on these observations, we set out to further evaluate the sensitivity of different human PDA cell lines to a panel of avian-origin IAVs. As reported in chapter 2, PDA cell lines were found to be sensitive to infection by human and avian IAV isolates. Investigation of cell viability and apoptosis induction following infection of PDA cell lines and a non-transformed pancreatic ductal cell line demonstrated the promising oncolytic potential of some avian-origin IAV isolates for virotherapy treatment. Based on these data the low pathogenicity avian influenza (LPAI) virus H7N3 A/turkey/Italy/2962/03, which displayed high levels of apoptosis in different PDA cell lines and beneficial effect in xenograft model (Kasloff et al., 2014), was selected for further development.

Using this work as a starting point, the aim of the present project was to engineer the avian-origin H7N3 influenza A virus to enhance its selectivity, safety and oncolytic activity for PDA treatment.

Specific aims of the presented study were:

1. Understand the mechanism by which the virus leads to high levels of cell death in PDA cell lines.
2. Generate a reverse genetics system for the H7N3 avian influenza virus suitable for engineering to improve its oncolytic potential.
3. Enhance the selectivity of the H7N3 virus to IFN-deficient cells, such as the majority of PDA cells (see paragraph 1.2.3).
4. Optimize the balance between levels of apoptosis induced and productive H7N3 virus replication in PDA cells to achieve the best therapeutic effect (see paragraph 1.5.4 and 1.5.5).
5. Enhance the safety of the avian isolate for clinical use by reducing the risk associated to antigenic shift with human circulating strains that may result in a potentially pandemic virus (see paragraph 1.6.1).
6. "Arm" the virus by engineering expression of the granulocyte-macrophage colony-stimulating factor (GM-CSF) gene during infection to increase potential potency of the treatment through stimulation of anti-tumour adaptive immunity (see paragraph 1.3.1.4).

Chapter 2. Oncolytic activity of avian-origin influenza A viruses in human pancreatic ductal adenocarcinoma cell lines.

2.1 Introduction

Pancreatic ductal adenocarcinoma (PDA) is one of the most lethal forms of human cancer mainly due to the lack of early methods of detection and to the asymptomatic form of the disease at the initial stages. Cancer therapies proven successful in other tumour types have shown little efficacy in treating PDA, thus development of new treatment strategies for pancreatic cancer patients is of crucial importance. Building on the observation that avian influenza A viruses (IAVs) appears to have a tropism for the pancreas *in vivo* (see paragraph 1.7) and human derived pancreatic cells are sensitive to IAV infection, investigations were undertaken to test the potential of different origin IAVs as oncolytic agents for PDA virotherapy treatment.

2.2 Results

2.2.1 Susceptibility of human PDA cell lines to avian-origin influenza A virus infection.

Preliminary data generated at the Istituto Zooprofilattico Sperimentale delle Venezie (IZSVe – Padova, Italy) using flow cytometry (FACS) with fluorescent labelled lectins specific for alpha-2,3 and alpha-2,6-linked sialic acids, demonstrated the presence of receptors for both human and avian influenza A viruses (see paragraph 1.6.2.1) on the surface of different human PDA cell lines (Table 3) (Kasloff et al., 2014). To further confirm the capability of avian IAVs to utilize receptors on the human PDA cells, a variety of cell lines were transduced with lentiviral pseudotypes bearing HA and NA glycoproteins of the avian influenza A virus A/Viet Nam/1194/2004 (H5N1). HA mediated entry of pseudotypes was monitored by the expression of GFP encoded from the packaged lentiviral

genome (Figure 21A). Bearing in mind that each cell line was transduced with an equal titre of pseudotypes, it appeared that the BxPC3 PDA line was the most susceptible to infection via the influenza H5 HA protein (Figure 21B).

Results generated at IZSVe demonstrated active viral RNA replication in all PDA cell lines (data not shown) infected with a panel of different IAVs of human or avian origin and of different subtypes (Table 4). This was detected both by accumulation of vRNA by RT-PCR from infected cells, and also by increases in virus titres released from the cells, although the infectious titres recorded were less than might have been expected, likely due to suboptimal proteolytic activation (Kasloff et al., 2014). Interestingly, MTT assay, an indicator of cell viability, which measures tetrazolium reduction by metabolically active and proliferating cells, highlighted different levels of virus-induced cell death in PDA cells depending on both the cell line and the virus isolate tested (Kasloff et al., 2014). The lowest levels of cell death were displayed by PANC-1 cells, and the highest by BxPC-3 and CFPAC-1 cell lines. Influenza A virus isolates H7N3 A/turkey/Italy/2962/03 and the H7N7 A/macaw/England/626/80 caused the greatest loss of cell viability across the panel of cell lines tested. The H7N3 isolate, in particular, triggered higher cell loss in BxPC-3 and CFPAC-1 cells than in the normal human pancreatic duct epithelial cell line HPDE6 (Kasloff et al., 2014).

CELL LINE	DERIVATION	KRAS[a]	CDKN2A	TP53[b]	SMAD4/DPC4
AsPC-1	62-year-old woman with adenocarcinoma of the head of the pancreas.	12 Asp	Δ2 bp; HD	135 Δ1 bp	WT
BxPC-3	61-year-old woman with adenocarcinoma of the body of the pancreas.	WT	HD	220 Cys	HD
CFPAC-1	Adenocarcinoma of the head of the pancreas derived from 26-year old male with cystic fibrosis.	12 Val	WT; Promoter methylation	242 Arg	HD
Mia paca2	65-year-old man with adenocarcinoma of the body and tail of pancreas.	12 Cys	HD	248 Trp	WT
PANC-1	56-year-old male with an adenocarcinoma in the head of the pancreas.	12 Asp	HD	273 His	WT

Table 3. ***Genotype of selected PDA cell lines used in this study with respect to the four most common mutations in pancreatic cancer.*** *Adapted from* (Deer et al., 2010). [a] *KRAS mutations involve amino acids that interfere with the GTPase function. In pancreatic cancer, mutations are essentially seen only at the twelfth position, (codon or amino acid 12), with rare exceptions seen at codon 13. The majority of KRAS mutations in pancreatic cancer change a glycine at codon 12 to a valine or aspartate.* [b] *Most of TP53 mutations consist of single amino acid change, which leads to the production of an altered version of the p53 protein that cannot bind effectively to DNA thus preventing the cell from undergoing apoptosis in response to DNA damage. WT—wild type, Δ—deletion, bp—base pair, HD—homozygous deletion*

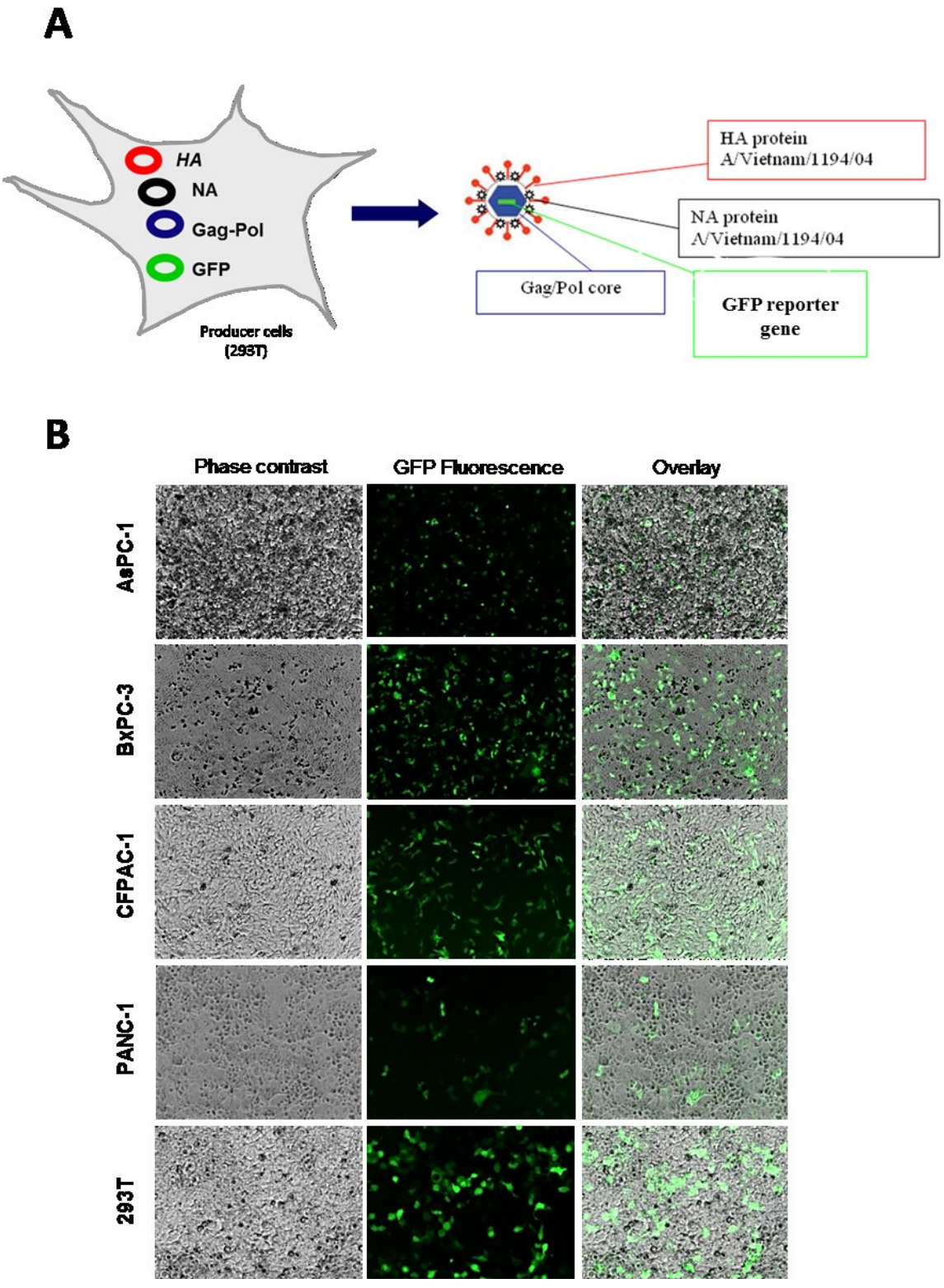

Figure 21. ***Influenza A virus pseudotypes structure and entry into PDA cells. A)*** *Generation of pseudotypes bearing avian signature HA and NA glycoproteins of A/VietNam/1194/2004 (H5N1).* ***B)*** *H5N1 pseudotype entry into PDA cells. AsPC-1, BxPC-3, CFPAC-1, and PANC-1 cell lines were transduced with fluorescent HA- and NA-bearing IAV pseudotypes as described in material and methods and visualized following 48 h of incubation. Human Embryonic Kidney (HEK or 293T) cells were included as positive control. Monolayers (left), GFP reporter gene expression (middle), and the merging of these two images (right) are shown for each cell line at a ×10 magnification. Cells were visualized with a Zeiss Axiovert 40 CFL, fluorescence, phase-contrast, inverted microscope equipped with an HBO50 mercury short-arc lamp.*

Subtype	Strain	Species	HA cleavage site
H5N1	A/mallard/Italy/3401/05	Avian	Monobasic
H7N3	A/turkey/Italy/2962/V03	Avian	Monobasic
H1N1	A/Puerto Rico/8/34	Human	Monobasic
H4N8	A/cockatoo/England/72	Avian	Monobasic
H7N7	A/macaw/England/626/80	Avian	Monobasic

Table 4. *Influenza A viruses subtypes and strains used in the preliminary experiments.*

The ability of Influenza A viruses to induce apoptosis in PDA cells was further evaluated in infected cells through annexin-V staining (see paragraph 1.5.3). The immortal human pancreatic duct epithelial cell line (HPDE6), which retains a genotype similar to pancreatic duct epithelia and is non-tumorigenic in nude mice (Furukawa et al., 1996; Ouyang et al., 2000), was employed as a "benign" control cell line. As a positive control treatment for apoptosis, cells were subject to a high concentration gemcitabine and cisplatin (gem+cisp), two commonly used chemotherapeutic agents (see paragraph 1.2.4).

Levels of apoptosis were highly variable between cell lines and virus isolates, ranging from only 5% of H7N7-infected PANC-1 cells to over 60% of H7N3-infected BxPC-3 cells by 16 hours post-infection (hpi) (Figure 22A). Surprisingly, BxPC-3, a PDA cell line previously shown "resistant" to other oncolytic viruses including Vesicular Stomatitis Oncolytic Virus (VSV), Conditionally Replicative Adenoviruses (CRAds), Sendai Virus (SeV) and Respiratory Syncytial Virus (RSV) (Murphy et al., 2012), was the most sensitive among the PDA cell lines to IAV-induced apoptosis, followed by AsPC-1, CFPAC-1, MIA paca 2 and PANC-1. Interestingly, the human H1N1 PR8 strain, whose oncolytic potential has been previously appraised for other tumour types (Bergmann et al., 2001; Muster et al., 2004), induced far less apoptosis compared to the avian isolates. Consistent with results from

MTT assays, the H7N3 A/turkey/Italy/2962/03 virus was the most potent inducer of apoptosis in the majority of PDA cell lines examined (Figure 22A). Replication of this avian strain in PDA cell lines was confirmed by quantitative Real-Time PCR and Western Blot targeting viral Matrix gene (M) and NP protein respectively (Figure 22 B-C). In line with results previously reported by Kasloff et al. (Kasloff et al., 2014), PDA cell lines displayed higher permissiveness to IAV replication than benign-like HPDE6 cell line.

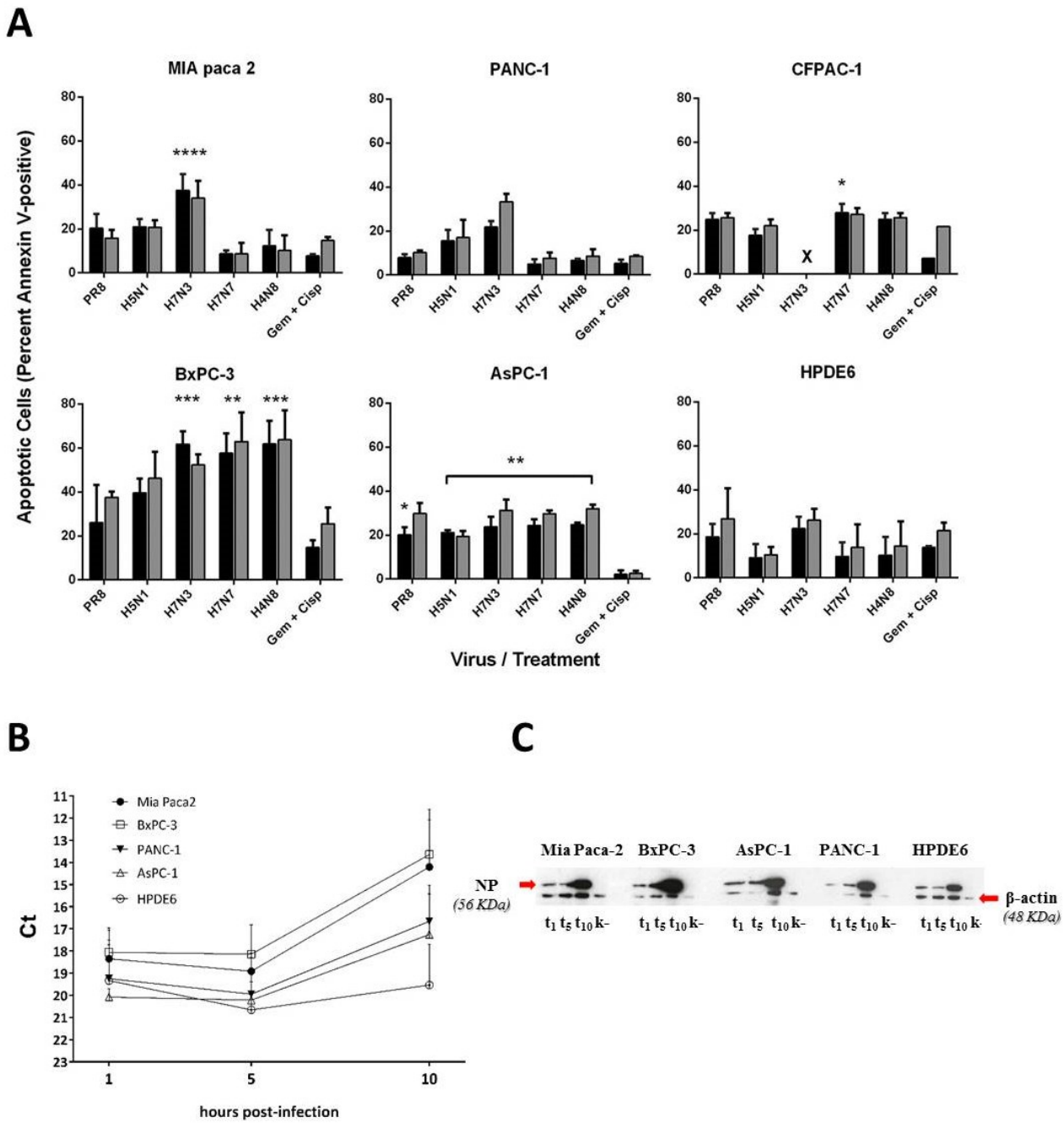

Figure 22. Influenza A viruses apoptosis induction and replication in PDA cell lines. A) Comparative induction of apoptosis in PDA cells following infection with different origin IAVs. Cells infected at MOI=1 with IAV or cultured with gemcitabine

(2 mM) plus cisplatin (0.8 µM) were assessed for induction of apoptosis at 16 hpi (black bars) and 24 hpi (grey bars) by Alexa Fluor 647-labelled Annexin V binding and flow cytometry. Results are normalized to uninfected controls and represent means plus standard deviation of two (Gem + Cisp treatment) or three (virus infections) independent experiments. Statistically significant differences between virus-induced and Gem + Cisp induced apoptosis at 16 hpi are indicated. Note - Severe cell death induced in H7N3-infected CFPAC-1 cells (X) prevented proper Annexin V cell labelling at time points examined. Virus-induced apoptosis is determined by subtracting the percentage of annexin V-positive control cells from infected cells. Adapted from (Kasloff et al., 2014). ***B)*** *Real-time PCR results obtained targeting IAV's M gene in different pancreatic cell lysates at 1, 5 and 10 hours post-infection with H7N3 A/turkey/Italy/2962/03 virus.* ***C)*** *Western blot analysis for the detection of viral nucleoprotein NP (56 KDa) in pancreatic ductal adenocarcinoma cells (MIA-PaCa-2, BxPC-3, AsPC-1, PANC-1) and human pancreatic ductal epithelial cell lines (HPDE6) infected with H7N3 A/turkey/Italy/2962/03. NP and Beta actin (46 KDa) were evaluated in cell lysates collected at 1, 5 and 10 h post-infection.*

2.2.2 The H7N3 A/turkey/Italy/2962/03 virus triggers high level of apoptosis in tumour BxPC-3 cells but not in "benign" HPDE6 cells.

Since some of the IAVs displayed high levels of apoptosis induction in BxPC-3 cells, a PDA cell line that was previously shown "resistant" to other oncolytic viruses (Murphy et al., 2012), we decided to focused on this line, together with the HPDE6 employed as a "benign" control (Furukawa et al., 1996; Ouyang et al., 2000), to further elucidate the mechanisms of IAV-induced PDA cell death.

Immunocytochemistry (ICC) targeting active caspase-3 was performed in BxPC-3 and HPDE6 cells at 16 and 24 hours post infection with the avian H7N3 A/turkey/Italy/2962/03 virus or with the human H1N1 A/Puerto Rico/8/1934 (PR8). The combination of gemcitabine and cisplatin was included as positive control treatment for apoptosis.

Acting at the cross-road between extrinsic and intrinsic pathway (see paragraph 1.5.3), caspase-3 can be considered as a general marker of apoptosis. Staining for activated caspase-3 revealed more positive cells after infection with H7N3 than for PR8 virus or the chemotherapeutic agents in BxPC-3 cells (Figure 23A-B). However, the effect of the H7N3 virus was much lower in the benign HPDE6 cells where it triggered levels of caspase-3 activation similar to those derived from infection with PR8 virus or treatment with the drugs (Figure 23A-C).

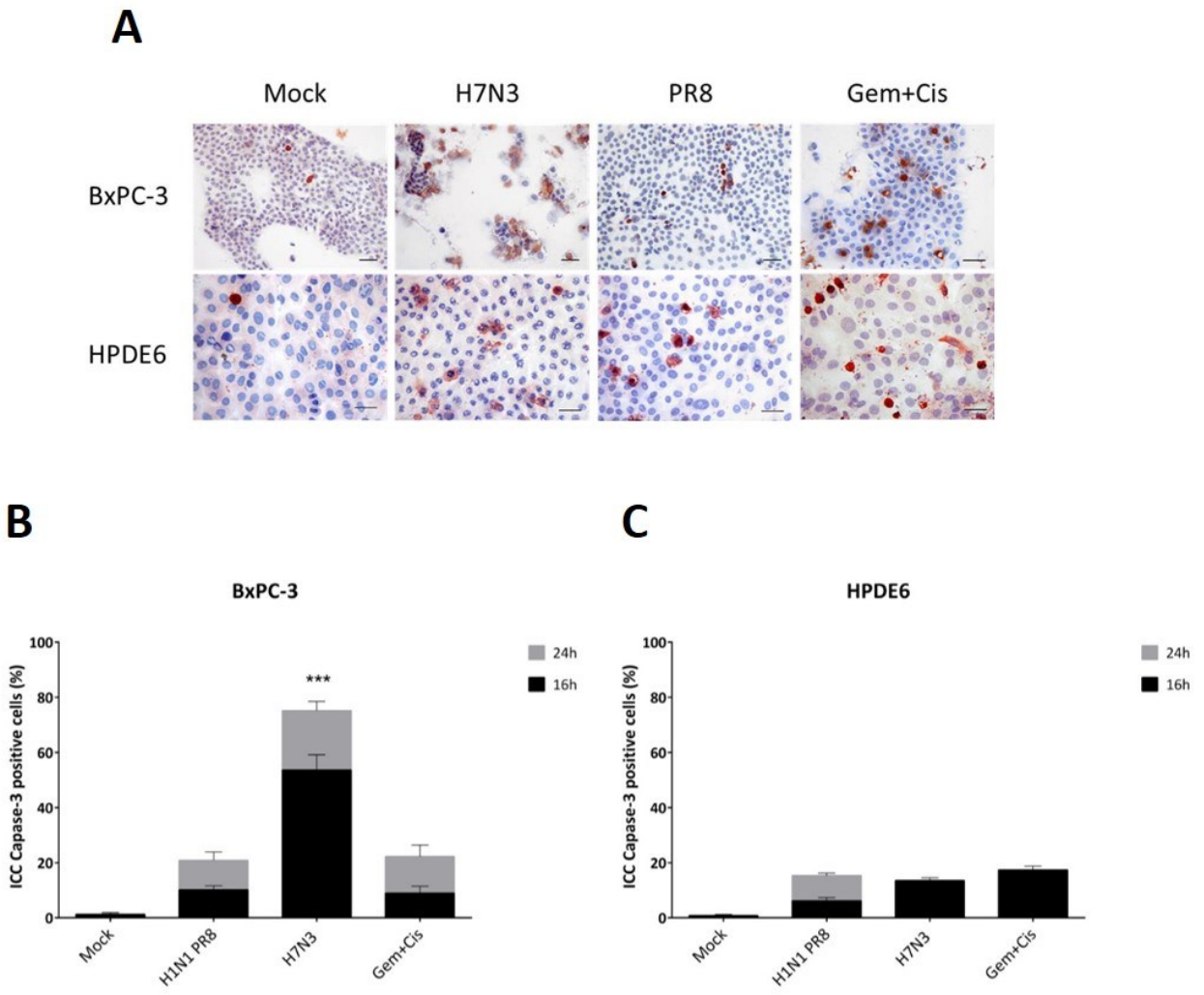

Figure 23. ***Immunocytochemistry (ICC) targeting active effector caspase-3 in BxPC-3 and HPDE6 cells following infection with IAVs.*** *(**A**) Semi-confluent monolayers of BxPC-3 and HPDE6 cells grown on glass chamber slides were infected with H1N1 A/Puerto Rico/8/34 (PR8) and H7N3 A/turkey/Italy/2602/2003 at an MOI of 1 and then tested by immunocytochemistry (ICC) for expression of cleaved caspase-3 at 16 and 24hours post-infection. Gemcitabine (2 mM) and cisplatin (0.8 µM) were included as positive controls. Quantification of BxPC-3 (**B**) and HPDE6 (**C**) cells positive to active caspase-3 in ICC. Results are means plus standard deviations for 10 repeat counts of 500 cells each, with significance shown for virus compared to gemcitabine plus cisplatin at 16 and 24 hours post-infection (*** p<0.001).*

HPDE6 cells resistance to Vesicular Stomatitis virus (VSV) oncolytic activity was previously suggested by Moerdyk-Schauwecker et al., 2012 as the result of constitutive high-level expression of IFN-stimulated antiviral genes (ISGs). BxPC-3 cells were not characterized in that paper. Therefore, in order to understand the differences in apoptosis recorded in the two cell lines, we investigated by RT-PCR the expression of IFNs and IFN-stimulated antiviral genes in BxPC-3 and HPDE6 cells mock

infected or infected with the H7N3 A/turkey/Italy/2962/03 virus. RT-PCR, using primers with sequence derived from those published by Moerdyk-Schauwecker et al. (Moerdyk-Schauwecker et al., 2012), confirmed that RIG-I and MAVS genes were expressed in both cell lines and the expression increased after infection (Figure 24). In contrast, while MxA and IFNα/β genes were constitutively expressed at low levels in HPDE6 cells, and their expression was increasing during infection, no expression was detected at all in BxPC-3 cells either constitutively (mock) or after infection with H7N3 virus. Thus differences in expression of and/or response to IFN, might account for the different infection rate and ensuing oncolytic ability displayed by H7N3 virus in BxPC-3 and HPDE6 cells.

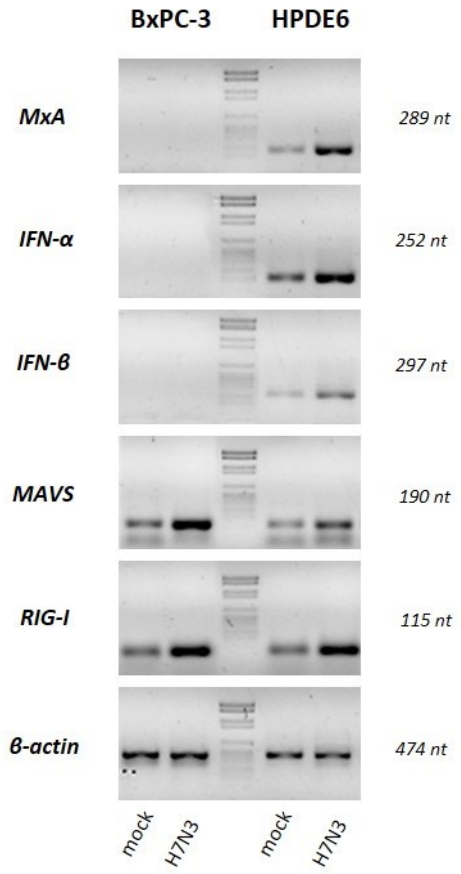

Figure 24. ***mRNA expression of IFN related genes in BxPC-3 and HPDE6 at 16 hours post-infection.*** *Cells were mock infected or infected with H7N3 A/turkey/Italy/2962/03 influenza viruses at M.O.I of 0.1. At 16 h post-infection cells were harvested and mRNA was reverse transcribed and analysed by PCR using the primers previously published* (Moerdyk-Schauwecker et al., 2012). *Amplified mRNA and corresponding product sizes are indicated on the left and on the right respectively.*

2.2.3 The H7N3 A/turkey/Italy/2962/03 virus induces apoptosis in tumour BxPC-3 cells mainly by affecting the intrinsic apoptotic pathway.

Although BxPC-3 cells remain sensitive to exogenous IFN (Murphy et al., 2012; Vitale et al., 2007), the lack of endogenous IFNα/β expression suggests that the cell death induced by IAV in this cell line was mainly a direct consequence of the virus activity (intrinsic pathway) rather than the result of paracrine cell signalling (extrinsic pathway). To confirm this hypothesis immunocytochemistry (ICC) targeting caspases 9 and 8, markers of the intrinsic and extrinsic apoptotic pathway respectively (see paragraph 1.5.3), was performed in BxPC-3 and HPDE6 cells infected with H7N3 or PR8 viruses. Treatment using Gemcitabine and Cisplatin was included as positive controls of apoptosis.

Most of the apoptosis driven by H7N3 virus in BxPC-3 cells was through the intrinsic pathway, since the percentage of caspase-9 positive cells at 16 hours post-infection was approximately double the number of those positive for caspase-8 (Figure 25A). The same trend was not observed in the case of PR8 virus for which caspase-8 and 9 positive cells reached comparable levels (Figure 25A). Conversely, HPDE6 cells infected with H7N3 virus tended to die more from apoptosis driven by the extrinsic pathway as showed by the higher levels of caspase-8 positive cells in comparison to those stained for caspase-9 (Figure 25B). Considering the data of IFNs and IFN-stimulated antiviral gene expression previously obtained (Figure 24), these results confirm that in BxPC-3 cells, unable to mount an IFN-mediated antiviral response, the H7N3 virus would more likely trigger apoptosis during its replication by direct targeting. Conversely, in HPDE6 cells the same virus, hindered in its replication by expression of IFN and ISGs such as MxA, would drive cell death mainly through IFN mediated cellular signalling. Taken together this finding emphasizes the H7N3 strain-specific ability to trigger high levels of cell death in tumour permissive BxPC-3 cells by activating the intrinsic apoptotic pathway.

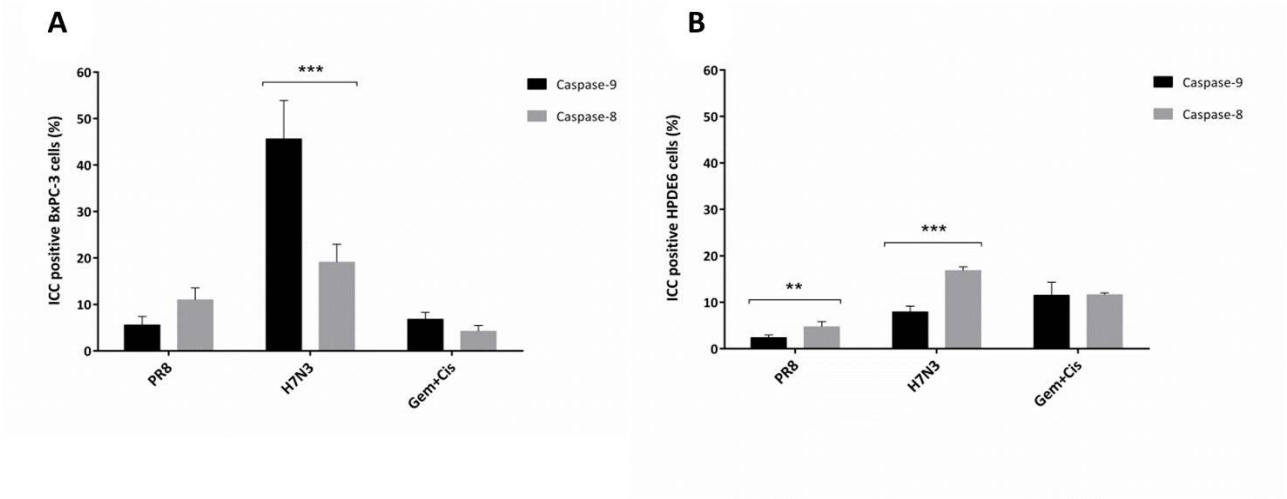

Figure 25. ***Immunocytochemistry (ICC) targeting active caspases 8 and 9 in BxPC-3 (A) and HPDE6 (B) cells at 16 hours post-infection.*** *Semi-confluent monolayers of BxPC-3 and HPDE6 cells were infected with H7N3 A/turkey/Italy/2602/2003 and H1N1 A/Puerto Rico/8/34 (PR8) at an M.O.I of 1 and then tested by ICC for expression of initiator caspases 8 and 9 at 16 hours post-infection. ICC results are normalized to uninfected controls of each cell line. All data represent means ± standard deviations (SD) of one representative experiment (n=10). Statistical significance was determined using Two-way ANOVA followed by Tukey's multiple comparison test.*

2.2.4 Oncolytic effects of H7N3 A/turkey/Italy/2962/03 influenza virus in mouse xenograft model.

The high level of apoptosis observed in BxPC-3 cells infected with H7N3 A/turkey/Italy/2962/03 virus *in vitro* appeared not to be due to the ability of the virus to infect these cells more efficiently than other isolates (Kasloff et al., 2014), but rather to its strain-dependent capability to induce cell death (Figure 22A-23B) by affecting mainly the intrinsic pathway (Figure 25A).

Aiming to confirm the H7N3 activity *in vivo* in a xenograft model, we firstly appraised the ability of human BxPC-3 cells to establish tumours in SCID-B17 mice. A group (n=5) of six-week-old female SCID-B17 mice were subcutaneously injected with 5 x 10^6 BxPC-3 cells in a volume of 100 µL into the right flank and observed for the development of a palpable tumour. All animals were sacrificed when the tumor volume had reached more than 1,000 mm^3. Post-mortem examination revealed solid hard tumours without involvement of other organs or evidence of metastasis (Figure 26A).

We next proceeded to test the H7N3 virus oncolytic activity in SCID mice (n=6) bearing BxPC-3 derived solid tumours. Following four successive virus inoculations into palpable BxPC-3 tumours over seven days (between day 8 and 15 post-implantation), the oncolytic effect of IAV on tumour reduction was compared to a PBS control group (Figure 26B). Overall, H7N3 treatment resulted in reduction of tumour growth in comparison to the control group, and all tumours collected from H7N3-treated mice sacrificed upon termination of the experiment yielded a positive result for IAV RNA by Real-Time RT-PCR targeting influenza virus Matrix (M) gene (Figure 26C).

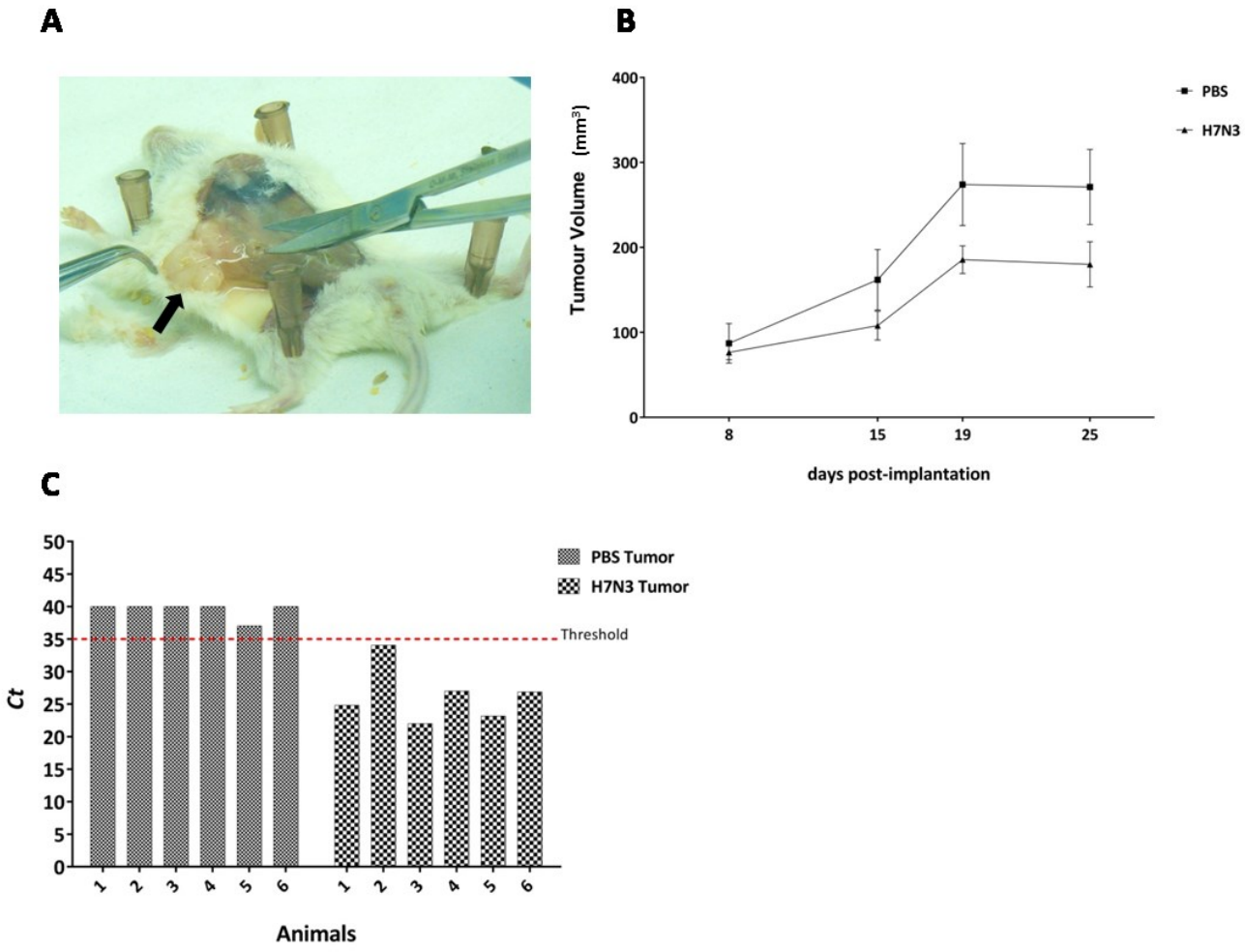

Figure 26. ***Oncolytic effects of H7N3 A/turkey/Italy/2962/03 influenza virus in SCID xenograft model. A****) BxPC-3 derived solid tumour in SCID-B17 mice.* ***B****) Oncolytic effect of H7N3 A/turkey/Italy/2962/03 virus in BxPC-3 xenograft mouse model. Twelve Six-week-old female SCID mice were subcutaneously implanted with 5 x 10^6 BxPC-3 cells in a volume of 100 µL into the right flank. At 8 days post-implantation palpable tumour became established, and mice were randomly divided in two groups (n=6 each), receiving either four intra-tumoural injections of 2.4 x 10^4 pfu of low pathogenic H7N3*

*virus (triangles) between day 8 and day 15 or four injections of PBS (squares). Caliper measurements of tumour dimensions were taken on indicated days post-implantation for calculation of tumour volumes. Data shown represent means of tumour volume + SEM. **C**) Real-time RT-PCR detecting influenza virus' Matrix (M) gene in tumour collected from different mice. Based on diagnostic procedures in place at IZSVe the Ct value of 35 is considered the threshold between a weak positive sample and a negative sample.*

2.3 Discussion and conclusion

The present data demonstrate that avian influenza A virus can infect, replicate in and induce apoptosis in several human PDA cell lines. Characterization of the receptor profiles of a panel of human PDA cell lines shown that these cells contained both α-2,6- and α -2,3-sialic acid linkages, explaining their susceptibility to infection by both avian and mammalian viruses. While the upper respiratory tract (URT) is the primary site of infection for human influenza viruses as a result of high levels of α-2,6-linked SAs, the expression of α-2,3-linked SAs has been detected in other human tissues, including endothelial cells of the heart, brain, intestines, and liver as well as nonciliated cells in the lungs (Yao et al., 2008). Although all PDA cell lines expressed both types of SA receptors on their surfaces, differences in expression levels were noted (Kasloff et al., 2014). Such heterogeneity in the levels of SA expression in different cell lines was not surprising, as altered levels of expression of sialyltransferases and fucosyltransferases have been demonstrated in different types of tumors, including pancreatic, breast, colon, gastric, cervical, and renal cancers (Mas et al., 1998; Peracaula et al., 2005).

Annexin V staining results demonstrated that levels of IAV-induced apoptosis in PDA cells varied depending on the virus isolate and cell line tested (Figure 22A). While several of the isolates tested showed a significantly enhanced ability to induce apoptosis compared to the treatment with gemcitabine and cisplatin, the H7N3 A/turkey/Italy/2962/03 isolate repeatedly outperformed the others, including the human PR8 virus currently tested as oncolytic virus for other tumour types, in terms of the rapidity and potency of cell death induced. Although it is not possible to completely

rule out an especial efficient ability of the H7N3 virus to bind and thus infect PDA cells, the results appear in line with the strain-specific variations in apoptotic induction previously documented in primary cultures and established cell lines in the cases of human, avian, and swine influenza viruses (Choi et al., 2006; Mok et al., 2007). These observations about the H7N3 isolate led us to further investigate its oncolytic potential.

Among the different tumour cell lines tested, we focused on BxPC-3, a PDA cell line previously shown "resistant" to other oncolytic viruses including Vesicular Stomatitis Oncolytic Virus (VSV), Conditionally Replicative Adenoviruses (CRAds), Sendai Virus (SeV) and Respiratory Syncytial Virus (RSV) (Murphy et al., 2012), but which surprisingly appeared to be highly sensitive to IAV infection (Figure 22A).

Immunocytochemistry (ICC) for the expression of effector caspase-3 in BxPC-3 and HPDE6 infected cells, confirmed the higher sensitivity of the tumour cell line over the resistant "benign" line (Figure 23A-B-C). Since KRAS mutations are known to increase resistance to apoptosis (Guerrero et al., 2000), the fact that BxPC-3 cells contain a wild-type KRAS (Table 3) may partially explain the higher levels of cell death observed in this tumour cell line compared to the others. However, the facts that non-transformed HPDE6 cells also contain wild-type KRAS and display a resistant phenotype suggests that other contributing factors are at play. Among these factors, the lack of expression of functional IFN and MxA (Figure 24) antiviral genes might exert a pivotal role. As discussed in chapter 1 (see paragraph 1.5.2), IFN expression can act in autocrine and/or paracrine manner to heighten the cell anti-viral defences; while MxA can counteract virus replication by preventing nuclear import of the vRNPs especially in the case of viruses presenting nucleoproteins (NPs) of avian origin (see paragraph 1.6.2.3). Thus the lack of expression of IFN and MxA genes, even at basal level, might contribute to the permissive phenotype displayed by BxPC-3 cells infected with the avian origin H7N3 A/turkey/Italy/2962/03 virus compared to the resistant HPDE6 cells.

Further ICC studies targeting initiator caspases 8 and 9 in infected BxPC-3 cells, demonstrated that H7N3-induced apoptosis was mainly the result of a strong strain-dependent activation of the intrinsic pathway (Figure 25A).

Building on results observed *in vitro*, an experiment using a SCID mouse xenograft model was performed to examine the oncolytic activity of the H7N3 A/turkey/Italy/2962/03 virus *in vivo*. As reflected by *in vitro* sensitivity, BxPC-3-derived tumours showed significantly reduced growth following H7N3 treatment compared to growth after treatment with PBS alone (Figure 26B). The presence of viral RNAs in neoplasm homogenates of all H7N3-treated animals sacrificed at the end of the experiment confirmed that all tumours were successfully infected with IAV (Figure 26C). Given the reduced ability of the LPAI viruses to undergo multiple rounds of replication in PDA cells *in vitro* (Kasloff et al., 2014), most likely due to protease-limiting conditions, the H7N3 virus was not expected to display numerous rounds of infection in BxPC-3 xenograft model. However, detection of viral RNAs in treated tumours up to 1 week following the final injection suggests that virus replication did occur within the tumour microenvironment. Indeed, previous papers immunohistochemically demonstrated the presence of mild to marked immunoreactivity to pancreatic trypsinogen in 75% of the 23 surgically resected pancreatic ductal adenocarcinomas (Ohta et al., 1994), reporting also that some human pancreatic ductal cancer cells, including BxPC-3, express and secreted pancreatic cationic-type tripsinogen in vitro, which can be spontaneously converted into active trypsin at acid pH of tumour microenvironment (Ohta et al., 1998). Thus it may well be that BXPC-3 cells can support multiple rounds of influenza virus infection because they secret activating proteases that can cleave the HA protein, a necessary step in the virus replication cycle.

In any case, the selective pro-apoptotic effect of the virus observed in tumour BxPC-3 cells, previously shown resistant to other oncolytic viruses, strengthen the idea that research in the area of oncolytic virology should not be focused on a short list of candidates, but rather on a broad

range of viruses characterized by specific cancer cell permissiveness, and that influenza virus could play a role in further studies on treatment of PDA. To this purpose the H7N3 A/turkey/Italy/2962/03 virus, which shown the highest oncolytic activity in PDA cells, was selected and the corresponding reverse genetics backbone was generated for additional development.

Chapter 3. NS1-77 truncation: enhancing IAV selectivity and oncolytic potential by reducing control of host antiviral response.

3.1 Introduction

Based on the sensitivity to IAVs displayed in preliminary results (see paragraph 2.2.1), our research focused on BxPC-3, a PDA cell line that was previously shown "resistant" to other oncolytic viruses including Vesicular Stomatitis Oncolytic Virus (VSV), Conditionally Replicative Adenoviruses (CRAds), Sendai Virus (SeV) and Respiratory Syncytial Virus (RSV) (Murphy et al., 2012). Like many PDA cells, BxPC-3 present homozygous deletion of genetic material within chromosome arm 9p21, where interferon alpha and beta (IFN-α/β) genes are located (see paragraph 2.2.2). Indeed, this loss has been shown to determine lack of functional IFN expression in nearly 80% of PDA cells, although responsiveness to exogenous IFN can be maintained in some cases (Murphy et al., 2012; Vitale et al., 2007). As such we reasoned that OV selectivity to these cells could be enhanced by creating viruses defective in IFN antagonism, which should not replicate efficiently if at all in interferon competent cells but can still replicate and trigger apoptosis in cells deficient in IFN induction or response.

Influenza A virus non-structural protein 1 (NS1) is a 219-237 amino acid protein expressed at very high levels in infected cells. Although it is a multi-functional protein, the major role ascribed to NS1

is to antagonize host IFN-mediated antiviral responses (see paragraph 1.5.4). Due to its role in counteracting host type I IFN expression, an IAV that lacks NS1 protein expression (ΔNS1) fails to replicate efficiently in normal cells. However, in cancer cells with deficient IFN responses, such mutants have been shown to be able to replicate and cause cell death (Bergmann et al., 2001; Muster et al., 2004). Moreover, a recombinant NS1 truncated influenza virus that has intermediate attenuation characteristics between ΔNS1 and wild-type viruses showed superior beneficial effect in mice due to an improved attenuation/replication balance (Muster et al., 2004).

Thus, to obtain a virus that could replicate efficiently in IFN deficient PDA cells but not in healthy IFN competent cells, we decided to introduce mutations within the IAV NS1 gene to create a premature termination codon and produce a protein of only 77 amino acids (NS1-77), resulting in complete loss of the effector domain (ED), which interacts with a variety of different cellular protein to mitigate host IFN expression and apoptosis (Figure 27A) (see paragraph 1.5.4). Position aa 77 was selected for the termination codon as mutations at this site did not affect the coding of the nuclear exporting protein (NEP), which is also expressed from viral RNA segment 8 (Figure 27B) (see paragraph 1.5.4). Furthermore, the truncation occurs within the linker region (LR) and thus should not change the folding of the RNA binding domain (RBD) (Figure 27C) or its ability to self-associate in dimers, although the loss of the ED domain might also reduce the dsRNA binding efficiency of the N-terminal domain by preventing higher-order multimerization of NS1 dimers (Hale, 2014).

Thus, we generated a complete reverse genetics system for the recovery of recombinant virus based on the backbone of the low pathogenicity avian influenza virus (LPAIV) H7N3 A/turkey/Italy/2962/03, which triggered high levels of apoptosis in different PDA cell lines (see paragraph 2.2.1) and displayed beneficial effect in mouse model (see paragraph 2.2.4). Using this system, a mutated virus bearing truncated NS1-77 gene was generated and propagated in Npro-MDCK cells that express NPro gene of Bovine Viral Diarrhea Virus (BVDV) and thus lack of IFN

expression. We then compared the H7N3 NS1-77 properties with those of the isogenic recombinant wild type virus bearing a full length NS1.

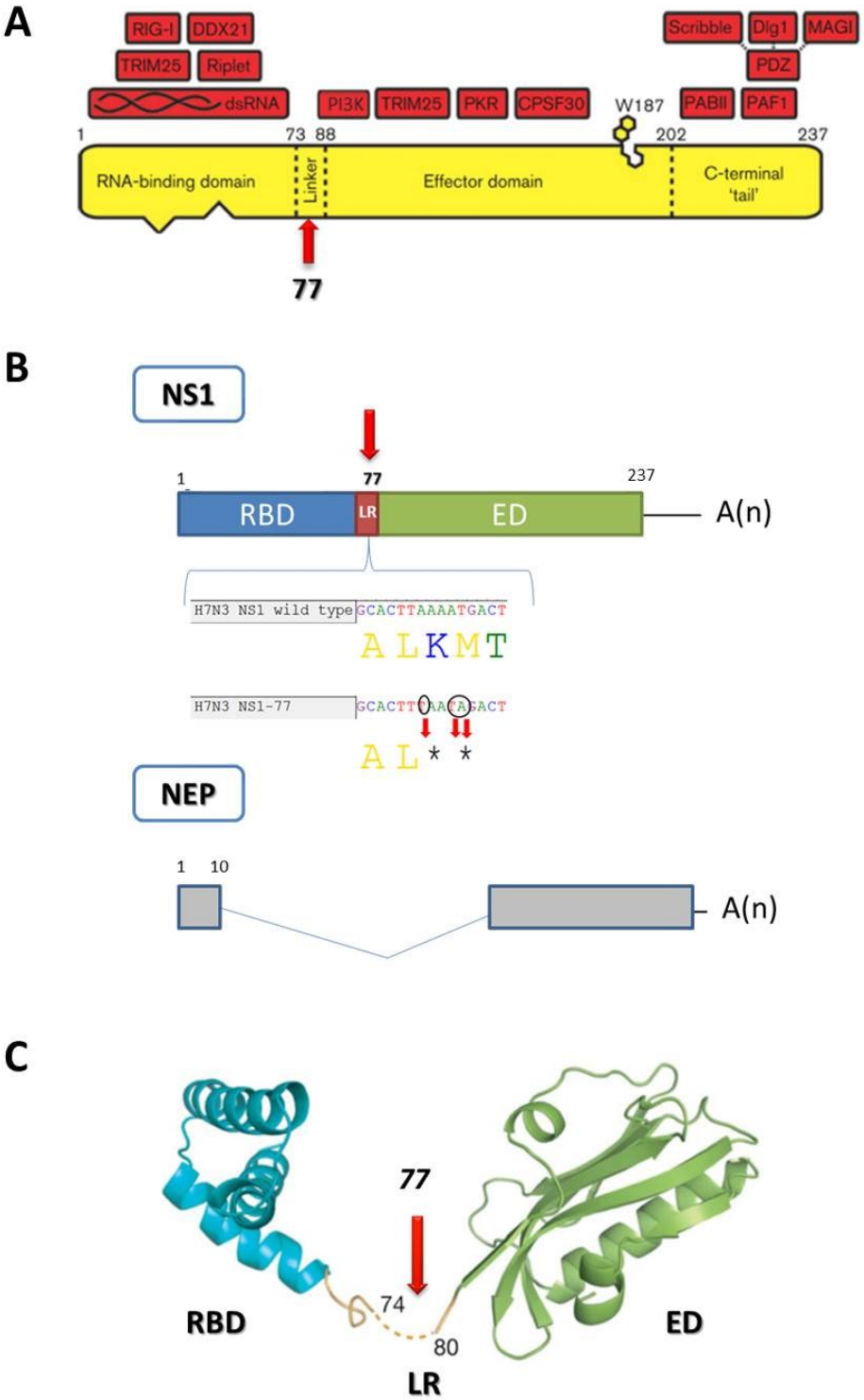

Figure 27. ***The H7N3 NS1-77 truncation. A)*** *Linear schematic representation of the NS1 domain layout (yellow) and host-proteins interaction sites (red). NS1 can be divided into three distinct regions: the N-terminal RNA-binding domain (RBD), the linker region (LR) and the effector domain (ED) which include also the "C-terminal tail". Interaction sites for NS1 to form homo-multimers are present in both the RBD (triangular cut-outs) and ED (W187). Adapted from* (Hale, 2014). ***B)***

Nonsense mutations introduced to obtain the H7N3 NS1-77 protein. The NS1 truncated protein possesses the RBD, but not the ED. The introduced mutations do not affect the NEP open reading frame, because they occur in a region that undergoes splicing during NEP mRNA synthesis. ***C)*** *Cartoon representation of the NS1 structure as viewed looking across the main a-helix of the RBD (aquamarine). The ED is coloured green, and the linker region (LR) orange. Red arrow indicates the aa position 77. Adapted from* (Bornholdt and Prasad, 2008)

3.2 Results

3.2.1 NS1-77 truncation determines faster progression of apoptosis in infected BxPC-3 cells.

To check whether NS1-77 truncation might have a detrimental effect on the apoptosis levels previously displayed by the wild type H7N3 virus, annexin V assay was performed in BxPC-3 and HPDE6 cells infected with full length or truncated NS1 viruses. Specific Cell Death (SCD%), defined as described in material and methods, was measured at 16 and 24 hours post-infection. Incubation of the cells with Gemcitabine and Cisplatin was included as positive control for apoptosis.

BxPC-3 and HPDE6 cells were equally susceptible to the treatment with chemotherapeutic agents (Figure 28A-B). However, in line with previous results (see paragraph 2.2.1), influenza virus induction of apoptosis was far more selective to tumour cells than to benign HPDE6 cells at both 16 and 24 hours post-infection (Figure 28A-B).

Interestingly, in permissive BxPC-3 cells, apoptosis induced by the NS1 truncated virus reached its peak at 16 hours post-infection, displaying significantly more cell death than the wild type at this time-point (Figure 28C). However, this effect was not maintained at later time post-infection (24h) when the levels of apoptosis triggered by the H7N3 NS1-77 virus were not further increased and the wild type reached similar SCD (Figure 28C). These data suggest that the NS1 truncation does not improve the pro-apoptotic skills of the virus in infected cells but rather allows the progression of cell death, once primed, to occur faster due to the loss of anti-apoptotic functions. The finding is consistent with previous publications showing that the NS1 ED can interact with cellular proteins

such as PKR (Li et al., 2006), PI3K/Akt (Shin et al., 2007b) and Scribble (Liu et al., 2010) implicated in the apoptotic pathway, contributing to delayed apoptosis during infection.

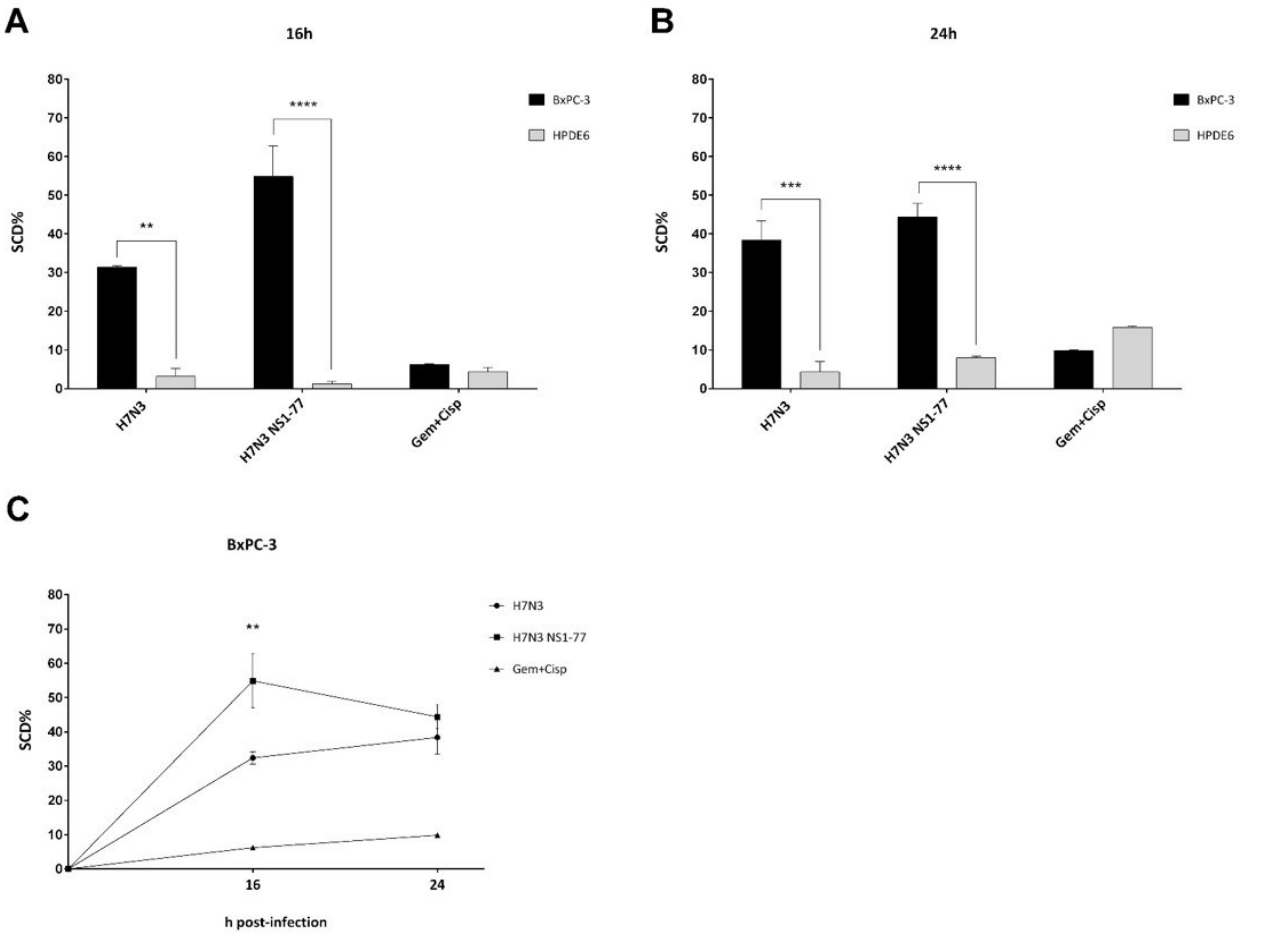

Figure 28. ***H7N3 and H7N3 NS1-77 annexin V results in BxPC-3 and HPDE6 cells.*** *Specific cell death (SCD) triggered by apoptosis in BxPC-3 and HPDE6 cells at 16 (**A**) and 24 (**B**) hours post-infection with H7N3 and H7N3 NS1-77 influenza virus (m.o.i.= 0.1). Treatment with Gemcitabine and Cisplatin was used as positive control for apoptosis. **C**) Time-course analysis of BxPC-3 SCD following infection with the different mutant viruses and chemotherapeutic agents. All data represent means ± standard deviations (SD) of two independent experiments. Statistical significance was determined using Two-way ANOVA followed by Tukey's multiple comparison test.*

3.2.2 H7N3 NS1-77 virus infection triggers high levels of IFN expression in benign cells.

Because of the strain-specific characteristics of NS1 protein, to investigate the effect of the truncation on the protein's ability to limit host IFN response during infection, a second pair of full

length NS1 or NS1-77 truncated IAVs were also generated using the genetic backbone of the well-studied laboratory human strain H1N1 A/Puerto Rico/8/34 (PR8).

The ability of the two pairs of IAVs to counteract the host IFN-mediated antiviral response was first assessed in A549-IFNLuc cells, a human lung cell line expressing a reporter construct in which the luciferase gene is downstream of an IFN-β promoter (Hayman et al., 2006). A549-IFNLuc cells were infected with the different engineered viruses at equal multiplicity (M.O.I. = 1) and after an eight hour infection they were lysed and measured for luciferase activity (Figure 29A). The resulting luciferase signal was an indirect measure of IFN expression and therefore it was inversely dependent on the virus ability to counteract IFN. Results showed that the H7N3 wild type virus efficiently controlled IFN induction as no difference was observed compared to the mock infection (Figure 29A). However, the H7N3 NS1-77 virus induced a significantly higher luciferase signal than the mock infection or the infection with the H7N3 wild type virus. Interestingly, while the truncation of the NS1 ED in this avian isolate led to a strong reduction of the ability to limit IFN induction, the difference in the IFN expression induced by human PR8 viruses with full length or truncated NS1 proteins was less pronounced.

To test the extent to which each of the recombinant influenza viruses would induce IFN in pancreatic cells, an indirect method was used (Figure 29B). Pancreatic ductal adenocarcinoma BxPC-3 cells and “benign” HPDE6 cells (Furukawa et al., 1996; Ouyang et al., 2000) were infected with an equal multiplicity of each recombinant IAV. Eight hours after infection, supernatants that would contain any induced secreted cytokines were collected, and any viruses present were inactivated under a germicidal lamp. The treated supernatants were transferred onto 293T cells previously transfected with ISG54Luc plasmid, which encoded the firefly luciferase gene driven by the interferon-inducible ISG54 promoter. A RenillaLuc plasmid encoding the renilla luciferase as transfection control was also included. The firefly luciferase signal from the ISG54 promoter was an indirect measure of IFN expression from BxPC-3 or HPDE6 cells during viral infection and as such it

was inversely dependent on the virus' ability to counteract IFN in these cells. Consistent with our preliminary data (see paragraph 2.2.2) and with previous publications reporting the lack of IFN-α/β expression in BxPC-3 cells due to chromosomal aberrations (see paragraph 1.2.3), the results showed no significant differences in the ISG54 stimulation between the supernatants derived from BxPC-3 cells infected with any of the influenza viruses and the mock infection (Figure 29B). However, supernatants from infected HPDE6 cells triggered luciferase signals from the ISG54 promoter and to a different extent depending on the virus used to infect. The trend was the same as previously shown in the A549-IFNLuc assay. The H7N3 NS1-77 bearing a truncated NS1 protein did not efficiently limit the IFN expression whereas parental H7N3 with full length NS1 gene did (Figure 29B). Recombinant PR8 NS1-77 virus was not affected as much as H7N3 NS1-77 by the truncation, since it did not show any significant difference in ISG54 stimulation compared to its wild type virus counterpart.

The likely explanation for the profound effect of H7N3 NS1 truncation on the virus' ability to control interferon compared to the same mutation in the PR8 virus is that the way in which different NS1 proteins can limit IFN expression differ between the influenza virus strains. Most NS1 protein can work to inhibit IFN at two different levels: first pre-transcriptionally by inhibiting RIG-I recognition of viral PAMPs and/or RIG-I ubiquitination by TRIM25, and second post-transcriptionally by binding to CPSF30 and inhibiting processing of induced host cell mRNAs such that they are not expressed (see paragraph 1.5.4). Previous studies showed that the NS1 protein of H1N1 A/PR/8/34 (PR8) limits pre-transcriptional events associated with IFN-β expression, but is apparently unable to block post-transcriptional processing of IFN-β pre-mRNAs due to amino acid substitutions in position 103 and 106 that block the interaction with the cleavage and polyadenylation specificity factor (CPSF30) (Kochs et al., 2007; Steidle et al., 2010). To appraise the ability of H7N3 NS1 to limit host gene expression, the NS1 proteins were cloned into pCAGG expression plasmids so they could be expressed in the absence of other viral proteins. To monitor expression of a gene that is transcribed

by host polymerase II, 293T cells were transfected with pCAGGLuc plasmid, which directs polymerase II mediated expression of firefly luciferase (Figure 29C). In addition, to measure the effect of NS1, one of the following plasmids: pCAGG/PR8 NS1, pCAGG/H7N3 NS1, pCAGG/H7N3 NS1-77 and empty pCAGG (K-) was co-transfected. The expression of luciferase in 293T was dependent on the ability of the different NS1 proteins to interfere with the maturation of the luciferase pre-mRNA. When full length PR8 NS1 protein was expressed, the levels of luciferase activity were comparable with those obtained if the empty pCAGG plasmid were transfected (Figure 29C). Conversely, the presence of full length H7N3 NS1 blocked luciferase expression, suggesting that the protein possesses the capability to interact with CPSF30. However, the truncation of the ED (NS1-77) resulted in the loss of this capability and restored luciferase expression to a level comparable with that measured with PR8 NS1 or empty pCAGG.

Western Blot results showed that all the NS1 proteins were expressed, although different levels of expression were observed (Figure 29C). During an infection the polyadenylation of IAV mRNAs is independent of cellular 3'-end processing factors (see paragraph 1.4.5.2); therefore in the context of the virus infection viral mRNAs are not affected by CPSF30 inhibition. However, in this assay the NS1 protein was encoded by a plasmid that underwent post transcriptional processing as a regular host cell mRNA. As a consequence the production of an NS1 protein efficiently able to interact with CPSF30 should limit its own expression. Accordingly, H7N3 NS1 protein showed lower levels of expression compared to PR8 NS1, but truncation of the ED restored expression of H7N3 NS1-77 protein to similar high levels as the PR8 NS1. Taken together, the luciferase assay and the western blot results also demonstrate that a small amount of functional H7N3 NS1 protein can trigger a high inhibition of host cell pre-mRNA processing.

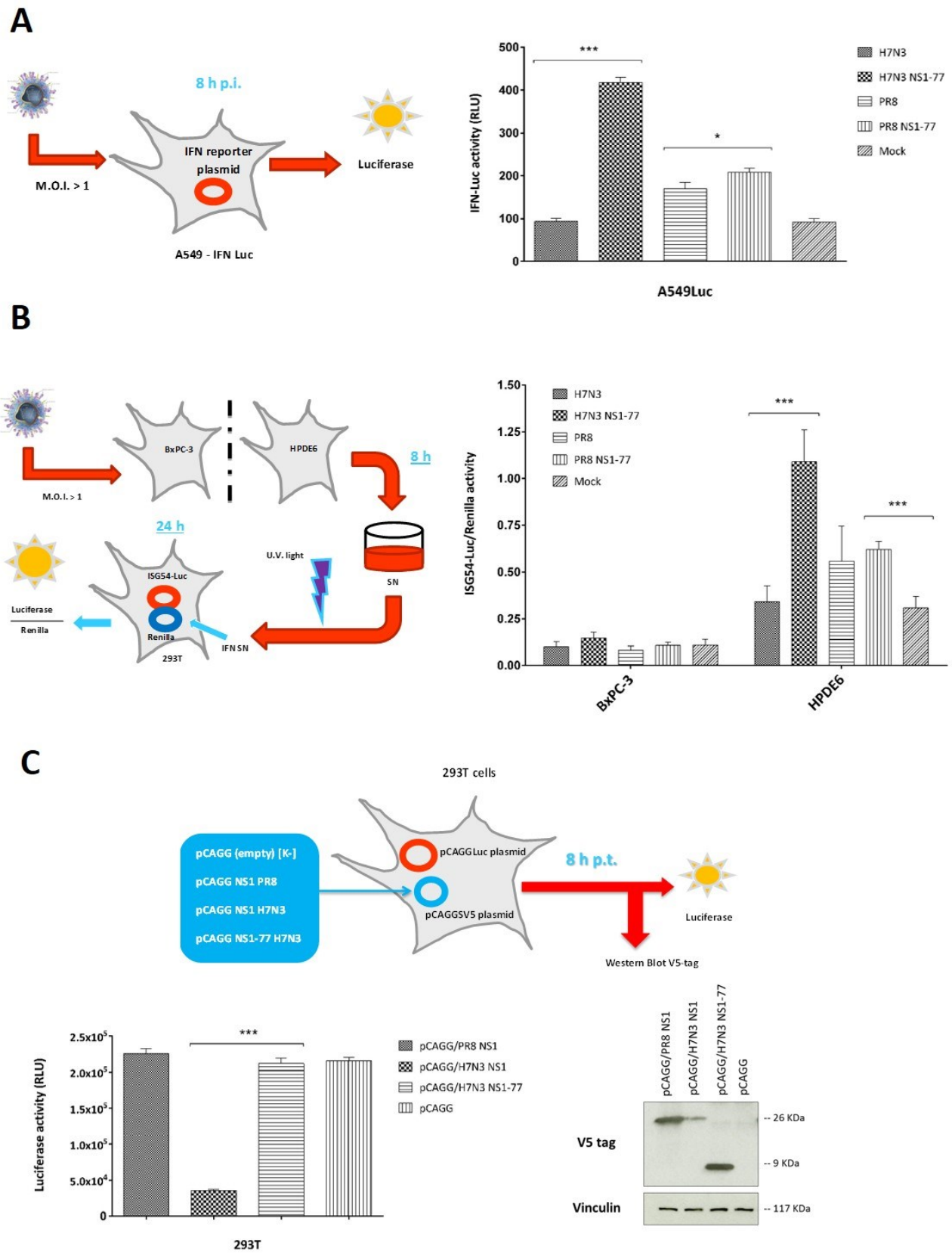

Figure 29. ***Strain specific effect of NS1-77 truncation on IFN expression in infected cells. A****) IFN-β expression in A549-IFNLuc cells infected with H7N3 and PR8 reverse genetics viruses bearing full length or truncated NS1 protein. Results are shown as raw data and expressed as RLU (relative light units).* ***B****) ISG54 expression induced by supernatant obtained from HPDE6 or BxPC-3 cells infected with recombinant IAVs. HPDE6 and BxPC-3 cells were infected with H7N3 or PR8 reverse*

genetics viruses bearing full length or truncated NS1 protein. At 8 hours post-infection, the supernatants were collected, inactivated under ultraviolet radiation and transferred on 293T cells previously transfected with ISG54Luc plasmid, encoding the firefly luciferase gene driven by the inducible promoter ISG54, and RenillaLuc, encoding the renilla luciferase. After 24 hours 293T cells were washed, lysed and tested for luciferase activity. Results are shown as Luciferase/Renilla ratio. ***C****) Luciferase expression in 293T cells co-transfected with pCAGGLuc, stably expressing firefly luciferase, and pCAGG/H7N3 NS1, pCAGG/H7N3 NS1-77, pCAGG/PR8 NS1 or empty pCAGG (K-). Results are shown as raw data and expressed as RLU (relative light units). Western Blot targeting SV5 tag was performed to confirm NS1 protein expression in the cell lysates following transfection of pCAGG plasmids encoding different NS1 genes. Vinculin was used as a loading control. All data represent means ± standard deviations (SD) of one representative experiment (n=3). Statistical significance was determined using One-way ANOVA followed by Bonferroni's multiple comparison test.*

3.2.3 H7N3 NS1-77 virus shows diminished replication in IFN-expressing targets.

Having proved that truncation of H7N3 NS1 protein significantly reduced the virus ability to antagonize the interferon response, we next tested whether this conferred a degree of preference for the virus to replicate in IFN deficient systems, representing the majority of PDA cells.

Replication of H7N3 and H7N3 NS1-77 viruses was monitored over a 72 hour time-course in IFN-competent HPDE6 cells and IFN-deficient BXPC-3 cells. Results confirmed that, although viral growth in either cell line was not high, overall, replication levels were higher in permissive tumour BxPC-3 cells than in HPDE6 cells (Figure 30A-B).

In IFN deficient BxPC-3 cells viral titres showed significant increase at 72 hours compared to those at 24 hours post-infection for both viruses and no significant differences between full length and truncated NS1 virus was observed at any given time-point (Figure 30A). Conversely, in IFN-competent HPDE6 cells only the wild-type virus showed significant growth between 24 and 72 hours post-infection, with the NS1-77 truncated virus displaying appreciable lower replication ability (Figure 30B). Although the results are in line with the data generated using direct and indirect IFN assay and seem to confirm that H7N3 NS1-77 virus had restricted replication in IFN expressing systems compared to the corresponding full length NS1 virus, we have to acknowledge that the truncation only appears to attenuate H7N3 virus in HPDE6 cells by about 2-fold, which is

extremely modest by virological standards. Because this might be due to suboptimal levels of proteases available (see paragraph 2.2.1) or to higher sensitivity of avian IAV isolates to mammalian ISGs (see paragraph 1.6.2.3), we decided to test the effect of NS1 truncation also in Embryonated Chicken Eggs (ECE), which represent a more standard laboratory medium for propagating avian influenza viruses.

The susceptibility of ECE to many viruses may change during the embryonic or neonatal development. Baron and Isaacs (Isaacs and Baron, 1960) first suggested that increasing resistance of the chicken embryo to certain viruses might be due to increased ability of older embryonic tissues to produce and respond to interferon. Morahan and Sidney (Morahan and Grossberg, 1970) showed that different viruses including IAV, VSV and NDV grew to lower titres in cells derived from older chicken embryos, capable of mounting a mature IFN response, than in those derived from younger embryos. Based on these reports, the growth of full length and truncated NS1 H7N3 viruses in 7 and 14 days old ECE was used to compare their replication in IFN impaired and competent systems.

Ten specific pathogen free (SPF) ECE of either 7 or 14 days of age were infected with 10^3 pfu/egg of recombinant H7N3 NS1-77 or full length NS1 viruses. Eggs were then incubated at 37°C and candled daily to monitor the embryo death for 5 days. Allantoic fluids harvested from all eggs were screened by rapid haemagglutination test and those positive in each group were pooled together. Viral titre of the pooled fluids was measured by haemagglutination assay (HA). Results showed that the two viruses reached the same HA titre in 7 day old ECE, whereas the HA titre of the wild type H7N3 virus was $3\log_2$ higher than the truncated virus in fully IFN competent 14 day old ECE (Figure 30C). These data confirm that H7N3 NS1-77 virus have restricted replication in IFN expressing systems compared to the corresponding full length NS1 virus, but displays the same growth as an otherwise isogenic wild type virus in IFN deficient systems.

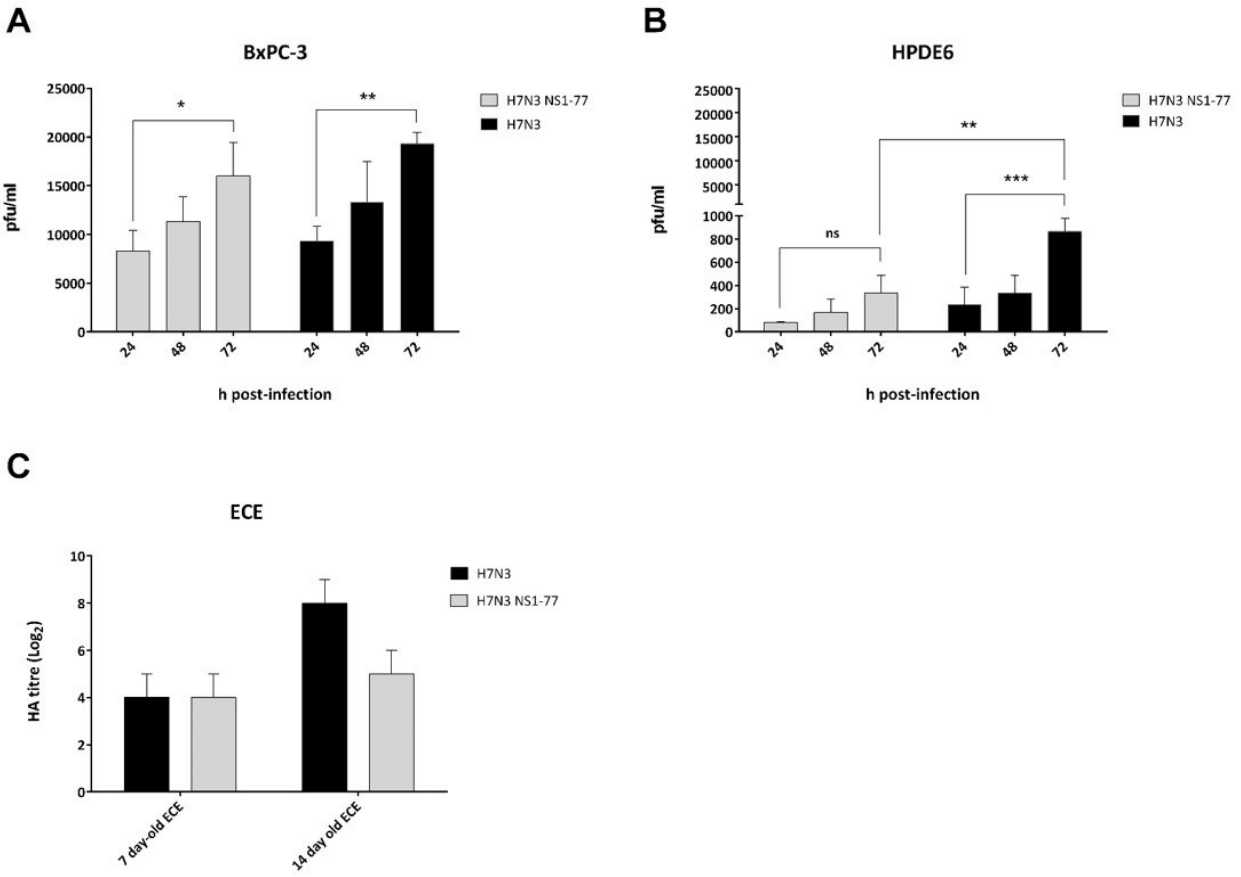

Figure 30. ***Replication kinetics of H7N3 and H7N3 NS1-77 IAVs in BxPC-3 and HPDE6 cell lines.*** *H7N3 and H7N3 NS1-77 virus replication was monitored over a 72 hour time-course in IFN-deficient BxPC-3 (**A**) and IFN-competent HPDE6 (**B**) cells. Cells were infected at an M.O.I. of 0.001 and virus titres of the supernatants were determined via plaque assay on MDCK-NPro cells at 24, 48 and 72 hours post-infection. Results represent means plus standard deviation (SD) of three independent experiments. Statistical differences for each virus at different time-points were determined using Two-way ANOVA followed by Tukey's multiple comparison test; while difference between the two viruses at each time-point were evaluated using Bonferroni post-test.* ***C)*** *H7N3 and H7N3 NS1-77 virus growth in 7 and 14 day old embryonated chicken eggs (ECE). PBS antibiotic solution containing each virus was inoculated into the allantoic cavity of 7 and 14 day-old ECE. The eggs were incubated at 37°C and candled daily for 5 days (120 h). For each group, the allantoic fluid of any eggs positive to rapid hemagglutination test after embryo's death or at the end of the incubation period were pooled together and the virus titre was measured using haemagglutination assay (HA assay).*

3.2.4 The immunostimulatory activity of H7N3 NS1-77 virus in infected healthy cells enhances its oncolytic effect via IFN-mediated cell killing of neighbouring uninfected PDA cells.

Different studies demonstrated the efficacy of IFN-α and β in the treatment *in vitro* and *in vivo* of several tumours types (Lindner et al., 1997; Vitale et al., 2006). Although IFN-α and β are multifunctional cytokines that binds the same receptors (IFNAR1 and IFNAR2), the latter possesses greater anti-tumour effect (Damdinsuren et al., 2003; Johns et al., 1992; Rosenblum et al., 1990; Vitale et al., 2006). In line with this considerations, as previously discussed (see paragraph 1.3.1.4), oncolytic viruses armed to express IFN-β are currently under clinical trials.

Vitale et al. (Vitale et al., 2007), showed that also in PDA cells, which often retain sensitivity to exogenous IFN (see paragraph 1.2.3), IFN-β is significantly more effective than IFN-α in inhibiting tumour cell growth by inducing more potent cell cycle arrest and apoptosis activation at very low doses, particularly in tumours with a high expression of IFNAR-1 and IFNA-2c receptors. A later publication by Tomimaru et al. (Tomimaru et al., 2011) demonstrated that IFN-β is able to act synergistically with gemcitabine to reduce the cell growth of pancreatic cancer cells, even in cell lines that are nonresponsive to IFN-α and have a low IFNAR-2 expression. In line with these observations, a recent study evaluating the effects of IFN-α and β in 11 human pancreatic cancer cell lines, showed that the expression level of the type I IFN receptor (IFNAR-1 and IFNAR-2c) is of predictive value for the direct antitumor effects of IFN-α, but not of IFN-β (Booy et al., 2014). Indeed IFN-β induced a potent antitumor effect at low concentrations and its activity was less dependent on IFN receptor expression, making it a more promising therapeutical agents than IFN-α. Local production of IFN-β was shown to induce a strong anti-tumour effect on PANC02-H7 cells, a highly metastatic mouse pancreatic adenocarcinoma cell line, successfully transfected with a vector containing a murine IFN-β gene (Wang et al., 2001). Thus, having demonstrated that the H7N3 NS1-

77 virus induces higher levels of IFN-β expression in IFN competent cells compared to the wild type (see paragraph 3.2.2), we hypothesized that by stimulating the antiviral response in healthy cells, which in a real situation are in contact with the tumour, the truncated virus might indirectly trigger a significant IFN-mediated killing of neighbouring uninfected PDA cells.

To test this hypothesis, confluent monolayers of IFN-competent HPDE6 cells, which present a near normal genotype and phenotype, were infected in 12 well plates with H7N3 and H7N3 NS1-77 at M.O.I=1 or mock infected (Figure 31A). After 24 hours supernatants were collected and treated under germicidal lamp to inactivate potential infectious particles in the suspension as confirmed by subsequent plaque assay. The VeriKine Human IFN-β ELISA kit (pbl Assay Science) was then used for quantitative measurement of IFN-β in the supernatants derived from HPDE6 infections (Figure 31A). Next different monolayers of PDA and HPDE6 cells were incubated with the conditioned media derived from previous infection. After 16 hours incubation the media was discharged and cells were tested for the presence of cytoplasmic histone-associated DNA fragments, a hallmark of apoptosis progression (see paragraph 1.5.3), using the Cell Death Detection ELISA^{PLUS} photometric enzyme immunoassay (Roche – Life Science) (Figure 31A).

Human IFN-β ELISA results showed higher concentration of the soluble cytokines in the HPDE6 supernatants derived from H7N3 infection than in those from mock infection (Figure 31B). This result slightly differed from the data obtained in the previous plasmid-based assays, where no significant difference was observed between these two conditions (Figure 29B), but this was likely due to the later time post-infection of the sampling (8h vs 24h). Nevertheless, consistent with previous results (Figure 29B), IFN-β concentration in the media from H7N3 NS1-77 virus infection was significantly higher compared to the supernatant from full length NS1 virus infection.

Cell death results (Figure 31C) showed that infectious particle-free HPDE6 cell supernatants containing IFN-β were capable of inducing apoptosis in various PDA cell lines to different extents. Indeed diverse degrees of sensitivity to exogenous IFN-β, depending on the PDA cell line, have been

previously reported (Booy et al., 2014; Vitale et al., 2007). Consistent with these publications, in comparison to the cell death triggered by supernatants derived from mock infection, BxPC-3 and AspC-1 cell lines displayed the highest sensitivity to conditioned media that contained IFN, followed by CFPAC-1 and by the more resistant Mia Paca-2. Benign HPDE6 cells were not affected by conditioned media, although it is not possible to exclude that longer incubation period might have also increased the amount of apoptosis occurring in this cell line.

In addition and even more interesting, the results showed that HPDE6 cell supernatants derived from H7N3 NS1-77 infection provoked significantly higher levels of cell death in all the PDA cells tested than those derived from full length NS1 virus infection. Thus, taken together, these data suggest that H7N3 NS1-77 virus might trigger higher apoptosis in uninfected PDA cells as consequence of a stronger stimulation of IFN production from infected neighbouring healthy cells, which would be also more resistant to this effect.

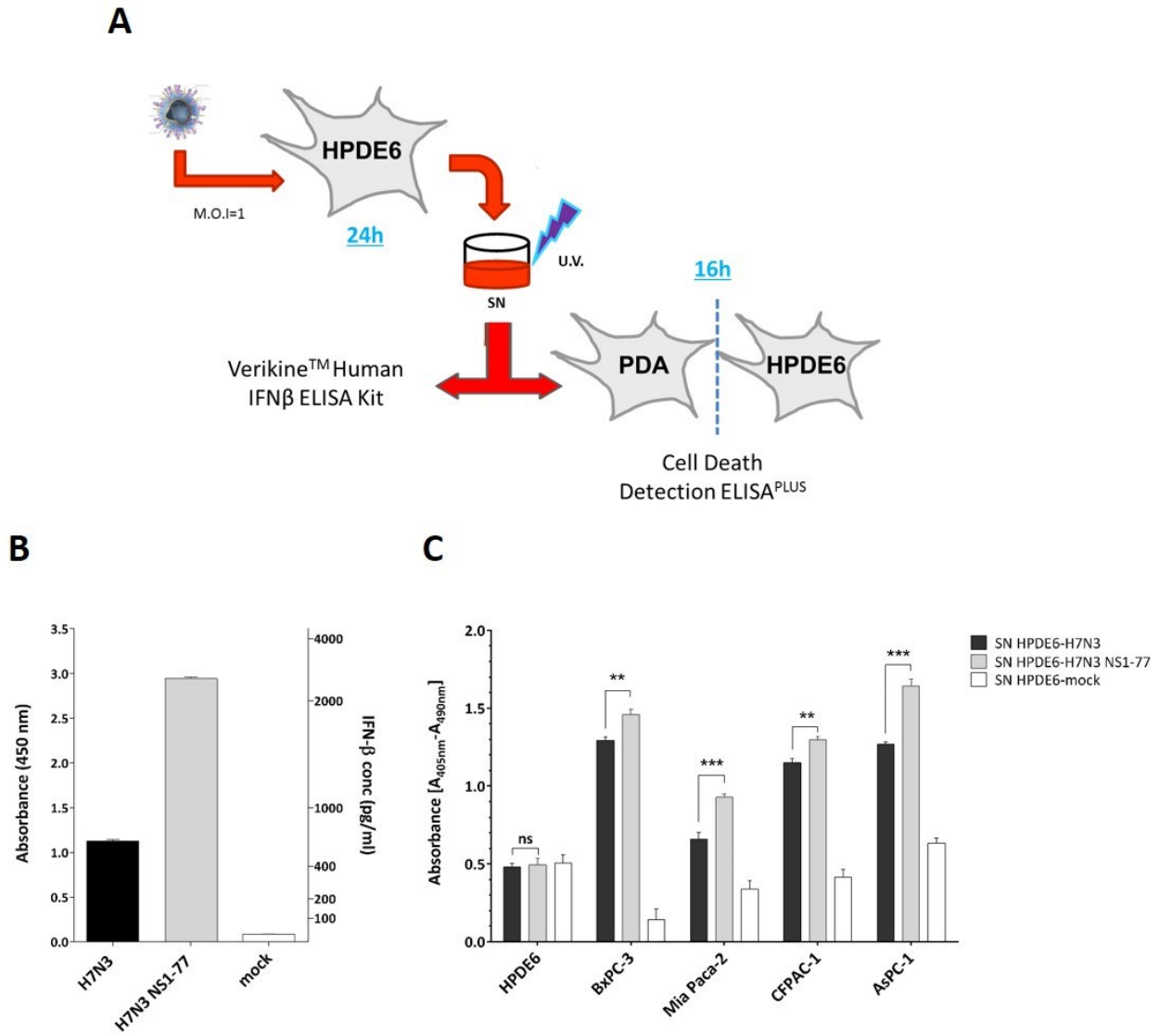

Figure 31. ***Sensitivity of PDA cells to exogenous IFN. A)*** *Schematic representation of the experiment. HPDE6 cells were infected at M.O.I = 1 pfu/cell with H7N3, H7N3 NS1-77 virus or mock infected. After 1 h absorption, the media were replaced with 3% FBS RPMI 1640 without trypsin, and the cells were incubated for further 24 hours. Next the supernatants were collected and exposed to the ultraviolet radiation from a germicidal lamp for 10 minutes in order to inactivate any infectious virus. Quantitative measurement of IFN-β in the supernatants was performed using the VeriKine Human IFN Beta ELISA kit (pbl Assay Science). The inactivated supernatants were then placed on different PDA and HPDE6 cells and incubated for 16 hours. Apoptosis triggered by conditioned media in the different cell lines was measured using Cell Death Detection ELISA^{PLUS} photometric enzyme immunoassay (Roche – Life Science).* ***B)*** *Human IFN-β ELISA kit results for HPDE6 cell supernatants collected at 24h post-infection with H7N3, H7N3 NS1-77 viruses or mock infected. For each group absorbance values at 450 nm are represented (left Y axis) and the correspondent IFN-β concentration (pg/ml) can be obtained by comparison with the standard curve values (right Y axis). All values represent means ± standard deviations (SD) of one representative experiment (n=3).* ***C)*** *Enzyme immunoassay targeting cytoplasmic histone-associated DNA fragments in PDA and HPDE6 cells after 16h incubation with virus-free supernatants derived from HPDE6 cells infected with H7N3, H7N3 NS1-77 virus or mock infected. Value represents means of*

$Absorbance_{450nm}$-$Absorbance_{490nm}$ ± standard deviations (SD) of one representative experiment (n=4). Statistical significance was determined using Two-way ANOVA followed by Tukey's multiple comparison test.

To further investigate the contribution of the immunostimulatory activity on the IAV's oncolytic potential, we tested the effect of infecting a confluent monolayer mix (ratio 1:1) of HPDE6 cells and a luciferase expressing BxPC-3 cell line derived from the original PDA cells, which was generated as part of this project and termed BxPC-3Luc. The mixture of HPDE6/BxPC-3Luc cells was infected with H7N3 or H7N3 NS1-77 viruses at different M.O.I or mock infected. Because the infection was performed in absence of exogenous trypsin and the media was enriched with foetal bovine serum (FBS), which possesses proteases inhibitory activity (Schultze et al., 1955), viral replication in both cell lines of the mix was limited to a single cycle. The virus ability to trigger BxPC-3Luc cell death in this experimental setting was evaluated through the decrease of luciferase activity compared to mock infection at 24 hours post-infection, a time-point at which the two viruses displayed similar levels of apoptosis by direct lysis (Figure 28C).

In this mixed scenario (Figure 32A), while IAV infection of BxPC-3Luc cells should trigger cell death via direct lysis, in HPDE6 cells it would result in a high levels of IFN-β production (see figure 31B), which, besides increasing the resistance of this cell line to virus infection (see paragraph 2.2.2), might also enhance the killing of IFN sensitive uninfected PDA cells (see figure 31C).

Results showed that reduction of luciferase activity following virus infection was detectable at 24h post-infection compared to mock infection and the extent of this decrease was overall greater at higher M.O.I (Figure 32B). Moreover, at equal M.O.I the amount of BxPC-3Luc cell death was higher for H7N3 NS1-77 virus infection than for the full length NS1 virus and the extent of this difference tended to increase at lower M.O.I. These data are in line with the mechanism of action proposed in which at high M.O.I. the lytic effect triggered by direct virus infection outcompetes the

immunostimulatory activity exerted on IFN competent cells. However at lower M.O.I., as the ratio between virus and cells decrease, the effect of the IFN induction became appreciable.

To confirm that PDA cell killing was at least partly due to the effect of virus infection of the HPDE6 cells, we repeated the test using confluent monolayers of BxPC-3Luc cells alone (Figure 32C).

Luciferase expression results at 24 hours post-infection showed significant difference at higher M.O.I only between virus treatments and the negative control (mock infection) (Figure 32D). However, no significant difference was observed in the decrease of luciferase activity between the H7N3 and H7N3 NS1-77 viruses at any M.O.I. used.

Taken together this results suggests that the NS1 truncated virus might have superior beneficial effect compared to the wild type virus in a clinical situation, by adding to the direct virus-mediated lysis of infected PDA cells a powerful immunostimulatory effect on healthy cells, which can trigger killing of uninfected tumour cells.

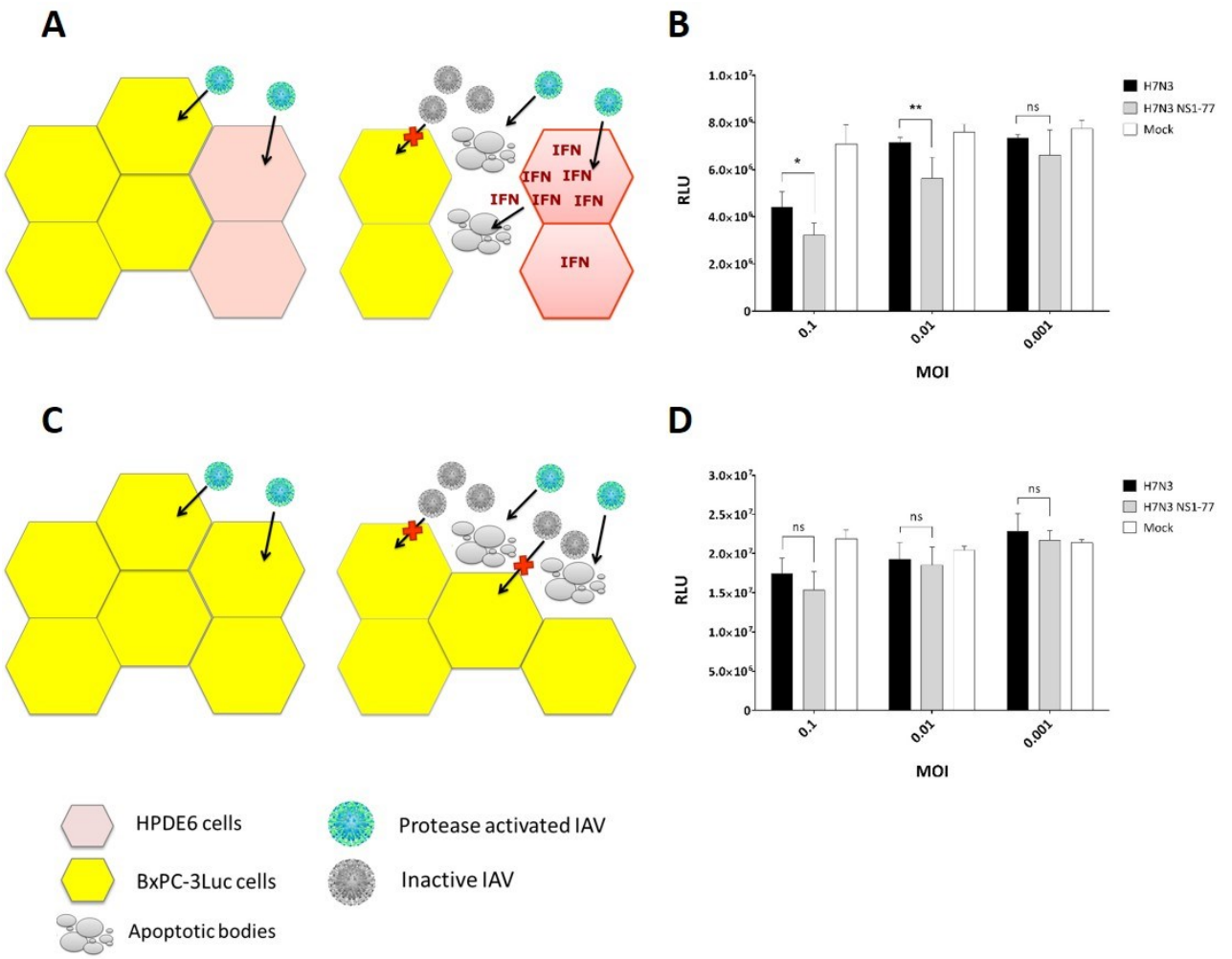

Figure 32. ***Evaluation of H7N3 viruses' immunostimulatory activity. A)*** *Proposed mechanism of IAVs action in a mixed monolayer of benign IFN-competent HPDE6 cells and tumour IFN-deficient BxPC-3Luc cells stably expressing the luciferase gene. Besides triggering direct lysis of infected BxPC-3Luc cells, IAV stimulates IFN production from HPDE6 cells, which in turn can promote cell death of uninfected IFN sensitive PDA cells enhancing the overall oncolytic activity of the virus.* ***B)*** *Luciferase activity results in mixed monolayers of HPDE6 and BxPC-3Luc cells at 24 hours post-infection with H7N3 and H7N3 NS1-77 viruses at different M.O.I. or following mock infection. The luciferase signal is expressed in relative light units (RLU) and provides a direct measurement of BxPC-3Luc cell viability.* ***C)*** *Proposed mechanism of IAV action in monolayers of tumour BxPC-3 cells. Since BxPC-3 cells lack of IFN expression, in monolayers of this cell line alone there will not be any contribution of the virus' immunostimulatory activity on the cell death, which will be exclusively the result of the direct virus-mediated lysis of infected cells.* ***D)*** *Luciferase activity in monolayers of BxPC-3Luc cells alone at 24 hours post-infection with H7N3 and H7N3 NS1-77 viruses at different M.O.I. or following mock infection. Luciferase signal (RLU) provides a direct measurement of BxPC-3Luc cell viability. All data displayed in panel B and D represent means + standard deviations (SD) of representative experiments (n=4 for each M.O.I). Statistical significance was determined using Two-way ANOVA followed by Tukey's multiple comparison test.*

3.2.5 H7N3 NS1-77 virus showed a beneficial effect in PDA xenograft mice model.

To further confirm the superior oncolytic activity of H7N3 NS1-77 virus compared to the corresponding wild type, we tested the efficacy of each virus in the treatment of SCID mice bearing BxPC-3Luc derived solid tumours.

Equal numbers of BXPC-3Luc cells were injected subcutaneously into the right flank of SCID mice. After the mice developed palpable tumours, they were divided equally into three groups (n=5). A control group received injections of PBS whilst the other two groups received four $5x10^4$ pfu/50 µl injections of H7N3 or H7N3 NS1-77 viruses around the tumour mass as described in material and methods. The amount of virus used in the present experiment for each injection was almost 3 log_{10} lower than in trials previously performed for other tumour types using PR8 strain (Sturlan et al., 2010). Such low virus dose was chosen to appraise the contribution of both lytic and immunostimulatory activity of the viruses. The mice were monitored for signs of distress and tumour size was measured twice a week from the beginning of the treatment using a microcaliper. The mean percentage of volume increase compared to the beginning of the treatment (day 9) was calculated for each group at any given time-point (Figure 33A). Tumour morphology, size and the presence of metastases were also evaluated at the end of the experiment by bioluminescence imagine (BLI) (Figure 33B).

Despite the low amount of virus used for each injection, a reduction in tumour growth was observed in both groups treated with IAVs in comparison to the control group (PBS). Moreover, although there was no statistically significant difference between the groups injected with wild type H7N3 and the NS1-77 mutant, the animals injected with NS1-77 virus showed lower mean tumour volume increase at all time-points than those treated with full length NS1 virus, displaying a significant beneficial effect with respect to the control group (Figure 33A).

Because the two viruses were shown to replicate at similar levels in tumour BxPC-3 cells (see figure 30A) and to trigger equivalent cell death by 24 hours post-infection in this cell line (see figure 28B-

C), the difference in the beneficial effect observed in comparison to the control group was unlikely ascribable to a higher viral growth (indeed similar level of viral RNA were detected in tumours infected by either virus see below). Thus, it might be due to the superior ability of the NS1-truncated virus to stimulate innate immune response from the healthy cells surrounding the tumour. Indeed different publications confirmed that SCID mice, which lack T and B lymphocytes (Bosma et al., 1983), possess normal innate immune mechanisms including IFN-α/β expression that can reach levels similar to the responses of immunocompetent controls (Bray, 2001; Falk et al., 1995; Murphy et al., 2003).

The stimulation of type I IFN production from healthy cells might also account for the lower levels of vascularization observed *post-mortem* in tumours derived from mice infected either with full length or truncated NS1 influenza viruses compared to those of the control group (observation orally reported by Dr. Micol Silic-Benussi who performed the trial at the IOV facilities). Previous publications, in fact, demonstrated the role of IFN-α as a powerful angiogenesis inhibitor (Indraccolo, 2010; von Marschall et al., 2003).

After all the mice were euthanized, 5 tumours and 1 lung, 1 liver and 1 kidney per group were collected and assessed by Real-Time PCR for influenza A virus M gene. All the lungs, livers and kidneys resulted negative for the viral RNAs (data not shown) confirming the absence of virus spreading. Conversely, all the tumours derived from mice injected with IAVs showed detectable virus RNA (Ct<35) (Figure 33C), which might indicate replication within the tumour site or might be just the result of the defective clearance derived from the lack of T and B lymphocytes in SCID mice.

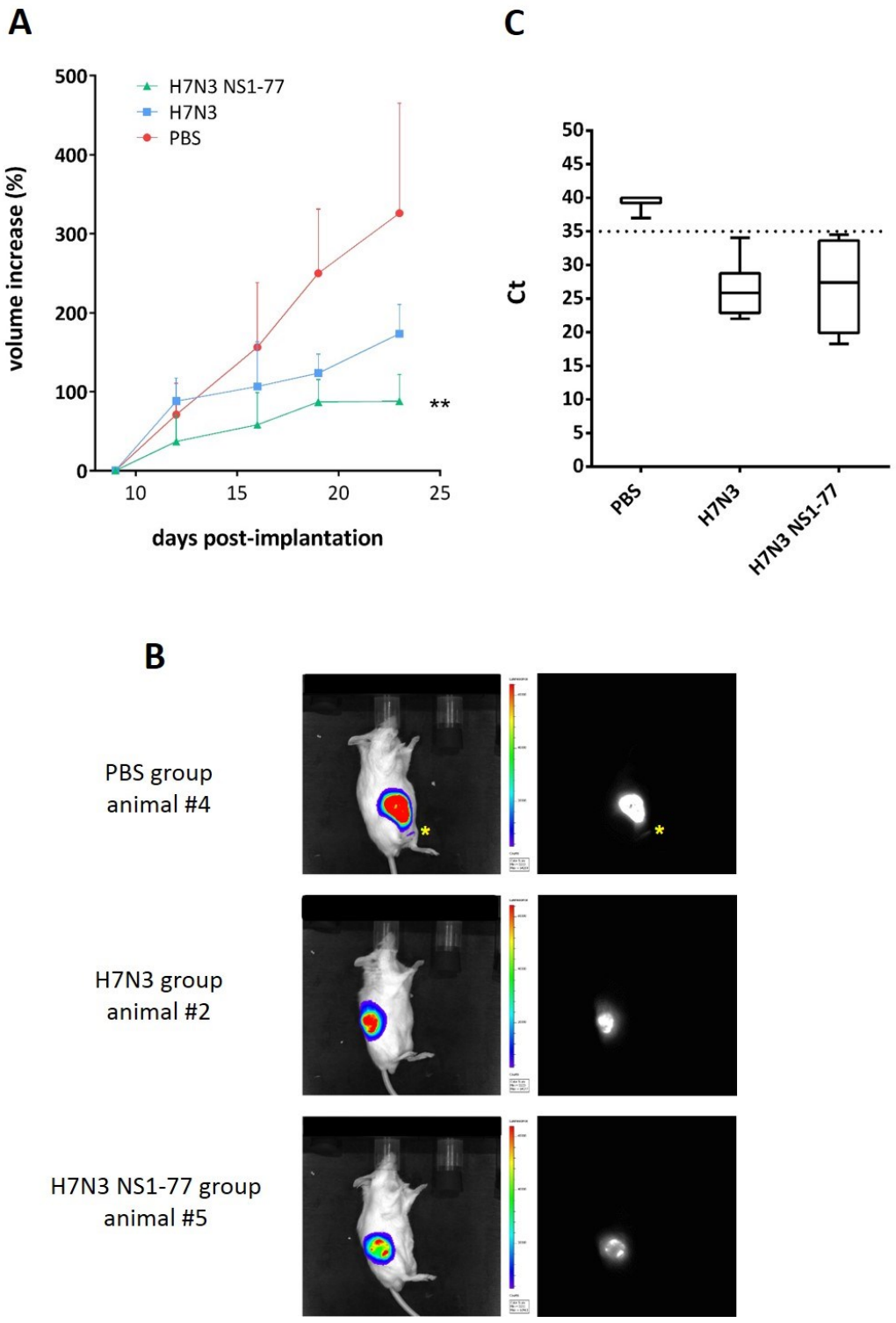

Figure 33. Efficacy of H7N3 and H7N3 NS1-77 virus treatment in SCID mice bearing human BxPC-3Luc derived tumours. A) Solid tumours were established by day 9 and mice were randomly divided into 3 groups (n=5 per group). Animals in each group were administered at the base of the tumour with 5x10^4 pfu of H7N3, H7N3 NS1-77 viruses or PBS (negative control). The procedure was subsequently repeated 3, 7, and 10 days later for a total of four intratumoural inoculations for each group. Tumour size was monitored by caliper measurements and percentage of volume increase was calculated as described in material and methods. The groups were observed twice a week within 23 days from the beginning of the

experiment. Comparison of groups was done by using Two-way ANOVA followed by the Tukey's multiple comparison test. ***B****) Bioluminescence imaging (BLI) of BxPC-3Luc solid tumour from selected animals of the 3 different challenge groups. (*) metastasis.* ***C)*** *Ct (cycle threshold) results of real-time RT PCR targeting viral matrix gene (M) in tumours homogenates derived from SCID mice treated with H7N3, H7N3 NS1-77 or PBS. Based on diagnostic standards in place at IZSVe samples with Ct>35 were considered negative.*

3.3 Discussion and conclusion.

In this study the oncolytic potential of an engineered avian-origin IAV has been tested for the first time in PDA cells characterized by deficient IFN expression. We focused our research on the BxPC-3 cell line as it displayed high sensitivity to IAV infection, although previously shown to be resistant to various oncolytic viruses. We selected the avian origin H7N3 A/turkey/Italy/2962/03 isolate because of its high apoptotic potential in PDA cells (see paragraph 2.2.1). Aiming to increase the selectivity of H7N3 virus for tumour IFN-deficient cells, such as BxPC-3, the NS1 protein was modified to express only its N-terminal 77 amino acids (NS1-77), resulting in almost complete loss of the ED, which predominantly mediates interactions with host-cell proteins (Figure 27A).

Annexin V results confirmed higher selectivity of H7N3 viruses' induced apoptosis for BxPC-3 cells than for HPDE6 cells in comparison to the Gemcitabine and Cisplatin treatment (Figure 28A-B), which is likely due to the capability of the benign cells to express IFN and activate specific IFN-stimulated genes following infection (see paragraph 2.2.2). Interestingly, progression of tumour cell death occurred faster with the H7N3 NS1-77 virus than for the wild type strain but cells infected by either virus reached the same final SCD (Figure 28C). The finding is consistent with an anti-apoptotic role for the NS1 ED (Li et al., 2006; Liu et al., 2010; Shin et al., 2007b).

The H7N3 NS1-77 virus was no longer able to counteract IFN expression in IFN-competent cells, as shown by several reporter based assays (Figure 29A-B). However, when the same truncation was engineered into a different viral genetic backbone, that of H1N1 A/Puerto Rico/8/34 (PR8), it did not result in significant differences in the ability to antagonize IFN mediated antiviral response

(Figure 29A-B), confirming the strain-specific IFN-antagonistic properties of different NS1 proteins (Figure 29C).

The inability to block host cell IFN expression during replication did not impair the growth of H7N3 NS1-77 virus in IFN-deficient BxPC-3 cells or in IFN-impaired 7 day-old ECE, (Figure 30A-C). Because the replication of the wild type virus in IFN competent HPDE6 cells was already very low, likely due to the activity of IFN and ISGs following infection, the effect of the truncation in this cell line was difficult to discern since released virus titres were almost at the limit of detection. Nevertheless, the H7N3 NS1-77 virus showed significant lower growth over time than the full length NS1 virus in HPDE6 cells (Figure 30B) and its reduced replication efficiency in IFN competent systems was further confirmed in 14 day-old ECE (Figure 30C).

In addition to an albeit small effect on improving virus selectivity compared to the wild type virus, the loss of the ability to counteract the innate immune response and the consequent increase in IFNs production from healthy cells appeared to enhance H7N3 NS1-77 cancer cell killing activity at appropriate M.O.I. Indeed, our results suggest that in a clinical situation, a limited amount of H7N3 NS1-77 virus infection of IFN-expressing healthy cells should not result in efficient virus replication (Figure 30B), but rather in stimulation of high levels of IFN-β expression (Figure 29B and 31B), which would then increase the killing of neighbouring uninfected BxPC-3 cells (Figure 31C) and thus improving the oncolytic potential of the virus compared to the wild type (Figure 32B and 33A). Furthermore, the presence of IFNs, such as IFN-α, in the tumour microenvironment might contribute to the inhibition of angiogenesis as previously reported (Indraccolo, 2010; von Marschall et al., 2003).

In conclusion, we generated an H7N3 NS1-77 avian origin IAV which was as efficient at inducing apoptosis as the parental strain in infected BxPC-3 cells but which overall possesses greater oncolytic activity than the wild type virus because of the superior ability to mediate the killing of uninfected cancer cells by stimulating IFN expression from neighbouring healthy cells.

Chapter 4. PB1-F2 mutation: looking for an optimal balance between apoptosis induction and virus replication in PDA cells.

4.1 Introduction

The H7N3 A/turkey/Italy/2962/03 avian-origin influenza virus was selected as oncolytic candidate for the present study due to its superior ability to trigger apoptosis in PDA cells compared to other isolates (Kasloff et al., 2014). The NS1-77 truncation was introduced to improve the specificity of virus for replication in IFN deficient cells (i.e. tumour cells) vs healthy cells. However, the overall replication of either wild type or NS1-77 H7N3 viruses was generally low, which might ultimately preclude the efficacy of the virus as single-shot treatment. Indeed, without high levels of virus replication, which can support rapid intra-tumoural spread, a single-shot administration of IAV would probably have modest or even innocuous effect on PDA *in vivo*.

As previously discussed (see paragraph 1.5.4 and 1.5.5), a proper timing between apoptosis delay and induction appears of paramount importance for optimal virus replication and packaging. As such, the highly efficient induction of apoptosis by the H7N3 virus might actually limit its replication if cell death were triggered too early during infection to allow onwards virus propagation. Thus in this chapter we were interested to explore what effect manipulating the extent of apoptosis induction triggered by the recombinant H7N3 virus would have on its efficacy as oncolytic agents.

Our caspase 9 results (see paragraph 2.2.3) showed that the H7N3 virus triggered apoptosis in BxPC-3 infected cells mainly by affecting the intrinsic apoptotic pathway. Based on the genetic aberration previously reported (Table 3) and on the expression profile of different apoptosis-related protein in untreated BxPC-3 cells presented in the following paragraph, the activation of this pathway appeared due to the direct effect of viral pro-apoptotic factors rather than represent the result of the host antiviral response to infection. Because the intrinsic pathway originates from the

mitochondria we investigated the role of pro-apoptotic protein PB1-F2 (see paragraph 1.5.5) and manipulated this gene in the context of recombinant virus in an effort to find an optimal balance between apoptosis induction and virus replication in PDA cells.

4.2 Results

4.2.1 The intrinsic apoptosis pathway in BxPC-3 cells.

As shown in paragraph 2.2.2, the lack of IFN and ISG expression might, at least partially, explain why BxPC-3 cells are more sensitive than HPDE6 cells to IAV infection and are subject to increased cell death. However, the reason why the H7N3 isolate displayed higher levels of apoptosis compared to other IAV strains in this PDA cell line is still unclear. As previously described (see paragraph 1.5.4), during influenza virus infection, apoptosis can be considered a host defence mechanism to limit pathogen spreading but also a condition promoted by the virus to enhance its genome replication and new virion release. In line with this bivalent effect, IAVs possess different proteins able to modulate host cell death by targeting cellular factors and thereby exerting either anti-apoptotic (Gaur et al., 2012; Zhirnov et al., 2002) or pro-apoptotic function (Chen et al., 2001; Halder et al., 2011; Schultz-Cherry et al., 2001; Tripathi et al., 2013).

The H7N3 A/turkey/Italy/2962/03 virus triggered cell death in BxPC-3 cells mainly as the result of activation of the intrinsic (or mitochondrial) apoptotic pathway (see paragraph 2.2.3). To elucidate whether the activation of this pathway might be the result of the host antiviral mechanism or a direct effect of viral pro-apoptotic proteins, the expression profile of 35 apoptosis-related proteins in untreated BxPC-3 and HPDE6 cell lysates was compared using a proteome profiler (Human Apoptosis Array Kit - R&D Systems).

In comparison to the “benign” HPDE6 cells, the expression profile of apoptosis-related proteins revealed up-regulation of p53 and Clusterin in BxPC-3 cells, two proteins with pivotal roles in the mitochondrial apoptotic pathway (Figure 34).

The p53 is a tightly regulated tumour suppressor protein that acts by stopping cell-cycle progression or promoting apoptosis when cells are exposed to stress stimuli such as oncogene activation or DNA damage. Having a short half-life, p53 is normally maintained at low levels in unstressed cells through continuous ubiquitylation and subsequent degradation, primarily due to the interaction with the RING-finger ubiquitin E3 ligase MDM2 (also known as HDM2) (Friedman et al., 1993). In response to genotoxic or cellular stress, p53 ubiquitylation is suppressed and the protein accumulates in the nucleus where it forms a homotetrameric transcription factor (Friedman et al., 1993; McLure and Lee, 1998) which regulates the expression of a wide variety of genes involved in cell-cycle arrest, apoptosis, DNA repair senescence, and differentiation (Ashcroft et al., 2000).

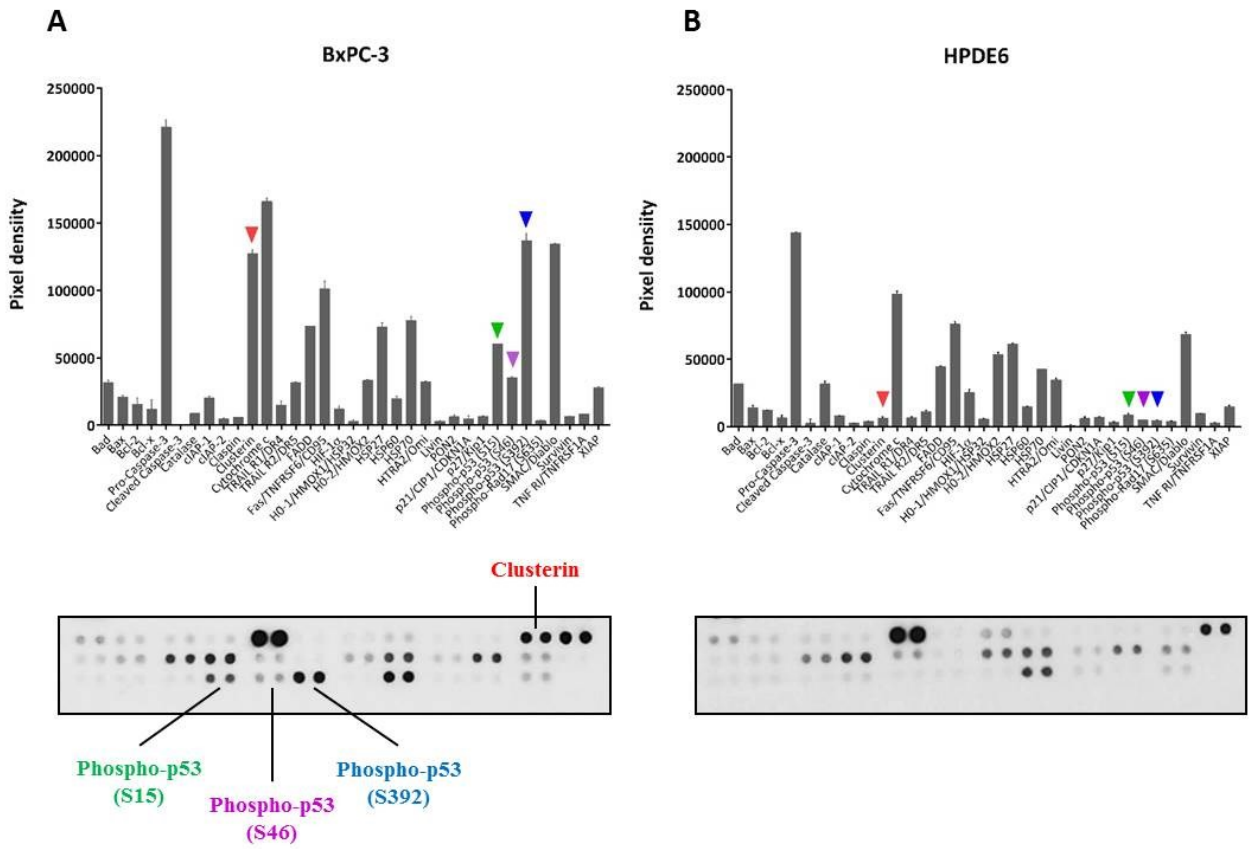

Figure 34. ***Apoptosis-related protein profiles of untreated BxPC-3 (A) and HPDE6 (B) cell lysates.*** *Cell lysates were diluted and incubated on nitrocellulose membrane spotted in duplicate with captured antibodies for 35 apoptosis-related proteins. Overexpression of Clusterin (Red arrow) and heavy levels of p53 expression and post-translational phosphorylation (green, purple and blue arrows) were observed in BxPC-3 compared to HPDE6 cells.*

In PDA cells, the vast majority (≈80%) of TP53 gene mutations resulted in alterations of the protein DNA-binding domain (see table 3 – paragraph 2.2.1) that can lead to loss of the tumour-suppressor function of p53 or to the accumulation of an oncogenic mutant version of p53. The mutation of just one allele of TP53 is potentially oncogenic since mutant p53 proteins are still capable of tetramerization but fail to bind efficiently to the specific DNA-binding motifs targeted by tetrameric wild-type p53 and can thus act in dominant negative fashion (Herskowitz, 1987). Post-translational phosphorylation of specific serines and/or threonines residues at the N- and C-termini of the protein has been reported to increase the stability of the tetramer and thus in the case of mutant p53 to enhance the inhibitory effect on wild-type p53. In agreement with previous publications, reporting the phosphorylation patterns of mutant p53 in different cancer cells (Minamoto et al.,

2001), the proteome profile of BxPC-3 cells revealed hyper-phosphorylation of p53 protein at serine 15 and serine 392 (S15; S392). Phosphorylation of the p53 regulatory C-terminal domain at S392, in particular, has been shown to regulate the oncogenic function of mutant p53 (Furihata et al., 2002; Yap et al., 2004) by inducing conformational changes within the tetramerization domain which increase its stability (Sakaguchi et al., 1997) and thereby contribute to dominant-negative effects and progression of tumours. Because of this effect, S392 phosphorylation has been suggested as a prognostic marker in patients with advanced-stage tumours (Matsumoto et al., 2006).

The other apoptosis-related protein overexpressed in BxPC-3 cells in comparison to HPDE6 is Clusterin (CLU), also known as testosterone-repressed prostate message-2 (TRPM-2), sulfated glycoprotein-2 (SGP- 2), apolipoprotein J (Apo J) or SP40, which is a ubiquitous heterodimeric glycoprotein of 75–80 KDa normally secreted to protect the cell in response to cellular stressors that may induce apoptosis. CLU exerts its chaperone-like activity (Loison et al., 2006) by interfering with the oligomerization of pro-apoptotic protein Bax (Zhang et al., 2005) (Bax itself is up-regulated by the tumour suppressor protein p53 (Miyashita et al., 1994; Miyashita and Reed, 1995)), which otherwise would lead to the release of cytochrome c from mitochondria and caspase 9 activation (see paragraph 1.5.3). Due to its activity, up-regulation of CLU can enhance tumorigenesis. Indeed, overexpression of CLU has been previously reported in numerous advanced stage and metastatic cancers (Bi et al., 2010; Redondo et al., 2000; Xie et al., 2005) and has been indicated as a key contributor to chemoresistance to anticancer agents (Koltai, 2014; Redondo et al., 2009; Springate et al., 2005; Tang et al., 2012; Zellweger et al., 2001; Zellweger et al., 2002).

Thus, due to the genetic aberration previously described in table 3 (see paragraph 2.2.1) and in the light of the proteome profiler results (Figure 34), the normal execution of the intrinsic (mitochondrial) apoptotic pathway appears to be tampered with at different levels in BxPC-3 cells. Based on these observations, together with the lack of IFN and MxA gene expression reported in paragraph 2.2.2, it is likely that the high level of cell death observed following H7N3 infection in

BxPC-3 cells was triggered by the direct activity of viral pro-apoptotic factors rather than represent the result of cellular antiviral mechanisms.

Different IAV proteins have been ascribed with pro-apoptotic activity. Recently, IAV nucleoprotein (NP) was shown to induce apoptosis by interacting with the host anti-apoptotic factor CLU weakening its association with Bax (Tripathi et al., 2013). Interestingly, overexpression of CLU was demonstrated to mitigate cell death induced by NP expression or IAV infection, whereas, siRNA-mediated knockdown of CLU enhanced the apoptosis triggered by the viral protein (Tripathi et al., 2013). Thus, in the light of the up-regulation of CLU observed in BxPC-3 cells, together with the high levels of conservation of the NP protein among avian species, we hypothesized that a viral protein other than NP was probably responsible for the apoptotic levels observed in the case of H7N3 A/turkey/2962/03 virus infection.

The influenza A virus matrix protein (M1) has also been associated with pro-apoptotic function by sequestering the chaperone heat shock protein 70 (Hsp70) from its binding to Apaf-1 complex, which prevents the formation of a functional apoptosome (Halder et al., 2011). Nevertheless this effect by itself is not sufficient to trigger apoptosis as it relies on previous mitochondria permeabilization and cytochrome c release. Therefore, although it was not possible to exclude the synergistic activity of other viral proteins, we hypothesized that the viral pro-apoptotic protein PB1-F2, which is able to directly target the mitochondria causing permeabilization of the MM and cytochrome c release (see paragraph 1.5.5), was the main determinant of apoptosis in BxPC-3 cells.

4.2.2 H7N3 PB1-F2 Mitochondrial Targeting Sequence (MTS) L75H mutation.

As previously discussed (see paragraph 1.5.5), PB1-F2 promotes apoptosis, usually during late stage of infection, by targeting and permeabilizing the MM. This in turn results in depolarization of membrane potential ($\Delta\Psi_m$), release of cyt c and activation of the caspase-9-mediated intrinsic apoptotic pathway (Gibbs et al., 2003; Lowy, 2003; Zamarin et al., 2005). Specific hydrophobic

residues within the PB1-F2 C-terminal MTS (minimal MTS aa 69-82 (Gibbs et al., 2003)) are essential for mitochondrial targeting. Indeed, Gibbs et al. reported that mitochondrial targeting was completely abolished by substituting specific non polar amino acids within the MTS with residues bearing electrically charged side chains (Gibbs et al., 2003). More recently, Chen et al. (Chen et al., 2010) demonstrated that the introduction of leucine (Leu/L) in positions 69 (Q69L) and 75 (H75L) of H5N1 A/Hong Kong/156/1997 PB1-F2 drove a 40.7% increase in the protein localization on the MM compared to the wild-type, strengthening the idea that a Leu-rich sequence in the C-terminus is important for mitochondrial targeting. In line with these observations, Schmolke M. et al (Schmolke et al., 2011), reported that the HPAI A/Viet Nam/1203/2004 (H5N1) PB1-F2, which does not contain the essential leucines at position 69 (69Q) and 75 (75R), did not predominately co-localize with the mitochondria in infected murine and duck cells.

Sequence analysis of the H7N3 A/turkey/Italy/2962/03 PB1-F2 MTS revealed a Leu in position 75 where other influenza viruses isolates, with lower ability to induce apoptosis but higher virus replication rates (Kasloff et al., 2014), had amino acids with electrically charged side chains (Histidine/H or Arginine/R) (Figure 35). We hypothesised that by targeting the MM very efficiently, the H7N3 PB1-F2 was triggering apoptosis prematurely during infection. Thus, we speculated that removal of Leu from this specific position might reduce PB1-F2 mitochondria targeting, and in turn enhance virus replication efficiency either by providing more time for replication (Gibbs et al., 2003) or by increasing the localization of PB1-F2 and co-localization of PB1 into the nucleus (Mazur et al., 2008). Thus, in order to study the effects of the L75H mutation on properties of the PB1-F2 protein itself we cloned the wild type or L75H mutated PB1-F2 ORF into the expression plasmids pCAGG. Next, seeking an optimal balance between apoptosis induction and virus replication, we generated two novel recombinant influenza viruses mutated at residue 75 of PB1-F2 in either the wild type H7N3 background or in combination with the NS1-77 truncation described in the previous chapter: H7N3 PB1-F2 L75H and H7N3 NS1-77 PB1-F2 L75H viruses.

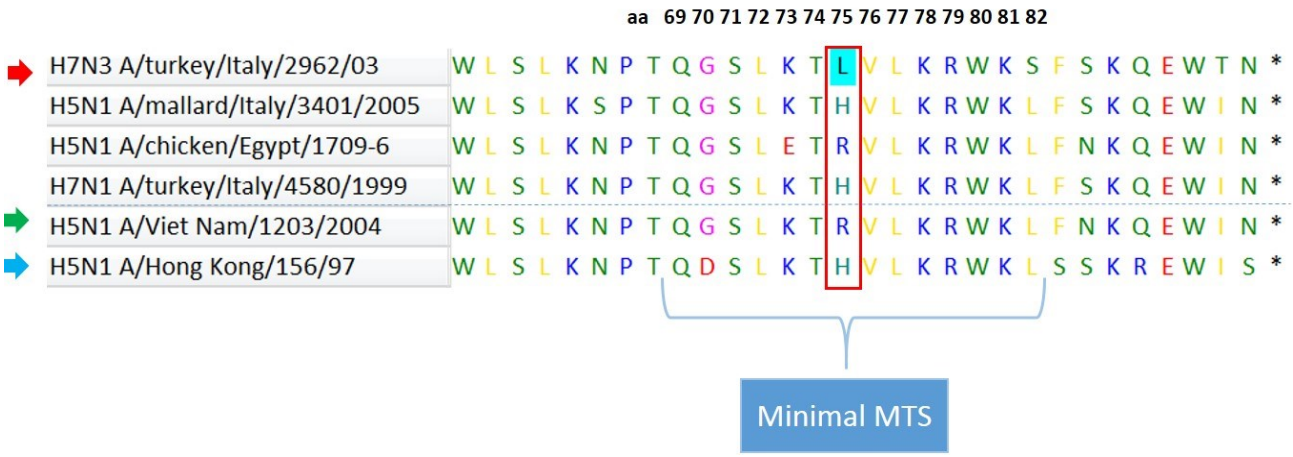

Figure 35. ***Comparison of PB1-F2 MTS between H7N3 A/turkey/Italy/2960/03 (red arrow) and other avian IAV strains previously characterized.*** *In position 75 (red box) the H7N3 virus presents a Leu (hydrophobic) compared to His or Arg (positively charged) possessed by the other strains. For comparison we included also (under the dashed line) the PB1-F2 MTS of H5N1 A/Viet Nam/1203/2004 (green arrow) and H5N1 A/Hong Kong/156/97 (blue arrow) viruses, which do not display predominant co-localization with mitochondria in infected cells* (Chen et al., 2010; Schmolke et al., 2011). *Sequence alignment was performed using MEGA (version 6.06) software.*

4.2.3 Mutation PB1-F2 L75H decreases H7N3 virus ability to counteract IFN via interaction with MAVS.

In the absence of antibody with which to detect the localization of PB1-F2, we chose to assess the effect of the L75H mutation on activities of PB1-F2 associated with its mitochondrial localization. In addition to triggering apoptosis from its mitochondrial localization, PB1-F2 protein has also been attributed with an ability to interfere with RLR pathway by interacting at the mitochondria level with MAVS (see paragraphs 1.5.1).

As previously discussed (see paragraph 1.5.5), PB1-F2 exerts IFN antagonist function by permeabilizing the MM and dissipating the membrane potential ($\Delta\Psi_m$) required for the activity of MAVS. Thus, any decrease of PB1-F2 mitochondrial targeting should reduce the inhibition of MAVS and increase IFN expression by the cell during infection. To test whether PB1-F2 L75H was compromised for inhibition of MAVS activity compared with wild type protein, 293T cells were co-

transfected with different pCAGG/PB1-F2 (H7N3) plasmids, which direct expression of SV5 epitope tagged PB1-F2, together with MAVS expression plasmid (MAVS+) that contains a flag tag for detection (Figure 36A). Overexpression of MAVS automatically triggers the induction of IFN. Cells were also transfected without MAVS plasmid (MAVS-) to evaluate the basal level of IFN expression. IFN-Luc was used as a reporter plasmid in which the luciferase gene was downstream of an IFN-β promoter (Hayman et al., 2006), while renilla luciferase (Renilla-Luc) was used to normalize the transfection (as described previously in chapter 3 to assess NS1 function – see paragraph 3.2.2). At 16 hours post-transfection the cell lysates were tested for luciferase activity. Firefly luciferase signal was an indirect measure of IFN expression triggered by MAVS.

Without MAVS plasmid (MAVS-) no luciferase signal was observed in any of the transfections (Figure 36A). Conversely, in presence of MAVS (MAVS+) the luciferase signal corresponding to IFN expression was modulated by co-expression of PB1-F2. Wild type PB1-F2 inhibited MAVS activity significantly more than PB1-F2 L75H. A western blot using an antibody to the flag and C-terminal SV5 epitope tag confirmed the expression of both MAVS and PB1-F2 constructs respectively (Figure 36B).

To appraise whether the effects of PB1-F2 L75H mutation would be altered in the presence of NS1 protein (as would be the case during virus infection) the previous experiment was repeated co-transfecting also H7N3 NS1, NS1-77 or empty pCAGG expression plasmids (Figure 36C). Full length H7N3 NS1 (pCAGG/NS1) strongly counteracted IFN expression induced by MAVS (Figure 36C) regardless of the PB1-F2 construct co-transfected. The truncation of the H7N3 NS1 ED (pCAGG/NS1-77) reduced this capability, as previously shown (see paragraph 3.2.2), but in this situation PB1-F2 could contribute to antagonize IFN expression triggered by MAVS (pCAGG/PB1-F2 vs pCAGG) and this effect was greater for wild type PB1-F2 than for the L75H mutant. In the absence of any NS1 construct (pCAGG) the single effect of different PB1-F2 proteins on MAVS and

IFN activity was again visible and PB1-F2 L75H showed higher levels of IFN expression than the corresponding wild type protein.

Taken together these results confirm that substitution L75H within the MTS affects H7N3 PB1-F2 ability to inhibit IFN expression probably by altering its localization.

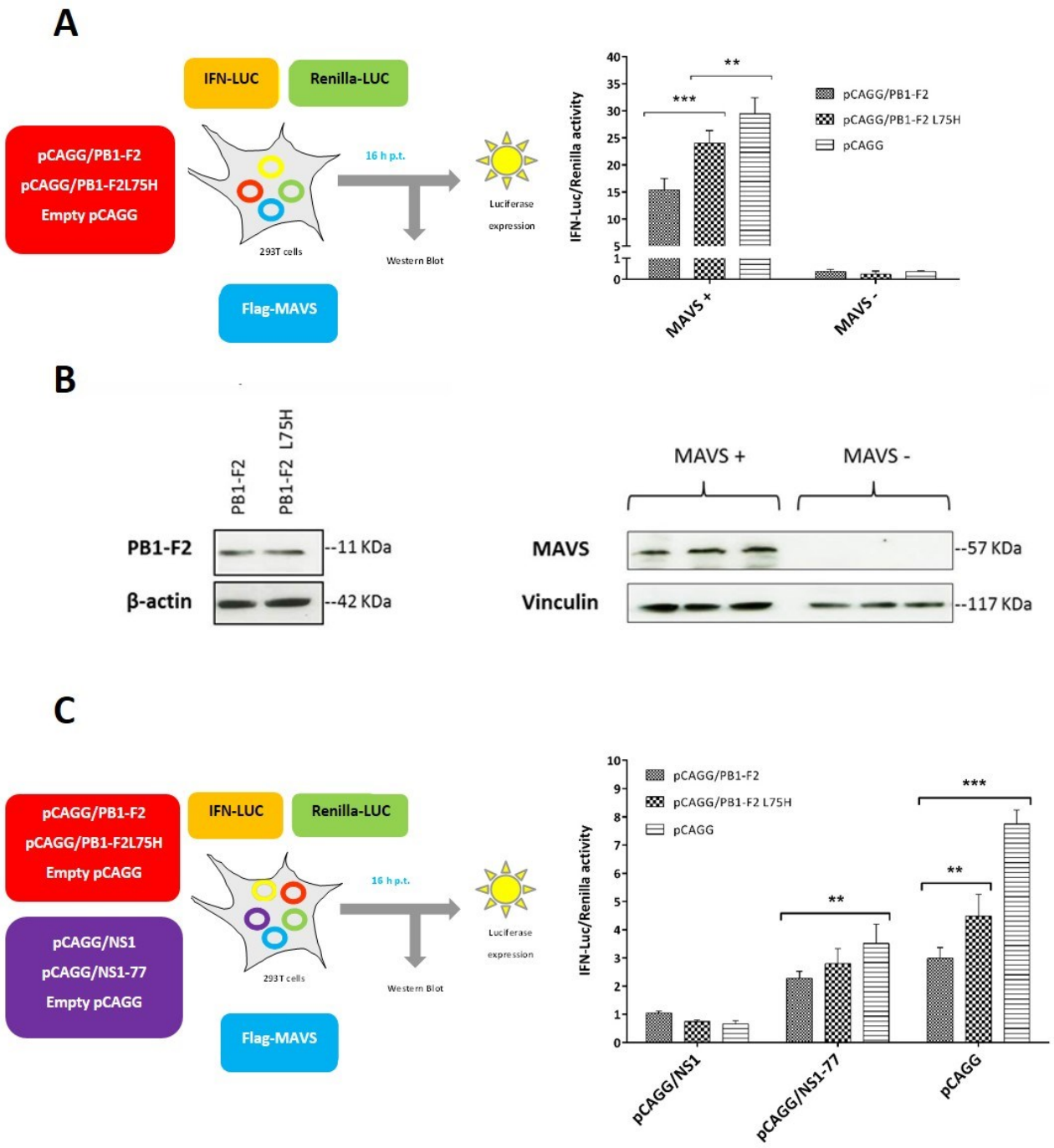

Figure 36. ***Mutation within the MTS of PB1-F2 modulates IFN induction at level of MAVS. A)*** *293T cells were transfected with an IFNLuc reporter encoding the firefly luciferase gene driven by the IFN-β promoter, a pCMV5-flag-MAVS (MAVS+) plasmid to direct overexpression of MAVS protein inducing the IFN-β reporter and one of the following: pCAGG/PB1-F2*

H7N3, pCAGG/PB1-F2 L75H H7N3 or pCAGG expression plasmids. A renilla plasmid was also transfected to normalise the luciferase signal. Control 293T cells (MAVS-) were transfected without including pCMV5-flag-MAVS plasmid to appraise the basal level of IFN-β expression. ***B)*** *Western blot targeting flag of pCMV5-flag-MAVS and SV5 tag of pCAGG/PB1-F2 plasmids were performed to confirm protein expression, while vinculin and β-actin were used as a loading control.* ***C)*** *The experiment described above was repeated including also pCAGG/NS1 H7N3, pCAGG/NS1-77 H7N3 or pCAGG expression plasmids to appraise the synergetic IFN antagonistic effect of NS1 and PB1-F2 proteins. All data represent means ± standard deviations (SD) of one representative experiment (n=3). Statistical significance was determined using Two-way ANOVA followed by Bonferroni post-test.*

4.2.4 Mutation L75H within PB1-F2 MTS affects H7N3 virus replication and apoptosis.

To evaluate whether the decrease in the number of leucines within the MTS could change the apoptotic potential displayed by H7N3 A/turkey/Italy/2962/03 virus, annexin V staining was performed in BxPC-3 and HPDE6 cells infected with H7N3 PB1-F2 L75H and H7N3 NS1-77 PB1-F2 L75H viruses. Incubation of the cells with Gemcitabine and Cisplatin was included as positive control for apoptosis and Specific Cell Death (SCD) was measured at 16 and 24 hours post-infection as described in material and methods.

Consistently with previous results (see paragraphs 2.2.1-2.2.2 and 3.2.1), both viruses induced higher levels of apoptosis in BxPC-3 than in HPDE6 cells, and in tumour cells infected with the NS1 truncated virus, apoptosis progression occurred faster than in the case of full length NS1 virus infection (data not shown).

Analysis of the annexin V results for H7N3 and H7N3 PB1-F2 L75H (Figure 37A) or H7N3 NS1-77 and H7N3 NS1-77 PB1-F2 L75H (Figure 37B) showed that mutation L75H within the MTS of PB1-F2 decreased the levels of apoptosis at the earlier stages of infection compared to influenza viruses bearing wild type PB1-F2 protein. However, the same levels of cell death were reached at 24 hours post-infection, suggesting slower progression of apoptosis in the L75H mutant virus-infected cells.

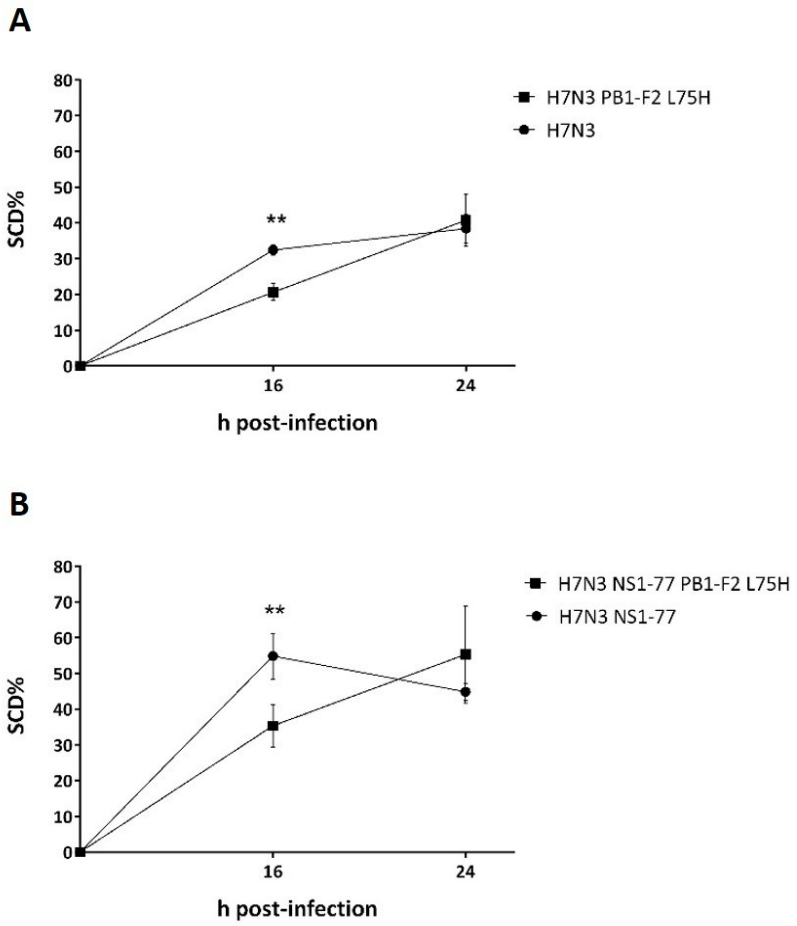

Figure 37. ***Annexin V results for H7N3 PB1-F2 L75H viruses at 16 and 24 hours post-infection.*** *Comparison of annexin V results between wild type and PB1-F2 L75H viruses bearing either full length (**A**) or truncated NS1 protein (**B**). All data represent means ± standard deviations (SD) of three independent experiments. Statistical significance was determined using Two-way ANOVA followed by Tukey's multiple comparison test.*

To confirm the lower levels of apoptosis observed following infection with PB1-F2 L75H mutants, western blot targeting the 89 KDa fragment derived from cleavage of poly(ADP-ribose) polymerases (PARP), a classical hallmark of apoptosis (see paragraph 1.5.3), was performed on BxPC-3 cell lysates collected at 8, 16 and 24 hours post-infection with the different H7N3 viruses (Figure 38A). PARP results confirmed that (i) NS1-77 truncated virus triggers higher levels of apoptosis at earlier time points compared to the corresponding wild type NS1 viruses (see paragraph 3.2.1) and that (ii) PB1-F2 L75H viruses shows reduced levels of apoptosis compared to the respective wild type PB1-F2 viruses.

In order to evaluate whether the variation in apoptosis induction might be associated with differences in replication activity, IAV Matrix (M) gene Real-Time PCR was performed on the supernatants derived from the infection described above (Figure 38B). Results showed a time related increase in M gene copy numbers for all the viruses, although different levels of replication were observed. In conjunction with full length or NS1-77 truncation, mutation L75H in PB1-F2 increased levels of replicated M gene.

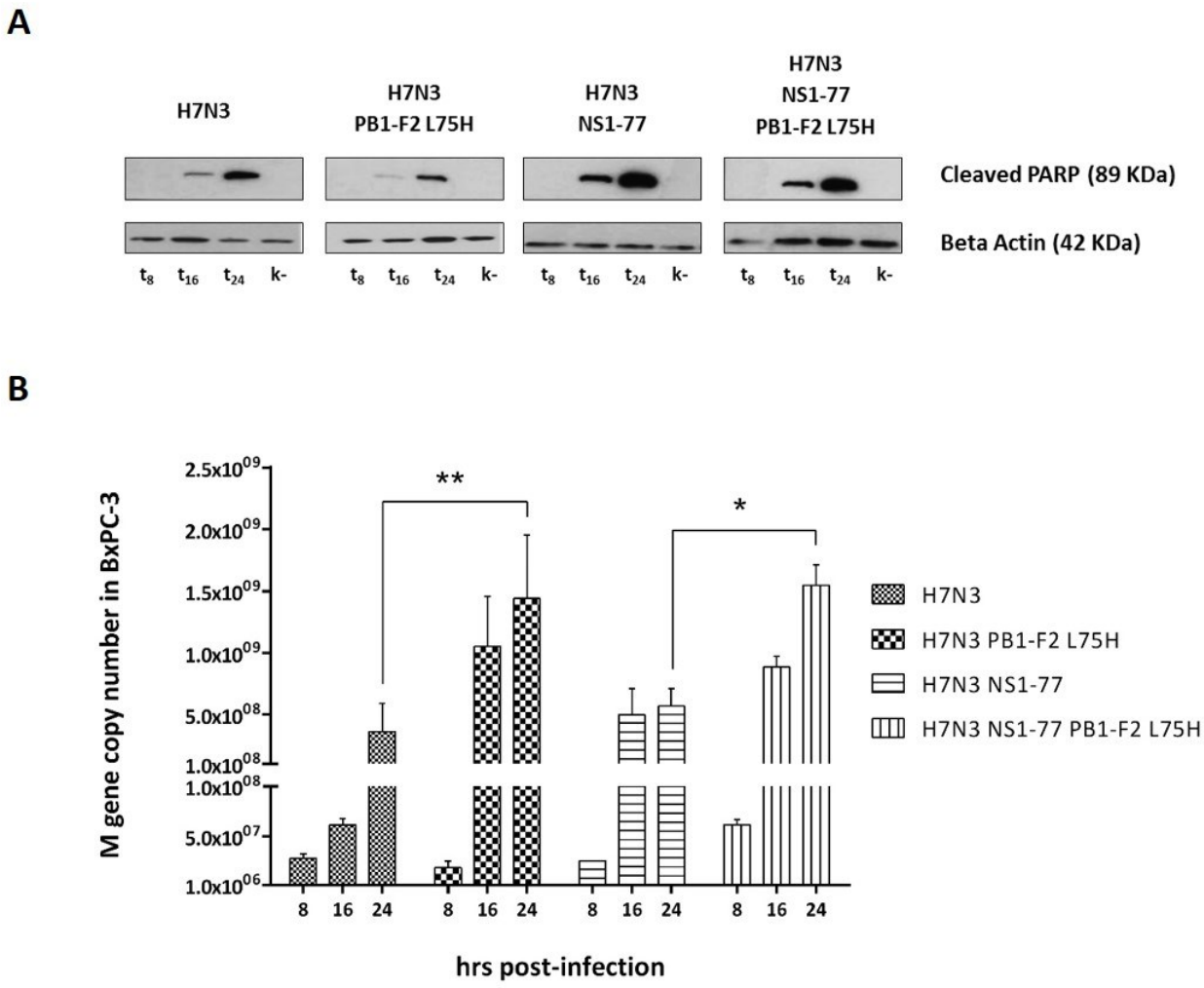

Figure 38. *PB1-F2 L75H mutation slows apoptosis promoting higher levels of virus replication. A) Western Blot targeting cleaved PARP 89 KDa fragment in BxPC-3 cells at 8, 16 and 24 hours post-infection with H7N3, H7N3 PB1-F2 L75H, H7N3 NS1-77 and H7N3 NS1-77 PB1-F2 L75H viruses (M.O.I.= 0.1).* ***B)*** *Quantitative real-time PCR targeting conserved M gene of type A influenza virus was applied on supernatants derived from BxPC-3 infected cells. All data represent means ± standard deviation (SD) of one representative experiment (n=3). Statistical significance was determined using Two-way ANOVA followed by Tukey's multiple comparison test.*

PB1-F2 has been suggested to play a role in polymerase function, perhaps by interacting with the PB1 subunit (Mazur et al., 2008).Therefore, it was possible that the L75H mutation was affecting viral M gene accumulation by enhancing viral polymerase activity. To assess this possibility a minireplicon assay was performed (Figure 39A). The minireplicon assay is based on plasmid expression of H7N3 A/turkey/Italy/2962/03 polymerase subunits PB1, PB2, PA, NP and a virus-like minigenome RNA molecule of negative polarity, containing a luciferase reporter gene, which mimic a viral genomic segment. In this assay pCAGG/PB1-F2 H7N3, pCAGG/PB1-F2 L75H H7N3 or empty pCAGG plasmids were also included and constituted the only variable. Therefore, differences in the expression of the reporter gene were an indirect measure of the reconstituted influenza virus polymerase activity, which was dependent on the ability of the different PB1-F2 to modulate replication. In the experiment PB1-F2 ORF of the PB1 gene was not silenced; therefore the PB1 plasmid retained the ability to also express wild type PB1-F2 protein. As such, there was no significant difference in the minireplicon assay performed using the wild type PB1-F2 or the empty pCAGG plasmid, suggesting that the additional expression of wild type PB1-F2 had little effect on the polymerase activity (Figure 39A). However, co-expression of PB1-F2 L75H construct showed significantly higher luciferase activity in comparison to co-expression of wild type PB1-F2, suggesting that the L75H protein was better able to support the viral polymerase activity. To test whether this effect translated to an increased virus yield, growth curves were performed in BxPC-3 cells using the recombinant viruses. The ability of the wild-type and PB1-F2 mutant H7N3 IAVs to replicate in BxPC-3 cells was monitored over a 72 hour time-course (Figure 39B). Due to the general low levels of IAVs replication previously reported in BxPC-3 (see chapter 3.3.3), it was possible to confirm a significant superior growth of H7N3 PB1-F2 L75H virus only at the latest time point. Nevertheless, the data show that the mutation L75H within the PB1-F2 MTS improves H7N3 replication likely by both decreasing apoptosis induction and simultaneously enhancing virus polymerase activity.

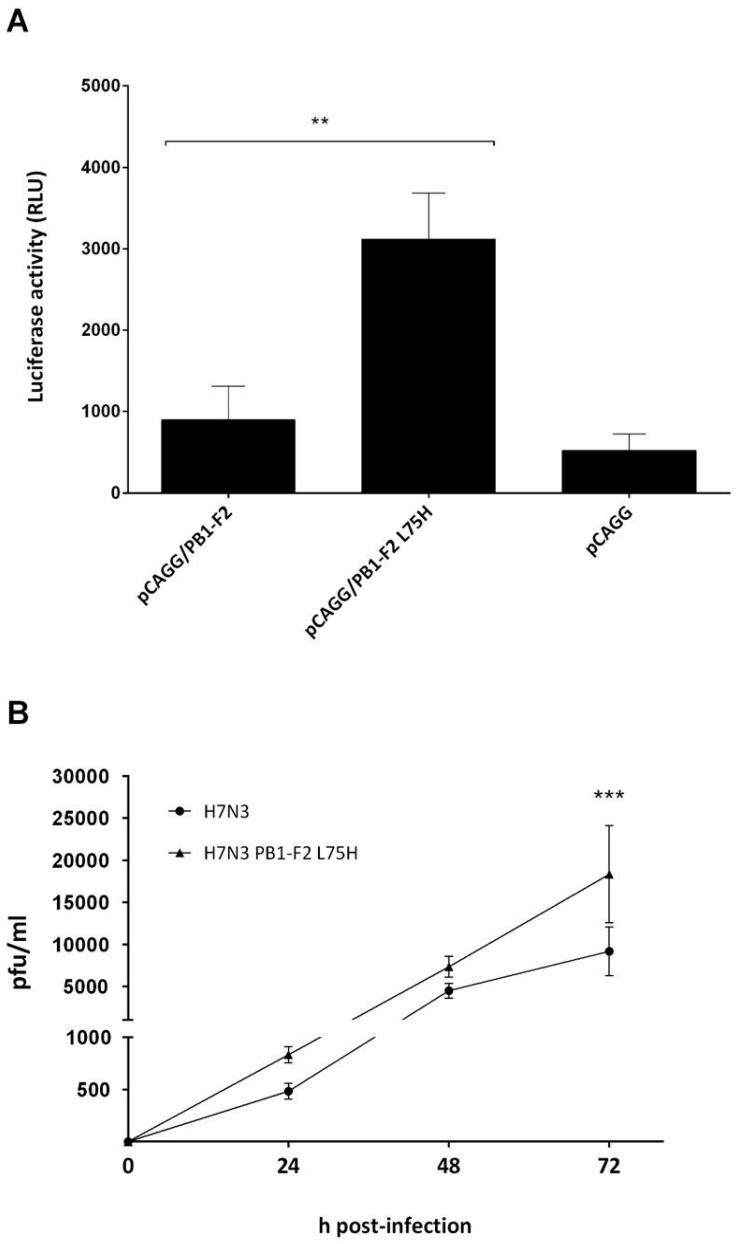

Figure 39. ***PB1-F2 L75H mutation enhances virus polymerase activity and virion production. A)*** *Minireplicon assay results for different PB1-F2 constructs. 293T cells were transfected with five plasmids, encoding PB2, PB1, PA, NP and either PB1-F2 or PB1-F2 L75H proteins derived from avian influenza virus H7N3 A/turkey/Italy/2962/03. A sixth plasmid directing the expression of a virus-like firefly luciferase reporter RNA minigenome, which mimic a viral genome segment, was co-transfected. At 24 h post-transfection, cells were lysed and firefly luciferase activity measured. Results are shown as raw data and expressed as RLU (relative light units). All data represent means + standard deviations (SD) of one representative experiment (n=3). Statistical significance was determined using One-way ANOVA followed by Bonferroni multiple comparison test.* ***B)*** *Replication kinetics of H7N3 and H7N3 PB1-F2 L75H influenza A viruses in BxPC-3 cell line. Cells were infected at an M.O.I of 0.001 and virus titres of the supernatants were determined via plaque assay on MDCK-NPro cells at 24, 48 and 72 hours post-infection. Results represent means ± standard deviation (SD) of one representative experiment (n=3). Statistical significance was determined using Two-way ANOVA followed by Sidak's multiple comparison test.*

4.2.5 Efficacy of H7N3 NS1-77 PB1-F2/L75H virus in SCID mice bearing BxPC-3Luc-derived tumours.

Although the differences in the viral growth between the PB1-F2 L75H virus and the correspondent wild type virus in BxPC-3 cells were modest (see figure 39B), the results presented in the course of this chapter suggested that a H7N3 NS1-77 PB1-F2 L75H virus might possess a better balance between attenuation, replication efficiency and apoptosis induction. As such, this virus was further tested for its oncolytic activity in SCID mice bearing BxPC-3 derived solid tumours.

The luciferase expressing line BxPC-3Luc, derived from the original BxPC-3 cells and generated as part of this project, was used. An equal number of BXPC-3Luc cells were injected subcutaneously into the right flank of SCID mice. After 9 days the mice developed palpable tumours and they were divided equally into four groups (n=5). A control group received intratumoral (IT) injections of PBS whilst the other three groups received a $5x10^4$ pfu/50 µl IT injections of H7N3, H7N3 PB1-F2 L75H or H7N3 NS1-77 PB1-F2 L75H respectively. The IT injections were repeated four times as described in material and methods. The mice were monitored for signs of distress and tumour size was measured twice a week from the beginning of the treatment using a microcaliper and bioluminescence imagine (BLI) (Figure 40).

All the viruses tested showed an effect in comparison to the group treated with PBS, with the H7N3 NS1-77 PB1-F2 L75H virus producing the most significant reduction in tumour growth. The virus harbouring full length NS1 and PB1-F2 L75H mutation also displayed a significant effect in reducing tumour volume. Although there was no statistically significant difference in the control of tumour volume between the wild type H7N3 and the PB1-F2 mutant, tumour size of mice treated with PB1-F2 mutant was lower at all time-points (Figure 40).

To appraise whether sustainable virus replication levels were occurring within the tumours the animals were maintained alive until thirty-three days after the beginning of the experiment. The mice were then euthanized and 5 tumours and 2 lungs per group were collected and assessed by

Real-Time PCR for influenza virus M gene. All the lungs tested were negative for the virus (data not shown) confirming the absence of viral spreading. Despite the oncolytic effect achieved in animals, only two tumour samples collected from the groups treated with H7N3 PB1-F2 L75H (Ct=33.91) and with H7N3 NS1-77 PB1-F2 L75H (Ct=32.75) had detectable virus presence at 10 days after the last viral administration.

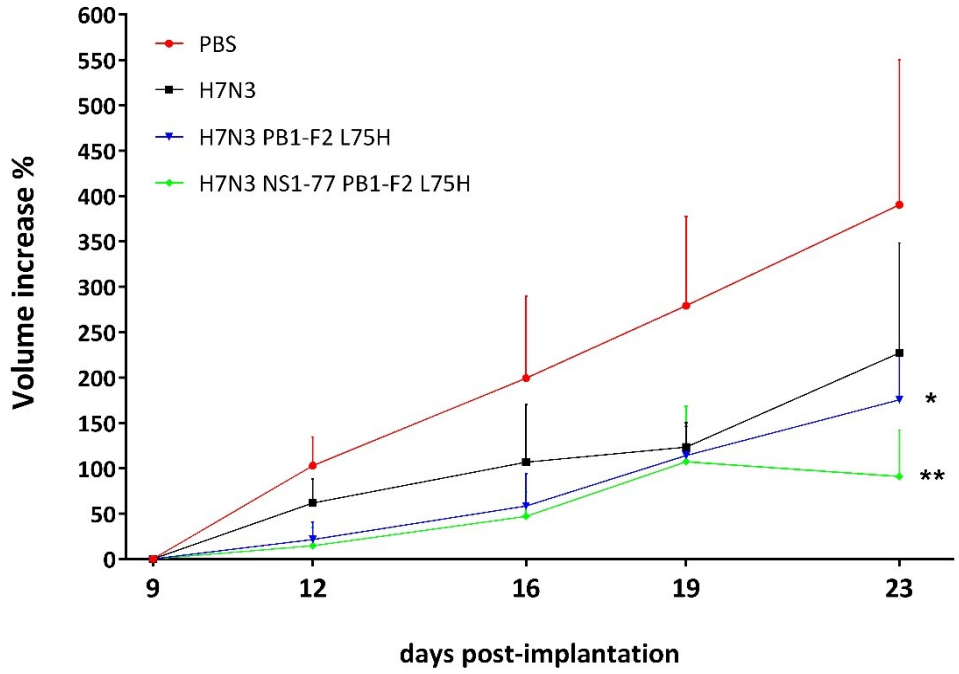

*Figure 40. **Efficacy of H7N3 reverse genetics viruses in SCID mice bearing human BxPC-3Luc derived tumors.** Solid tumours were established by day 9 and mice were randomly divided into 4 groups (n=5 per group). Animals in each group were administered IT with 5x10^4 pfu of H7N3 A/turkey/Italy/2962/V03, H7N3 PB1-F2 L75H, H7N3 NS1-77 PB1-F2 L75H viruses or PBS (negative control). The procedure was subsequently repeated 3, 7, and 10 days later for a total of four intratumoural inoculations for each group. Tumour sizes were monitored by caliper measurements and bioluminescence imaging (BLI). Tumour volume and percentage of volume increase were calculated as described in material and methods. The groups were observed twice a week within 23 days from the beginning of the experiment. Comparison of groups was done by using Two-way ANOVA followed by the Tukey's multiple comparison test.*

4.3 Discussion and conclusion

Previously, Kasloff et al. (Kasloff et al., 2014) showed that the H7N3 A/turkey/Italy/2962/03 virus triggered higher levels of apoptosis but achieved lower titres in PDA cells compared to other strains

tested. Immunocytochemistry (ICC) results confirmed the ability of H7N3 virus to induce high levels of apoptosis in BxPC-3 cells by directly affecting the intrinsic apoptotic pathway (see paragraph 2.2.3). We speculated that the virus was promoting apoptosis prematurely during infection limiting its own replication and that this might ultimately decrease its oncolytic potential as single-shot treatment *in vivo*.

The apoptosis-related protein profile (Figure 34) of untreated tumour BxPC-3 cells revealed that these cells were aberrant at various levels along the mitochondrial pathway. The up-regulation of anti-apoptotic cellular proteins together with the lack of expression of IFNs and other ISGs (see paragraph 2.2.2) suggested that the apoptosis process seen in virus infected cells was likely the result of viral pro-apoptotic factors rather than the consequence of activation of the cellular antiviral mechanism. Thus, in the attempt to rebalance apoptosis induction in favour of virus replication, we investigated the influenza virus pro-apoptotic protein PB1-F2. Based on previous studies demonstrating the importance of specific leucine residues within the MTS for mitochondrial targeting (see paragraph 4.2.2), L75H substitution was introduced to decrease PB1-F2 MM localization and delay apoptosis induction during infection thus enhancing virus rescue.

An indirect measure of the decrease in mitochondrial targeting was the reduced ability of PB1-F2 L75H to affect the mitochondrial antiviral-signalling protein (MAVS) (Figure 36A-C), which led to higher host IFN expression and might contribute to enhance even further the selectivity of H7N3 virus for IFN-deficient cells.

Besides having an effect on the activity of MAVS, the reduction of mitochondrial targeting also modulated the timing of apoptosis in infected PDA cells. Indeed, in the annexin V assay, which measures early-stage of apoptosis (see paragraph 1.5.3), PB1-F2 L75H mutant viruses showed lower but steady progression of BxPC-3 cell death compared to the corresponding viruses bearing a wild type protein (Figure 37A-B). Analysis of cleaved PARP (Figure 38A), a late stage signature of

programmed cell death (see paragraph 1.5.3), also showed that apoptosis induced by the PB1-F2 L75H viruses was decreased at early time points.

The data obtained are consistent with an effect of the L75H mutation on the potency of the MTS. While the wild-type protein would predominantly target the MM, priming the intrinsic apoptotic pathway early during infection, the L75H mutation would decrease the accumulation of PB1-F2 at the mitochondria level. This in turn would determine lower levels of apoptosis coupled with higher influenza M gene copy numbers (Figure 38B) resulting from deferring the induction of apoptosis during infection and/or enhancing the viral polymerase activity (Figure 39A). It is likely that these factors synergistically contributed to increase virion production in tumour cells (Figure 39B), although it was difficult to show enhanced replication of the mutated virus in BxPC-3 cells that were rather poorly permissive for multiple cycles of influenza infection under laboratory conditions. Nonetheless, the H7N3 PB1-F2 L75H virus displayed a higher therapeutic effect than the wild-type virus in xenograft model (Figure 40). In line with the findings presented in chapter 3 (see paragraph 3.3.5), the effect of the treatment was further increased by NS1 truncation.

Although intra-tumoural replication levels of the H7N3 virus might be promoted in some PDA patients suffering with pre-existing chronic pancreatitis (see paragraph 1.2.2) as the result of auto-activation of trypsinogen and chymotrypsinogen within the pancreas (see paragraph 1.1.2), the low viral growth displayed in BxPC-3 cell lines and BxPC-3 derived solid tumours by wild-type and PB1-F2 L75H mutant virus suggests that they could be cleared very rapidly in immune competent systems. Based on these considerations, we decided not to incorporate the mutation PB1-F2L75H within the H7N3 NS1-77 virus so far developed in order to maintain the highest levels of apoptosis of the oncolytic candidate with the aim of using it in a multiple injection treatment.

Nevertheless, the results obtained confirm the involvement of viral protein PB1-F2 in modulating IFN expression and apoptosis during infection. Furthermore, our data show that it may be possible

to tune the strain specific characteristics of IAV by manipulating its genome to obtain optimal apoptosis/replication balance.

Chapter 5. Enhancing safety of the treatment: generation of a 6:2 recombinant virus.

5.1 Introduction

Although the low pathogenicity H7N3 A/turkey/Italy/2962/03 NS1-77 influenza virus displays restricted replication in benign human cells (see paragraphs 2.2.1-2.2.2-3.3.3) due to specific proteases-limiting conditions, species barrier factors and antiviral mechanisms which can prevent virus spreading outside the site of injection, the use of an avian strain for cancer treatment might still carry potential threats. Indeed, as previously discussed (see paragraph 1.6.1), the possibility of "antigenic shift" with circulating human strains is an important concern. Although 16 HA subtypes have been identified in wild birds, only H1, H2 and H3 have been stably introduced into the human population. Therefore, the H7N3 virus belongs to an avian subtype for which the human population is almost completely naïve and thus its use for cancer treatment carries risk of further recombination within a treated patient that might result in new potentially pandemic strains. Furthermore, despite being a rare event, the spontaneous introduction of basic amino acids into the haemagglutinin cleavage site, which can determine the passage to a "highly pathogenic" (HP) phenotype, can occur naturally within the H7 subtype (see paragraph 1.4.4.1). This feature allows ubiquitous HA activation and permits the virus to evade restriction associated to trypsin-like proteases availability (Klenk et al., 1975; Lazarowitz and Choppin, 1975) thus conferring to it potential systemic spread which might cause an acute generalized disease.

Based on these considerations, we generated a reassortant virus containing the 2 genes expressing surface antigens haemagglutinin (HA) and neuraminidase (NA) of the well characterized human strain H1N1 A/Puerto Rico/8/1934 and the 6 gene segments encoding the internal viral proteins (PB2, PB1, PA, NP, M and NS) of the H7N3 A/turkey/Italy/2962/03 NS1-77 virus (Figure 41). The properties of the 6:2 reassortant virus, named PR8 H1/N1-2962 NS1-77, were then compared with those of the H7N3 viruses bearing either full length or truncated NS1 proteins.

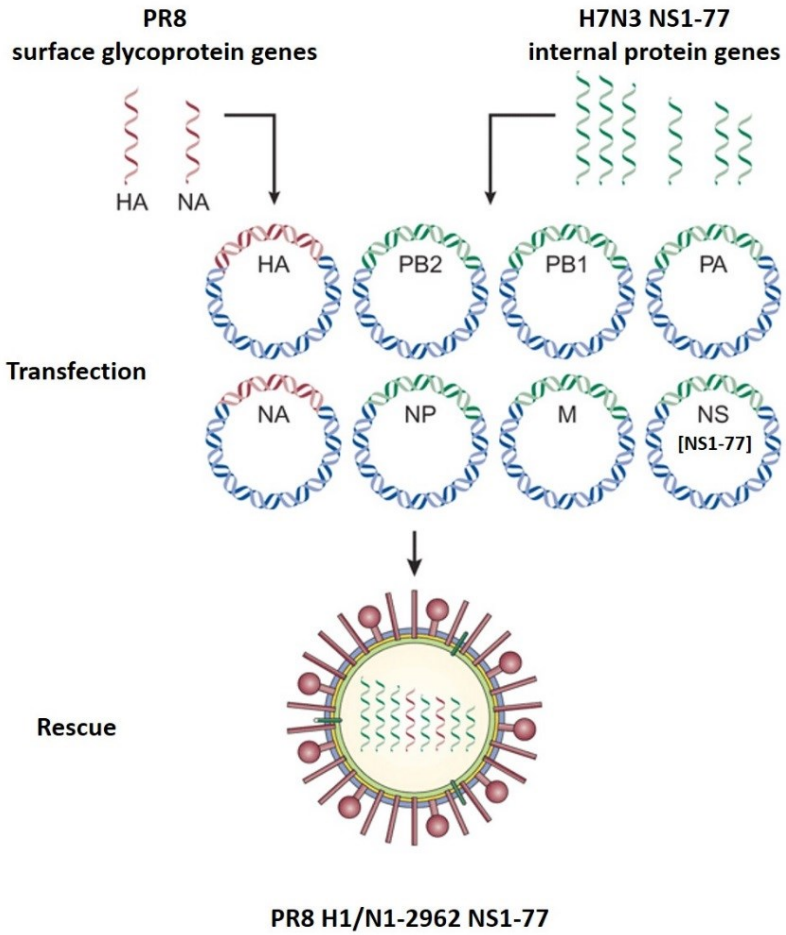

Figure 41. ***Use of reverse genetics to generate 6:2 recombinant influenza A virus.*** *The HA and NA genes from well characterized human strain H1N1 A/Puerto Rico/8/34 were transfected together with the 6 genes (PB2, PB1, PA, NP, M, NS) encoding the internal viral proteins of the avian origin H7N3 A/turkey/Italy/2962/03 NS1-77 to generate the recombinant PR8 H1/N1-2962 NS1-77 virus. Adapted from* (Palese, 2004).

5.2 Results

5.2.1 PR8 H1/N1-2962 NS1-77 virus retains growth and apoptotic skills similar to those of H7N3 viruses.

To evaluate whether the new HA and NA proteins might have affected the receptor binding efficiency of the recombinant virus and hence its ability to infect pancreatic cancer cells, growth curves were performed for H7N3 and PR8 H1/N1-2962 NS1-77 in different benign and cancer cell lines (Figure 42). According to previous results (see paragraphs 2.2.1-3.3.3), although IFN-competent HPDE6 cells produced the lowest viral growth among the cell lines tested, PR8 H1/N1-2962 NS1-77 virus reached lower titres than the full length NS1 H7N3 isolate. Conversely, in IFN deficient PDA cell lines both viruses produced similar titres at any given time post-infection showing higher growth in BxPC-3 and Mia Paca-2 than in CFPAC-1 cells (Figure 42 B-C-D).

Based on these results the introduction of exogenous surface glycoprotein genes had no effect on the virus growth in PDA cell lines. However, to rule out a decrease in the level of virus mediated apoptosis caused by the reassortant compared to the parental strain the amount of cytoplasmic histone-associated DNA fragments (see paragraph 1.5.3) were measured in BxPC-3 and benign HPDE6 cells following infection with PR8 H1/N1-2962 NS1-77, H7N3, H7N3 NS1-77 or H1N1 PR8 viruses (Figure 43).

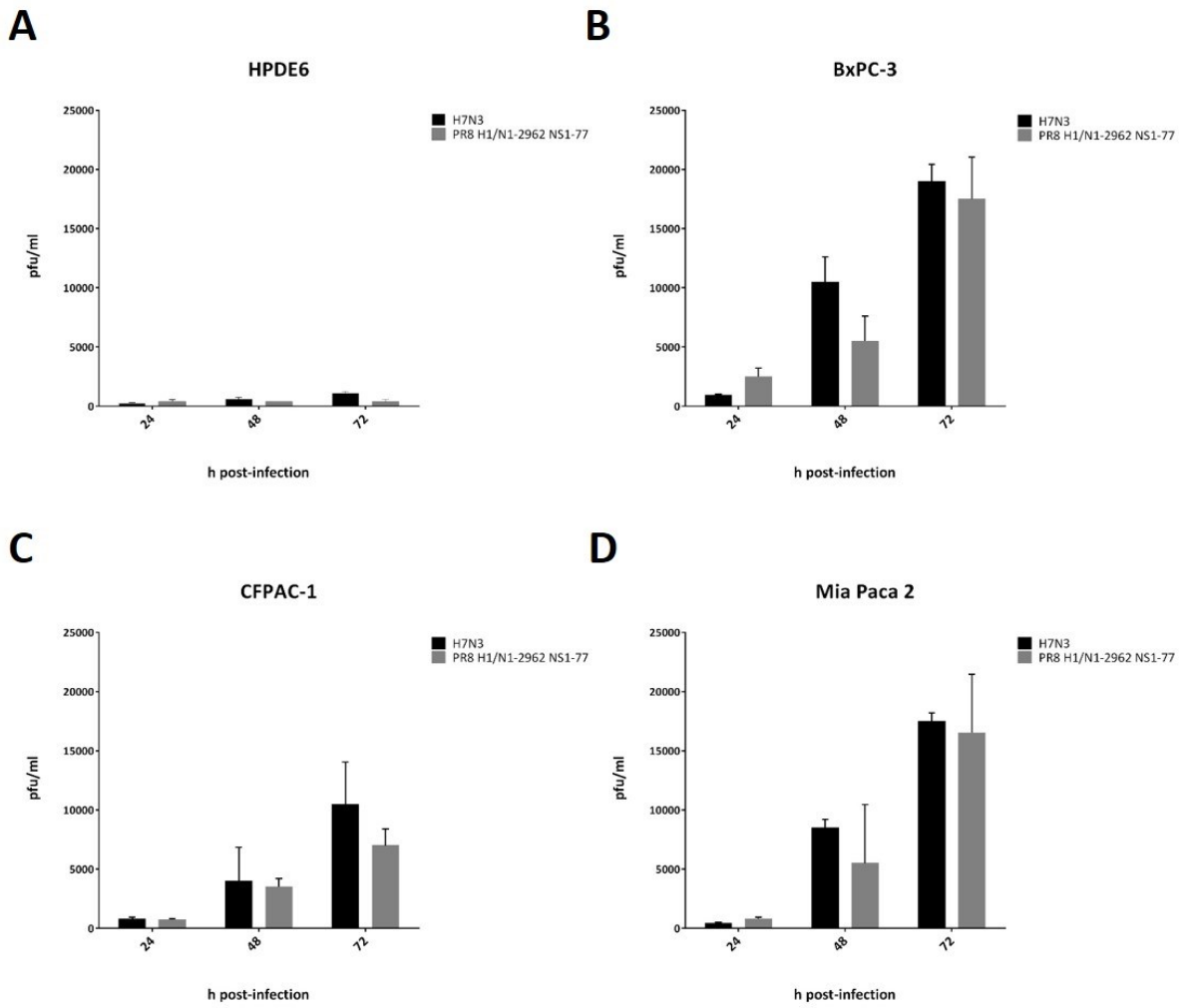

Figure 42. ***Replication kinetics of H7N3 and PR8 H1/N1-2962 NS1-77 IAVs in human pancreatic cell lines.*** *H7N3 and PR8 H1/N1-2962 NS1-77 virus replication was monitored over a 72 hour time-course in HPDE6 (**A**), BxPC-3 (**B**), CFPAC-1 (**C**) and Mia Paca 2 (**D**) cell lines. Cells were infected at an m.o.i of 0.001 and virus titres of the supernatants were determined via plaque assay on MDCK-NPro cells at 24, 48 and 72 hours post-infection. Results represent means plus standard deviation (SD) of three independent experiments.*

Consistently with previous data (see paragraphs 2.2.1), lower apoptosis was measured in HPDE6 cells than in the tumour BxPC-3 cell line. In addition, in the benign cell line both NS1 truncated viruses triggered less cell death than the full length NS1 H7N3 and H1N1 PR8 viruses. According with earlier findings (see paragraph 2.2.1), in BxPC-3 cell line the H7N3 isolate induced higher apoptosis compared to the human H1N1 PR8 strain. However, both PR8 H1/N1-2962 NS1-77 and H7N3 NS1-77 viruses displayed levels of cell death similar to those observed for the avian isolate

bearing full length NS1 protein. Taken together, these data confirm that the superior apoptotic skills displayed by the H7N3 virus are not the result of the virus' ability to bind PDA cells more efficiently than other strains (i.e. dependent on the HA) but rather they reside in the intrinsic capability of the avian isolate to promote apoptosis during infection (i.e. dependent on pro-apoptotic factors expressed by virus internal genes).

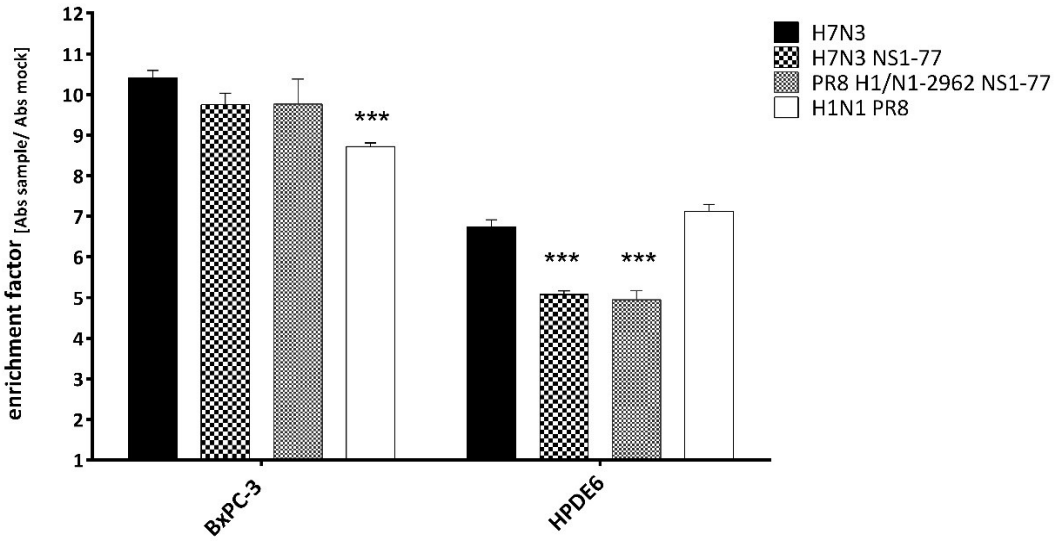

Figure 43. ***Enrichment of nucleosomes in the cytoplasm of BxPC-3 and HPDE6 cells at 24 hours post-infection with H7N3, H7N3 NS1-77, PR8 H1/N1-2962 NS1-77 and H1N1 PR8 viruses (M.O.I=1).*** *Cell Death Detection ELISA^{PLUS} (Roche) results are represented as mean enrichment factors [Abs sample/ Abs mock] ± standard deviations (SD) of one representative experiment (n=2). Statistical significance respect the H7N3 virus was determined in each cell line using Two-way ANOVA followed by Dunnett's multiple comparison test.*

5.2.2 PR8 H1/N1-2962 NS1-77 retains the IFN stimulatory ability of the H7N3 NS1-77 truncated virus.

Since the loss of ability to counteract IFN in healthy cells has been shown to improve the oncolytic potential of the H7N3 NS1-77 virus by contributing to both selectivity (see paragraph 3.3.3) and killing of uninfected cancer cells (see paragraph 3.3.4), we investigated whether the incorporation of PR8 HA and NA gene segments was detrimental for this feature. Thus, we compared the stimulation and the production of IFN-β in monolayers of different PDA cell lines and HPDE6 cells

infected with H7N3, H7N3 NS1-77, PR8 H1/N1-2962 NS1-77 viruses (M.O.I=0.1) or mock infected. Twenty-four hours post infection supernatants were collected and tested using the human IFN-β ELISA kit as described in material and methods. In line with earlier papers (Moerdyk-Schauwecker et al., 2012; Murphy et al., 2012), HPDE6 was the only cell line among those tested to mount an efficient IFN response to infection (Figure 44). Coherently with our previous results (see paragraph 3.2.2), HPDE6 cells produced higher levels of IFN-β following both NS1-77 truncated virus infections than for the H7N3 virus bearing full length NS1. The fact that H7N3 NS1-77 and PR8 H1/N1-2962 NS1-77 viruses induced similar production of this cytokine in the supernatants of infected HPDE6 cells confirmed that the new surface glycoprotein did not affect the ability of the recombinant virus to enter the benign cells and induce a powerful innate immune response.

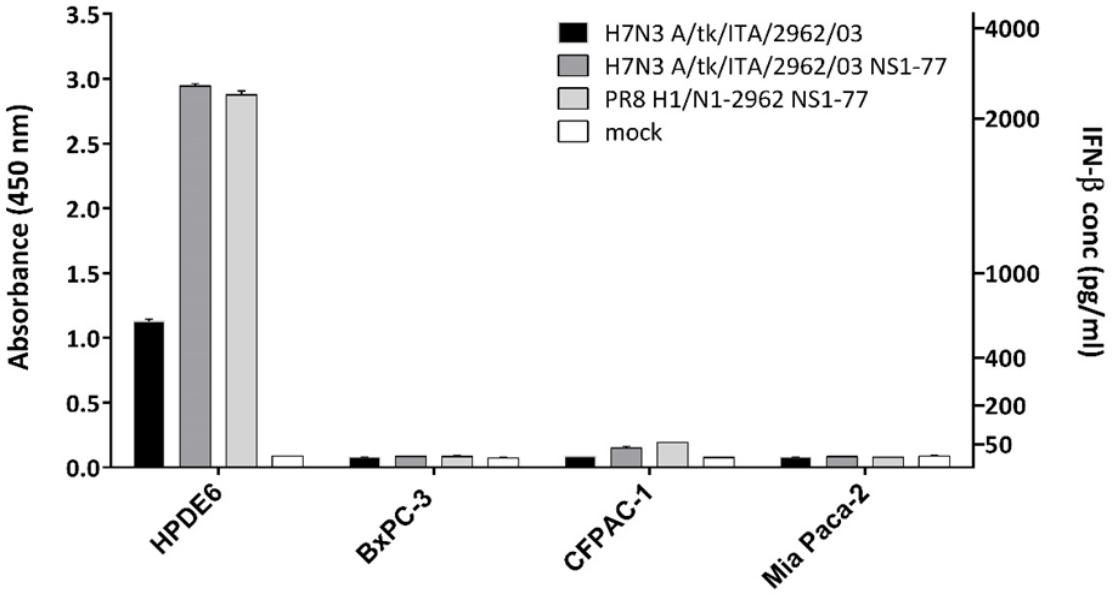

Figure 44. IFN-β ELISA kit results for supernatants derived from different pancreatic cell lines infected with H7N3, H7N3 NS1-77 and PR8 H1/N1-2962 NS1-77 viruses or mock infected. For each group absorbance values at 450 nm are represented (left Y axis) and the correspondent IFN-β concentration (pg/ml) can be obtained by comparison with the standard curve values (right Y axis). All values represent means ± standard deviations (SD) of one representative experiment (n=2).

5.3 Discussion and conclusion

Although in previous chapters we demonstrated that the H7N3 NS1-77 virus is attenuated in IFN competent systems, the use of an H7 avian influenza A virus strain for tumour treatment would face several concerns due to the possibility of (i) recombination with circulating human strains which might result in a potentially new pandemic virus and/or (ii) evolution to an highly pathogenic phenotype.

To address these safety issues we generated a 6:2 recombinant virus, named PR8 H1/N1-2962 NS1-77, possessing the backbone of the previously tested H7N3 A/turkey/Italy/2962/03 NS1-77 virus but the HA and NA genes from the well characterized human strain H1N1 A/Puerto Rico/8/1934.

The change of the surface glycoproteins, which represents the major antigens of IAV (Wang et al., 2010), altered neither the PR8 H1/N1-2962NS1-77 virus growth (Figure 42) nor its apoptotic potency (Figure 43) compared to the parental H7N3 NS1-77 strain. These results confirm that the marked ability of H7N3 virus to trigger PDA cell death does not depend on the HA binding and fusion activity, strengthening the idea that it rather resides in the effect of internal pro-apoptotic genes as discussed in chapter 4.

Furthermore, the PR8 H1/N1-2962 NS1-77 virus also retained the interferon-stimulatory properties displayed by the H7N3 NS1-77 virus (Figure 44) that can contribute to improve the final outcome of the treatment by allowing the killing of uninfected PDA cells (see paragraph 3.3.4-3.3.5).

Although the 6:2 recombinant does not show any enhancement in its oncolytic potential compared to the parental virus, its safety for therapeutic use is strongly improved as it presents a human origin H1 glycoprotein which (i) has never been associated to a highly pathogenic phenotype and (ii) is not completely new to human population (indeed since the pH1N1 2009 virus emerged, many people have antibodies that may cross protect against PR8 virus (Skountzou et al., 2010)). Thus in case of antigenic shift with other circulating human strains, the PR8 H1N1-2962 NS1-77 virus would represent a limited risk in terms of both systemic spreading and pandemic threat.

Furthermore, if a recombination occurred, several internal genes provided by the PR8 H1/N1-2962 NS1-77 virus could also contribute to curb the replication of the new virus in healthy mammalian cells. Indeed, as a turkey isolate without prior adaptive passages in mammals, the H7N3 virus presents internal genes characterized by typical avian signatures which have been associated to low transmission from birds to mammals and between mammals (for the sequence of all the virus segments please refer to materials and methods section). Examples of these signatures are those within the H7N3 PB2 gene, which has a pivotal role in the adaptation process of avian IAV to mammals (see paragraph 1.6.2.2). As previously discussed, glutamic acid to lysine change at position 627 (E627K) or an aspartic acid to asparagine change at position 701 (D701N) are key adaptive mutations for efficient replication of avian-origin IAVs in human cells. In the absence of PB2-627K or 701N, replacement of the highly conserved glutamine at position 591 with lysine (Q591K) or substitution of threonine at position 271 with alanine (T271A) can facilitate mammalian adaptation in the context of an avian-type PB2 protein (Yamada et al., 2010). Because the PB2 gene shared by H7N3 NS1-77 and PR8 H1/N1-2962 NS1-77 presents a typical avian signature without any of the above substitutions, the incorporation of this segment in a recombinant virus would result in limited replication in human cells and low transmissibility within the human population.

Besides PB2, avian NP has also been previously reported to contribute to the species barrier due to its high sensitivity to the antiviral activity exerted by human MxA protein (see paragraph 1.6.2.3). Conversely human IAV are often able to cope with Mx gene product thanks to mutation within specific recognition sites on the NP. Indeed, presence of isoleucine at position 100 (100I), proline at position 283 (283P) and tyrosine at position 313 (313Y) have been associated with the ability to escape MxA binding, while asparagine at position 52 (52N) has been shown to partially compensate the absence of some of the previous amino acids (Riegger et al., 2015). Because the H7N3 NP protein displays a typical avian signature (100R, 283L, 313F and 52Y), which makes it sensitive to

the antiviral activity exerted by human MxA (see paragraph 2.2.2), the integration of PR8 H1/N1-2962 NS1-77 NP gene into a recombinant virus would contribute to limit viral fitness in human cells. Finally, besides the factors associated with the species barrier, NS1-77 truncation would also strongly reduce the risk associated with the use of PR8 H1/N1-2962 NS1-77 virus as proven by the fact that different IAVs with truncated or modified NS1 proteins have been proposed as attenuated vaccines (Ngunjiri et al., 2015; Richt and Garcia-Sastre, 2009).

In conclusion to address issues related to the potential risk of antigenic shift and systemic spreading we generated a 6:2 recombinant virus which preserves the oncolytic properties previously shown by the parental H7N3 NS1-77 virus but which is safer for therapeutic use.

Chapter 6. "Arming" the virus: expression of granulocyte colony-stimulating factor (GM-CSF).

6.1 Introduction.

The immune system can identify and destroy nascent tumour cells in a process termed cancer immunosurveillance, which plays an important role in the defence against neoplasm (Vesely et al., 2011; Zitvogel et al., 2006). As with foreign tissues or infectious pathogens, following recognition of transformed cells, our immune cells secrete signal proteins that travel to the bone marrow where they promote proliferation of hematopoietic stem cells and subsequently their maturation and differentiation into leukocytes. One of the most important proteins in this process is the granulocyte macrophage colony-stimulating factor (GM-CSF, also known as CSF2), which stimulates blood stem cells to produce granulocytes and monocytes (Metcalf et al., 1986; Smith, 1990). GM-CSF leads to protective immunity, mainly by stimulating the recruitment, maturation, and function

of dendritic cells (DCs) (Dranoff, 2003; Li et al., 2009), the most potent antigen-presenting cell (APC) (Huang et al., 1994), which can activate the immune system against tumour-specific antigens (Dranoff, 2004).

The ability of the immune system to fight tumour cells has been used in the development of cancer immunotherapy treatments based on enhancing host antitumor responses (Dougan and Dranoff, 2009). Sipuleucel-T (trade name Provenge), as an example, is an autologous dendritic cell-based vaccine in which DCs are loaded with a fusion protein (PA2024) consisting of two parts: the antigen prostatic acid phosphatase (PAP), which is present in 95% of prostate cancer cells, and the GM-CSF that helps the APCs to mature. Reinfusion of such activated cells (APC8015) into the prostate cancer patients showed a 4-month benefit relative to the control group in randomized phase III clinical trials (Kantoff et al., 2010; Le et al., 2010). In addition, as previously discussed (see paragraph 1.3.1-1.3.1.4), clinical outcomes for the oncolytic vaccinia virus JX-594 (Pexa-Vec) and more recently for the herpes virus talimogene laherparepvec (T-Vec), both of which are armed with GM-CSF, confirmed that superior beneficial effect can be achieved when localized oncolytic activity is coupled with immune cell recruitment (Donnelly et al., 2013; Goins et al., 2014; Heo et al., 2013).

Based on these successful examples, to enhance the therapeutic activity of the PR8 H1/N1-2962 NS1-77 virus, we further engineered the viral NS segment to express the human GM-CSF gene. Expression of this cytokine during PR8 H1/N1-2962 NS1-77 GM-CSF virus infections was then tested in comparison to the parental strains.

6.2 Results

6.2.1 Design of NS1-77/2A/GM-CSFV5/NSend plasmid for reverse genetics.

Successful insertion of exogenous genes into the IAV genome has been previously achieved by different groups (Manicassamy et al., 2010; Pena et al., 2013; Shinya et al., 2004; Strobel et al.,

2000). The choice of the viral segment in which to insert the foreign gene depends on several factors. Increasing the length of the segment may have a detrimental effect on the packaging of the viral genome into new virus progeny. The segment may encode multiple viral proteins through splicing or frame shifts, as a result co-expression of the foreign gene might alter the expression levels of or even abrogate the correct production of the authentic viral genes with detrimental effect on virus fitness.

Based on its small size and on the low number of proteins currently known to be co-encoded, the segment 8 (NS) is often an easy choice for insertion of exogenous genes in the IAV genome (Figure 45A). Indeed, many publications demonstrated the possibility to express different non-viral proteins (e.g. GFP and luciferase) by fusing their ORF with the NS1 gene on segment 8, which has the advantages of being directly transcribed by a continuous RNA sequence and being expressed at very high levels during infection (see paragraph 3.1).

Segment 8 encodes two viral proteins NS1 and NEP. The NEP is produced following mRNA splicing and the levels of its expression are tightly controlled because the splice consensus sites are suboptimal so that NEP only slowly accumulates during infection (Chua et al., 2013). Nonetheless manipulation of segment 8 by abrogating this splicing mechanism has been adopted to allow expression of foreign proteins from the viral segment.

Although different strategies have been used to insert an exogenous gene into the NS1 ORF, many of them exploited the incorporation of a 2A autoproteolytic cleavage sequence within the NS segment. This sequence provides the opportunity to engineer in either whole proteins or domains that can be cleaved co-translationally with high efficiency (Ryan and Drew, 1994). In fact, during translation, the small 2A peptide interacts with the exit tunnel of the ribosome to induce the "skipping" of its last peptide bond. Crucially, the ribosome is able to continue translating the downstream gene, after releasing the first protein fused in its C-terminus to 2A (Ryan et al., 2002).

The first successful use of the foot-and-mouth disease virus (FMDV) 2A sequence to stably express a foreign protein from a recombinant influenza A virus was shown by Barclay et al. (Percy et al., 1994). Much later Basler et al. (Basler et al., 2001) used a similar strategy to express functionally active NS1 and NEP from a single polyprotein by (i) placing the FMDV 2A autoproteolytic cleavage site downstream of NS1 ORF, (ii) restoring the whole NEP ORF downstream the FMDV 2A sequence and (iii) silencing the NS splicing acceptor (SA) site (Figure 45B).

Extending this work, Manicassamy et al. (Manicassamy et al., 2010) designed a NS segment expressing the NS1-GFP and NEP as a single polyprotein with a 19 aa porcine teschovirus–1 (PTV-1) 2A autoproteolytic cleavage site (Kim et al., 2011) between them in order to allow NEP release from the upstream NS1-GFP fusion protein during translation (Figure 45C). Also in this study, silent mutations were introduced in the SA site to prevent unnecessary splicing of NS mRNA.

A different strategy was used by Pena et al. (Pena et al., 2013) who cloned the FMDV 2A autoproteolytic cleavage site sequence downstream of a truncated NS1 ORF (1–99) and then placed after it the transgene of interest (i.e. GFP, or luciferase). The NEP sequence, in this case, was deleted from segment 8 and re-introduced within segment 2, which was modified such that a FMDV 2A sequence separated the PB1 and the NEP ORF (Figure 45 D). Finally, in both segments 2 and 8, the vRNA specific packaging signals (see paragraph chapter 1.4.5.3) were reconstituted after the 3’ end of the inserted gene sequences.

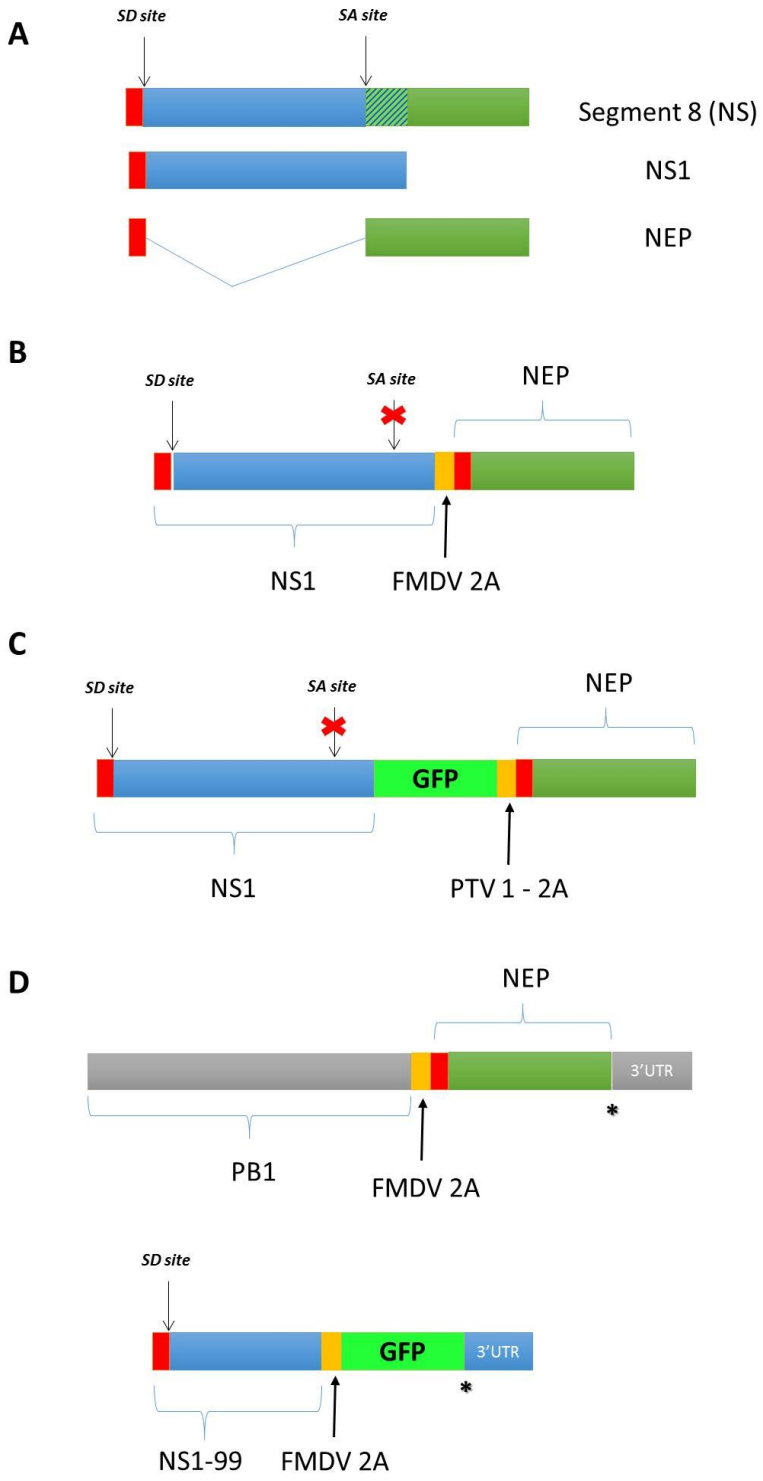

*Figure 45. **Different strategies adopted to express exogenous genes from the IAV NS segment. A)** Schematic representation of IAV NS segment structure and mRNAs expressed. **B)** In the NS1–2A-NEP constructs* (Basler et al., 2001)*, the NS1 and the NEP coding sequences do not overlap. In addition the two coding sequences are separated by the foot-and-mouth disease virus (FMDV) 2A autoprotease and are expressed as a single polyprotein. At the ribosome level, the polyprotein is then cleaved into two peptides: an NS1 with 16 additional 2A-derived amino acids at its carboxy terminus and an NEP with a single 2A-derived proline at its amino terminus. **C)** Schematic representation of IAV NS segment expressing NS1-GFP fusion protein* (Manicassamy et al., 2010)*. NS1 is fused to GFP via a GSGG linker and then followed by PTV-1 2A autproteolytic cleavage site and the whole NEP coding sequence. The NS splice acceptor (SA) site is mutated to prevent*

mRNA splicing. ***D)*** *Schematic representation of rearranged influenza viruses generated from Pena et al.* (Pena et al., 2013). *Exploiting the FMDV 2A autoproteolytic sequence, NEP is expressed from a single ORF downstream of the PB1 gene, whereas the foreign gene of interest (GFP) is expressed downstream of a C-terminal truncated NS1 gene translating only the first 99 amino acids. The packaging signals span both the untranslated region (UTR) and part of the ORF at both ends of each RNA segment. (*stop codon/s)*

Although all the strategies described successfully allow the generation of viruses expressing exogenous genes, it has to be noted that while in wild type IAV infected cells the steady-state amount of spliced NEP mRNA is only approximately 10% that of unspliced NS1 mRNA (Herz et al., 1981; Lamb and Lai, 1980; Lamb et al., 1980), in all the designs mentioned above, due to the shared ORFs, the rate of NEP expression would be the same as that of NS1 (Figure 45B-C) or PB1 (Figure 45D) genes. This would result in overexpression of NEP, which, besides exerting a central role in exporting vRNPs outside the nucleus, has also been implicated in the polymerase switch between viral transcription and replication (see paragraph 1.4.5.2). This might result in important changes in the behaviour of the virus compared to the parental strain as shown by Chua et al. (Chua et al., 2013). Since IAVs are not able to grow with high efficiency in PDA cells, high rates of viral genes production (mRNAs) would be required in order to assure significant amount of transgene expression. Based on these considerations we devised a novel NS segment which could retain, as much as possible, the original structure and preserve NEP splicing rate.

In our design the FMDV 2A peptide (17aa) was inserted after codon 77 of NS1 protein and then followed by the GM-CSF gene (Figure 46). A V5 epitope tag peptide (14 aa) from the simian virus 5 was then fused at the C-terminus of the GM-CSF gene to allow the detection of the cytokine without affecting its interaction sites with the GM-CSF Receptor Complex (Hansen et al., 2008). The remaining part of the NS segment was moved downstream of the GM-CSFV5 stop codon in the attempt to preserve splicing and thus the natural expression of NEP.

This NS design would have also assured that (i) the GM-CSF was produced at high levels by being encoded together with the NS1 protein that is abundantly expressed during infection (see paragraph 1.5.4), (ii) that the full length NS1 genotype could not be restored, an event that might have occurred following reversion of nonsense mutation in the previous NS1-77 constructs (see paragraph 3.1), and that (iii) the proper packaging signals were maintained at both ends of the vRNA segment (see paragraph chapter 1.4.5.3).

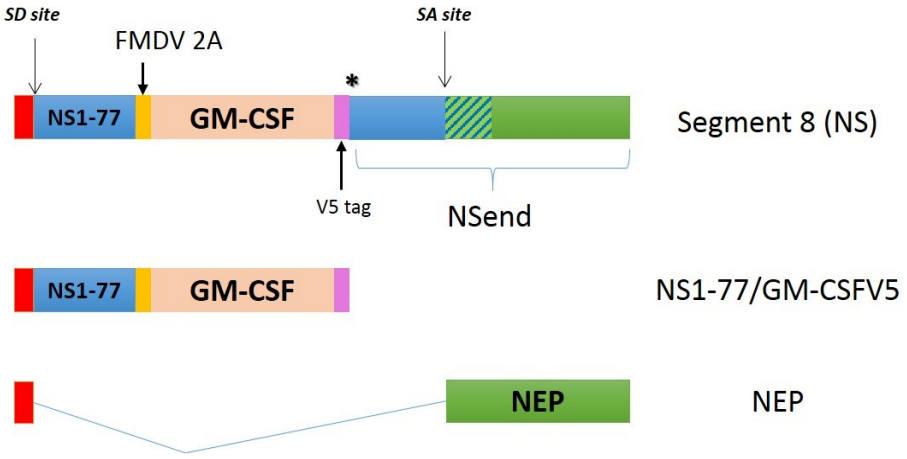

Figure 46. Schematic representation of the NS1-77/2A/GM-CSFV5/NSend segment structure and mRNAs expressed. The NS1-77 and the downstream GM-CSFV5 coding sequences flank the foot-and-mouth disease virus (FMDV) 2A auto-proteolytic motif and are expressed as a single polyprotein. The sequence from NS1 codon 78 until the C terminus of the original segment 8 is moved downstream of the GM-CSFV5 stop codon. Both splice donor (SD) and acceptor (SA) sites are preserved to allow mRNA splicing and production of NEP. (stop codon).*

6.2.2 Analysis of expression of NS1-77/2A/GM-CSF polyprotein.

To generate the structure desired the human GM-CSF gene, consisting only of the exon coding sequences, was obtained in pEx-A2 vector from Eurofins MWG - Operon. Using PCR overlapping and restriction enzymes, as described in material and methods (see paragraph 8.2.1.8), the first part of the NS segment, consisting of NS1-77/2A/GM-CSF sequence, was inserted into a pCAGG plasmid, which permits the fusion of the expressed protein with a V5 tag.

To evaluate the production of GM-CSF from the construct, 293T cells were transfected with the pCAGG/NS1-77/2A/GM-CSF and the previously generated pCAGG/NS1 H7N3 and pCAGG/NS1-77 H7N3 expression plasmids (see paragraph 3.2.2) (Figure 47A). At twenty-four hours post-transfection supernatants and cells were collected and protein expression was evaluated by western blot using Anti-V5 tag antibody (Lifetechnologies) (Figure 47B).

The western blot confirmed that transfection efficiently occurred in 293T, as both positive controls (pCAGG/NS1 and pCAGG/NS1-77) displayed intense signals in the cell lysates, additionally the higher expression levels of NS1-77 protein compared to the full length one reiterated the loss of the truncated protein's ability to inhibit the activity of CPSF30 (see paragraph 3.2.2). Consistent with the nuclear and cytoplasmic localization reported for NS1 (Hale et al., 2008), the signals for both the truncated and the full length proteins were detected only in the cell lysates.

Human GM-CSF codes for a protein of 144 amino acids, with a N-terminal leading peptide of 17 amino acids which is essential for protein targeting to the endoplasmic reticulum (ER) membrane and entry into the translocon (Walter and Johnson, 1994). In addition, GM-CSF undergoes heavy glycosylation which can target two N-linked glycosylation sites and four potential O-linked glycosylation sites (Kaushansky et al., 1987). Because of these different degrees of glycosylation the apparent molecular mass of the mature GM-CSF proteins can vary producing a broad band on SDS-Page between 18 and 30 KDa (Wong et al., 1985).

Although a continuous signal consistent with variations in glycosylation was observed, in the pellet of 293T cells transfected with pCAGG/NS1-77/2A/GM-CSF plasmid two major bands were visible. Based on molecular weight prediction the 144 aa non-glycosylated precursor form of human GM-CSF should have migrated in SDS-page around 16 KDa. However, the cytokine generated from the pCAGG plasmid was fused at its C-teminus with 16 amino acids consisting of the 2 aa-long Mlu I restriction site and the 14 aa-long V5 tag (see chapter 9 – Appendix for the detailed sequence and structure of the construct). As such, the final length of the GM-CSFV5 protein expressed from the

plasmid was 160 aa with an expected molecular weight around 18 KDa. Thus, we ascribed the lower band in the pellet (column 3 - blue arrow) to the expression of the non-glycosylated GM-CSFV5 precursor protein. As for the upper band (column 3 - red arrow) located above the signal for NS1 protein (≈26 KDa), although heavy post-translational glycosylation can further increase the molecular weight of GM-CSFV5 up to 30 KDa (Wong et al., 1985), we cannot rule out the possibility that this band might correspond to an uncleaved form of the NS1-77/2A/GM-CSFV5 polyprotein (predicted molecular weight ≈28.5 KDa) derived from sub-optimal cleavage of the 2A sequence.

In contrast with the NS1 and NS1-77 proteins, due to the presence of secretory signal peptide at its N-terminus, the human GM-CSF protein was also abundantly detected in the supernatant of transfected cells (column 6). In line with previous data (Wong et al., 1985), the heavy post-translational glycosylation on both O-linked and N-linked sites produced a heterogeneous population of mature GM-CSFV5 proteins in the supernatants that migrated as a broad band between 18 and 30 KDa. The presence of GM-CSF in the supernatants derived from pCAGG/NS1-77/2A/GM-CSF transfection was further confirmed using the Human GM-CSF ELISA kit (Thermo Scientific™) (Figure 47C).

The detection of the cytokine in the supernatants was an indirect evidence of the proteolytic cleavage of the NS1-77/2A/GM-CSFV5 polyprotein. If the cleavage had not occurred the GM-CSF signal peptide would have been embedded within the polyprotein and hence the cytokine could not have been secreted (Futatsumori-Sugai and Tsumoto, 2010; Rapoport, 1992).

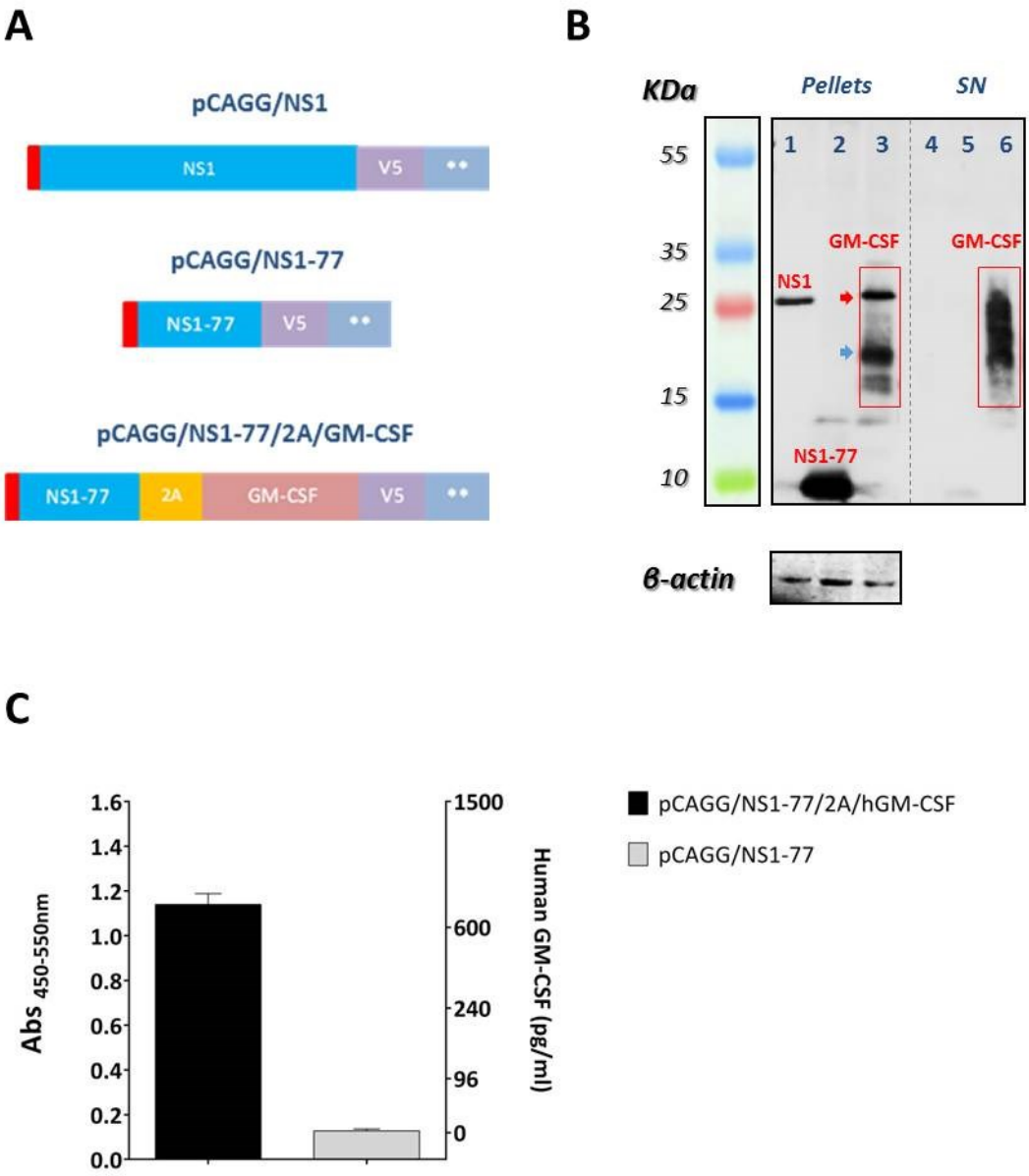

Figure 47. ***Expression of human GM-CSF from pCAGG/NS1-77/2A/GM-CSF plasmid. A)*** *Schematic representation of the pCAGG plasmids used for transfection of 293T cells.* ***B)*** *Western Blot analysis targeting V5 tag in pellets (Column 1-3) and supernatants (column 4-6) derived from 293T transfection with pCAGG/NS1 H7N3 (columns 1 and 4), pCAGG/NS1-77 H7N3 (columns 2 and 5) and pCAGG/NS1-77/2A/GM-CSF (columns 3 and 6) plasmids. Expected protein sizes: NS1≈ 26 KDa, NS1-77≈ 9 KDa, hGM-CSFV5 precursor form (nonglycosylated)≈ 18 KDa [blue arrow], NS1-77/2A/GM-CSFV5 ≈ 28.5 KDa [red arrow], hGM-CSFV5 mature form (glycosylated) ≈ 18-30 KDa.* ***C)*** *Human GM-CSF ELISA kit quantitative results for the supernatants derived from pCAGG/NS1-77/2A/GM-CSF and pCAGG/NS1-77 transfections. For each group mean absorbance (n=2) (Abs 450-550nm) is represented (left Y axis) + standard deviation (SD) and the correspondent concentration (pg/ml) can be obtained by comparison with the standard curve values (right Y axis).*

6.2.3 Generation of RF483-NS1-77/2A/GM-CSFV5/NSend plasmid for reverse genetics.

A series of overlapping PCRs were then performed to obtain the final NS1-77/2A/GM-CSFV5/NSend construct (see chapter 9 – Appendix for the detailed sequence and structure of the construct), which was eventually inserted into the rescue plasmid RF483 as described in materials and methods (see paragraph 8.2.1.8). The RF483 rescue plasmid, derived from the pHW2000 plasmid previously generated by Hoffmann et al. (Hoffmann et al., 2000) (see paragraph 1.6.3), allows synthesis of the same viral RNA species produced during virus infection by using a RNA pol I–pol II transcription system (Figure 48A).

We next tested the capability of the new reverse genetics construct to produce NEP mRNA following splicing of the full length NS mRNA in transfected cells. Thus, semi-confluent monolayers of 293T cells were transfected in a 24 well plate with RF483-NS1-77/2A/GM-CSFV5/NSend plasmid at concentration of 1 µg/well. As positive controls for segment 8 mRNA splicing, the rescue plasmids RF483-H7N3 NS and RF483-H7N3 NS1-77, previously used for the generation of H7N3 and H7N3 NS1-77 viruses respectively, were also transfected (Figure 48B). Forty-eight hours post-transfection, the media was removed and the cells pelleted at 12000 g x 5 minutes. Total RNA was extracted from cell lysates using the Nucleospin RNA extraction kit (Macherey-Nagel) and then mRNAs were isolated trough the PolyATtract mRNA Isolation Systems (Promega). Using the primers H7N3 NEP Fw1-23 and H7N3 NEP Rv322-344, which target the NS1 and NEP shared mRNA sequences (Figure 48B), RT-PCR was performed to investigate the expression of the mRNAs produced from NS1-77/2A/GM-CSFV5/NSend construct.

Visualization of PCR products in agarose gel (Figure 48C) confirmed production of a different NS1 mRNA species from the NS1-77/2A/GM-CSFV5/NSend segment when compared to the NS and NS1-77 reverse genetics plasmids. Indeed, in line with the construct design, NS1-77/2A/GM-CSFV5/NSend segment generated longer NS1 mRNAs (PCR product ≈ 1347nt) than the wild type

segment (PCR product ≈ 693nt). Nevertheless, all the plasmids tested produced an additional band of the same size and similar intensity which migrated at a molecular weight compatible with the NEP mRNAs (PCR product ≈ 344nt). Purification of the bands from agarose gel and subsequent sequencing confirmed the identity of the NEP mRNAs (data not shown). Taken together these results show that the structure of the new construct does not affect the ability of NS segment to undergo splicing and that NEP production occurs at similar rates as for the original segment.

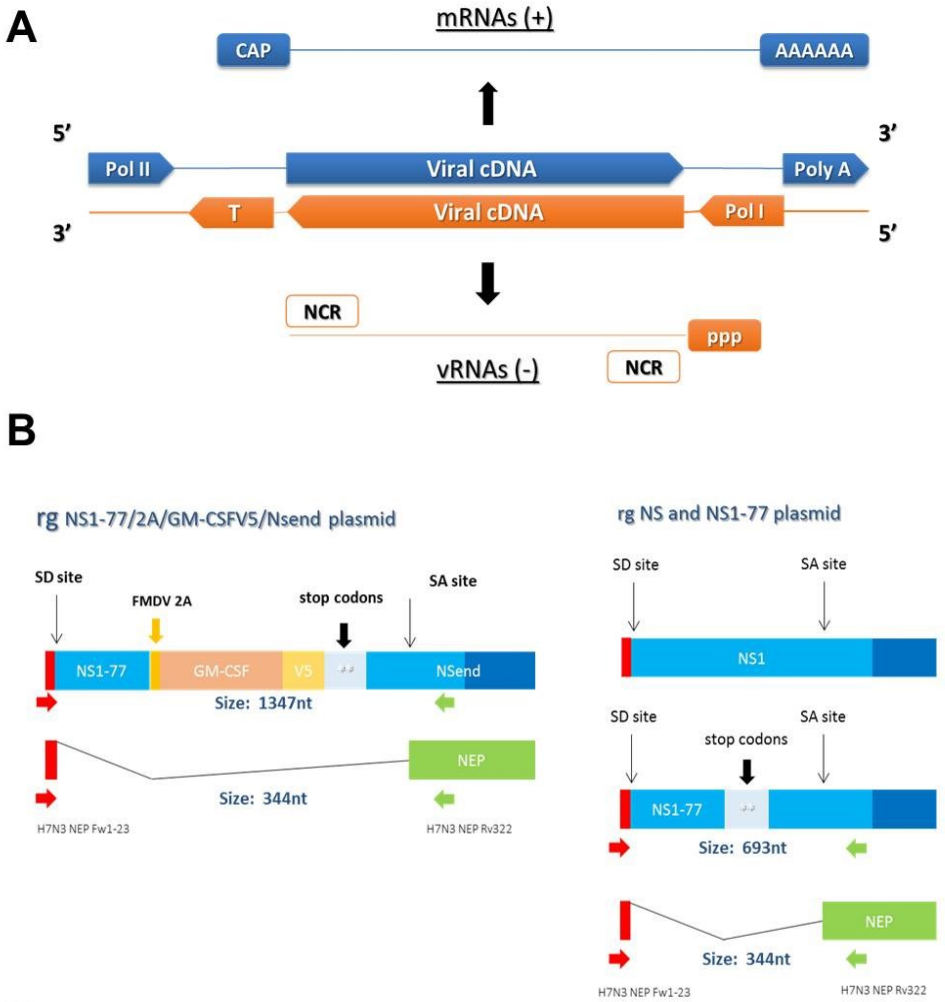

Figure 48. ***Detection of mRNA species produced from RF483-NS1-77/2A/GM-CSFV5/NSend rescue plasmid. A)*** *Schematic representation of RF483 dsDNA pol I–pol II transcription system for synthesis of vRNAs and mRNAs to generate reverse genetics viruses. The cDNA of each of the eight influenza virus segments is inserted between the RNA pol II promoter (pol II) and the polyadenylation signal (Poly A). This pol II transcription unit is flanked by the RNA pol I promoter (pol I) and the pol I terminator (T) in the opposite orientation (-). After transfection of the plasmid, two types of molecules are synthesized. From the human pol I promoter, negative-sense vRNA(-) is synthesized by cellular pol I. The synthesized vRNA contains the noncoding regions (NCR) at the 5′ and 3′ ends. Transcription by pol II yields mRNAs with 5′ cap structures and 3′ poly(A) tails; these positive-sense mRNAs (+) are translated into viral proteins.* ***B)*** *Schematic representation of RF483-NS1-77/2A/GM-CSFV5/NSend, RF483-H7N3 NS and RF483-H7N3 NS1-77 rescue plasmids used in the experiment and their corresponding mRNA products. Red and green arrows represent the forward and reverse primers respectively used to target shared NS1 and NEP mRNA sequences in the RT-PCR reaction. Expected sizes of PCR products are reported below each mRNA species.* ***C)*** *Left - upper panel: agarose gel visualization of PCR amplified mRNA products transcribed from NS1-77/2A/GM-CSFV5/NSend (1), wild type NS (2) and NS1-77 (3) segments. Left - lower panel: Beta-actin was also tested as loading control. Right panel: agarose gel visualization of purified PCR products confirming the expected size of the different mRNA species.*

6.2.4 PR8 H1/N1-2962 NS1-77 GM-CSF virus rescue and propagation.

Although mRNA transcribed from the NS1-77/2A/GM-CSFV5/NSend segment was able to support NS1-77, GM-CSF and NEP expression in mammalian cells following transfection, we still had to confirm that (i) the corresponding vRNA could be packaged into the virion and (ii) that it could be efficiently transcribed by the viral RNA polymerase complex. Thus, to address these points, we tested whether PR8 H1/N1-2962 viruses could be rescued by reverse genetics using the new NS segment.

Human embryonic kidney cells (HEK) 293T were transfected with the seven reverse genetics plasmids used for the production of the PR8 H1/N1-2962 virus (H7N3 PB2/PB1/PA/NP/M and PR8 HA/NA) (see paragraph 5.1) plus the RF483-NS1-77/2A/GM-CSFV5/NSend plasmid to generate the novel PR8 H1/N1-2962 NS1-77 GM-CSF virus. Transfections with the RF483-NS1-77/2A/GM-CSFV5/NSend or pCAGG/NS1-77/2A/GM-CSF plasmids alone were also performed as controls. Twenty four hours post-transfection aliquots of the supernatants were collected and tested for the

presence of GM-CSF protein using the Human GM-CSF ELISA kit. The ELISA assay confirmed the expression of the cytokine from all the transfections except the mock (Figure 49A).

To evaluate whether the NS construct was efficiently packaged into virions, a RT-PCR using a forward primer targeting the 5' end of the NS1 gene and a reverse primer annealing downstream the GM-CSFV5 sequence was performed on supernatants derived from the eight plasmid transfection (Figure 49B). Supernatant derived from transfection of RF483-NS1-77/2A/GM-CSFV5/NSend plasmid alone was also appraised as negative control. Results showed amplification of the NS1-77/2A/GM-CSFV5/NSend segment only in the supernatants derived from transfection with all the 8 plasmids suggesting efficient packaging of the NS segment into newly synthesized viruses released from the cells (Figure 48B). Accordingly, electron microscopy confirmed the presence in this supernatant of IAV particles (Figure 49C), in which subsequent RNA extraction and sequencing verified the presence of the NS1-77/2A/GM-CSFV5/NSend segment (data not shown).

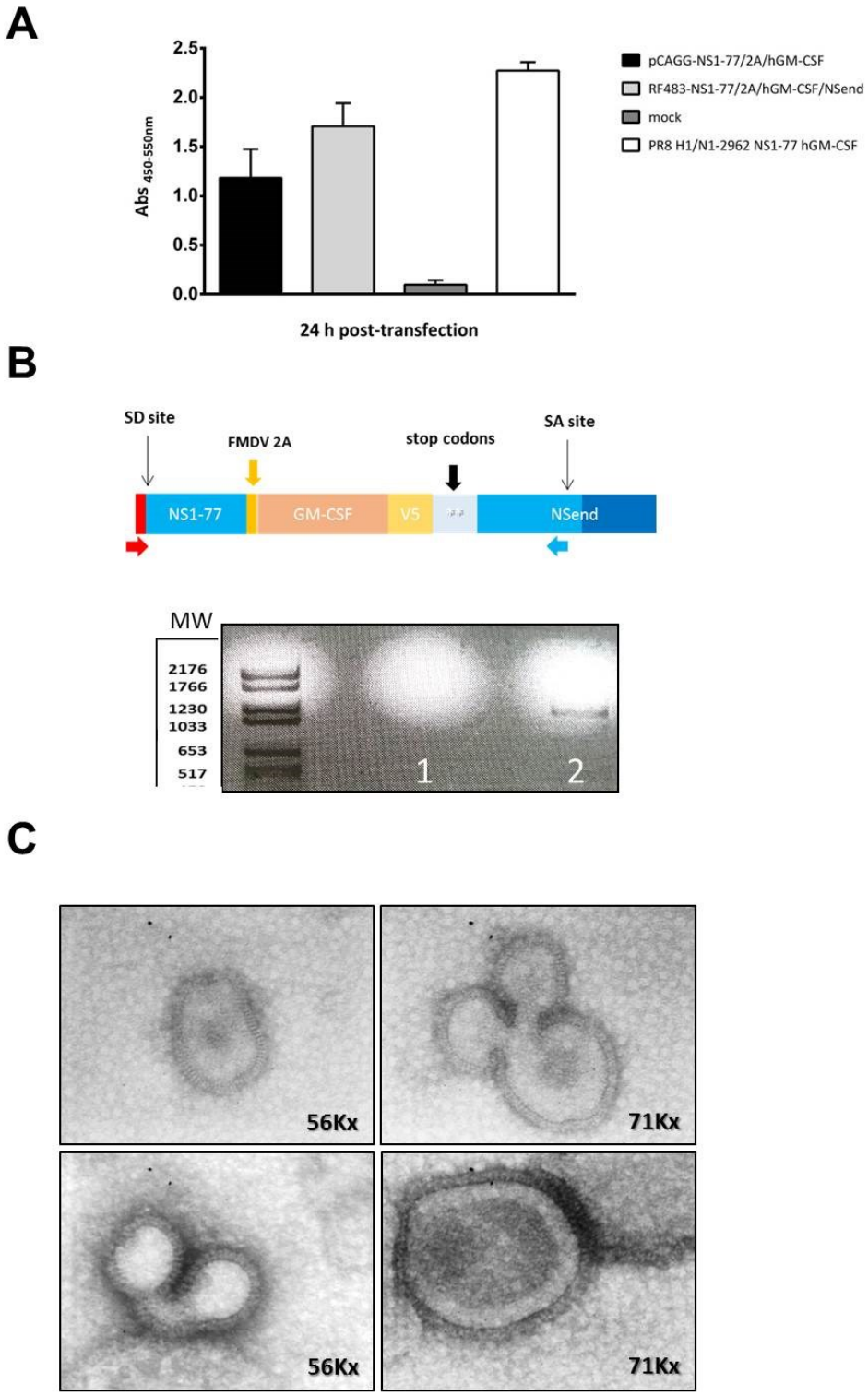

Figure 49. ***Rescue of PR8 H1/N1-2962 NS1-77 GM-CSF virus. A)*** *Human GM-CSF ELISA results for supernatants derived from 293T cells transfected with pCAGG/NS1-77/2A/GM-CSF plasmid, RF483-NS1-77/2A/GM-CSF/NSend plasmid, RF483-NS1-77/2A/GM-CSF/NSend plus the other segments required for the generation of PR8 H1/N1-2962 NS1-77 GM-CSF virus or mock transfected.* ***B)*** *Agarose gel results for RT-PCR targeting the NS1-77/2A/GM-CSFV5/NSend segment in the supernatant of 293T cells transfected either with the segment alone (1) or in combination with the other 7 reverse genetics plasmids (2).* ***C)*** *Electron microscopy confirming the presence of IAV particles in the supernatant from the eight plasmid transfection. Magnifications: 56Kx=56000x; 71Kx=71000x.*

Although the PR8 H1/N1-2962 NS1-77 GM-CSF virus was successfully rescued the corresponding titre was extremely low to perform a direct growth curve. Therefore, the virus had to undergo serial passages in MDCK-Npro cells, during which we monitored its ability to retain and express the cytokine. RT-PCR and subsequent sequencing of virus NS segment confirmed the presence of the NS1-77/2A/GM-CSFV5/Nsend vRNA in the supernatants of infected cells in passage 1 and 2 (Figure 50A). The production of the human cytokine during PR8 H1/N1-2962 NS1-77 GM-CSF virus infection was monitored at the end of the second passage in Npro cells through a 72 hour time course (M.O.I=0.1) using the Human GM-CSF ELISA kit (Figure 50B). PR8 H1/N1-2962 NS1-77 virus and mock infection were performed as negative controls. A significant increase in the amount of human GM-CSF was observed within the first 48 hours post-infection, confirming the ability of PR8 H1/N1-2962 NS1-77 hGM-CSF virus to efficiently express the exogenous gene at high rate in infected cells. No appreciable signals were recorded for any of the other infections.

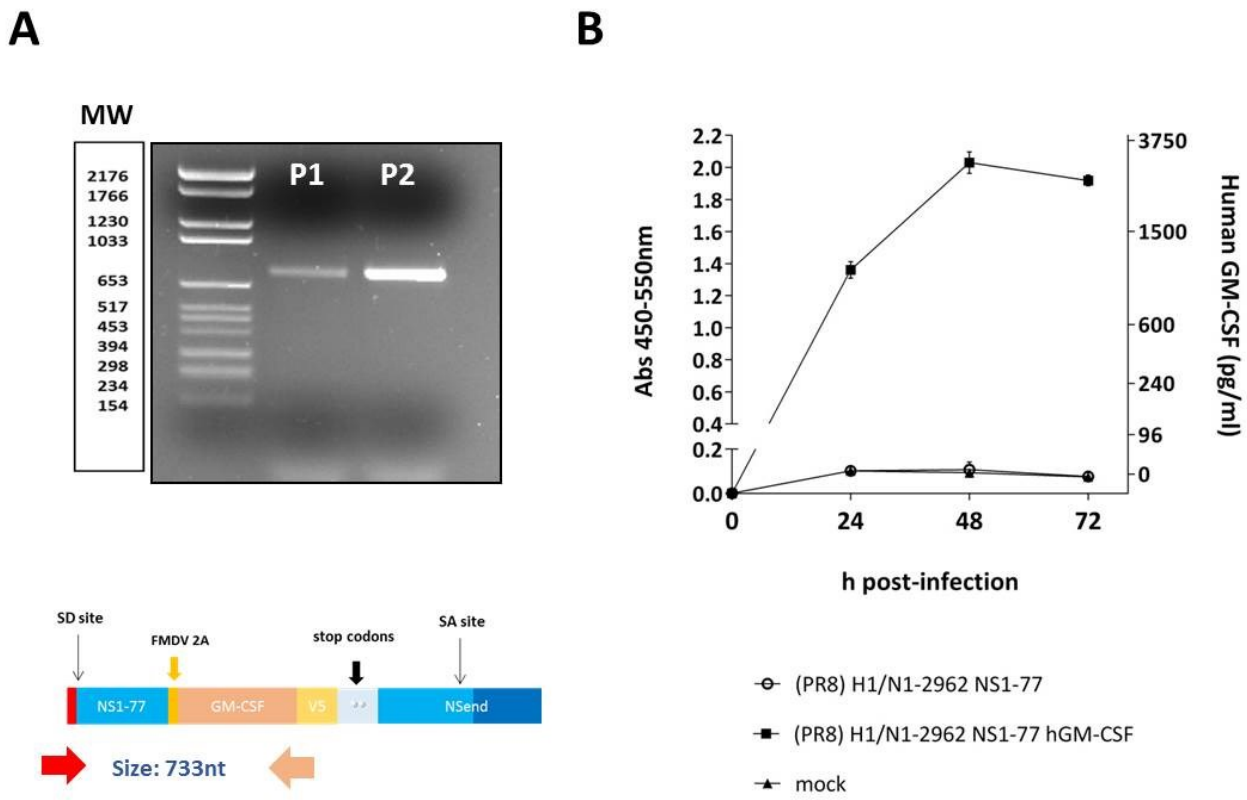

*Figure 50. **Ability of the PR8 H1/N1-2962 NS1-77 GM-CSF virus to mantain and express the human GM-CSF gene. A)** RT-PCR analysis of NS1-77/2A/GM-CSFV5/Nsend vRNA in the supernatants of infected Npro cells after the first (P1) and the second (P2) passages. RT-PCR was carried out for viral RNA isolated from cell culture supernatants by using a forward*

primer annealing to the 5'end of NS1 gene while the reverse primer was targeting the GM-CSF/V5 overlapping region (expected product size ≈733nt). PCR products were separated by agarose gel electrophoresis and visualized by ethidium bromide staining. ***B)*** *Time-course expression of human GM-CSF during PR8 H1/N1-2962 NS1-77 GM-CSF virus infection in Npro cells. The cells were infected with PR8 H1/N1-2962 NS1-77 GM-CSF or PR8 H1/N1-2962 NS1-77 viruses at M.O.I 0.1 or mock infected. Supernatants were collected and analysed for human GM-CSF using the Human GM-CSF ELISA kit. Mean absorbance (Abs 450-550nm) values derived from one representative experiment (n=3) are represented ± standard deviation (SD) and the correspondent concentration (pg/ml) can be obtained by comparison with the standard curve values on the right Y axis.*

A truncation involving the major part of the human GM-CSF sequence was revealed by RT-PCR and sequence analysis (data not shown) at the end of the third passage in Npro cells and further confirmed at the end of passage 4 (Figure 51A-B). Previously, Wolschek et al. (Wolschek et al., 2011) showed that the human interleukin-2 (IL-2) gene, co-expressed immediately downstream the SD site (aa 10) of the NS1 gene, was deleted from the virus after only one passage in Vero cells. However, the same gene was stably retained until passage five when the NS1 gene was allowed to express the first 125 amino acids (Kittel et al., 2005), suggesting that the introduction of a foreign sequence in close proximity of the SD or SA sites might compromise NS mRNA splicing due to an interfering RNA secondary structure (Wolschek et al., 2011). Wolschek et al. addressed this issue by constructing different IL-2-expressing chimeric segments endowed with specific changes in the sequences surrounding the splicing sites and the branch point to enhance NS mRNA splicing efficacy (Wolschek et al., 2011). Although this strategy improved the stability of the foreign gene expression, at least until passage number 5, it also entailed a change in the splicing rate of the NS segment. Differently to Wolschek et al., we tried to avoid affecting NEP expression by keeping intact the sequence surrounding the splicing sites and maintaining the natural distance between the splicing acceptors site and the branch point sequence within the "NSend" part of the construct. Nevertheless, it appears that an optimal distance between the SA and SD sequences is preferred in order to allow a stable propagation of the NS segment. In line with this consideration following few

passages the selective pressure promoted the emergence of a truncated form of segment 8 that likely restored a more suitable distance between the different splicing regulatory elements.

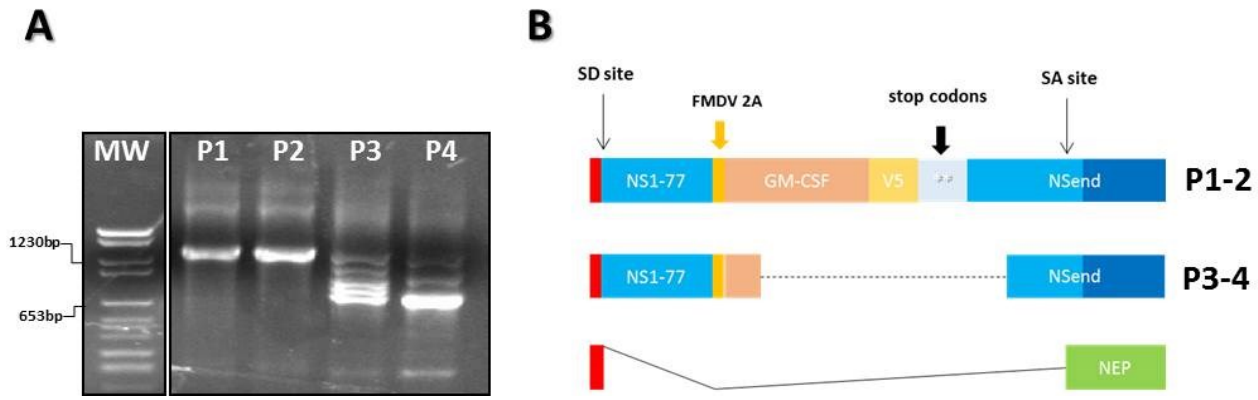

Figure 51. ***Progressive truncation of the NS1-77/2A/GM-CSFV5/NSend segment during serial passages in Npro cells. A)*** *RT-PCR analysis of the novel NS segment following serial passages of the PR8 H1/N1-2962 NS1-77 GM-CSF virus in Npro cells. RT-PCR was carried out from viral RNA isolated from cell culture supernatants by using primers targeting 5' and 3' ends of NS1-77/2A/GM-CSFV5/NSend segment. Decrease of the size of the engineered NS segment was observed after passage number 3 and further confirmed at the end of passage number 4. RT-PCR product expected sizes: NS1-77/2A/GM-CSFV5/NSend = 1347 nt; wild type NS segment= 693nt.* ***B)*** *Schematic representation of the truncation occurring within the NS1-77/2A/hGM-CSFV5/Nsend segment following serial passages in Npro cells. After agarose gel purification of the lowest band displayed for passage 3 and subsequent sequencing, a truncation spreading from 75nt after the beginning of the hGM-CSF gene to 59nt following the V5 tag stop codon was revealed. Results were further confirmed sequencing samples from passage number 4. The deletion affected the expression of the cytokine but not those of NS1-77 and NEP proteins.*

6.2.5 Expression of GM-CSF genes in PDA cells following infection.

Although the expression of the exogenous gene appears compromised after multiple rounds of infection, this issue might represent a problem for the production of large viral stock rather than for the efficacy of the treatment itself. Indeed, since PDA cells do not support high growth of H7N3 derived viruses (see paragraphs 3.3.3 – 4.2.1) and hence the virus oncolytic activity cannot rely on multiple cycles of infection in these cells, the loss of GM-CSF, even after few passages, would have unlikely a dramatic effect on the final outcome of a multiple injection treatment as long as the input

virus is able to express significant amount of the cytokine. Therefore, to appraise the level of human GM-CSF expression during a single round of infection in PDA cells, the PR8 H1/N1-2962 NS1-77 GM-CSF virus collected in passage 2 was tested in BxPC-3 cell line.

In order to confirm the cytokine expression in tumour cells, immunofluorescence (IF) targeting the V5 tag, fused to the C-terminus of GM-CSF (see Figure 46), was performed in BxPC-3 cells at 8 hours post-infection with PR8 H1/N1-2962 NS1-77 GM-CSF, PR8 H1/N1-2962 NS1-77 viruses (M.O.I=0.1) or following mock infection (negative controls). The results displayed a very strong signal only for the PR8 H1/N1-2962 NS1-77 GM-CSF virus, confirming the production of the V5-tagged protein early during infection, a data in line with the timing of NS1 gene expression with which GM-CSF is co-transcribed (Figure 52).

However, higher magnification (400X) revealed that the IF signal for the V5 tag was mainly nuclear rather than cytoplasmic. This result would be consistent with the production of an uncleaved form of NS1-77/2A/GM-CSFV5 polyprotein, which was previously hypothesized on the basis of western blot data generated in paragraph 6.2.2 (Figure 47B). Indeed, sub-cellular localization might be explained because the uncleaved polyprotein would be directed to the nucleus by the nuclear localization signal 1 (NLS1) within the RBD (residues Arg-35, Arg-38 and Lys-41) at the N-terminus of NS1-77 protein (Hale et al., 2008). Due to its localization, this polyprotein would represent the main target of IF antibodies as the cleaved form of GM-CSFV5 protein is rapidly secreted outside the plasma membrane. Indeed, the successful secretion of human GM-CSF from transfected 293T cells reported earlier (see paragraph 6.2.2) suggests that the uncleaved and unsecreted form of GM-CSFV5 might represent only a fraction of the whole product generated from the new NS segment. Since IF appraises the presence of V5-tagged protein inside the cells, we next investigated the amount of GM-CSF secreted in the supernatant during PR8 H1/N1-2962 NS1-77 GM-CSF infection.

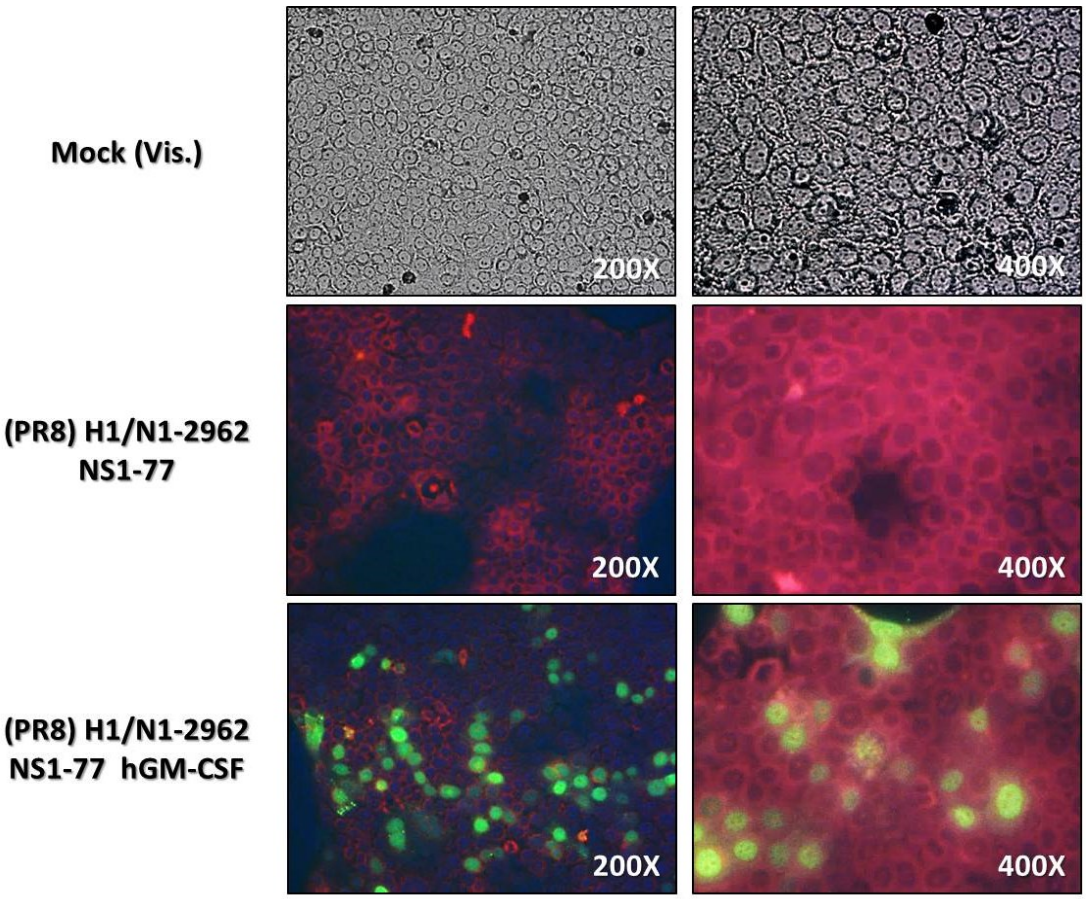

*Figure 52. **Immunofluorescence (IF) targeting GM-CSFV5 in BxPC-3 cells at 8 hrs post-infection.** Tumour BxPC-3 cells were infected with PR8 H1/N1-2962 NS1-77 GM-CSF or PR8 H1/N1-2962 NS1-77 viruses (M.O.I= 0.1) or mock infected. After fixation and permeabilization, BxPC-3 cells were incubated with the Mouse anti-V5 Antibody (Lifetechnologies) and then with the Goat anti-mouse IgG-FITC (SIGMA). Each antibody was diluted in PBS containing 1% BSA, 0.1% Tween-20 and 0.2% Evan's Blue contrast solution.*

To appraise the levels of human GM-CSF expression in benign and tumor cell lines, semiconfluent monolayers of HPDE6 and BxPC-3 cells were infected with PR8 H1/N1-2962 NS1-77 GM-CSF virus (M.O.I=0.1). PR8 H1/N1-2962 NS1-77 virus and mock infections were also performed as negative controls. At 24 hours post-infection supernatants were collected and tested for presence of GM-CSF using the Human GM-CSF ELISA kit (Thermo Scientific). The results confirmed production of the cytokine only in the case of PR8 H1/N1-2962 NS1-77 GM-CSF virus infection in both cell lines (Figure 53). However, while in the supernatants of tumour BxPC-3 cells GM-CSF reached values above 1500 pg/ml, in those derived from benign HPDE6 cells the concentration was almost 2 fold lower. Indeed,

although the virus can infect both cell lines as no selectivity is exerted at cell entry, the ability of benign HPDE6 to efficiently mount an IFN-mediated antiviral response (see paragraph 2.2.2) and the fact that GM-CSF is encoded together with a truncated NS1-77 protein, which cannot counteract this response (see paragraph 3.2.2), could explain the lower levels of the cytokine in this cell line.

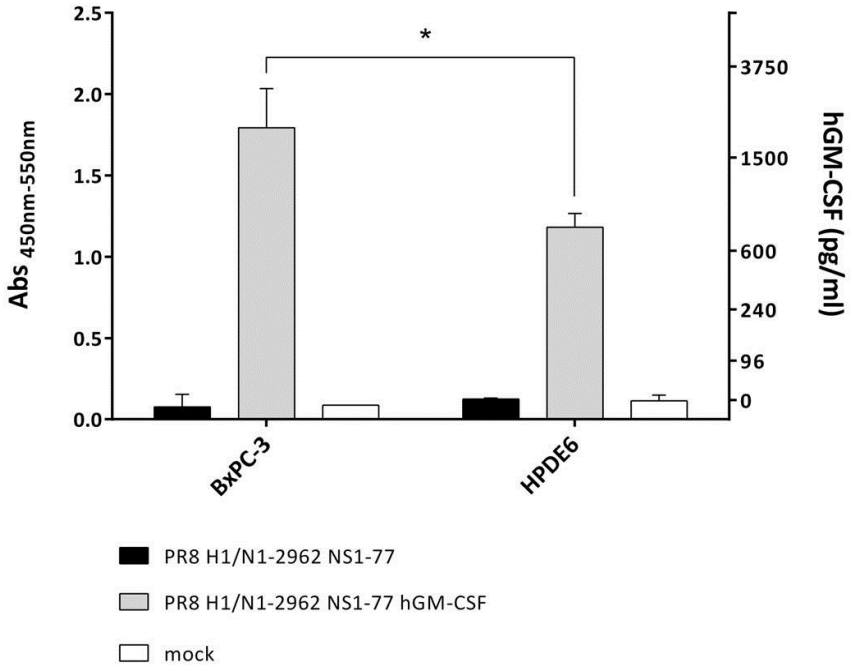

*Figure 53. **Human GM-CSF ELISA results for BxPC-3 and HPDE6 supernatants collected at 24 hours post-infection with PR8 H1/N1-2962 NS1-77 GM-CSF, PR8 H1/N1-2962 NS1-77 viruses (M.O.I = 0.1) or following mock infection.** Values represent means of Absorbance$_{450nm}$- Absorbance$_{550nm}$ ± standard deviations (SD) of one representative experiment (n=4). For each absorbance value the correspondent GM-CSF concentration (pg/ml) can be obtained by comparison with the standard curve values (right Y axis). Statistical significance was determined using Two-way ANOVA followed by Tukey's multiple comparison test.*

6.3 Discussion and conclusion

The granulocyte macrophage colony-stimulating factor (GM-CSF or CSF2) is produced by various cell types including macrophages, mast cells, T cells, fibroblasts and endothelial cells (Cousins et al., 1994; Nimer and Uchida, 1995), mostly in response to immune activation and cytokines that mediate inflammation. Under physiological conditions, GM-CSF in the circulation is at low or even

undetectable levels (20-100 pg/ml) (Conti and Gessani, 2008), which can readily reach high values (200-7000 pg/mL) in response to immune stimuli (Shi et al., 2006).

T cell-derived GM-CSF, which is produced by both CD4+ and CD8+ T cells after TCR (T-cell receptor) activation along with the appropriate co-stimulatory signals, has a particularly important role in the crosstalk between antigen-presenting cells and T cells (Conti and Gessani, 2008). Indeed, It has been shown that GM-CSF is critical for DCs development and maturation by activating different cellular signalling pathways such as the janus kinase/signal transducer and activator of transcription (JAK/STAT) pathway, the mitogen-activated protein kinase (MAPK) pathway and the phosphatidylinositol 3-kinase (PI3K) pathway. These pathways can act synergistically promoting proliferation and differentiation of DCs (van de Laar et al., 2012) which can then move by chemotactic (Wang et al., 1987) in the blood stream toward the site of cytokine expression and boost both Th1 and Th2 mediated immune response against foreign antigen or tumour associated antigens.

Based on the encouraging results showed by different armed oncolytic viruses and vectors, demonstrating the beneficial effect of GM-CSF stimulated anticancer immunity even in the case of low or no replication (Andtbacka et al., 2015; Hellebrand et al., 2006; Heo et al., 2013), we decided to incorporate the gene encoding for this cytokine into the PR8 H1/N1-2962 NS1-77 influenza A virus backbone.

Using information generated by earlier studies co-expressing exogenous genes linked with the viral NS1 ORF, we designed a novel NS segment in which the foot-and-mouth disease virus (FMDV) 2A auto-proteolytic cleavage sequence and the human GM-CSF gene fused to V5 tag were placed “in frame” downstream of codon 77 of NS1 gene (NS1-77) (Figure 46). The rest of the NS segment was then moved downstream of the V5 tag stop codon, maintaining both splicing acceptor site and branch sequences with the aim to preserve splicing site selection (Corvelo et al., 2010; Taggart et al., 2012) for the generation of NEP mRNA.

Following transfection of 293T cells the construct allowed efficient production and secretion of human GM-CSF (Figure 47B-C) and expression of NEP at level similar to those of the original NS segment (Figure 48C). Moreover the elongated vRNA was packaged into novel virions since we were able to generate a PR8 H1/N1-2962 NS1-77 GM-CSF virus bearing the human cytokine gene (Figure 49B-C). Infection of cells with this virus led to secretion of GM-CSF from MDCK Npro cells during passage of stocks (Figure 50A-B) and after infection of tumour BxPC-3 cells (Figure 53). Although GM-CSF was also detected in the supernatants of infected HPDE6 cells, the efficient antiviral response against the truncated NS1-77 virus mounted by the benign cells (see paragraphs 2.2.2-3.2.2) mitigated the production of the cytokine to significantly lower concentrations than in tumour cells (Figure 53).

The results collected in this chapter show that the novel NS segment can “arm” the previously generated PR8 H1/N1-2962 NS1-77 virus to abundantly express the human GM-CSF during PDA cell infection. The high levels of GM-CSF expression in BxPC-3 cells (Figure 53) suggest that infection of PDA cells with the recombinant virus could promote recruitment of immune cell to the proximity of the neoplasm where tumour antigens might be present in larger number compared to normal cell components as results of virus preferential lytic (see paragraph 2.2.1) and immunostimulatory activity (see paragraph 3.3.4).

Chapter 7: Discussion.

7.1 Why should IAV make any difference for PDA virotherapy?

Pancreatic cancer is the fourth commonest cause of cancer related death in men. Late detection, early metastases, difficult surgical approach and cancer resistance for chemo and radiotherapy all contribute to the worst prognosis among various gastro-intestinal cancers (see paragraph 1.2.4).

Pancreatic cell carcinogenesis develops through accumulation of mutations and genetic lesions which lead to activation of oncogenes and inactivation of tumour suppressor genes. Although characteristic patterns of genetic lesions have been revealed (see paragraph 1.2.3), accumulating evidence suggests that PDAs are characterized by marked genetic heterogeneity. Indeed the latest genomic sequencing efforts demonstrate that most of the secondary mutations occurring in PDAs have a prevalence of <5% (Biankin et al., 2012; Yachida and Iacobuzio-Donahue, 2013). Therefore, although molecular signatures of this malignancy, consisting of mutations in KRAS, CDKN2A, TP53 and SMAD4/DPC4 genes, are pivotal in pancreatic cancer evolution, their combination with different secondary events may lead to diverse PDA sub-classes possessing disparate phenotypes and genotypes, as shown by various cancer-derived cell lines (Deer et al., 2010). This may have substantial implications for therapeutic responsiveness and targeted intervention strategies (Biankin et al., 2012; Collisson et al., 2011).

With technological advancement, more specific cancer treatments targeted to key genetic aberrations are becoming available, leading the way for better care through patient-tailored personalized treatment.

As previously discussed (see paragraph 1.3), virotherapy is a treatment based on oncolytic viruses, which exploit the genetic aberrations in tumours to selectively or preferentially infect, replicate and ultimately kill cancer cells with minor or no effect on the healthy cells. Although some oncolytic

viruses have already been thoroughly investigated and even successfully reached advanced clinical trials (see paragraph 1.3.2), due to the genetic heterogeneity of PDA tumour cells together with the different replicative mechanisms adopted by each virus, virotherapy should not rely on a short list of possible candidates. Instead, a broad range of viruses characterized by specific cancer cell permissiveness would represent a better opportunity to find the best treatment for each specific PDA patient. As an example reovirus, a naturally occurring, replication competent oncolytic virus, which has shown positive results in different clinical trials across a variety of cancer types (Comins et al., 2008), replicates specifically in cells that have a constitutive activated KRAS pathway. Because of the prevalence of KRAS-mediated neoplasms associated with pancreatic cancer (see paragraph 1.2.3), the majority of PDA cell lines results sensitive to treatment by reovirus. However, this virus fails to produce the same beneficial effect in BxPC-3 cells (Lee et al., Dec. 6, 2011) which carry a wild-type gene and do not present enhanced KRAS activity (Yip-Schneider et al., 1999). Indeed different publications showed that PDA cells are highly heterogeneous in their permissiveness to various OVs (Moerdyk-Schauwecker et al., 2012; Murphy et al., 2012; Wennier et al., 2011). Therefore the potent pro-apoptotic effect of IAVs in tumour PDA cells, previously shown resistant to other oncolytic viruses (see paragraph 2.2.1), suggested that IAV might be a useful treatment option for specific sub-classes of PDA and might play a role in further studies on virotherapy for pancreatic cancer.

7.2 An engineered avian influenza A virus for PDA virotherapy.

In the present study for the first time the oncolytic potential of engineered avian-origin influenza A virus (AIV) was evaluated against PDA cells. Indeed, to our knowledge, no IAV of any origin has been appraised so far for PDA treatment and the relative small number of previous investigations concerning the use of this virus for virotherapy were focused on the well characterized human strain H1N1 A/Puerto Rico/8/34 (Bergmann et al., 2001; Muster et al., 2004; Sturlan et al., 2010;

Wolschek et al., 2011) (Table 5). However, as shown in the thesis, the choice of a particular viral isolate does affect the corresponding oncolytic performances as it can influence for example the ability to counteract host IFN response (see paragraph 3.2.2), the extent of apoptotic induction (see paragraphs 2.2.1 – 2.2.2) or the sensitivity to host ISGs (see paragraph 1.6.2.3). As such, the possibility to select a virus strain from the diverse natural avian reservoir on the basis of its inherent oncolytic potency in PDA cells and, through engineering, improve its safety and debulking activity represents a novel approach for IAV therapy.

Publications	IAV backbone (origin)	Genetic changes	Tumour cells
Bergmann et al., 2001	H1N1 A/Puerto Rico/8/34 (human)	• delNS1	Ras-transfectant cell line 518-L1
Muster et al., 2004	H1N1 A/Puerto Rico/8/34 (human)	• delNS1 or NS1-99	Human melanoma cell lines
Sturlan et al., 2010	H1N1 A/Puerto Rico/8/34 (human)	• NS1-80	Human colon cancer cell lines
van Rikxoort et al., 2012	H1N1 A/Puerto Rico/8/34 (human)	• delNS1 • Armed with IL-15, (based on NS design from Wolschek et al., 2011).	Human melanoma cell lines
Present work	H7N3 A/turkey/Italy/2962/03 (avian)	• NS1-77 • PB1-F2 L75H • H1-N1 (PR8) • Armed with hGM-CSF • Novel NS design	Human pancreatic ductal adenocarcinoma (PDA) cell lines

Table 5. ***Novel aspects of the present study (blue line) in comparison to previous publications on IAV as an oncolytic virus (white lines).*** *delNS1, lack of NS1 gene expression; NS1-99/NS1-80/NS1-77, NS1 gene express only the N-terminal 99, 80 or 77 amino acids, respectively; IL-15, Interleukin-15; hGM-CSF, human granulocyte macrophage colony-stimulating factor.*

Specific targeting of cancer cells is the *conditio sine qua non* for oncolytic virotherapy since it contributes to enhance both safety and efficacy of the treatment. Some viruses, such as reovirus, Newcastle disease virus and mumps virus have a natural preference for cancer cells, while others such as measles, adenovirus, vesicular stomatitis virus (VSV), vaccinia and herpes simplex virus (HSV) can be adapted to make them cancer specific (Russell et al., 2012).

Among the different strategies to improve cancer selectivity (see paragraph 1.3.1.2) oncolytic viruses can be engineered to exploit the defective antiviral defences of tumour cells (Naik and Russell, 2009). Like many types of cancer cells, the majority of PDA cells are deficient in IFN alpha and beta gene expression (see paragraph 1.2.3). As such, it is possible to enhance preferential replication in these cells by decreasing the virus' ability to counteract IFN-mediated antiviral response in the healthy cells. In case of IAV this strategy involves the impairment of the NS1 protein, which is the major viral antagonist of host IFN expression during infection (see paragraph 1.5.4). Thus, to further increase selectivity for IFN-deficient PDA cells, the low pathogenicity avian influenza virus H7N3 A/turkey/Italy/2962/03 (see paragraph 2.2.1) was mutated to express a truncated NS1-77 protein (see paragraph 3.1).

The NS1 deletions or truncations have most often been described in the literature as potential novel attenuated influenza virus vaccines (Ngunjiri et al., 2015; Pica et al., 2012; Wacheck et al., 2010). In addition the previous works developing the PR8 strain of IAV as an OV also turned to NS1 deletion or truncation for improving the selectivity of the virus to replicate in IFN deficient tumour cells (Muster et al., 2004; Sturlan et al., 2010). However none of these previous studies had described the bystander effect that we directly tested here whereby H7N3 NS1 truncation significantly enhanced the killing of uninfected PDA cells, through stimulation of IFN expression from the healthy cells (see paragraph 3.3.4).

In order to further enhance the potency for tumour killing by giving the virus more time for genome replication within each round of PDA infection, we next attempted to engineer mutations to the

virus that might delay induction of apoptosis by mutating the viral PB1-F2 protein, which normally exerts a pro-apoptotic function. However, the increase in virus yield following the PB1-F2 L75H mutation was extremely modest compared to the wild type H7N3 PB1-F2 virus. The overall titre of the mutated virus might have been limited by the availability of proteases in the cell culture system that are required for activation of influenza HA to support multiple rounds of replication. Although previous studies showed that trypsin-like protease endogenously expressed in different PDA cell lines were sufficient to allow multi-cycle replication of lentogenic Newcastle disease virus (NDV) (Buijs et al., 2014), under our experimental conditions vRNA replication did not appear to correlate with a proportional increase of infectious virus titres (see chapters 2 and 4). In other words the *in vitro* system we use to measure virus replication might not support multicycle replication and that makes it difficult to test whether engineered mutations really do enhance replication or not. These effects might be more readily seen *in vivo* in the orthotropic pancreatic tumour mouse model because of an excess of activating trypsin that may result from pancreatitis often associated with tumour progression that could support more efficiently multiple rounds of infection.

Since the stimulation of the immune system is often detrimental for pathogen replication and viral gene expression, the development of antitumor immune-based strategies and oncolytic viruses (OVs) have occurred on separate tracks for long time. However, it has become increasingly clear that the immune responses play a critical role on the clinical benefit of virotherapy such that, in some models, virus replication and direct oncolysis are not even necessarily required for therapy (Prestwich et al., 2009).

The granulocyte macrophage colony-stimulating factor (GM-CSF) is the immune gene most usually inserted into clinically advanced OVs (Andtbacka et al., 2015; Heo et al., 2013). This preference for GM-CSF derives from its potent ability to generate systemic adaptive antitumour immunity *in vivo* after expression in cancer cells, (Dranoff et al., 1993) which is associated with the recruitment and differentiation of activating DC in the tumour microenvironment. Coupling virus infection with

concomitant expression of an immunostimulatory signal, able to boost anti-tumour immunity, appears a suitable strategy to improve the oncolytic performances of a virus which displays low replication but high lysis in PDA cells. Thus, oncolytic IAV H1/N1-2962 NS1-77 virus was "armed" to express the human GM-CSF gene during infection (chapter 6). Although the use of 2A autoproteolytic sequence has been widely reported by different authors for the expression of polyprotein mRNAs (see paragraph 6.2.1), we devised a novel NS segment which (i) allows high levels of GM-CSF expression and secretion, (ii) retains the natural production of NEP by preserving both splicing sites and (iii) further enhances the safety of the virus by eliminating the possibility of reversion to the full length NS1 genotype.

Of course a possible downside of coupling oncolytic activity with immune cell recruitment might be that the activated immune system may also act prematurely to suppress therapeutic virus replication. However, as previously reported (see paragraphs 3.3.3 – 4.2.1), the avian origin IAV displayed moderate replication in PDA cells and thus its use as oncolytic agent in these cells does not rely (at least at the moment) on multiple rounds of infection. Moreover, the direct method of administration (IT), the quickly ability of the H7N3-derived viruses to trigger high level of cell death (see paragraph 3.2.1) and to express significant levels of GM-CSF in PDA cells (see paragraph 6.2.5) together with the possibility to exploit HA exchange with other human IAV subtypes (H1, H2, H3) preserving the original apoptotic properties (see paragraphs 5.2.1), may allow the virus to perform its lytic and immunostimulatory activity before adaptive immunity could promote pathogen clearance.

Although immunodeficient animal models (e.g. SCID mice) are suitable for the evaluation of effective replication in and destruction of human tumours by OVs, they cannot assess the complete safety and efficacy profile of the virus in normal tissue, nor do they permit evaluation of the impact of adaptive immunity on overall virus potency, which is especially important when such virus is armed with immunomodulatory transgenes. However, the cost associated with generating or

buying and housing immunocompetent mice are prohibitive and tumour latency and progression to invasive diseases are also highly variable (Tseng et al., 2010). In addition, in our specific case, the use of immunocompetent pancreatic cancer mouse models would have also required the injections of murine PDA cell lines and the insertion into the viral NS segment of the murine variant of GM-CSF, which shares modest structural homology at the level of the nucleotide (70%) and amino acid (56%) sequences with the human gene (Shi et al., 2006).

An alternative to common immunocompetent mouse models may be represented by humanized mice, which are immunodeficient mice that have been engrafted with human primary haematopoietic cells and tissues that generate a functional human immune system. These models address many of the limitations of translating discoveries in rodents into clinical applications for studies of human hematopoiesis, immunity, cancers, and infectious diseases (Shultz et al., 2012). With respect to oncology, humanized mice have already been used to study human tumours *in vivo* (Shultz et al., 2007), to characterize tumour biology (Barabe et al., 2007) and to study anti-tumour therapies (Wege et al., 2011). Nevertheless, there are still a number of limitations in the currently available humanized mouse models as investigators are continuing to identify molecular mechanisms underlying the remaining defects in the engrafted human immune system and are generating "next generation" models to overcome these final deficiencies (Brehm et al., 2013; Shultz et al., 2012).

Due to all these issues the oncolytic activity of the GM-CSF “armed” IAV was not tested in immunocompetent PDA mouse model during this project. Therefore, future studies will be necessary to appraise the timing and the extent of GM-CSF expression and the corresponding overall oncolytic activity of the PR8 H1N1-2962 NS1-77 GM-CSF virus in the more complex context of an immunocompetent system. In addition, infection of appropriate immunocompetent system should also preclude overexpression of GM-CSF, which has been previously associated with

pathological changes mainly due to autoimmune response (Biondo et al., 2001; Hamilton and Anderson, 2004; Johnson et al., 1989).

Nevertheless, taken together, our work demonstrates the possibility to improve the oncolytic potential of an influenza A virus isolate, chosen on the basis of its strain-specific apoptotic potency in PDA cells, by enhancing its selectivity (see chapter 3) and safety (see chapter 5) and by combining its tumour debulking activity via direct viral lysis (see chapter 2) with the possible activation of innate (see chapter 3) and adaptive (see chapter 6) immune responses (Figure 54). Based on all these considerations, we believe that the study hereby presented is novel and is an example of how to develop information from current literature to solve difficult medical problems.

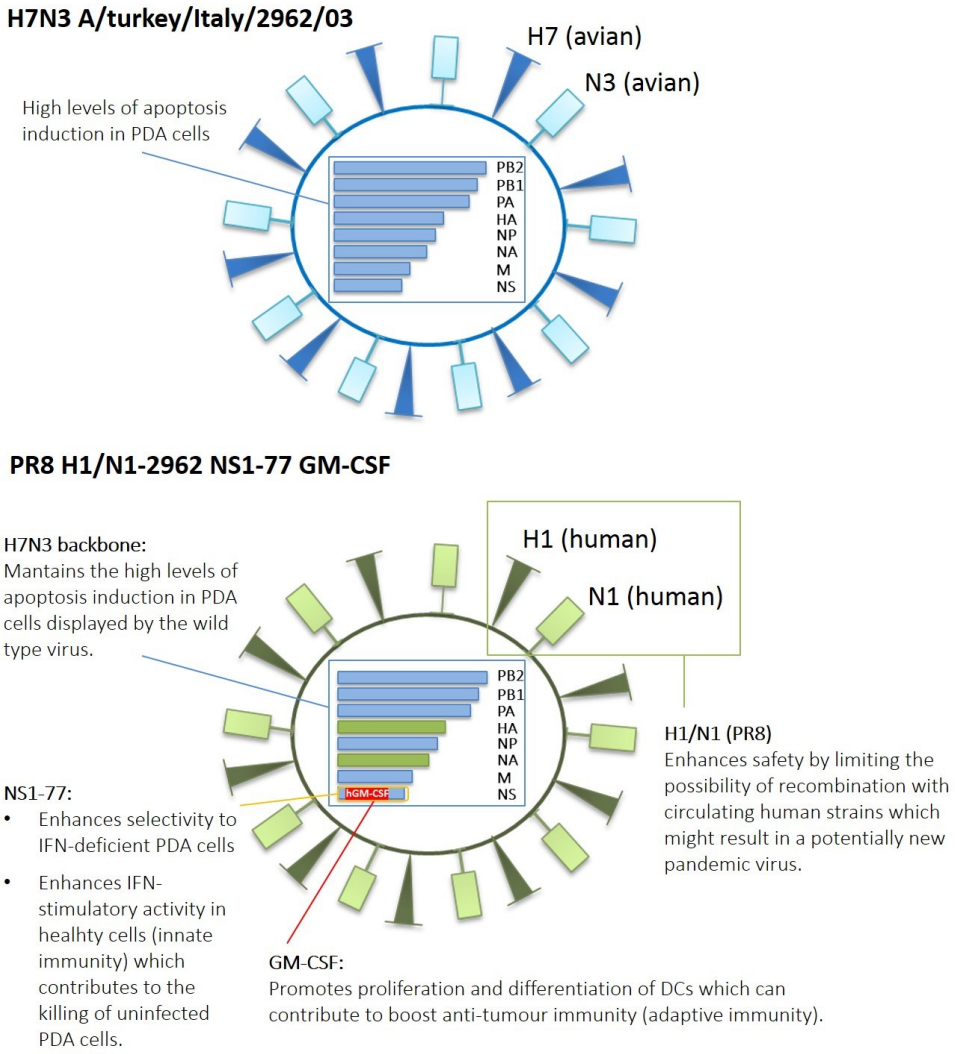

Figure 54. ***Graphical abstract of the main findings of the present work.*** *The wild type avian influenza virus H7N3 A/turkey/Italy/2962/03, which was selected for its strain-specific apoptotic potency in PDA cells (upper panel), was*

further improved by engineering. The resulting reverse genetics virus, named PR8 H1/N1-2962 NS1-77 GM-CSF (lower panel) preserves the apoptotic potential of the parental strain in PDA cells, but possesses enhanced selectivity, safety and oncolytic potential.

In addition, the project also generated useful reagents and findings. We generated a BxPC-3 cell line stably expressing the luciferase gene (BxPC-3Luc), which might be a useful tool to monitor both tumour growth and virotherapy beneficial effect in future *in vivo* studies. We also contributed to the characterization of the PDA cells in terms of (i) sialic–acids receptor distribution (see paragraph 2.2.1), (ii) IFN and ISG genes expression (see paragraph 2.2.2 and 5.2.2) and (iii) apoptosis related protein activation (see paragraph 4.2.1). Although these data may represent important information especially for further investigation in oncology and virotherapy, they are also relevant for interpreting basic virological studies. Indeed, since many cell lines used for virological experiments are either immortalized or derived from tumours, they might possess genetic aberrations which might affect the final outcome of the research. Therefore a better characterization of the cell lines in laboratory use can improve the study of the virus determinants and their interaction with the host cell pathways.

Finally, in light of an increasing level of criticism about the lack of reproducibility in modern scientific publications, it is worth noting that our results also consolidate previous findings, including those confirming the strain-specific ability of NS1 protein to counteract IFN mediated antiviral response (see paragraph 3.2.2) or the data supporting the lack of IFN expression and the sensitivity to exogenous IFN of different PDA cell lines (see paragraph 3.3.4).

7.3 Future developments.

Oncolytic viruses can constantly be subjected to improvement, refinement and perfection through engineering efforts. For example surface markers that are expressed selectively by specific tumour

cells can be targeted by engineering viruses to use them as receptors for virus entry (Cattaneo et al., 2008). Besides increasing the efficacy of the treatment, this transductional targeting can also be used to eliminate toxicities, particularly when the oncolytic virus binds a ubiquitous receptor. VSV, for example, was pseudotyped with the surface glycoprotein from a non-neurotropic lymphocytic choriomeningitis virus or retargeted measles virus, thereby eliminating its neurotoxicity without compromising its ability to infect and kill cancer cells (Ayala-Breton et al., 2012; Muik et al., 2011). Modification of the hypervariable loop of the adenovirus hexon protein ablated the ability of that virus to infect normal hepatocytes but not tumour cells (Shashkova et al., 2009).

Further modifications to enhance specific PDA targeting, thus increasing its anti-tumour effect and reducing undesirable tropism, might be introduced also into the PR8 H1/N1-2962 NS1-77 GM-CSF virus. Indeed, IAV infection begins with a specific interaction between the viral hemagglutanin (HA) and a sialic acid (SA)-containing host cell receptor (see paragraph 1.4.5.1). The degree of receptor affinity is further influenced by oligosaccharide length, sulfation, fucosylation, and specific subterminal residues of the SA-containing glycoconjugate, all affecting the interaction at the HA receptor binding site (RBS) (Nicholls et al., 2008). Sialyl Lewis x (SLex)-related antigens, which contain fucose adjacent to the terminal SA, have been found in the majority of pancreatic cancer tissues while absent from normal tissues, and correlate with poor patient prognosis in the clinical setting (Kim et al., 1988; Mas et al., 1998; Perez-Garay et al., 2010). Thus to increase IAV specific-targeting of PDA cells, the HA RBS might be mutated to optimize binding with tumour-associated SA species, creating a PDA-specific virus with lowered affinity for cells from the normal pancreas. A possible way to engineer viruses with altered preferences for different silaic acid species has recently been pioneered using an experimental evolution approach (Imai et al., 2012). Here random mutations were introduced into the region of HA encoding the globular head, which includes the receptor-binding pocket, of IAV HA to generate a virus library from which mutants that displayed enhanced binding for particular sialic acids were enriched. In our case such a library would be

screened by panning for PDA cell binding (Imai et al., 2012) or by using synthetic Sialyl lewis glycans (Stencel-Baerenwald et al., 2014). De-targeting or re-targeting the virus could be pivotal to success, especially in the case of the treatment of the pancreas, where, an undesired tropism could cause pancreatic disorders. Indeed, a possible viral involvement in the aetiology of type I diabetes (T1D), for example, has been suggested by several authors (Filippi and von Herrath, 2008; Richer and Horwitz, 2008; von Herrath et al., 1998). Viruses associated with human type I diabetes include enterovirus such as Coxsakievirus B (CVB) (Hyoty and Taylor, 2002; Jaidane and Hober, 2008; Yin et al., 2002), but also measles, congenital rubella, mumps, cytomegalovirus and influenza B (Hyoty et al., 1993; Lindberg et al., 1999; Sano et al., 2008). Viral infections such as Coxsackie B 4 (CVB4) (Coleman et al., 1973; Jaidane et al., 2009), rotavirus (Honeyman et al., 2000), and reovirus (Onodera et al., 1978) have shown to be diabetogenic in mice. Therefore, although pancreatitis and T1D might likely be pre-existing conditions in patient suffering PDA (see paragraph 1.2.2), the re-targeting of IAV HA to specific tumour cell receptors could be essential to decrease the likelihood of undesired side effects and increase the safety of the treatment.

Once the issue of unwanted toxicity is addressed, further engineering could take the virus closer to the goal of a single-shot virotherapy (Russell et al., 2012), which might enhance the beneficial effect of the treatment and reduce the stress of multiple interventions for the patients. Indeed, without rapid, destructive intra-tumoural spread, a single-shot administration of IAV for PDA virotherapy would probably have a modest or even innocuous effect. Thus, to enhance efficacy, further engineering of the viral HA could be performed, to increase its activation only in the environment of the pancreatic tumour. A second key event in the IAV infection process is the cleavage of HA by host proteases from its inactive precursor, HA0, to its functionally active forms HA1 and HA2 (see paragraph 1.4.5.1). The amino acid sequence of the HA cleavage site determines the proteases capable to process it, and, thus its tropism based on the protease distribution in different organs (see paragraph 1.4.4.1). Previous publication showed that the IAV HA cleavage site can be modified

to host novel proteolytic sites, making virus replication dependent on the presence of specific proteases (Stech et al., 2005). Alterations of protease production and secretion are well-documented in cancers, such as over-expression of matrix metalloproteinases (MMPs) in numerous types of tumours, including PDA (Kinoh et al., 2004; Schneider et al., 2003; Springfeld et al., 2006; Vartak and Gemeinhart, 2007). Therefore, modification of the HA cleavage site to render it specific for tumour-associated proteases could provide a further mechanism to increase viral replication specifically in the tumour cells (Cattaneo, 2010; Springfeld et al., 2006; Szecsi et al., 2006).

7.4 Personal considerations

Because the research described in this thesis contributed not only to generate scientific data but also to my vocational training, I would like to conclude with a personal remark. When I began my PhD I considered this project a fantastic opportunity to improve my knowledge concerning two extremely interesting area of science to me: virology and oncology. I still do. Nonetheless, as with many projects, in the following years I had to face diverse scientific, technical and financial challenges. In solving them when I could, or bypassing them through the devising new experiments and strategies when I could not, I developed as a scientist. Although a very straightforward project would have been appreciated, I am thankful for the challenges and problems that I encountered as they correspond to the moments where I learnt the most and sometimes I had the chance to surprise myself with some good ideas. I do not know if what I adsorbed during these years is enough but I am aware of what I knew at the beginning of this thesis and what I know now about IAV and pancreatic cancer. Looking back I would have done some things differently but I will value this experience as preparation for the next challenges that I will face in my scientific career.

Chapter 8. Materials and Methods

8.1 Materials

8.1.1 Cell lines

Table 6. Cell lines used in this study.

Cell line	Origin / Modification	Source
293T	Human embryonic kidney cells expressing large T antigen of SV-40	ATCC
A549- IFNLuc	Human lung cell line stably expressing Firefly luciferase reporter gene under the control of IFN-β promoter	Barclay Lab
MDCK-NPro	Madin Darby Canine Kidney cells expressing the NPro gene of Bovine Viral Diarrhea Virus (BVDV)	Barclay Lab
BxPC-3	Human pancreatic ductal adenocarcinoma cell line	ATCC
BxPC-3Luc	BxPC-3 cells stably expressing Firefly luciferase reporter gene.	This study
AsPC-1	Human pancreatic ductal adenocarcinoma cell line	ATCC
CFPAC-1	Human pancreatic ductal adenocarcinoma cell line	ATCC
MIA PaCa-2	Human pancreatic ductal adenocarcinoma cell line	ATCC
PANC-1	Human pancreatic ductal adenocarcinoma cell line	ATCC
HPDE6	Human pancreatic ductal cells from normal pancreatic ducts immortalized by transfection with the E6 gene of human papilloma virus (HPV).	Dr. Lorenzo Piemonti (HSR - Milan)

8.1.2 Animals

Table 7. Animal species used in this study.

Species	Age/Use	Source
Embryonated Chicken Eggs (ECE)	7 and 14-days / Virus infection	Charles River Laboratories
SCID-B17 mice	6 weeks/ Evaluation of the treatment in xenograft model	Dr. Vincenzo Ciminale Instituto Oncologico Veneto (IOV)

8.1.3 Viruses

Table 8. Viruses used in this study.

Viruses	Genome	Source
H1N1 A/Puerto Rico/8/34 (PR8)	Reverse genetics virus based on wild type strain.	Fouchier lab Erasmus Medical Centre
PR8 NS1-77	PR8 genetic backbone bearing the NS1-77 gene truncation.	This study
H7N3 A/turkey/Italy/2962/03	Reverse genetics virus based on wild type strain.	This study

H7N3 NS1-77	H7N3 genetic backbone bearing the NS1-77 gene truncation.	This study
H7N3 PB1-F2 L75H	H7N3 genetic backbone bearing L75H substitution in the PB1-F2 gene.	This study
H7N3 NS1-77 PB1-F2 L75H	H7N3 genetic backbone bearing NS1-77 gene truncation and L75H substitution in the PB1-F2 gene.	This study
(PR8) H1/N1-2962 NS1-77	Internal gene segments (PB2, PB1, PA, NP, M, NS) from the H7N3 NS1-77 virus and HA and NA genes from H1N1 PR8.	This study
(PR8) H1/N1-2962 NS1-77 GM-CSF	PB2, PB1, PA, NP, M gene segments from H7N3 virus, HA and NA from H1N1 PR8 and novel NS1-77/2A/GM-CSFV5/NSend segment.	This study

8.1.4 Plasmid vectors

All plasmids used in this study contain genetic antibiotic resistance to Ampicillin unless otherwise stated.

Table 9. List of plasmid vectors used in this study.

Plasmid	Description	Use	Source
pI.18/VN1194 HA	Express the HA from the influenza H5N1 virus isolate A / Viet Nam/ 1194 / 2004 (Genbank: AY651333).	Generation of pseudotypes	Prof. N.J. Temperton, University of Kent
pI.18/VN1194 NA	Express the NA from the influenza H5N1 virus isolate A / Viet Nam/ 1194 / 2004 (Genbank: AY651445).	Generation of pseudotypes	Prof. N.J. Temperton, University of Kent
pCMV-Δ8.91	Express HIV- type 1 (HIV-1) gag-pol construct.	Generation of pseudotypes/ lentivector	Prof. N.J. Temperton, University of Kent
pCSFLW	Reporter plasmid expressing firefly luciferase.	Generation of pseudotypes	Prof. N.J. Temperton, University of Kent
VSV-G	Express the Vesicular Stomatitis Virus G protein.	Generation of pseudotypes/ lentivector	Prof. N.J. Temperton, University of Kent
pRRL-Firefly	Reporter plasmid expressing firefly luciferase.	Generation of pseudotypes/ lentivector	Olivier Moncorgé Barclay Lab
pCMV-Victoria-PB2	Express human influenza Victoria PB2 protein	Helper plasmid for reverse genetics virus rescue	Barclay Lab
pCMV-Victoria-PB1	Express human influenza Victoria PB1 protein	Helper plasmid for reverse genetics virus rescue	Barclay Lab
pCMV-Victoria-PA	Express human influenza Victoria PA protein	Helper plasmid for reverse genetics virus rescue	Barclay Lab
pCMV-Victoria-NP	Express human influenza Victoria NP protein	Helper plasmid for reverse genetics virus rescue	Barclay Lab

RF483- PR8 PB2	Pol I-Pol II vector containing H1N1 A/Puerto Rico/8/34 (PR8) Segment 1 cDNA.	Reverse genetics	Fouchier lab Erasmus Medical Centre
RF483- PR8 PB1	Pol I-Pol II vector containing H1N1 A/Puerto Rico/8/34 (PR8) Segment 2 cDNA.	Reverse genetics	Fouchier lab Erasmus Medical Center
RF483- PR8 PA	Pol I-Pol II vector containing H1N1 A/Puerto Rico/8/34 (PR8) Segment 3 cDNA.	Reverse genetics	Fouchier lab Erasmus Medical Center
RF483- PR8 HA	Pol I-Pol II vector containing H1N1 A/Puerto Rico/8/34 (PR8) Segment 4 cDNA.	Reverse genetics	Fouchier lab Erasmus Medical Center
RF483- PR8 NP	Pol I-Pol II vector containing H1N1 A/Puerto Rico/8/34 (PR8) Segment 5 cDNA.	Reverse genetics	Fouchier lab Erasmus Medical Center
RF483- PR8 NA	Pol I-Pol II vector containing H1N1 A/Puerto Rico/8/34 (PR8) Segment 6 cDNA.	Reverse genetics	Fouchier lab Erasmus Medical Center
RF483- PR8 M	Pol I-Pol II vector containing H1N1 A/Puerto Rico/8/34 (PR8) Segment 7 cDNA.	Reverse genetics	Fouchier lab Erasmus Medical Center
RF483- PR8 NS	Pol I-Pol II vector containing H1N1 A/Puerto Rico/8/34 (PR8) Segment 8 cDNA.	Reverse genetics	Fouchier lab Erasmus Medical Center
RF483- PR8 NS1-77	Pol I-Pol II vector containing H1N1 A/Puerto Rico/8/34 (PR8) Segment 8 cDNA modified to express a NS1 protein of 77 amino acids (NS1-77), without affecting NEP ORF.	Reverse genetics	This study
RF483- H7N3 PB2	Pol I-Pol II vector containing H7N3 A/turkey/Italy/2962/03 Segment 1 cDNA.	Reverse genetics	This study
RF483- H7N3 PB1	Pol I-Pol II vector containing H7N3 A/turkey/Italy/2962/03 Segment 2 cDNA.	Reverse genetics	This study
RF483- H7N3 PB1-F2 L75H	Pol I-Pol II vector containing H7N3 A/turkey/Italy/2962/03 Segment 2 cDNA mutated to create L75H amino acid changes, without affecting PB1 and N40 ORFs.	Reverse genetics	This study
RF483- H7N3 PA	Pol I-Pol II vector containing H7N3 A/turkey/Italy/2962/03 Segment 3 cDNA.	Reverse genetics	This study
RF483- H7N3 HA	Pol I-Pol II vector containing H7N3 A/turkey/Italy/2962/03 Segment 4 cDNA.	Reverse genetics	This study
RF483- H7N3 NP	Pol I-Pol II vector containing H7N3 A/turkey/Italy/2962/03 Segment 5 cDNA.	Reverse genetics	This study
RF483- H7N3 NA	Pol I-Pol II vector containing H7N3 A/turkey/Italy/2962/03 Segment 6 cDNA.	Reverse genetics	This study
RF483- H7N3 M	Pol I-Pol II vector containing H7N3 A/turkey/Italy/2962/03 Segment 7 cDNA.	Reverse genetics	This study
RF483- H7N3 NS	Pol I-Pol II vector containing H7N3 A/turkey/Italy/2962/03 Segment 8 cDNA.	Reverse genetics	This study
RF483- H7N3 NS1-77	Pol I-Pol II vector containing H1N1 A/turkey/Italy/2962/03 Segment 8 cDNA modified to express a NS1 protein of 77 amino acids (NS1-77), without affecting NEP ORF.	Reverse genetics	This study
RF483- H7N3 NS1-77/2A/GM-CSFV5/NSend	Pol I-Pol II vector containing H1N1 A/turkey/Italy/2962/03 Segment 8 cDNA engineer to express a NS1 protein of 77 amino acids (NS1-77) and human GM-CSF, without affecting NEP ORF.	Reverse genetics	This study

pCAGG/NS1 PR8	pCAGG vector expressing PR8 NS1 protein	Protein expression	This study
pCAGG/NS1 H7N3	pCAGG vector expressing H7N3 NS1 protein.	Protein expression	This study
pCAGG/NS1-77 H7N3	pCAGG vector expressing H7N3 NS1-77 protein.	Protein expression	This study
ISG54Luc	Reporter plasmid expressing the firefly luciferase gene driven by the inducible promoter ISG54.	Protein expression	Barclay Lab
RenillaLuc	Reporter plasmid expressing renilla luciferase	Protein expression	Barclay Lab
pCAGGLuc	Expression of firefly luciferase	Protein expression	Barclay Lab
pCAGG/PB1-F2 H7N3	pCAGG vector expressing H7N3 PB1-F2 protein.	Protein expression	This study
PCAGG/ PB1-F2 L75H H7N3	pCAGG vector expressing H7N3 PB1-F2 L75H protein.	Protein expression	This study
pCMV5-FLAG-MAVS	Expressing MAVS adaptor protein	Protein expression	Barclay Lab
IFN-Luc	Reporter plasmid expressing the firefly luciferase gene driven by the IFN-β promoter.	Protein expression	Barclay Lab
pCAGG/PB2 H7N3	pCAGG vector expressing H7N3 PB2 protein.	Protein expression	This study
pCAGG/PB1 H7N3	pCAGG vector expressing H7N3 PB1 protein.	Protein expression	This study
pCAGG/PA H7N3	pCAGG vector expressing H7N3 PA protein.	Protein expression	This study
pCAGG/NP H7N3	pCAGG vector expressing H7N3 NP protein.	Protein expression	This study
pHuman-PolI-Firefly	Negative-sense firefly luciferase-expressing plasmid used as reporter to measure the polymerase activity	Minireplicon assay	Olivier Moncorgé Barclay Lab
pEX-A2-2AhGM-CSF	pEX-A2 vector for gene synthesis containing the human GM-CSF gene without introns sequences.	Cloning	Eurofins-MGW Operon
pCAGG/ NS1-77/2A/GM-CSF	pCAGG vector expressing H7N3 NS1-77/2A/GM-CSF polyprotein.	Protein expression	This study

8.1.5 Oligonucleotides

Oligonucleotide primers were synthesised by MWG Eurofins and stock solutions of 100 pmol/µl were made using sterile water.

Table 10. List of the main oligonucleotides used in this study.

Primer	Sequence	Use
mpFUS-PB2H7N3f	CCGAAGTTGGGGGGGAGCGAAAGCAGGTCAAATA	To generate RF483-H7N3 PB2 reverse genetics plasmid
abFUS-PB2-r	GGCCGCCGGGTTATTAGTAGAAACAAGGTCGTTTTTA	To generate RF483- H7N3 PB2 reverse genetics plasmid
abFUS-PB1-G-f	CCGAAGTTGGGGGGGAGCGAAAGCAGGCAAAC	To generate RF483- H7N3 PB1 reverse genetics plasmid

abFUS-PB1-r	GGCCGCCGGGTTATTAGTAGAAACAAGGCATTTTTTC	To generate RF483- H7N3 PB1 reverse genetics plasmid
mpFUS-PAH7N3f	CCGAAGTTGGGGGGGAGCGAAAGCAGGTACTGATC	To generate RF483- H7N3 PA reverse genetics plasmid
abFUS-PA-r	GGCCGCCGGGTTATTAGTAGAAACAAGGTACTTTTTTGG	To generate RF483- H7N3 PA reverse genetics plasmid
abFUS-H7-A-f	CCGAAGTTGGGGGGGAGCAAAAGCAGGGGATACG	To generate RF483- H7N3 HA reverse genetics plasmid
abFUS-HA-r	GGCCGCCGGGTTATTAGTAGAAACAAGGGTGTTTTTTC	To generate RF483- H7N3 HA reverse genetics plasmid
abFUS-NP-A-f	CCGAAGTTGGGGGGGAGCAAAAGCAGGGTAGATAAT	To generate RF483- H7N3 NP reverse genetics plasmid
abFUS-NP-r	GGCCGCCGGGTTATTAGTAGAAACAAGGGTATTTTTCTT	To generate RF483- H7N3 NP reverse genetics plasmid
mpFUS-NAH7N3f	CCGAAGTTGGGGGGGAGCAAAAGCAGGTGCGAG	To generate RF483- H7N3 NA reverse genetics plasmid
mpFUS-NAH7N3r	GGCCGCCGGGTTATTAGTAGAAACAAGGTGCTTTTTTC	To generate RF483- H7N3 NA reverse genetics plasmid
abFUS-MA-A-f	CCGAAGTTGGGGGGGAGCAAAAGCAGGTAGATATTG	To generate RF483- H7N3 M reverse genetics plasmid
abFUS-MA-r	GGCCGCCGGGTTATTAGTAGAAACAAGGTAGTTTTTTACT	To generate RF483- H7N3 M reverse genetics plasmid
abFUS-NS-A-f	CCGAAGTTGGGGGGGAGCAAAAGCAGGGTGACA	To generate RF483- H7N3 NS reverse genetics plasmid
mpFUS-NSH7N3r	GGCCGCCGGGTTATTAGTAGAAACAAGGGTGTTTTTTATC	To generate RF483- H7N3 NS reverse genetics plasmid
PR8/NS1-77fw	AATCCGATGAGGCACTTTAAATGACCATGGCCTCT	Mutagenic primer to introduce a stop codon (TAA) in the H1N1 A/Puerto Rico/8/34 NS1 ORF after 77 amino acids.
PR8/NS1-77rv	AGAGGCCATGGTCATTTAAAGTGCCTCATCGGATT	Mutagenic primer to introduce a stop codon (TAA) in the H1N1 A/Puerto Rico/8/34 NS1 ORF after 77 amino acids.
H7N3/NS1-77fw	GGAGGAAGAATCTGATGAGGCACTTTAATAGACTATTACT TCAGTGCCG	Mutagenic primer to introduce two stop codons (TAATAG) after 77 amino acids in the H7N3 A/turkey/Italy/2962/03 NS1 ORF (NS1-77).
H7N3/NS1-77rv	CGGCACTGAAGTAATAGTCTATTAAAGTGCCTCATCAGAT TCTTCCTCC	Mutagenic primer to introduce two stop codons (TAATAG) after 77 amino acids in the H7N3 A/turkey/Italy/2962/03 NS1 ORF (NS1-77).
H7N3/PB1-F2_L75H_fw	CAGGGATCTTTGAAAACTCATGTCTTGAAACGATGGAAG	Mutagenic primer to introduce PB1-F2 L75H amino acid changes, without affecting PB1 and N40 ORF.
H7N3/PB1-F2_L75H_rv	CTTCCATCGTTTCAAGACATGAGTTTTCAAAGATCCCTG	Mutagenic primer to introduce PB1-F2 L75H amino acid changes, without affecting PB1 and N40 ORF.
H7N3/NS1NotIF	TAT***GCGGCCGC***AGCAAAAGCAGGGTGACAAAAACA	To clone the H7N3 NS1 and NS1-77 into pCAGGS plasmid
SAMR	TCCTCATCAGTATGTCC***G***GGAAGAGAAGGTAATGG	PCR mutagenesis was used to remove the splice acceptor site (AG) from the H7N3 NS1 coding

		sequence in pCAGG plasmid.
SAMF	CCATTACCTTCTCTTCC***C***GGACATACTGATGAGGA	PCR mutagenesis was used to remove the splice acceptor site (AG) from the H7N3 NS1 coding sequence in pCAGG plasmid.
H7N3/NS1MluIR	GCG***ACGCGT***AACTTCTGACTCAATTGTTCTCGCCA	To clone the H7N3 NS1 into pCAGG plasmid.
H7N3/NS1-77MluIR	GCG***ACGCGT***AAGTGCCTCATCAGATTCTTCCTCC	To clone the H7N3 NS1-77 into pCAGG plasmid.
H7N3/PB1-F2NotIF	TATGCGGCCGCCATACAGCCATGGAACAGGAAC	To clone the H7N3 PB1-F2 into pCAGG plasmid.
H7N3/PB1-F2MluIR	GCGACGCGTGTTTGTCCACTCTTGTTTGCTG	To clone the H7N3 PB1-F2 into pCAGG plasmid.
H7N3 PB2 NotIF	TAT***GCGGCCGC***GTCAAATATATTCAATATGGAGAG	To clone the H7N3 PB2 into pCAGG plasmid.
H7N3 PB2 MluIR	GCGACGCGTATTGATGGCCATCCGAATTC	To clone the H7N3 PB2 into pCAGG plasmid.
H7N3 PB1 NotIF	TAT***GCGGCCGC***CATTTGAATGGATGTCAATCCG	To clone the H7N3 PB1 into pCAGG plasmid.
H7N3 PB1 MluIR	GCGACGCGTTTTTTGCCGTCTGAGCTCTTC	To clone the H7N3 PB1 into pCAGG plasmid.
H7N3 PA NotIF	TAT***GCGGCCGC***TCCAAAATGGAAGATTTTGTGCG	To clone the H7N3 PA into pCAGG plasmid.
H7N3 PA MluIR	GCGACGCGTTTTCAGTGCATGTGTGAGGAAG	To clone the H7N3 PA into pCAGG plasmid.
H7N3 NP NotIF	TAT***GCGGCCGC***ATCAGCATCATGGCGTCTCAAG	To clone the H7N3 NP into pCAGG plasmid.
H7N3 NP MluIR	GCGACGCGTATTGTCATACTCCTCTGCATTG	To clone the H7N3 NP into pCAGG plasmid.
2A/NS1-77 rv1	GGTCAAAATTAAGTGCCTCATCAGATTCTTCC	To generate RF483- H7N3 NS1-77/2A/GM-CSFV5/NSend and pCAGG/ NS1-77/2A/GM-CSF plasmids.
2A/NS1-77 rv2	GCAAGTTTAAGAAGGTCAAAATTAAGTGCCTC	To generate RF483- H7N3 NS1-77/2A/GM-CSFV5/NSend and pCAGG/ NS1-77/2A/GM-CSF plasmids.
2A rv1	TCGACGTCTCCCGCAAGTTTAAGAAGGTC	To generate RF483- H7N3 NS1-77/2A/GM-CSFV5/NSend and pCAGG/ NS1-77/2A/GM-CSF plasmids.
2A rv2	GTTGGACTCGACGTCTCCCGCAAG	To generate RF483- H7N3 NS1-77/2A/GM-CSFV5/NSend and pCAGG/ NS1-77/2A/GM-CSF plasmids.
IIMlul/GM-CSF rv2	ATAT***ACGCGT***CTCCTGGACTGGCTCC	To generate RF483- H7N3 NS1-77/2A/GM-CSFV5/NSend and pCAGG/ NS1-77/2A/GM-CSF plasmids.
II2A fw2	AGACGTCGAGTCCAACCCTGGG	To generate RF483- H7N3 NS1-77/2A/GM-CSFV5/NSend and pCAGG/ NS1-77/2A/GM-CSF plasmids.
MluI/GM-CSF rv	TAT***ACGCGT***CTCCTGGACTGGCTCCCAGCAGTCAAAG	To generate RF483- H7N3 NS1-77/2A/GM-CSFV5/NSend and pCAGG/ NS1-77/2A/GM-CSF plasmids.

V5/stops rv	GAAGTAATAGTCTATTACGTTGAGTCGAGTCCCAG	To generate RF483- H7N3 NS1-77/2A/GM-CSFV5/NSend plasmid.
Stops/NSend fw	TGGGACTCGACTCAACGTAATAGACTATTACTTCAG	To generate RF483- H7N3 NS1-77/2A/GM-CSFV5/NSend plasmid.
H7N3 NEP Fw1-23	ATGGATTCCAACACTGTGTCAAG	NS1-77/2A/GM-CSF and NEP mRNAs amplification
H7N3 NEP Rv322-344	GTTCTTATCTCTTGCTCCACTTC	NS1-77/2A/GM-CSF and NEP mRNAs amplification
VG 150	GCAAAGACCTGTACGCCAACA	β-actin mRNA amplification
VG 151	CCTCGGCCACATTGTGAAC	β-actin mRNA amplification

8.1.6 Antibodies

Table 11. List of antibodies used in this study.

Antibody	Description	Source
Mouse ANTI-V5 tag antibody	Mouse monoclonal antibody against SV5 tag	AbD Serotec
Monoclonal ANTI-FLAG antibody produced in mouse	Monoclonal ANTI-FLAG antibody produced in mouse	Sigma
Cleaved PARP (Asp214) Rabbit monoclonal antibody	Rabbit monoclonal antibody against 89KDa cleaved PARP fragment.	Cell Signalling Technology
Goat anti-mouse IgG horseradish peroxidase linked whole antibody	Secondary antibody conjugated to HRP	GE Healthcare
Goat anti-rabbit IgG HRP-linked Antibody	Secondary antibody conjugated to HRP	Cell Signalling Technology
Goat anti-vinculin (N-19) antibody	Goat monoclonal antibody against Vinculin	Santa Cruz Biotechnology
Donkey anti-goat IgG-HRP antibody	Secondary antibody conjugated to HRP	Santa Cruz Biotechnology
Mouse monoclonal to beta Actin	Mouse monoclonal antibody against B-actin	abcam
Mouse anti-V5 Antibody	Mouse monoclonal antibody against SV5 tag	Lifetechnologies
Goat anti-mouse IgG-FITC	Secondary antibody conjugated to FITC	Sigma
Alexa Fluor® 647 Annexin V conjugate	Analysis of apoptosis in infected cells	Invitrogen

8.1.7 Buffers and culture media

Table 12. List of Buffers and culture media used in this study.

Solution	Recipe	Use
DMEM	Dulbecco's Modified Eagle Medium (DMEM) (Gibco) Fetal Bovine Serum 10% (v/v) (Biosera) Non-essential amino acids (NEAA) 1% (v/v) (Sigma) Penicillin and Streptomycin (P/S) 1% (v/v) (Gibco)	Maintence of 293T, PANC-1 and MIA PaCa-2 cell lines
DMEM G-418	Dulbecco's Modified Eagle Medium (DMEM) (Gibco) Fetal Bovine Serum 10% (v/v) (Biosera) Non-essential amino acids (NEAA) 1% (v/v) (Sigma) Penicillin and Streptomycin (P/S) 1% (v/v) (Gibco) Geneticin (G-418) (Gibco) (0.5 mg/ml)	Maintence of Npro-MDCK and A549 IFN-Luc cell lines
RPMI 1640	RPMI 1640 (Gibco) Fetal Bovine Serum 10% (v/v) (Biosera) Non-essential amino acids (NEAA) 1% (v/v) (Sigma) Penicillin and Streptomycin (P/S) 1% (v/v) (Gibco)	Maintence of BxPC-3, BxPC-3Luc, AsPC-1, HPDE6 cell lines
Iscove	Iscove's medium (Gibco)	Maintence of CFPAC-1 cell

	Fetal Bovine Serum 10% (v/v) (Biosera) Non-essential amino acids (NEAA) 1% (v/v) (Sigma) Penicillin and Streptomycin (P/S) 1% (v/v) (Gibco)	line.
Phosphate Buffered Saline (PBS)	155 mM NaCl 1 mM KH2PO4 3 mM Na2HPO4	Cell washes
Cell trypsin	2x solution 200ml PBS (Gibco) 4ml 2.5% (10x) Trypsin solution (Gibco) 0.5mM EDTA	Cell passage
Virus plaque assay overlay	100 ml 10 x Earle's minimal essential medium (EMEM) 28 ml 7.5% BSA 1% glutamine (200mM) 20 ml 7.5% NaHCO3 10 ml 1M HEPES 5 ml 1% DEAE Dextran (Sigma) 1% penicillin-streptomycin (5000IU/ml) 2% Agarose (Oxoid)	Virus plaque assays
2,5% Avicel	2,5 g of Avicel powder (FMC Corporation) 100 ml distilled water	Virus plaque assay
Crystal violet solution	100 ml Crystal violet stock solution 300 ml ethanol 1.6 l water	Virus plaque assay - cell monolayer staining
TAE Buffer	40mM Tris-acetate pH 8 1mM EDTA	DNA gel electrophoresis
Lysogeny Broth (LB)	1% Oxoid tryptone 0.5% Oxoid yeast extract 0.5% NaCl 0.1% glucose	Culturing transformed bacterial cells
SOC Medium	2% Oxoid tryptone 0.5% Oxoid yeast extract 10mM NaCl 2.5mM KCl 10mM MgCl2 10mM MgSO4 20mM glucose	Recovery medium used during transformation of Escherichia coli DH10B cells
6X DNA loading dye	0.25% Bromophenol blue 40% (w/v) sucrose.	DNA gel electrophoresis
Dissociation buffer	50 mM Tris-Cl pH 6.8 5% β-mercaptoethanol 2% SDS 0.1% bromophenol blue 10% glycerol	Cell lysis
6X protein loading dye	375 mM Tris-HCl pH 6.8 6% SDS 30% glycerol 9% 2-Mercaptoethanol 0.03% bromophenol blue	Protein gel electrophoresis
SDS-Page running buffer	25 mM Tris 250 mM glycine 0.1% SDS	Protein gel electrophoresis
Western Blot transfer buffer	39 mM glycine 48mM Tris base 0.037% SDS 20% methanol	Protein gel electrophoresis

8.2 Methods

8.2.1 Molecular biology

8.2.1.1 Reverse Transcriptase and Polymerase Chain Reaction (PCR).

Reverse transcriptase PCR reactions were performed either using Qiagen OneStep RT-PCR kit or a two steps reaction consisting of cDNA synthesis followed by PCR.

Qiagen OneStep RT-PCR

RT-PCRs were carried out in a total volume of 25 µl. Reaction mixture contained 1 pg – 2 µg/reaction of template RNA, 5x QIAGEN OneStep RT-PCR Buffer, dNTP Mix (final concentration 400 µM of each dNTP), 1 µM of sense and anti-sense oligonucleotides, RNase Inhibitor (8U/reaction), 1U/reaction of OneStep RT-PCR Enzime Mix. OneStep PCR conditions are presented in Table 13.

Table 13. Qiagen OneStep PCR thermal cycling conditions.

Passage	Temperature	Time	Reaction
1	50°C	30 min	Reverse transcription
2	94°C	15 min	Initial PCR activation step
3	94°C	1 min	Denaturation
4	55°C	1 min	Annealing
5	68°C	1-2 min	Extension
6	Go to step 3, repeat 34-39 times		
7	68°C	7 min	Final extension
8	4°C	Hold	

cDNA

Complementary DNA (cDNA) was synthesised through two sequential reactions: (i) annealing of random primer mix (RF671) to RNA and then (ii) reverse transcription. The reaction mixture for the first reaction consists of 0.1 µM random oligonucleotides (RF671 -Operon), 0.5mM dNTPs Mix, 20U rRNAsin (Promega), 1 pg – 2 µg/reaction template RNA. After 5 minutes incubation at 65°C the reaction mixture was cooling down on ice for 5 minutes and ten mixed with a second reaction mixture containing 1X RT buffer (Invitrogen), DTT 0.005M, rRNAsin 20U, SuperScript III RT 200U (Invitrogen). The final reaction mixture was incubated at 25°C for 5 minutes and then at 60°C for 50 minutes to obtain cDNA.

PCR

PCR for sequencing and DNA insert construction was performed using a reaction mix containing 50-100 ng of cDNA, PFU Buffer 1X (Stratagene), dNTPs Mix 0.25 μM, 0.2 μM of sense and anti-sense oligonucleotide primers, 1.75 U of Turbo PFU (Stratagene). PCR conditions are presented in Table 14.

Table 14. PCR thermal cycling conditions.

Passage	Temperature	Time	Reaction
1	95°C	2 min	Initial Denaturation
2	95°C	45 sec	Denaturation
3	55-65°C	1 min	Annealing
4	72°C	2 min	Extension
5	Go to step 2 and repeat 39 times		
6	72°C	10 min	Final extension
7	4°C	Hold	

8.2.1.2 Agarose gel electrophoresis

DNA fragments were separated on 1% or 2% agarose gels diluted with 0.5X TAE buffer and supplemented with 1x gel red (Cambridge Bioscience). DNA was loaded with 5x Gel loading dye (Qiagen). Gels were run in 0.5X TAE buffer. Samples were run alongside markers at 80-120V until the bands had sufficiently separated. DNA was visualised using a UV trans-illuminator.

8.2.1.3 DNA purification

DNA fragments were cut from the agarose gel under UV light, and DNA extracted using a QIAquick Gel extraction kit (Qiagen) following manufacturer's instructions. Similarly, digestion products or PCR product (directly) were purified using the Gel extraction kit. DNA fragments were eluted with 35-50 μl sterile water.

8.2.1.4 Double restriction enzyme digest

In order to clone genes into the pCAGG vector, the NotI and MluI restriction enzymes were utilized. Double digests were performed in 40 μl total volume using 4 μl of the 10X NEB buffer 3, 2 μl of each

NotI and MluI enzyme (NEB), 4 µl of 10X NEB BSA and 28 µl of PCR purified DNA or purified plasmid DNA in nuclease free water. All reactions were carried out at 37°C for 2 - 3 hours.

8.2.1.5 DNA ligation

Constructs were ligated into the pCAGG vector using T4 DNA Ligase kit (Promega) as recommended by the manufacturer's guidelines. Typically, DNA ligation was performed in a total volume of 20 µl using a 1:3 vector:insert ratio and 2 hours incubation at room temperature (RT).

8.2.1.6 Transforming competent bacterial cells

1 to 3 µl of the DNA ligation (or ~50ng of plasmid) was mixed with 50µl OneShot®TOP10 chemically competent E.coli. (Invitrogen) and incubated on ice for 30 minutes. Cells were heat shocked for 30 seconds at 42°C and replaced on ice for 2 minutes. 250µl of pre-warmed S.O.C. media (Invitrogen) was added to the mix and incubated for 1 hour at 37°C in a shaking incubator, after which a suitable volume was spread on to pre-warmed LB agar plates containing 1% Ampicillin and incubated overnight at 37C for colony formation. Colonies were screened by PCR, and grown in 5ml LB supplemented with Ampicillin (100µg/ml).

8.2.1.7 Plasmid purification

Small scale. Bacterial cells grown in 5ml LB (100µg/ml Ampicillin) were pelleted by centrifugation at 3000xg for 5 minutes. The supernatant was discarded and DNA purified by the QIAprep Spin Miniprep kit (QIAGEN) following the manufacturers guidelines. DNA was eluted with 50µl warm sterile water and stored at -20°C.

Large scale. 250ml of LB supplemented with 100µg/ml Ampicillin was inoculated with 200µl bacterial cells and incubated at 37°C for 16 hours. Cells were pelleted by centrifugation at 3000xg for 5 minutes. The supernatant was discarded and DNA purified by the QIAfilter Plasmid Maxi kit (QIAGEN) following the manufacturers guidelines. The DNA pellet was resuspended with 500-1000 µl of nuclease free water and stored at -20°C. The concentration and quality of DNA was measure using a NANODROP spectrophotometer. Good quality DNA was considered such with a A260/A280 ratio of 1.7-2.0.

8.2.1.8 Plasmid constructs

The empty RF483, which is derived from the pHW2000 plasmid previously generated by Hoffmann et al. (Hoffmann et al., 2000), and the virus PR8 rescue plasmids were supplied by Dr. R. Fouchier, Erasmus University, Rotterdam, Netherlands.

Viral RNA segments from A/turkey/Italy/2962/03 (H7N3) were extracted by using RNA extraction kit NucleoSpin RNA II (Macherey-Nagel) according to manufacturer's instructions and circularized to sequence their Non-Coding Regions (NCR) as previously described (de Wit et al., 2007). Based on the NCR sequences sense and antisense primers were designed according to the In-Fusion® Dry-Down PCR Cloning Kit recommendations (Clontech) for subsequent amplification of the viral genes by reverse transcription-PCR (RT-PCR). cDNA copies of viral RNAs were sequenced in order to very their fidelity to the original segments and inserted into RF483 vector by using In-Fusion® Dry-Down PCR Cloning Kit (Clontech). Plasmids obtained were propagated in One Shot® TOP10 Chemically Competent E. coli (Invitrogen), purified by EndoFree® Plasmid Maxi Kit (Qiagen) and confirmed by sequencing. Mutations of interest in the NS1 and PB1-F2 genes (segment 8 and 2 respectively) were introduced by PCR using QuikChange Site-Directed Mutagenesis kit (Stratagene) as follows:

- *RF483 - PR8 NS1-77*

A single nucleotide mutation A232T was introduced in segment 8 of H1N1 A/PR/8/34 using PR8/NS1-77fw and PR8/NS1-77rv primers in order to create a stop codon (TAA) in the NS1 ORF after 77 amino acids. The resulting construct was called RF483- PR8 NS1-77 and confirmed by sequencing.

- *RF483 - H7N3 NS1-77*

Using the set of primers H7N3/NS1-77fw and H7N3/NS1-77rv two stop codons (TAATAG) were generated by three site mutations (A232T, A235T, T236A) after 77 amino acid in the H7N3 A/turkey/Italy/2962/03 NS1 ORF (see chapter 9 – appendix). The resulting construct was called RF483- H7N3 NS1-77 and was confirmed by sequencing.

- *RF483 - H7N3 PB1-F2 L75H*

A single nucleotide mutation T224A was introduced in the PB1-F2 gene of either full length or truncated NS1-77 H7N3 A/turkey/Italy/2962/03 virus using H7N3/PB1-F2_L75H_fw and H7N3/PB1-F2_L75H_rv primers to create L75H amino acid changes, without affecting PB1 and N40 ORF (see chapter 9 – appendix). The resulting constructs was called RF483- H7N3 PB1-F2 L75H and was confirmed by sequencing.

The *RF483-NS1-77/2A/GM-CSFV5/NSend* plasmid (see chapter 9 – appendix) was generated through multiple steps as summarized in figure 55. Briefly, using the RF483- H7N3 NS plasmid as template a first PCR was performed with the H7N3 NS1NotIFw and the 2A/NS1-77rv1 oligonucleotides to amplify the H7N3 NS1 gene sequence until codon 77. The reverse primers added to the final PCR product the docking sequence for further elongation of the FMDV 2A autoproteolytic site through a series of successive PCRs that eventually produced the NS1-77/2A fragment (Figure 55A). pEX-A2 vector containing the FMDV 2A sequence upstream of the human GM-CSF gene (without intron sequences) was obtained from Eurofins-MGW Operon and used as PCR template to generate the 2A/GM-CSF product (Figure 55B). Next overlapping PCR was performed using the two previous products as templates to obtain the NS1-77/2A/GM-CSF fragment bearing NotI and MluI restriction sites at its 5' and 3' ends respectively (Figure 55C). Using DNA restriction and subsequent ligation the PCR product was inserted into pCAGG plasmid, which allowed the fusion of the construct expressing the polyprotein with a 14-amino-acid long SV5 tag at its carboxyl terminus (Figure 55D). The resulting plasmid was named pCAGG/NS1-77/2A/GM-CSF and used to test the expression of both NS1-77 and human GM-CSF proteins. Next, using the pCAGG/NS1-77/2A/GM-CSF plasmid as template, the H7N3 NS1NotIFw and V5/stops rv primers allowed the PCR amplification of the sequence from NS1-77 until V5 tag and the introduction of two stop codons at the 5' terminus (Figure 55D). Using the RF483-H7N3 NS rescue plasmid as template another PCR was performed to amplify the NS sequence from aa position 77 on the NS1 ORF to the 3' UTR of the viral segment (Figure 55E). The sense oligonucleotide (Stops/NSend fw) provided two stop codons at 5' of the PCR product which overlap the sequence at 3' end of the NS1-77/2A/GM-CSFV5 segment previously generated. Finally, overlapping PCR was performed using the sense and anti-sense oligonucleotides bearing the viral NS segment NCR (abFUS-NS-A-f and mpFUS-NSH7N3r), which were previously designed according to the In-Fusion® Dry-Down PCR Cloning Kit recommendations (Clontech) (Figure 55F).

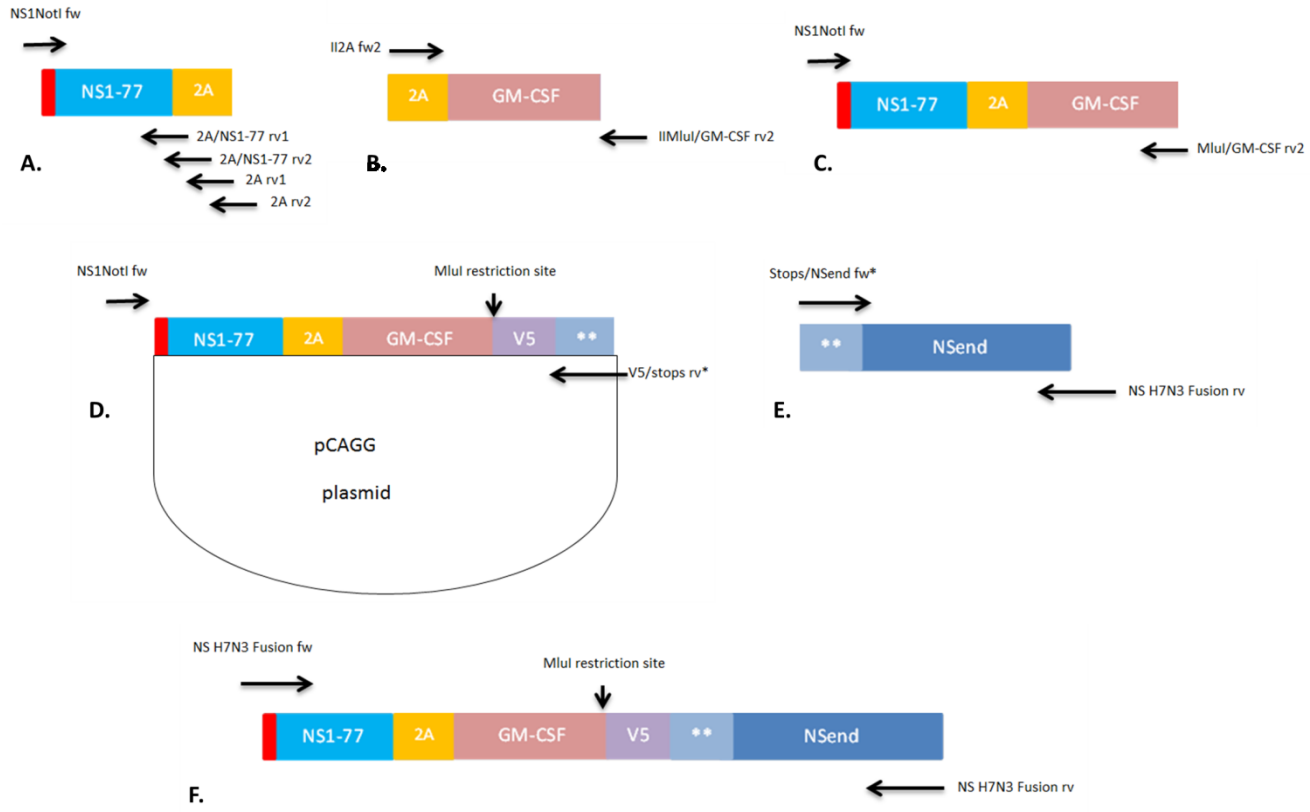

*Figure 55. **Schematic representation of the steps performed to construct the pCAGG/NS1-77/2A/GM-CSF and the RF483-NS1-77/2A/GM-CSFV5/NSend plasmids.** Red box: NS1/NEP shared coding region; NS1-77: sequence encoding 77 N-terminal aa of the H7N3 NS1 protein, 2A: FMDV autoproteolytic cleavage site; GM-CSF: human granulocyte macrophage colony-stimulating factor; V5: SV5 tag; ** stop codons; NSend: sequence from NS1 codon 78 until the end of the H7N3 NS segment. For specific primers sequences refer to table 10.*

pCAGG/NS1 H7N3 expression construct was generated as previously described by Hayman A. et al., 2006 (Hayman et al., 2006). Briefly, PCR mutagenesis was used to remove the splice acceptor site (AG) from the H7N3 A/turkey/Italy/2962/03 NS1 coding sequence (see chapter 9 – appendix). In PCR1 the primer pairs H7N3/NS1NotIF and SAMR (see table 10) were used, producing a ~550 bp amplicon. PCR2 included primers SAMF and H7N3/NS1MluIR (see table 10) and resulted in a ~ 210 bp product. PCR1 and PCR2 were performed starting from the viral RNA as template using Qiagen OneStep RT-PCR kit (Qiagen). A third overlapping PCR3 was then carried out using the NS1NotIF and NS1MluIR primers. The 720 bp PCR3 product was then digested with NotI and MLu restriction enzymes (NEB, New England Biolabs) and ligated into pCAGG vector, which allow the fusion of the expressed protein with a 14-amino-acid long SV5 tag at its carboxyl terminus. The construct was then propagated in One Shot® TOP10 Chemically Competent *E. coli* (Invitrogen), purified by EndoFree® Plasmid Maxi Kit (Qiagen) and confirmed by sequencing.

A second construct pCAGG/NS1-77 H7N3, encoding the first 77 amino acids of the NS1 protein from H7N3 A/turkey/Italy/2962/03, was generated by PCR using the forward primer H7N3/NS1NotIF and the reverse primer H7N3/NS1-77MluIR. The PCR product was then cloned into the pCAGG vector using the NotI and MluI restriction sites as previously described. A pCAGG/NS1 PR8 construct containing the full length NS1 from H1N1/PR/8/34 modified to remove the splice acceptor site was previously generated in our laboratory. Empty pCAGG vector was used as negative control.
Different pCAGG/PB1-F2 H7N3 and pCAGG/PB1-F2 L75H H7N3 constructs were generated by PCR using the forward primer H7N3/PB1-F2NotIF, the reverse primer H7N3/PB1-F2MluIR and as templates the wild type PB1 or PB1-F2 L75H plasmids previously employed to produce the reverse genetics viruses. PCR products were then cloned into pCAGG vector as described above.

8.2.1.9 Sequencing of constructs

All plasmid constructs were verified by DNA sequencing. Briefly, PCR amplification was performed by using specific primers (primer sequences are available on request) and then the complete coding sequences were generated using the Big Dye Terminator v3.1 cycle sequencing kit (Applied Biosystems, Foster City, CA). The products of the sequencing reactions were cleaned-up using the Performa DTR Ultra 96-well kit (Edge BioSystems, Gaithersburg, MD) and sequenced in a 16-capillary ABI Prism 3130xl Genetic Analyzer (Applied Biosystems, Foster City, CA). Sequence data were assembled and edited with SeqScape software v2.5 (Applied Biosystems).

8.2.2 Cell lines and transfection

8.2.2.1 Cell culture

293T, Mia Paca-2, PANC-1, Npro-MDCK that express NPro gene of Bovine Viral Diarrhea Virus (BVDV) thus lacking of IFN expression and A549-IFNLuc cells, which contain a stable integrate firefly luciferase gene driven by the IFN-β promoter, were grown in Dulbecco's modification of Eagle's medium DMEM (Gibco) supplemented with 10% Fetal Bovine Serum FBS (Biosera), 1% MEM Non-essential amino acid solution NEAA (SIGMA) and 1% penicillin-streptomycin (P/S) (Gibco). Geneticin (G-418) (Gibco) was added at the concentration of 0.5 mg/ml in A549-IFNLuc and Npro-MDCK media. The immortalized epithelial cell line from normal human pancreatic ducts HPDE6 and the pancreatic ductal adenocarcinoma cell lines AsPC-1 and BxPC-3 were maintained in RPMI 1640 (Gibco) supplemented with 10% FBS, 1% P/S solution and 1% NEAA solution. Iscove's medium

(Gibco) supplemented with FBS 10%, 1% NEAA (Sigma) and 1% P/S solution (Gibco) was used to grow CFPAC-1 ductal adenocarcinoma cell line. All cell lines were grown in a humidified incubator at 37°C with 5% CO_2, and sub-cultured twice weekly.

8.2.2.2 Transfection

Transfections were performed using Lipofectamine 2000 reagent (Invitrogen) following manufacturer's instructions. DNA:reagent ratio volumes were scaled appropriately for cell transfections. DNA and Lipofectamine were diluted in the appropriate volumes using OptiMEM (Invitrogen). Transfection of RG plasmids for RG virus generation was carried out with Fugene 6 (Promega), as described in paragraph 8.2.2.4.

8.2.2.3 Generation of BxPC-3Luc cell line.

BxPC-3 cells stably expressing Luciferase gene (BxPC-3Luc) were generated using lentivector transduction (Figure 55). Briefly, semiconfluent monolayers of 293T cells were co-transfected in 10 cm^2 Petri dishes with 8 µg of HIV gag/pol construct 4 µg Vesicular Stomatitis Virus G protein (VSV-G) construct and 4 µg of pRRL-Firefly luciferase reporter constructs using Lipofectamine 2000 (Invitrogen). Supernatant was harvested 48 h post-transfection, filtered through 0.45-µm filters, and stored at -80°C. Transduction was performed in a 12 well plate by adding 500 µl/well of lentivector suspension in serum free DMEM onto 10 fold dilutions of BxPC-3 cells. After 24 hours incubation the media were replaced with fresh media containing 3% FBS DMEM and cells were left at 37°C for 72h. The lentivector transduction efficiency was assessed by monitoring expression of luciferase in the target cells using the Luciferase Assay Reporter System (Promega). BxPC-3Luc cells were maintained in RPMI 1640 (Gibco) supplemented with 10% FBS, 1% Pen-Strep solution and 1% NEAA solution.

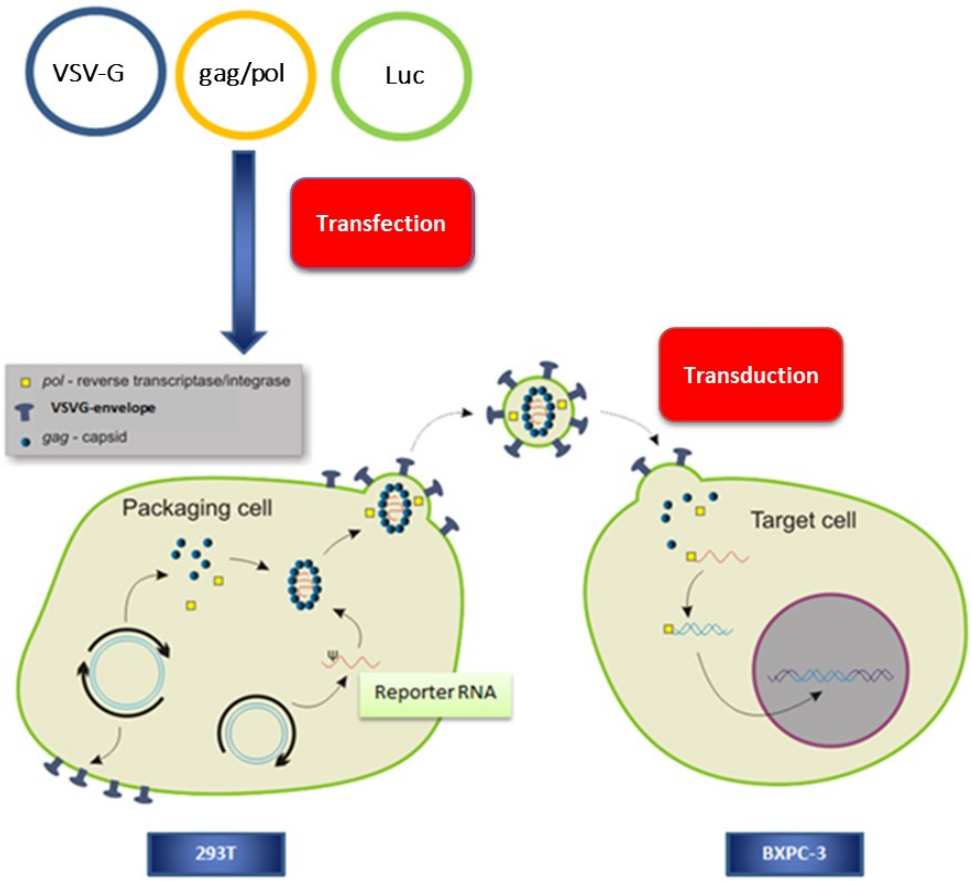

Figure 56. Lentivector transduction used to establish a BXPC-3 cell line stably expressing the firefly luciferase, termed BXPC-3Luc.

8.2.2.4 Virus rescue

Virus rescue was carried out using a set consisting of 12 plasmids. Four expression "helper" plasmids with a CMV promoter directed the expression of the proteins of the viral polymerase complex PB1, PB2, PA, and NP from the human strain A/Victoria/3/75 (H3N2). The remaining eight plasmids contained cDNA copies of viral RNAs derived from the avian A/turkey/Italy/2962/03 (H7N3) or the human A/Puerto Rico/8/34 (H1N1) inserted into the RF483 vector. The rescue method used was adapted from Neumann et al. (1999) (Neumann et al., 1999) as previously described (Elleman and Barclay, 2004). Briefly, all 12 plasmids were transfected into 293T cells in 12-well plates using Fugene 6. To generate recombinant NS1-77 and/or PB1-F2 L75H viruses, different plasmids (see table 9) corresponding to mutated segment 8 and 2 RNAs were substituted in place of the equivalents H7N3 or human PR8 plasmids. The PR8 H1/N1-2962 NS1-77 virus was obtained by co-transfecting the plasmids for the surface antigens haemagglutinin (HA) and neuraminidase (NA) of the H1N1 PR8 virus together with the 6 plasmids expressing the internal viral genes (PB2, PB1, PA, NP, M and NS) of the H7N3 NS1-77 virus. To generate the PR8 H1/N1-2962

NS1-77 GM-CSF virus the RF483 – H7N3 NS1-77 plasmid was substituted with the RF483-H7N3 NS1-77/2A/GM-CSFV5/NSend plasmid. After 24 hours, the transfected cells were removed from the wells and mixed with Npro-MDCKs and co-cultured in 25ml flasks. The first 6–8 h of the co-culture was carried out in DMEM media supplemented with 10% FBS after which the cells were washed briefly in serum-free media and the media was replaced with serum-free media containing 2.5 µg /ml TPCK-trypsin (Worthington). The cells were monitored daily thereafter and supernatants containing recombinant viruses were harvested once the cell layers were completely destroyed by the virus. The harvested supernatants were spun at 4000 x g at 4 °C for 20 min to remove the cell debris and stored in aliquots at -80 °C. Viral titres were determined by plaque assay on MDCK-Npro cells (Matrosovich et al., 2006).

8.2.2.5 A549-IFNLuc luciferase assay

A549-IFNLuc cells were incubated with different reverse genetics viruses diluted in serum-free DMEM at an M.O.I. of 1 in a 24 well plate at 37°C. After 1 hour absorption, the input viruses were replaced with 3% FBS DMEM and then cells were further incubated for 8 hours. Next, the cells were washed once with PBS and then lysed with 100 µl/well of Passive Lysis Buffer (Promega), rocking the plate for 15 minutes at room temperature. In order to assure the maximum release of the luciferase proteins from the cells the plates were frozen and thawed for 3 times at -80°C. The luciferase activity was measured in a luminometer using the Luciferase Assay System (Promega).

8.2.2.6 ISG54 luciferase assay

HPDE6 and BxPC-3 cells were incubated with reverse genetics viruses diluted in serum-free DMEM at an M.O.I of 1 pfu/cell in a 24 well plate at 37°C. After 1 h, the viruses were replaced with 3% FBS DMEM and the cells were incubated for further 8 hours. The supernatants were collected and exposed on ice to the ultraviolet radiation from a germicidal lamp for 5 minutes in order to inactivate any possible viral particle then they were stored at -80°C.

Plasmids ISG54Luc, encoding the firefly luciferase gene driven by the inducible promoter ISG54 and RenillaLuc, encoding the renilla luciferase, were co-transfected into 293T cells using Lipofectamine 2000 (Roche). After 8 h, the medium was replaced with the supernatans previously inactivated and cells were incubated at 37°C. After 24 hours 293T cells were washed once with PBS and then lysed with 100 µl/well of Passive Lysis Buffer (Promega), rocking the plate for 15 minutes at room temperature. In order to assure the maximum release of the luciferase proteins from the cells were

frozen and thawed for 3 times at -80°C. The firefly and the renilla luciferase activities were measured in a luminometer using the Dual-Luciferase Reporter Assay System (Promega).

8.2.2.7 Post-transcriptional limitation of IFN-β induction

293T cells were co-transfected with pCAGGLuc plasmid, which constitutively expresses firefly luciferase and one of the following plasmids: pCAGG/NS1 PR8, pCAGG/NS1 H7N3, pCAGG/NS1-77 H7N3 and empty pCAGG (K-). After 8 hours incubation at 37°C, cells were lysed in Passive Lysis Buffer (Promega), rocking the plate for 15 minutes at room temperature. In order to assure the maximum release of the luciferase proteins the cells were frozen and thawed for 3 times at -80°C. The firefly luciferase activity was measured in a luminometer using the Luciferase Reporter Assay System (Promega).

8.2.2.8 Western blot

Cells lysates were treated in dissociation buffer for 5 minutes at 96°C and then electrophoresed in 12% polyacrylamide gels using running buffer. Following SDS-PAGE the proteins were transferred from the gel onto immuno-blot Hybond-ECL membrane (GE Healthcare) by electroblotting with transfer buffer. Membranes were washed with PBS and then incubated overnight at 4°C in PBS solution containing 5% skymmed milk (Bio-rad). After further washing with PBS, membrane was incubated for 1 h at room temperature under constant shaking with PBS containing 0.05% Tween-20 (Sigma), 5% skymmed milk (Bio-Rad) and mouse ANTI-V5 tag antibody (AbD Serotec), Mouse anti-V5 Antibody (Lifetechnologies), Monoclonal ANTI-FLAG antibody produced in mouse (Sigma) or Cleaved PARP (Asp214) Rabbit monoclonal antibody (Cell Signalling Technology). After incubation the membrane was washed again as previously described and then incubated with goat anti-mouse IgG horseradish peroxidase linked whole antibody (GE Healthcare) or Anti-rabbit IgG HRP-linked Antibody (Cell Signalling Technology). Vinculin and β-actin were detected as loading controls using goat anti-vinculin (N-19) antibody (Santa Cruz Biotechnology) followed by incubation with donkey anti-goat IgG-HRP antibody (Santa Cruz Biotechnology) and Mouse monoclonal to beta Actin (abcam) followed by incubation with goat anti-mouse IgG horseradish peroxidase linked whole antibody (GE Healthcare), respectively. Visualization of protein bands in Amersham Hyperfilm™ ECL (GE Healthcare) was performed using ECL Plus Western Blotting Detection System (GE Healthcare).

8.2.2.9 BxPC-3 and HPDE6 cells apoptosis-related proteins profile

BxPC-3 and HPDE6 cells were seeded at density of $1x10^5$ cells/well in 12 well plates. After 24 hours media was removed and cells were washed 3 times with PBS and then lysed in dissociation buffer. Cell lysates from 3 different wells for each cell line were pooled together and microcentrifuged at 14000 g for 5 min. The supernatant was collected and the expression of 35 apoptosis-related proteins was evaluated using the Human Apoptosis Array kit (R&D Systems). Transfer of protein dots in Amersham Hyperfilm™ ECL (GE Healthcare) was performed using ECL Plus Western Blotting Detection System (GE Healthcare). Data analysis was performed using Gel Doc EZ system and the Image Lab Software (Bio-Rad).

8.2.2.10 PB1-F2/MAVS luciferase assay

PB1-F2/MAVS luciferase assay was performed in a 24-well plate transfecting 293T cells with pCAGG/PB1-F2 H7N3, pCAGG/PB1-F2 L75H H7N3 or empty pCAGG plasmids (1 μg/well), together with IFNβ-Luc plasmid (0.250 μg/well), which contain a firefly luciferase gene driven by the IFN-β promoter and renilla expression plasmid (0.125 μg/well). pCMV5-FLAG-MAVS plasmid, stably expressing MAVS adaptor protein, was added to half of the plate (1 μg/well) (MAVS+). The other half was transfected without pCMV5-FLAG-MAVS plasmid (MAVS-) to appraise the basal levels of IFN expression in 293T. At 8 hours post-transfection the media was replaced with DMEM supplemented with 10% FBS, 1% NEEA and 1% P/S solution and cells were incubated for further 16 hours. At the end of the incubation, 293T cells were lysed with 300 μl of lysis buffer (Promega) then firefly luciferase activity was measured in a luminometer using the Dual-Luciferase Reporter Assay System (Promega).

The PB1-F2/MAVS/NS1 assay was performed including also pCAGG/NS1 H7N3, pCAGG/NS1-77 H7N3 or empty pCAGG expression plasmids in the MAVS+ condition described above, aiming to evaluate the synergetic effect of NS1 and PB1-F2 antagonistic effect on the IFN-mediated antiviral response.

8.2.2.11 Minireplicon assay

293T cells were transfected in 24-well plates with pCAGG expression plasmids encoding PB2, PB1, PA, NP and different PB1-F2 (wild type or L75H) proteins derived from the H7N3 A/turkey/Italy/2962/V03 (NP, 320 ng; PB1 and PB2, 160 ng; PA, 80 ng; PB1-F2 or PB1-F2 L75H or empty pCAGG, 500 ng) using Lipofectamine 2000 (Invitrogen). A negative-sense firefly luciferase-expressing plasmid (pHuman-PolI-Firefly; 80 ng) was used as reporter to measure the polymerase

activity. At 24 hrs post-transfection, cells were lysed with 300 µl of lysis buffer then firefly luciferase activity was measured in a luminometer using the Luciferase Reporter Assay System (Promega).

8.2.2.12 NS1-77/2A/GM-CSFV5 and NEP mRNAs detection.

Semi-confluent monolayers of 293T cells were transfected in a 24 well plate with RF483-NS1-77/2A/GM-CSFV5/NSend, RF483-H7N3 NS1 or RF483-H7N3 NS1-77 plasmids at concentration of 1 µg/well. Forty-eight hours post-transfection, the media was removed and the cells were pelleted at 12000 g x 5 minutes. Total RNA was extracted from cell lysates using the Nucleospin RNA extraction kit (Macherey-Nagel) and then mRNAs were isolated using the PolyATtract mRNA Isolation Systems (Promega). RT-PCR was performed using the primers H7N3 NEP Fw1-23 and H7N3 NEP Rv322-344, which target the NS1 and NEP shared mRNA sequences, to investigate the expression of mRNAs produced from NS1-77/2A/GM-CSFV5/NSend construct. Amplification of β-actin mRNA was performed as a loading control using VG 150 and VG 151 primers previous published by Moerdyk-Schauwecker et al. (Moerdyk-Schauwecker et al., 2012).

8.2.3 Infectious studies

8.2.3.1 Annexin-V staining

The ability of reverse genetics influenza viruses to kill pancreatic cells via apoptosis was measured using annexing V staining. BxPC-3 and HPDE6 cells were infected with virus isolates at M.O.I. of 0.1 and the inoculum was removed after one hour of absorption and replaced with 1 ml of serum-free media. Combination of Gemcitabine (2 mM) and Cisplatin (0.8 µM) treatment served as positive controls for apoptosis. FBS was added to each well one hour prior to harvesting for a final concentration of 10% to ensure cell membrane integrity for the labelling process. At 16 and 24 hours post-infection, cells were harvested from two infected and one control well and incubated with Alexa Fluor® 647 Annexin V conjugate (Invitrogen) (1 µl per 375,000 cells) and propidium iodide (PI, 2 µl per 375,000 cells) in a volume of 300 µl of media with 10% FBS for 10 minutes in the dark. Samples were then fixed for 15 minutes in 3.6% paraformaldehyde, spun for 5 minutes at 1200 RPM, resuspended in 300 ul of PBS-FBS and read within 24 hours on a BD Facscalibur. The percentage of Specific Cell Death (SCD %) was calculated according to the formula SCD% = [(% annexin V positive cells (AV+) following virus infection - % AV+ not treated) / (100% - % AV+ not

treated)] x 100. A minimum of 5,000 events were recorded and all infections were repeated in three independent experiments.

8.2.3.2 Expression of IFN related genes in BxPC-3 and HPDE6 cells.

Cells were either mock-treated or infected with H7N3 A/turkey/Italy/2962/03 at M.O.I. of 0.1. Total RNA was extracted from cells at 16 h post-infection (p.i.) using NucleoSpin RNA II kit (Macherey-Nagel) in accordance with manufacturer instructions. RNA (0.5 mg/reaction) was reverse transcribed and amplified by RT-PCR using OneStep RT-PCR kit (Qiagen). PCR was carried with the following conditions: reverse transcription at 50°C at 30m, denaturation at 94 °C for 15 min followed by denaturation at 94°C for 45 s, annealing at 57 °C for 45 s, extension at 72 °C for 45 s for 35 cycles and a finishing step at 72 °C for 8 min. All the primers used for the PCR were previously published and designed to amplify cellular mRNAs (Moerdyk-Schauwecker et al., 2012). PCR products were electrophoresed on a 1% agarose gel with Gel Red™ Nucleic Acid Stain (Biotium) and photographed using a Gel Doc™ EZ Imager (Bio-Rad).

8.2.3.3 Immunocytochemistry (ICC) targeting apoptotic markers.

BXPC-3 and HPDE6 cells previously seeded on sterile glass chamber slides (BD) and high-binding slides were infected at M.O.I. of 1. At 16 h post-infection supernatants were removed, slides were air-dried under the biosafety cabinet, fixed in ice-cold acetone for 20 minutes, and then stored at -20°C until analysis. Gemcitabine and Cisplatin treatment served as positive controls for apoptosis. Prior to staining, frozen slides were thawed and washed 3 times for five minutes with deionized water to remove residual acetone, blocked with 3% H_2O_2 for eight minutes at RT to remove endogenous peroxidases, washed 3 times with deionized water and once with PBS-Tween 20. Slides were then blocked for 30 minutes with 1% BSA, washed with PBS-Tween and permeabilized with 0.1% Triton X-100 for 10 minutes. Caspase-specific primary antibodies, including anti-active/cleaved caspase-8 (1:50, Imgenex), anti-active-caspase-9 (1:10, BioVision), and anti-active-caspase-3 (1:30, Cambridge, UK) were applied for 1 hour in a humidified chamber at room temperature. Immunoreactivity was revealed by the avidin–biotin method (LSAB+/System-HRP, DakoCytomation Glostrup) using aminoetile-carbazole substrate (AEC + Substrate-Chromogen Ready-to-use, DakoCytomation). Carazzi's haematoxylin was used as a counterstain and Faramount Mounting Medium (DakoCytomation) was used to mount coverslips on slides. Ten histological counts of 500

cells each were performed per cell line/treatment/time point using Nis Elements BR software (Nikon) to determine the percentage of caspase-positive cells.

8.2.3.4 Influenza A virus M gene one step RRT-PCR.

BxPC-3 cells were infected with H7N3, H7N3 PB1-F2 L75H, H7N3 NS1-77, H7N3 NS1-77 PB1-F2 L75H A/turkey/Italy/2962/03 viruses at M.O.I. of 1. Total RNA was extracted from cells at 8, 16 and 24 h post-infection (p.i.) using NucleoSpin RNA II kit (Macherey-Nagel) in accordance with manufacturer instructions. The isolated RNA was amplified using the published primers and probes from *Spackman et al., 2002* (Spackman et al., 2002), targeting the conserved Matrix (M) gene of type A influenza virus. 5 µl of RNA were added to the reaction mixture composed of 300 nM of the forward and reverse primers (M25F and M124-R respectively), and 100 nM of the fluorescent label probe (M+64). The amplification reaction was performed in a final volume of 25 µl using the commercial kit QuantiTect Multiplex RT-PCR kit (Qiagen, Hilden, Germany). The PCR reaction was performed using the following protocol: 20 minutes at 50 °C and 15 minutes at 95 °C followed by 40 cycles at 94 °C for 45 sec and 60 °C for 45 sec. Target RNA *in vitro* transcribed was obtained using the Mega Short Script 7 (High Yield Transcription kit, Ambion), according to the manifacturer's instructions, quantified by NanoDrop 2000 (Thermo Scientific) and used to create a standard calibration curve for viral RNA quantification. Copy numbers of M gene were obtained through the extrapolation of Ct values of the test samples against the corresponding standard curve.

8.2.3.5 Virus replication kinetics in pancreatic cell lines.

The ability of H7N3 and H7N3 NS1-77 to replicate in IFN competent HPDE6 cells and IFN deficient BxPC-3 cells was monitored over a 72 hour time-course. Cells were seeded in a 24 well plate and then infected with both viruses at an M.O.I. of 0.001. After 1 hour absorption the inoculum was removed and replaced with 500 µl/well of serum-free RPMI 1640 media containing 0.1 µg/ml of TPCK-trypsin (SIGMA). At 24, 48 and 72 hours post-infection cells were scraped and for each virus cell suspensions from three infected wells were harvested centrifuged and then the supernatants were store ad -80°C.

The ability of H7N3 and H7N3 PB1-F2 avian influenza viruses to replicate in tumour derived BxPC-3 cells was monitored over a 72 hour time-course in 24-well plates using an MOI of 0.001. Following one hour of incubation the inoculum was removed and replaced with 500 µl/well of serum-free RPMI 1640 media containing 0.5 µg/ml of TPCK-trypsin. At 24, 48 and 72 hours post-infection cell

suspensions from three infected wells were harvested, centrifuged and then the supernatants were store ad -80°C. Viral titres were determined for all the samples within the same plaque assay session on MDCK-Npro cells (Matrosovich et al., 2006).

8.2.3.6 Viral growth in 7 and 14-day-old embryonated chicken eggs (ECE)

Ten specific pathogen free (SPF) embryonated chicken eggs ECE (Charles River) of both 7 and 14 day-old were infected with 10^3 pfu/egg of recombinant H7N3 A/turkey/Italy/2962/03 NS1-77 or full length NS1 viruses. Infected eggs were incubated at 37°C and candled daily to monitor the embryo viability. Once the number of dead eggs in each group exceeded 50%, they were incubated at +4°C overnight. Allantoic fluids harvested from all eggs were screened by rapid HA and those positive in each group were pooled together. Viral titres of the pooled fluids were measured by Haemagglutination assay (HA) according to the EU Council Directive 2005/94/EC and the OIE diagnostic manual (COUNCIL DIRECTIVE 2005/94/EC of 20 December 2005, 2006; Office International des Epizooties (OIE), May 2012).

8.2.3.7 Evaluation of H7N3 NS1-77 virus' immunostimulatory activity.

Confluent monolayers of IFN-competent HPDE6 cells were infected in 12 well plates with H7N3 and H7N3 NS1-77 at M.O.I=1 or mock infected. After 1 h absorption, the media were replaced with RPMI 1640 supplemented with 3% FBS, 1% Pen/Strep, 1% NEEA and cells were incubated for further 24 hours. After 24 hours supernatants were collected and exposed for 10 minutes under germicidal lamp to inactivate potential infectious particles in the suspension as confirmed by subsequent plaque assay. The VeriKine Human IFN-β ELISA kit (pbl Assay Science) was then used for quantitative measurement of IFN-β in the supernatants. Next different monolayers of PDA and HPDE6 cells in 24 well plates were incubated with the conditioned media derived from previous infection. After 16 hours incubation the media was discharged and cells were washed with PBS and tested for the presence of cytoplasmic histone-associated DNA fragments using the Cell Death Detection ELISAPLUS photometric enzyme immunoassay (Roche – Life Science).

Confluent mixture of HPDE6/BxPC-3Luc cells or BxPC-3Luc cells alone were growth in 96 well-plates using RPMI 1640 with 10% FBS, 1% Pen/Strep, 1% NEEA. Cells were then washed 3 times with PBS and infected with H7N3 or H7N3 NS1-77 viruses at M.O.I=0.1; 0.01; 1 or mock infected. After 1 hour absorption the cells were supplemented with RPMI 1640 with 0.5% FBS, 1% Pen/Strep, 1% NEEA and further incubated at 37°C until 24 hours post-infection when they were washed carefully with

PBS and lysed in Passive Lysis Buffer (Promega). Next, 5µl of cell lysates were combined with 100ul of BrightGlow buffer and substrate mixture (Bright-Glo™ Luciferase Assay System, Promega). Luciferase signal reading was performed within 5 minutes in GloMax-Multi Detection System (Promega).

8.2.3.8 Packaging and conservation of NS1-77/2A/GM-CSFV5/NSend segment following serial virus passages in Npro cells.

Packaging (Figure 49B). Supernatants derived from transfection with RF483-NS1-77/2A/GM-CSFV5/NSend alone or in combination with the other 7 plasmids required to generate PR8 H1/N1-2962 NS1-77 GM-CSF virus, were tested for the presence of the novel NS segment. Total RNA was extracted using the Nucleospin RNA extraction kit (Macherey-Nagel) and cDNA was generated. PCR reaction was performed using PFU turbo polymerase (invitrogen) and H7N3/NS1NotIF and H7N3/NS1MluIR sense and antisense oligonucleotides.

The conservation of the NS1-77/2A7GM-CSF segment following PR8 H1/N1-2962 NS1-77 GM-CSF virus passage 1 and 2 in Npro cells (Figure 50A) was evaluated through Onestep RT-PCR using H7N3/NS1NotIF and IIMluI/GM-CSF rv2 primers.

Analysis of truncation of the novel segment between passage 1 and 4 in Npro cells (Figure 51A) was performed on RNA extracted from the supernatant of infected cells by RT-PCR using H7N3/NS1NotIF and H7N3 NEP Rv322-344 sense and antisense oligonucleotides.

8.2.3.9 Visualisation of GM-CSF expression in PR8 H1/N1-2962 NS1-77 GM-CSF virus infected BxPC-3 cells.

BxPC-3 cells were grown on slides to 80% confluence and then infected with PR8 H1/N1-2962 NS1-77 and PR8 H1/N1-2962 NS1-77 GM-CSF viruses at an M.O.I. of 0.1 or mock infected. After 8 hours post-infection the supernatants were collected and cells were carefully washed with PBS and then fixed and permeabilized with chilled acetone (80%). Blocking was performed with PBS containing 1% BSA and 0.1% Tween-20 (Sigma), then the cells were incubated for 1 h at 37°C in a humidified chamber with mouse Anti-V5 antibody (Lifetechnologies), washed 3 times in PBS and further incubated with goat anti-mouse IgG-FITC antibody (Sigma) in PBS containing 1% BSA and 0.2% Evan's Blue. After 1 hour at 37°C the staining solution was decanted and the slides were washed three times and observed under UV light.

8.2.3.10 Human GM-CSF and IFN-β quantitative measurement.

Quantitative measurement of GM-CSF and IFN-β in cell supernatants was performed using the Human Gm-CSF ELISA kit (Thermo Scientific) and the VeriKine^{TM} Human IFN Betas ELISA kit (pbl assay science) following manufacturers' recommendations.

8.2.3.11 In vivo tumour model

The *in vivo* experimental protocol was investigated and approved by the Italian Ministry of Health (protocol 130/2011). Six weeks old pathogen-free SCID-B17 female mice were maintained in laminar flow racks and micro isolator cages under pathogen-free conditions and received autoclaved food and water ad libitum.

For the experiment described in chapter 2 twelve 6-week-old female SCID mice were subcutaneously injected with $5x10^6$ BxPC-3 cells in a volume of 100 µl into the right flank. Palpable tumours developed after 8 days, and mice were then randomly divided into two groups (n=6), one group receiving an intratumoral inoculation of $2.4x10^4$ PFU of H7N3 in a volume of 100 µl and the other receiving 100 µl of PBS. The procedure was subsequently repeated 3, 5, and 7 days later for a total of four intratumoral inoculations per treatment group. The overall physical condition and behaviour of the mice were monitored daily, and measurements of tumour size were taken on days 8, 15, 19, and 25 following initial injection. Caliper measurements of tumour sizes were taken at regular intervals throughout the experiment, and the length (L) and width (W) were recorded to determine tumour volumes according to the formula $V = L * W^2 * (\pi/6)$ (V=volume; L=length; W=width). At 25 days post-infection, mice were sacrificed and tumours were snap-frozen for RNA extraction and IAV-specific RT-PCR as described above.

For the experiments described within chapters 3 and 4, mice were inoculated subcutaneously in the right flank with 100 µl of 5×10^6 BxPC-3Luc cells, stably expressing firefly luciferase gene. Palpable tumours developed after nine days and mice were then randomly divided into different groups (n=5 per group), each one receiving an intratumoural (IT) inoculation of 5×10^4 pfu/50 µl of H7N3 A/turkey/Italy/2962/V03, H7N3 NS1-77, H7N3 PB1-F2 L75H, H7N3 NS1-77 PB1-F2 L75H viruses or PBS (negative control). The procedure was subsequently repeated for a total of four inoculations per treatment group. The overall physical condition and behaviour of the mice were monitored daily, and caliper measurements of tumour size were performed at regular interval following initial injection. The percentage of volume increase from the beginning of the treatment was calculated as

follows: Volume increase (%) = $(Vt_x-Vt_0)/(Vt_0*100)$. Tumour size and presence of metastasis were monitored also by bioluminescence imaging (BLI).In the case of H7N3 NS1-77 PB1-F2 L75H experiment (chapter 4 – paragraph 4.2.5) at day 23 a fifth IT virus injection was performed to appraise the clearance of the virus by the animals. All animals were sacrificed at the end of the experiments and in any case before reaching the threshold tumour volume of 1000 mm^3. Following post-mortem examination tumours and lungs, livers and kidneys were collected, snap-frozen and tested for viral RNA presence using Real-Time RT-PCR for influenza A virus M gene as described above.

8.2.4 Bioinformatic analysis

8.2.4.1 Sequence analysis

The sequences of all eight influenza genome segments belonging to H7N3 A/turkey/Italy/2962/2003 were submitted to GenBank and assigned accession numbers JX515660, JX515661, JX515662, JX515663, JX515664, JX515665, JX515666, DQ090062.

Influenza plasmids and virus sequences were aligned and analysed using MEGA 6.06 software (Tamura et al., 2013). Sequences used for comparison were downloaded from the NCBI Influenza Virus Resource (Bao et al., 2008).

8.2.4.2 Statistical analysis

Analysis of data was done using GraphPad Prism 6 for Windows (GraphPad Software Inc., La Jolla, CA). Symbol and meaning: *, $p \leq 0.05$; **, $p \leq 0.01$; ***, $p \leq 0.001$; ****, $p \leq 0.0001$.

Chapter 9. Appendix

Sequences and corresponding ORFs of the main plasmids used in this study. Analysis was performed using Geneious v5.0 software (Kearse et al., 2012).

RF483- H7N3 NS1 and RF483-H7N3 NS1-77

Three site mutations (red boxes) were introduced to obtain the RF483-H7N3 NS1-77 plasmids from the Rf483-H7N3 NS1.

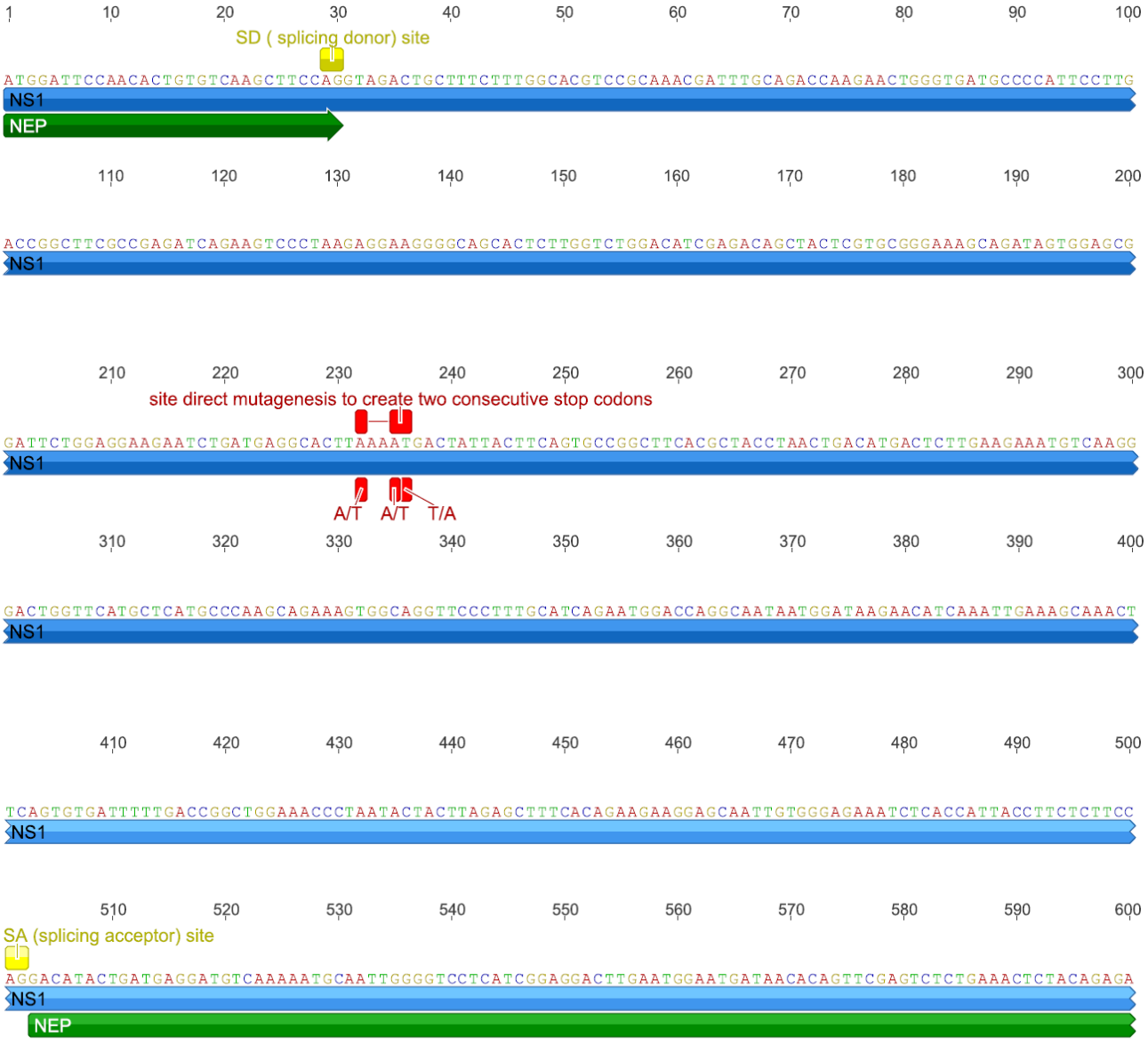

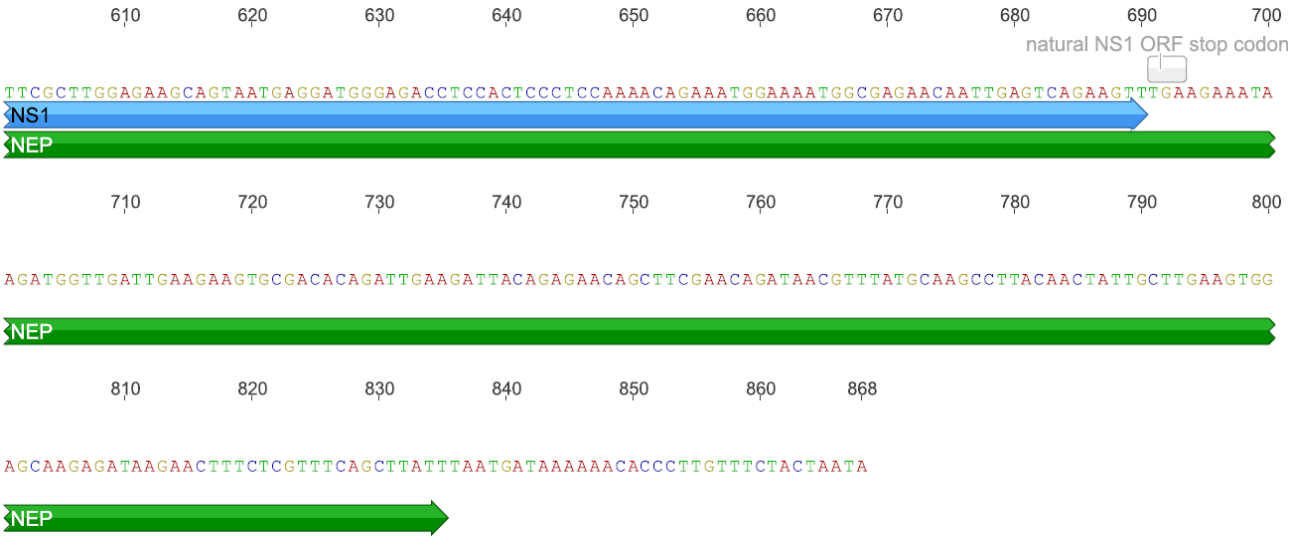

pCAGG/NS1 H7N3

Site specific mutagenesis (A/C) was performed on pCAGG/NS1 H7N3 plasmid to abrogate NEP expression.

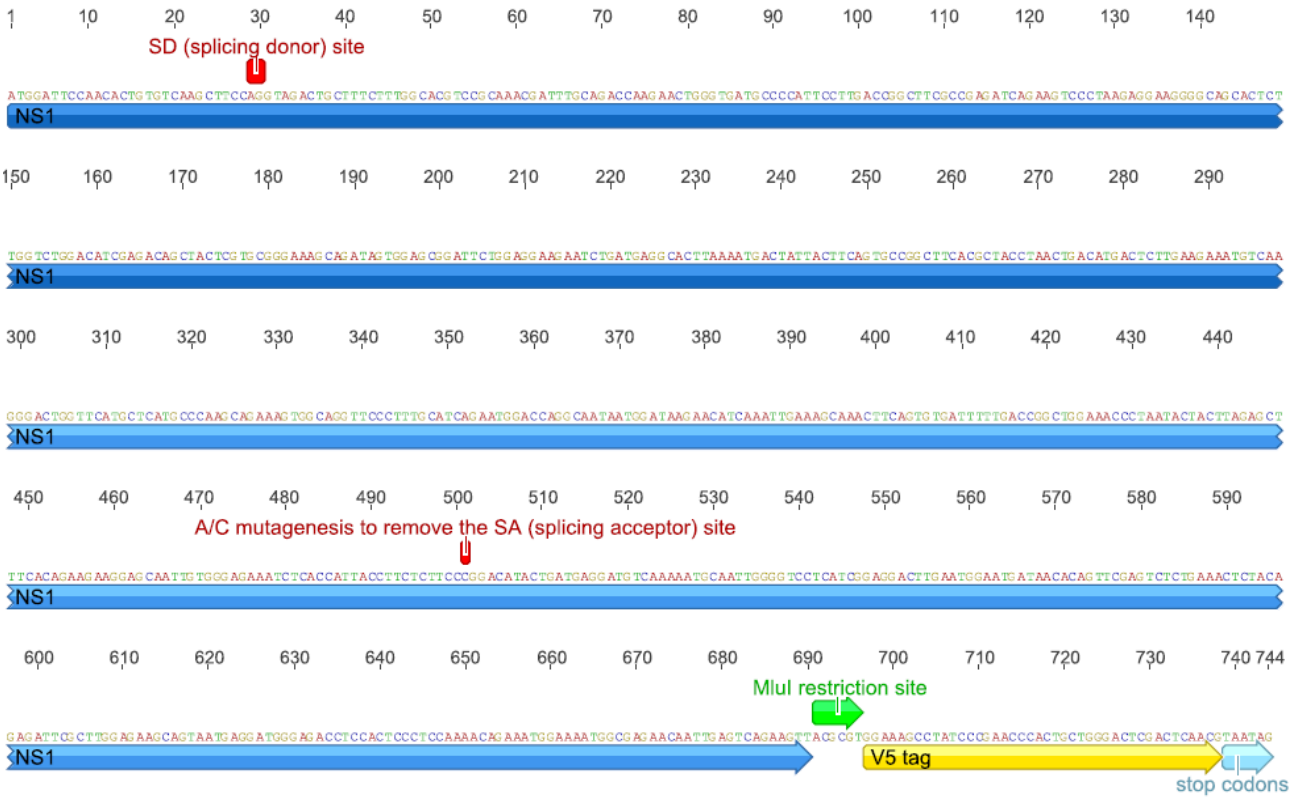

RF483- H7N3 PB1-F2 and RF483-PB1-F2 L75H

Site direct mutagenesis (red box) was used to substitute Leucine (L) in position 75 within the PB1-F2 ORF to Histidine (H).

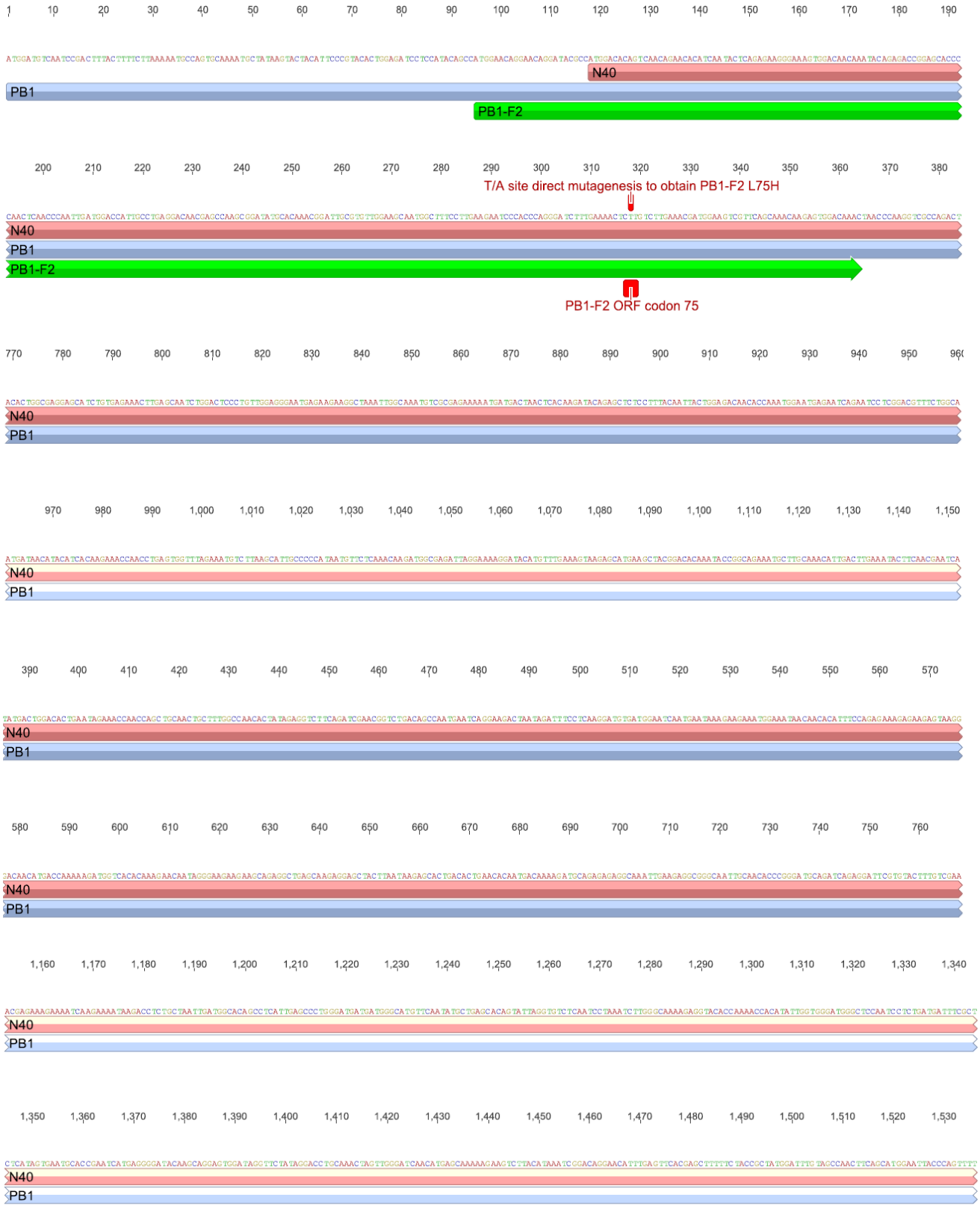

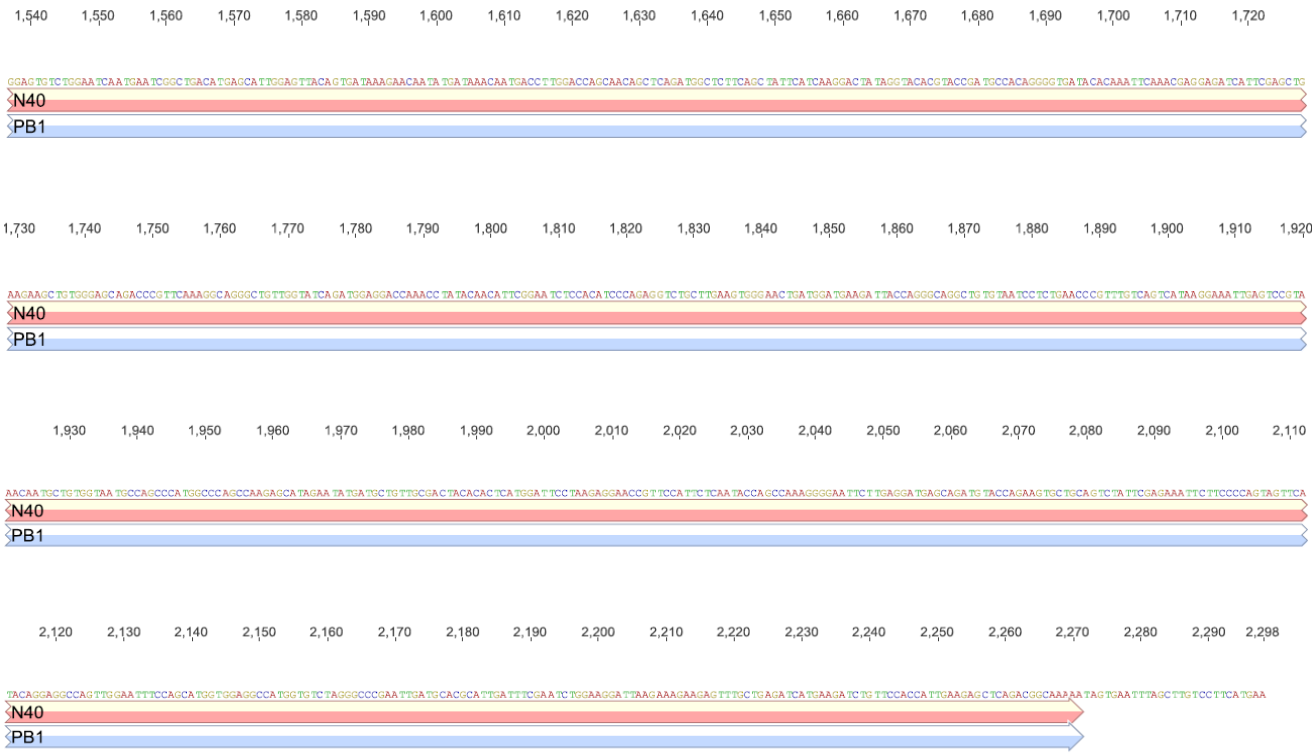

RF483-NS1-77/2A/GM-CSF/NSend

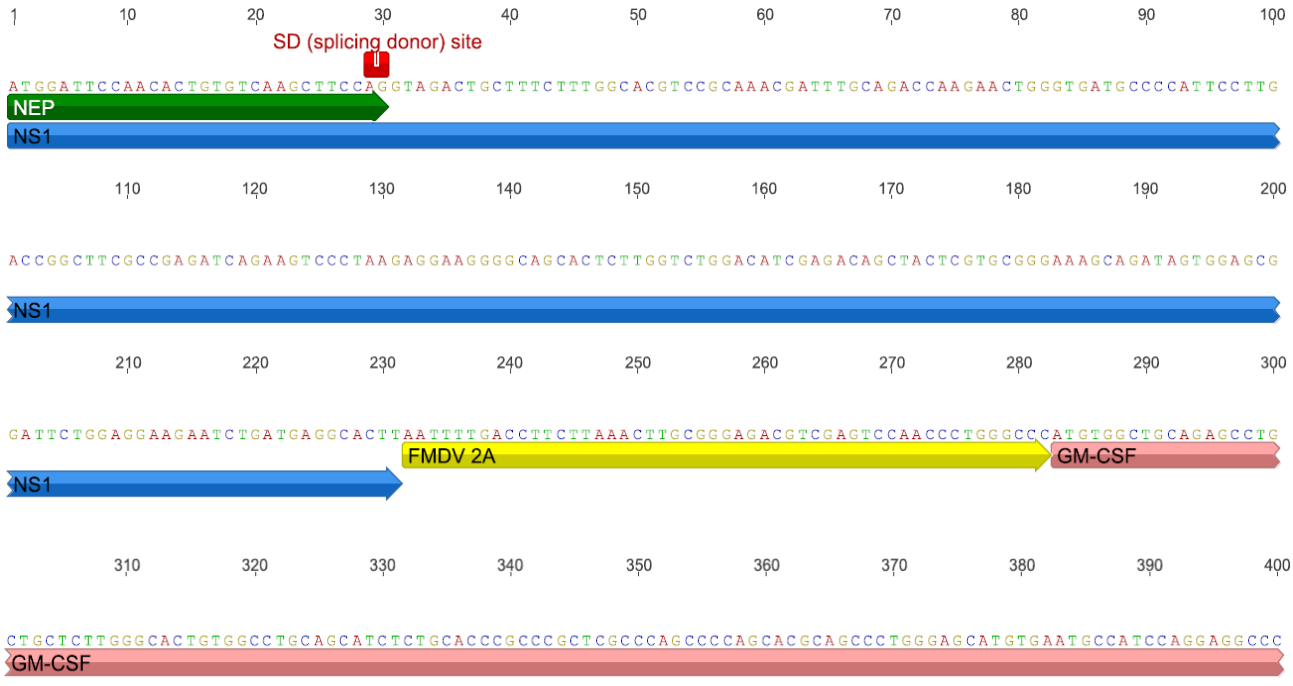


410 420 430 440 450 460 470 480 490 500
GM-CSF
510 520 530 540 550 560 570 580 590 600
GM-CSF
610 620 630 640 650 660 670 680 690 700
GM-CSF
710 720 730 740 750 760 770 780 790 800
MluI restriction site
stop codons
GM-CSF
V5 tag
NS1
810 820 830 840 850 860 870 880 890 900
NS1
910 920 930 940 950 960 970 980 990 1,000
NS1
1,010 1,020 1,030 1,040 1,050 1,060 1,070 1,080 1,090 1,100
SA (splicing acceptor) site
NEP
NS1
1,110 1,120 1,130 1,140 1,150 1,160 1,170 1,180 1,190 1,200
NEP
NS1
1,210 1,220 1,230 1,240 1,250 1,260 1,270 1,280 1,290 1,300
NEP
NS1
1,310 1,320 1,330 1,340 1,350 1,360 1,370 1,380 1,390 1,399
NEP

Chapter 10. References

Akarsu, H., Burmeister, W.P., Petosa, C., Petit, I., Muller, C.W., Ruigrok, R.W., and Baudin, F. (2003). Crystal structure of the M1 protein-binding domain of the influenza A virus nuclear export protein (NEP/NS2). EMBO J. *22,* 4646-4655.

Alexander, D.J. (2007). An overview of the epidemiology of avian influenza. Vaccine *25,* 5637-5644.

Ali, A., Avalos, R.T., Ponimaskin, E., and Nayak, D.P. (2000). Influenza virus assembly: effect of influenza virus glycoproteins on the membrane association of M1 protein. J. Virol. *74,* 8709-8719.

Almoguera, C., Shibata, D., Forrester, K., Martin, J., Arnheim, N., and Perucho, M. (1988). Most human carcinomas of the exocrine pancreas contain mutant c-K-ras genes. Cell *53,* 549-554.

American Cancer Society. (2014). Cancer Facts & Figures 2014. (Atlanta: American Cancer Society).

American Cancer Society. (2013). Cancer Facts & Figures 2013. (Atlanta: American Cancer Society).

Amorim, M.J., Bruce, E.A., Read, E.K., Foeglein, A., Mahen, R., Stuart, A.D., and Digard, P. (2011). A Rab11- and microtubule-dependent mechanism for cytoplasmic transport of influenza A virus viral RNA. J. Virol. *85,* 4143-4156.

Andree, H.A., Reutelingsperger, C.P., Hauptmann, R., Hemker, H.C., Hermens, W.T., and Willems, G.M. (1990). Binding of vascular anticoagulant alpha (VAC alpha) to planar phospholipid bilayers. J. Biol. Chem. *265,* 4923-4928.

Andtbacka, R.H., Kaufman, H.L., Collichio, F., Amatruda, T., Senzer, N., Chesney, J., Delman, K.A., Spitler, L.E., Puzanov, I., Agarwala, S.S*., et al.* (2015). Talimogene Laherparepvec Improves Durable Response Rate in Patients With Advanced Melanoma. J. Clin. Oncol.

Aramini, J.M., Hamilton, K., Ma, L.C., Swapna, G.V., Leonard, P.G., Ladbury, J.E., Krug, R.M., and Montelione, G.T. (2014). (19)F NMR reveals multiple conformations at the dimer interface of the nonstructural protein 1 effector domain from influenza A virus. Structure *22,* 515-525.

Aramini, J.M., Ma, L.C., Zhou, L., Schauder, C.M., Hamilton, K., Amer, B.R., Mack, T.R., Lee, H.W., Ciccosanti, C.T., Zhao, L*., et al.* (2011). Dimer interface of the effector domain of non-structural protein 1 from influenza A virus: an interface with multiple functions. J. Biol. Chem. *286,* 26050-26060.

Aredia, F., and Scovassi, A.I. (2014). Poly(ADP-ribose): A signaling molecule in different paradigms of cell death. Biochem. Pharmacol. *92,* 157-163.

Arndt, U., Wennemuth, G., Barth, P., Nain, M., Al-Abed, Y., Meinhardt, A., Gemsa, D., and Bacher, M. (2002). Release of macrophage migration inhibitory factor and CXCL8/interleukin-8 from lung epithelial cells rendered necrotic by influenza A virus infection. J. Virol. *76,* 9298-9306.

Arranz, R., Coloma, R., Chichon, F.J., Conesa, J.J., Carrascosa, J.L., Valpuesta, J.M., Ortin, J., and Martin-Benito, J. (2012). The structure of native influenza virion ribonucleoproteins. Science *338,* 1634-1637.

Ashcroft, M., Taya, Y., and Vousden, K.H. (2000). Stress signals utilize multiple pathways to stabilize p53. Mol. Cell. Biol. *20,* 3224-3233.

Avilov, S.V., Moisy, D., Munier, S., Schraidt, O., Naffakh, N., and Cusack, S. (2012). Replication-competent influenza A virus that encodes a split-green fluorescent protein-tagged PB2 polymerase subunit allows live-cell imaging of the virus life cycle. J. Virol. *86,* 1433-1448.

Ayala-Breton, C., Barber, G.N., Russell, S.J., and Peng, K.W. (2012). Retargeting vesicular stomatitis virus using measles virus envelope glycoproteins. Hum. Gene Ther. *23,* 484-491.

Babcock, H.P., Chen, C., and Zhuang, X. (2004). Using single-particle tracking to study nuclear trafficking of viral genes. Biophys. J. *87,* 2749-2758.

Baglioni, C., Minks, M.A., and Maroney, P.A. (1978). Interferon action may be mediated by activation of a nuclease by pppA2'p5'A2'p5'A. Nature *273,* 684-687.

Balachandran, S., Kim, C.N., Yeh, W.C., Mak, T.W., Bhalla, K., and Barber, G.N. (1998). Activation of the dsRNA-dependent protein kinase, PKR, induces apoptosis through FADD-mediated death signaling. EMBO J. *17,* 6888-6902.

Bao, Y., Bolotov, P., Dernovoy, D., Kiryutin, B., Zaslavsky, L., Tatusova, T., Ostell, J., and Lipman, D. (2008). The influenza virus resource at the National Center for Biotechnology Information. J. Virol. *82,* 596-601.

Barabe, F., Kennedy, J.A., Hope, K.J., and Dick, J.E. (2007). Modeling the initiation and progression of human acute leukemia in mice. Science *316,* 600-604.

Barber, G.N. (2004). Vesicular stomatitis virus as an oncolytic vector. Viral Immunol. *17,* 516-527.

Barber, G.N. (2001). Host defense, viruses and apoptosis. Cell Death Differ. *8,* 113-126.

Bardeesy, N., and DePinho, R.A. (2002). Pancreatic cancer biology and genetics. Nat. Rev. Cancer. *2,* 897-909.

Barman, S., Ali, A., Hui, E.K., Adhikary, L., and Nayak, D.P. (2001). Transport of viral proteins to the apical membranes and interaction of matrix protein with glycoproteins in the assembly of influenza viruses. Virus Res. *77,* 61-69.

Barman, S., and Nayak, D.P. (2000). Analysis of the transmembrane domain of influenza virus neuraminidase, a type II transmembrane glycoprotein, for apical sorting and raft association. J. Virol. *74,* 6538-6545.

Basler, C.F., Reid, A.H., Dybing, J.K., Janczewski, T.A., Fanning, T.G., Zheng, H., Salvatore, M., Perdue, M.L., Swayne, D.E., Garcia-Sastre, A., Palese, P., and Taubenberger, J.K. (2001). Sequence of the 1918 pandemic influenza virus nonstructural gene (NS) segment and characterization of recombinant viruses bearing the 1918 NS genes. Proc. Natl. Acad. Sci. U. S. A. *98,* 2746-2751.

Batabyal, P., Vander Hoorn, S., Christophi, C., and Nikfarjam, M. (2014). Association of diabetes mellitus and pancreatic adenocarcinoma: a meta-analysis of 88 studies. Ann. Surg. Oncol. *21,* 2453-2462.

Baudin, F., Petit, I., Weissenhorn, W., and Ruigrok, R.W. (2001). In vitro dissection of the membrane and RNP binding activities of influenza virus M1 protein. Virology *281,* 102-108.

Baum, J., Simons, B.E.,Jr, Unger, R.H., and Madison, L.L. (1962). Localization of glucagon in the alpha cells in the pancreatic islet by immunofluorescent technics. Diabetes *11,* 371-374.

Ben, Q., Xu, M., Ning, X., Liu, J., Hong, S., Huang, W., Zhang, H., and Li, Z. (2011). Diabetes mellitus and risk of pancreatic cancer: A meta-analysis of cohort studies. Eur. J. Cancer *47,* 1928-1937.

Bergmann, M., Romirer, I., Sachet, M., Fleischhacker, R., Garcia-Sastre, A., Palese, P., Wolff, K., Pehamberger, H., Jakesz, R., and Muster, T. (2001). A genetically engineered influenza A virus with ras-dependent oncolytic properties. Cancer Res. *61,* 8188-8193.

Berrington de Gonzalez, A., Sweetland, S., and Spencer, E. (2003). A meta-analysis of obesity and the risk of pancreatic cancer. Br. J. Cancer *89,* 519-523.

Bertran, K., Perez-Ramirez, E., Busquets, N., Dolz, R., Ramis, A., Darji, A., Abad, F.X., Valle, R., Chaves, A., Vergara-Alert, J.*, et al.* (2011). Pathogenesis and transmissibility of highly (H7N1) and low (H7N9) pathogenic avian influenza virus infection in red-legged partridge (Alectoris rufa). Vet. Res. *42,* 24-9716-42-24.

Bi, J., Guo, A.L., Lai, Y.R., Li, B., Zhong, J.M., Wu, H.Q., Xie, Z., He, Y.L., Lv, Z.L., Lau, S.H.*, et al.* (2010). Overexpression of clusterin correlates with tumor progression, metastasis in gastric cancer: a study on tissue microarrays. Neoplasma *57,* 191-197.

Biankin, A.V., Waddell, N., Kassahn, K.S., Gingras, M.C., Muthuswamy, L.B., Johns, A.L., Miller, D.K., Wilson, P.J., Patch, A.M., Wu, J.*, et al.* (2012). Pancreatic cancer genomes reveal aberrations in axon guidance pathway genes. Nature *491,* 399-405.

Biondo, M., Nasa, Z., Marshall, A., Toh, B.H., and Alderuccio, F. (2001). Local transgenic expression of granulocyte macrophage-colony stimulating factor initiates autoimmunity. J. Immunol. *166,* 2090-2099.

Blum, A., Podvitzky, O., Shalabi, R., and Simsolo, C. (2010). Acute pancreatitis may be caused by H1N1 influenza A virus infection. Isr. Med. Assoc. J. *12,* 640-641.

Booy, S., van Eijck, C.H., Dogan, F., van Koetsveld, P.M., and Hofland, L.J. (2014). Influence of type-I Interferon receptor expression level on the response to type-I Interferons in human pancreatic cancer cells. J. Cell. Mol. Med. *18,* 492-502.

Bornholdt, Z.A., and Prasad, B.V. (2008). X-ray structure of NS1 from a highly pathogenic H5N1 influenza virus. Nature *456,* 985-988.

Bosma, G.C., Custer, R.P., and Bosma, M.J. (1983). A severe combined immunodeficiency mutation in the mouse. Nature *301,* 527-530.

Boyer, J.C., and Haenni, A.L. (1994). Infectious transcripts and cDNA clones of RNA viruses. Virology *198,* 415-426.

Bray, M. (2001). The role of the Type I interferon response in the resistance of mice to filovirus infection. J. Gen. Virol. *82,* 1365-1373.

Brehm, M.A., Shultz, L.D., Luban, J., and Greiner, D.L. (2013). Overcoming current limitations in humanized mouse research. J. Infect. Dis. *208 Suppl 2,* S125-30.

Breitbach, C.J., Thorne, S.H., Bell, J.C., and Kirn, D.H. (2012). Targeted and armed oncolytic poxviruses for cancer: the lead example of JX-594. Curr. Pharm. Biotechnol. *13,* 1768-1772.

Bridgen, A., and Elliott, R.M. (1996). Rescue of a segmented negative-strand RNA virus entirely from cloned complementary DNAs. Proc. Natl. Acad. Sci. U. S. A. *93,* 15400-15404.

Brown, I.H. (2000). The epidemiology and evolution of influenza viruses in pigs. Vet. Microbiol. *74,* 29-46.

Brown, J.M., and Attardi, L.D. (2005). The role of apoptosis in cancer development and treatment response. Nat. Rev. Cancer. *5,* 231-237.

Bui, M., Wills, E.G., Helenius, A., and Whittaker, G.R. (2000). Role of the influenza virus M1 protein in nuclear export of viral ribonucleoproteins. J. Virol. *74,* 1781-1786.

Buijs, P.R., van Eijck, C.H., Hofland, L.J., Fouchier, R.A., and van den Hoogen, B.G. (2014). Different responses of human pancreatic adenocarcinoma cell lines to oncolytic Newcastle disease virus infection. Cancer Gene Ther. *21,* 24-30.

Bullido, R., Gomez-Puertas, P., Saiz, M.J., and Portela, A. (2001). Influenza A virus NEP (NS2 protein) downregulates RNA synthesis of model template RNAs. J. Virol. *75,* 4912-4917.

Bullough, P.A., Hughson, F.M., Skehel, J.J., and Wiley, D.C. (1994). Structure of influenza haemagglutinin at the pH of membrane fusion. Nature *371,* 37-43.

Burke, J.M., Lamm, D.L., Meng, M.V., Nemunaitis, J.J., Stephenson, J.J., Arseneau, J.C., Aimi, J., Lerner, S., Yeung, A.W., Kazarian, T., Maslyar, D.J., and McKiernan, J.M. (2012). A first in human phase 1 study of CG0070, a GM-CSF expressing oncolytic adenovirus, for the treatment of nonmuscle invasive bladder cancer. J. Urol. *188,* 2391-2397.

Burris, H.A.,3rd, Moore, M.J., Andersen, J., Green, M.R., Rothenberg, M.L., Modiano, M.R., Cripps, M.C., Portenoy, R.K., Storniolo, A.M., Tarassoff, P.*, et al.* (1997). Improvements in survival and clinical benefit with gemcitabine as first-line therapy for patients with advanced pancreas cancer: a randomized trial. J. Clin. Oncol. *15,* 2403-2413.

Bush, R.M., Fitch, W.M., Bender, C.A., and Cox, N.J. (1999). Positive selection on the H3 hemagglutinin gene of human influenza virus A. Mol. Biol. Evol. *16,* 1457-1465.

Bussey, K.A., Bousse, T.L., Desmet, E.A., Kim, B., and Takimoto, T. (2010). PB2 residue 271 plays a key role in enhanced polymerase activity of influenza A viruses in mammalian host cells. J. Virol. *84,* 4395-4406.

Call, J.A., Eckhardt, S.G., and Camidge, D.R. (2008). Targeted manipulation of apoptosis in cancer treatment. Lancet Oncol. *9,* 1002-1011.

Cannell, J.J., Vieth, R., Umhau, J.C., Holick, M.F., Grant, W.B., Madronich, S., Garland, C.F., and Giovannucci, E. (2006). Epidemic influenza and vitamin D. Epidemiol. Infect. *134,* 1129-1140.

Cano, M., Iglesias, P., Perez, G., and Diez, J.J. (2010). Influenza A virus (H1N1) infection as a cause of severe diabetic ketoacidosis in type 1 diabetes. Endocrinol. Nutr. *57,* 37-38.

Capua, I., Mercalli, A., Pizzuto, M.S., Romero-Tejeda, A., Kasloff, S., De Battisti, C., Bonfante, F., Patrono, L.V., Vicenzi, E., Zappulli, V.*, et al.* (2013). Influenza A viruses grow in human pancreatic cells and cause pancreatitis and diabetes in an animal model. J. Virol. *87,* 597-610.

Carrillo, B., Choi, J.M., Bornholdt, Z.A., Sankaran, B., Rice, A.P., and Prasad, B.V. (2014). The influenza A virus protein NS1 displays structural polymorphism. J. Virol. *88,* 4113-4122.

Cattaneo, R. (2010). Paramyxovirus entry and targeted vectors for cancer therapy. PLoS Pathog. *6,* e1000973.

Cattaneo, R., Miest, T., Shashkova, E.V., and Barry, M.A. (2008). Reprogrammed viruses as cancer therapeutics: targeted, armed and shielded. Nat. Rev. Microbiol. *6,* 529-540.

Chaitanya, G.V., Steven, A.J., and Babu, P.P. (2010). PARP-1 cleavage fragments: signatures of cell-death proteases in neurodegeneration. Cell. Commun. Signal. *8,* 31.

Chen, B.J., Leser, G.P., Jackson, D., and Lamb, R.A. (2008). The influenza virus M2 protein cytoplasmic tail interacts with the M1 protein and influences virus assembly at the site of virus budding. J. Virol. *82,* 10059-10070.

Chen, C.J., Chen, G.W., Wang, C.H., Huang, C.H., Wang, Y.C., and Shih, S.R. (2010). Differential localization and function of PB1-F2 derived from different strains of influenza A virus. J. Virol. *84,* 10051-10062.

Chen, R., and Holmes, E.C. (2006). Avian influenza virus exhibits rapid evolutionary dynamics. Mol. Biol. Evol. *23,* 2336-2341.

Chen, W., Calvo, P.A., Malide, D., Gibbs, J., Schubert, U., Bacik, I., Basta, S., O'Neill, R., Schickli, J., Palese, P.*, et al.* (2001). A novel influenza A virus mitochondrial protein that induces cell death. Nat. Med. *7,* 1306-1312.

Chen, Z., Li, Y., and Krug, R.M. (1999). Influenza A virus NS1 protein targets poly(A)-binding protein II of the cellular 3'-end processing machinery. EMBO J. *18,* 2273-2283.

Chen, Z.H., Zhang, H., and Savarese, T.M. (1996). Gene deletion chemoselectivity: codeletion of the genes for p16(INK4), methylthioadenosine phosphorylase, and the alpha- and beta-interferons in human pancreatic cell carcinoma lines and its implications for chemotherapy. Cancer Res. *56,* 1083-1090.

Choi, Y.K., Kim, T.K., Kim, C.J., Lee, J.S., Oh, S.Y., Joo, H.S., Foster, D.N., Hong, K.C., You, S., and Kim, H. (2006). Activation of the intrinsic mitochondrial apoptotic pathway in swine influenza virus-mediated cell death. Exp. Mol. Med. *38,* 11-17.

CHOPPIN, P.W., MURPHY, J.S., and TAMM, I. (1960). Studies of two kinds of virus particles which comprise influenza A2 virus strains. III. Morphological characteristics: independence to morphological and functional traits. J. Exp. Med. *112,* 945-952.

Chou, Y.Y., Heaton, N.S., Gao, Q., Palese, P., Singer, R.H., and Lionnet, T. (2013). Colocalization of different influenza viral RNA segments in the cytoplasm before viral budding as shown by single-molecule sensitivity FISH analysis. PLoS Pathog. *9,* e1003358.

CHU, C.M., DAWSON, I.M., and ELFORD, W.J. (1949). Filamentous forms associated with newly isolated influenza virus. Lancet *1,* 602-top-frame" src="./pubmed_files/top.

Chua, M.A., Schmid, S., Perez, J.T., Langlois, R.A., and Tenoever, B.R. (2013). Influenza A virus utilizes suboptimal splicing to coordinate the timing of infection. Cell. Rep. *3,* 23-29.

Clemens, M.J. (2003). Interferons and apoptosis. J. Interferon Cytokine Res. *23,* 277-292.

Clemens, M.J., and Williams, B.R. (1978). Inhibition of cell-free protein synthesis by pppA2'p5'A2'p5'A: a novel oligonucleotide synthesized by interferon-treated L cell extracts. Cell *13,* 565-572.

Coleman, T.J., Gamble, D.R., and Taylor, K.W. (1973). Diabetes in mice after Coxsackie B 4 virus infection. Br. Med. J. *3,* 25-27.

Collisson, E.A., Sadanandam, A., Olson, P., Gibb, W.J., Truitt, M., Gu, S., Cooc, J., Weinkle, J., Kim, G.E., Jakkula, L.*, et al.* (2011). Subtypes of pancreatic ductal adenocarcinoma and their differing responses to therapy. Nat. Med. *17,* 500-503.

Comins, C., Heinemann, L., Harrington, K., Melcher, A., De Bono, J., and Pandha, H. (2008). Reovirus: viral therapy for cancer 'as nature intended'. Clin. Oncol. (R. Coll. Radiol) *20,* 548-554.

Compans, R.W., Content, J., and Duesberg, P.H. (1972). Structure of the ribonucleoprotein of influenza virus. J. Virol. *10,* 795-800.

Conti, L., and Gessani, S. (2008). GM-CSF in the generation of dendritic cells from human blood monocyte precursors: recent advances. Immunobiology *213,* 859-870.

Corvelo, A., Hallegger, M., Smith, C.W., and Eyras, E. (2010). Genome-wide association between branch point properties and alternative splicing. PLoS Comput. Biol. *6,* e1001016.

Couch, F.J., Johnson, M.R., Rabe, K.G., Brune, K., de Andrade, M., Goggins, M., Rothenmund, H., Gallinger, S., Klein, A., Petersen, G.M., and Hruban, R.H. (2007). The prevalence of BRCA2 mutations in familial pancreatic cancer. Cancer Epidemiol. Biomarkers Prev. *16,* 342-346.

Coughlan, L., Vallath, S., Saha, A., Flak, M., McNeish, I.A., Vassaux, G., Marshall, J.F., Hart, I.R., and Thomas, G.J. (2009). In vivo retargeting of adenovirus type 5 to alphavbeta6 integrin results in reduced hepatotoxicity and improved tumor uptake following systemic delivery. J. Virol. *83,* 6416-6428.

COUNCIL DIRECTIVE 2005/94/EC of 20 December 2005. (2006). Community measures for the control of avian influenza and repealing Directive 92/40/EEC. Official Journal of the European Union

Cousins, D.J., Staynov, D.Z., and Lee, T.H. (1994). Regulation of interleukin-5 and granulocyte-macrophage colony-stimulating factor expression. Am. J. Respir. Crit. Care Med. *150,* S50-3.

Cripe, T.P., Ngo, M.C., Geller, J.I., Louis, C.U., Currier, M.A., Racadio, J.M., Towbin, A.J., Rooney, C.M., Pelusio, A., Moon, A.*, et al.* (2014). Phase 1 Study of Intratumoral Pexa-Vec (JX-594), an Oncolytic and Immunotherapeutic Vaccinia Virus, in Pediatric Cancer Patients. Mol. Ther.

Cros, J.F., Garcia-Sastre, A., and Palese, P. (2005). An unconventional NLS is critical for the nuclear import of the influenza A virus nucleoprotein and ribonucleoprotein. Traffic *6,* 205-213.

Cross, K.J., Burleigh, L.M., and Steinhauer, D.A. (2001). Mechanisms of cell entry by influenza virus. Expert Rev. Mol. Med. *3,* 1-18.

Croyle, M.A., Callahan, S.M., Auricchio, A., Schumer, G., Linse, K.D., Wilson, J.M., Brunner, L.J., and Kobinger, G.P. (2004). PEGylation of a vesicular stomatitis virus G pseudotyped lentivirus vector prevents inactivation in serum. J. Virol. *78,* 912-921.

Cubilla, A.L., and Fitzgerald, P.J. (1984). Tumours of the Exocrine Pancreas. (Washington, D.C.: AFIP).

Cui, S., Eisenacher, K., Kirchhofer, A., Brzozka, K., Lammens, A., Lammens, K., Fujita, T., Conzelmann, K.K., Krug, A., and Hopfner, K.P. (2008). The C-terminal regulatory domain is the RNA 5'-triphosphate sensor of RIG-I. Mol. Cell *29,* 169-179.

Damdinsuren, B., Nagano, H., Sakon, M., Kondo, M., Yamamoto, T., Umeshita, K., Dono, K., Nakamori, S., and Monden, M. (2003). Interferon-beta is more potent than interferon-alpha in inhibition of human hepatocellular carcinoma cell growth when used alone and in combination with anticancer drugs. Ann. Surg. Oncol. *10,* 1184-1190.

Dauber, B., Martinez-Sobrido, L., Schneider, J., Hai, R., Waibler, Z., Kalinke, U., Garcia-Sastre, A., and Wolff, T. (2009). Influenza B virus ribonucleoprotein is a potent activator of the antiviral kinase PKR. PLoS Pathog. *5,* e1000473.

De Pace, N. (1912). Sulla scomparsa di un enorme cancro vegetante del callo dell'utero senza cura chirurgica (Italian). Ginecologia *9,* 82-88.

de Wit, E., Bestebroer, T.M., Spronken, M.I., Rimmelzwaan, G.F., Osterhaus, A.D., and Fouchier, R.A. (2007). Rapid sequencing of the non-coding regions of influenza A virus. J. Virol. Methods *139,* 85-89.

de Wit, E., Kawaoka, Y., de Jong, M.D., and Fouchier, R.A. (2008). Pathogenicity of highly pathogenic avian influenza virus in mammals. Vaccine *26 Suppl 4,* D54-8.

Deer, E.L., Gonzalez-Hernandez, J., Coursen, J.D., Shea, J.E., Ngatia, J., Scaife, C.L., Firpo, M.A., and Mulvihill, S.J. (2010). Phenotype and genotype of pancreatic cancer cell lines. Pancreas *39,* 425-435.

Desselberger, U., Racaniello, V.R., Zazra, J.J., and Palese, P. (1980). The 3' and 5'-terminal sequences of influenza A, B and C virus RNA segments are highly conserved and show partial inverted complementarity. Gene *8,* 315-328.

Dias, A., Bouvier, D., Crepin, T., McCarthy, A.A., Hart, D.J., Baudin, F., Cusack, S., and Ruigrok, R.W. (2009). The cap-snatching endonuclease of influenza virus polymerase resides in the PA subunit. Nature *458,* 914-918.

Diop-Frimpong, B., Chauhan, V.P., Krane, S., Boucher, Y., and Jain, R.K. (2011). Losartan inhibits collagen I synthesis and improves the distribution and efficacy of nanotherapeutics in tumors. Proc. Natl. Acad. Sci. U. S. A. *108,* 2909-2914.

Dittmann, J., Stertz, S., Grimm, D., Steel, J., Garcia-Sastre, A., Haller, O., and Kochs, G. (2008). Influenza A virus strains differ in sensitivity to the antiviral action of Mx-GTPase. J. Virol. *82,* 3624-3631.

Dock, G. (1904). The influence of complicating diseases upon leukemia. Am J Med Sci *127,* 563-592.

Doloff, J.C., Jounaidi, Y., and Waxman, D.J. (2011). Dual E1A oncolytic adenovirus: targeting tumor heterogeneity with two independent cancer-specific promoter elements, DF3/MUC1 and hTERT. Cancer Gene Ther. *18,* 153-166.

Doms, R.W., and Helenius, A. (1986). Quaternary structure of influenza virus hemagglutinin after acid treatment. J. Virol. *60,* 833-839.

Donelan, N.R., Basler, C.F., and Garcia-Sastre, A. (2003). A recombinant influenza A virus expressing an RNA-binding-defective NS1 protein induces high levels of beta interferon and is attenuated in mice. J. Virol. *77,* 13257-13266.

Dong, B., and Silverman, R.H. (1997). A bipartite model of 2-5A-dependent RNase L. J. Biol. Chem. *272,* 22236-22242.

Donnelly, O., Harrington, K., Melcher, A., and Pandha, H. (2013). Live viruses to treat cancer. J. R. Soc. Med. *106,* 310-314.

Doronin, K., Shashkova, E.V., May, S.M., Hofherr, S.E., and Barry, M.A. (2009). Chemical modification with high molecular weight polyethylene glycol reduces transduction of hepatocytes and increases efficacy of intravenously delivered oncolytic adenovirus. Hum. Gene Ther. *20,* 975-988.

Dougan, M., and Dranoff, G. (2009). Immune therapy for cancer. Annu. Rev. Immunol. *27,* 83-117.

Dranoff, G. (2004). Cytokines in cancer pathogenesis and cancer therapy. Nat. Rev. Cancer. *4,* 11-22.

Dranoff, G. (2003). GM-CSF-secreting melanoma vaccines. Oncogene *22,* 3188-3192.

Dranoff, G., Jaffee, E., Lazenby, A., Golumbek, P., Levitsky, H., Brose, K., Jackson, V., Hamada, H., Pardoll, D., and Mulligan, R.C. (1993). Vaccination with irradiated tumor cells engineered to secrete murine granulocyte-macrophage colony-stimulating factor stimulates potent, specific, and long-lasting anti-tumor immunity. Proc. Natl. Acad. Sci. U. S. A. *90,* 3539-3543.

Dreyer, W.J., and Neurath, H. (1955). The activation of chymotrypsinogen; isolation and identification of a peptide liberated during activation. J. Biol. Chem. *217,* 527-539.

Duell, E.J., Holly, E.A., Bracci, P.M., Liu, M., Wiencke, J.K., and Kelsey, K.T. (2002). A population-based, case-control study of polymorphisms in carcinogen-metabolizing genes, smoking, and pancreatic adenocarcinoma risk. J. Natl. Cancer Inst. *94,* 297-306.

Duell, E.J., Lucenteforte, E., Olson, S.H., Bracci, P.M., Li, D., Risch, H.A., Silverman, D.T., Ji, B.T., Gallinger, S., Holly, E.A.*, et al.* (2012). Pancreatitis and pancreatic cancer risk: a pooled analysis in the International Pancreatic Cancer Case-Control Consortium (PanC4). Ann. Oncol. *23,* 2964-2970.

Duke, R.C., and Cohen, J.J. (1986). IL-2 addiction: withdrawal of growth factor activates a suicide program in dependent T cells. Lymphokine Res. *5,* 289-299.

Ehrhardt, C., Wolff, T., Pleschka, S., Planz, O., Beermann, W., Bode, J.G., Schmolke, M., and Ludwig, S. (2007). Influenza A virus NS1 protein activates the PI3K/Akt pathway to mediate antiapoptotic signaling responses. J. Virol. *81,* 3058-3067.

Eisfeld, A.J., Kawakami, E., Watanabe, T., Neumann, G., and Kawaoka, Y. (2011). RAB11A is essential for transport of the influenza virus genome to the plasma membrane. J. Virol. *85,* 6117-6126.

Elankumaran, S., Chavan, V., Qiao, D., Shobana, R., Moorkanat, G., Biswas, M., and Samal, S.K. (2010). Type I interferon-sensitive recombinant newcastle disease virus for oncolytic virotherapy. J. Virol. *84,* 3835-3844.

Elena, J.W., Steplowski, E., Yu, K., Hartge, P., Tobias, G.S., Brotzman, M.J., Chanock, S.J., Stolzenberg-Solomon, R.Z., Arslan, A.A., Bueno-de-Mesquita, H.B.*, et al.* (2013). Diabetes and risk of pancreatic cancer: a pooled analysis from the pancreatic cancer cohort consortium. Cancer Causes Control *24,* 13-25.

Elleman, C.J., and Barclay, W.S. (2004). The M1 matrix protein controls the filamentous phenotype of influenza A virus. Virology *321,* 144-153.

Enari, M., Sakahira, H., Yokoyama, H., Okawa, K., Iwamatsu, A., and Nagata, S. (1998). A caspase-activated DNase that degrades DNA during apoptosis, and its inhibitor ICAD. Nature *391,* 43-50.

Everitt, A.R., Clare, S., Pertel, T., John, S.P., Wash, R.S., Smith, S.E., Chin, C.R., Feeley, E.M., Sims, J.S., Adams, D.J.*, et al.* (2012). IFITM3 restricts the morbidity and mortality associated with influenza. Nature *484,* 519-523.

Falk, L.A., McNally, R., Perera, P., Kenny, J., and Vogel, S.N. (1995). LPS-inducible responses in severe combined immunodeficiency (SCID) mice. Innate Immun. *2 (4),* 273-280.

Farrell, P.J., Balkow, K., Hunt, T., Jackson, R.J., and Trachsel, H. (1977). Phosphorylation of initiation factor elF-2 and the control of reticulocyte protein synthesis. Cell *11,* 187-200.

Feldmann, G., Beaty, R., Hruban, R.H., and Maitra, A. (2007). Molecular genetics of pancreatic intraepithelial neoplasia. J. Hepatobiliary. Pancreat. Surg. *14,* 224-232.

Fesq, H., Bacher, M., Nain, M., and Gemsa, D. (1994). Programmed cell death (apoptosis) in human monocytes infected by influenza A virus. Immunobiology *190,* 175-182.

Filippi, C.M., and von Herrath, M.G. (2008). Viral trigger for type 1 diabetes: pros and cons. Diabetes *57,* 2863-2871.

Fitch, W.M., Bush, R.M., Bender, C.A., and Cox, N.J. (1997). Long term trends in the evolution of H(3) HA1 human influenza type A. Proc. Natl. Acad. Sci. U. S. A. *94,* 7712-7718.

Fodor, E., Devenish, L., Engelhardt, O.G., Palese, P., Brownlee, G.G., and Garcia-Sastre, A. (1999). Rescue of influenza A virus from recombinant DNA. J. Virol. *73,* 9679-9682.

Fodor, E., Pritlove, D.C., and Brownlee, G.G. (1994). The influenza virus panhandle is involved in the initiation of transcription. J. Virol. *68,* 4092-4096.

Fouchier, R.A., Munster, V., Wallensten, A., Bestebroer, T.M., Herfst, S., Smith, D., Rimmelzwaan, G.F., Olsen, B., and Osterhaus, A.D. (2005). Characterization of a novel influenza A virus hemagglutinin subtype (H16) obtained from black-headed gulls. J. Virol. *79,* 2814-2822.

Franko, J., Feng, W., Yip, L., Genovese, E., and Moser, A.J. (2010). Non-functional neuroendocrine carcinoma of the pancreas: incidence, tumor biology, and outcomes in 2,158 patients. J. Gastrointest. Surg. *14,* 541-548.

Freeman, A.I., Zakay-Rones, Z., Gomori, J.M., Linetsky, E., Rasooly, L., Greenbaum, E., Rozenman-Yair, S., Panet, A., Libson, E., Irving, C.S., Galun, E., and Siegal, T. (2006). Phase I/II trial of intravenous NDV-HUJ oncolytic virus in recurrent glioblastoma multiforme. Mol. Ther. *13,* 221-228.

Friedman, P.N., Chen, X., Bargonetti, J., and Prives, C. (1993). The p53 protein is an unusually shaped tetramer that binds directly to DNA. Proc. Natl. Acad. Sci. U. S. A. *90,* 3319-3323.

Fromont-Racine, M., Senger, B., Saveanu, C., and Fasiolo, F. (2003). Ribosome assembly in eukaryotes. Gene *313,* 17-42.

Fukuda, K., Abei, M., Ugai, H., Seo, E., Wakayama, M., Murata, T., Todoroki, T., Tanaka, N., Hamada, H., and Yokoyama, K.K. (2003). E1A, E1B double-restricted adenovirus for oncolytic gene therapy of gallbladder cancer. Cancer Res. *63,* 4434-4440.

Furihata, M., Kurabayashl, A., Matsumoto, M., Sonobe, H., Ohtsuki, Y., Terao, N., Kuwahara, M., and Shuin, T. (2002). Frequent phosphorylation at serine 392 in overexpressed p53 protein due to missense mutation in carcinoma of the urinary tract. J. Pathol. *197,* 82-88.

Furukawa, T., Duguid, W.P., Rosenberg, L., Viallet, J., Galloway, D.A., and Tsao, M.S. (1996). Long-term culture and immortalization of epithelial cells from normal adult human pancreatic ducts transfected by the E6E7 gene of human papilloma virus 16. Am. J. Pathol. *148,* 1763-1770.

Futatsumori-Sugai, M., and Tsumoto, K. (2010). Signal peptide design for improving recombinant protein secretion in the baculovirus expression vector system. Biochem. Biophys. Res. Commun. *391,* 931-935.

Gabel, F., Wang, D., Madern, D., Sadler, A., Dayie, K., Daryoush, M.Z., Schwahn, D., Zaccai, G., Lee, X., and Williams, B.R. (2006). Dynamic flexibility of double-stranded RNA activated PKR in solution. J. Mol. Biol. *359,* 610-623.

Gabriel, G., Herwig, A., and Klenk, H.D. (2008). Interaction of polymerase subunit PB2 and NP with importin alpha1 is a determinant of host range of influenza A virus. PLoS Pathog. *4,* e11.

Gabriel, G., Klingel, K., Otte, A., Thiele, S., Hudjetz, B., Arman-Kalcek, G., Sauter, M., Shmidt, T., Rother, F., Baumgarte, S.*, et al.* (2011). Differential use of importin-alpha isoforms governs cell tropism and host adaptation of influenza virus. Nat. Commun. *2,* 156.

Gack, M.U., Albrecht, R.A., Urano, T., Inn, K.S., Huang, I.C., Carnero, E., Farzan, M., Inoue, S., Jung, J.U., and Garcia-Sastre, A. (2009). Influenza A virus NS1 targets the ubiquitin ligase TRIM25 to evade recognition by the host viral RNA sensor RIG-I. Cell. Host Microbe *5,* 439-449.

Gack, M.U., Shin, Y.C., Joo, C.H., Urano, T., Liang, C., Sun, L., Takeuchi, O., Akira, S., Chen, Z., Inoue, S., and Jung, J.U. (2007). TRIM25 RING-finger E3 ubiquitin ligase is essential for RIG-I-mediated antiviral activity. Nature *446,* 916-920.

Galabru, J., and Hovanessian, A. (1987). Autophosphorylation of the protein kinase dependent on double-stranded RNA. J. Biol. Chem. *262,* 15538-15544.

Gale, M.,Jr, and Katze, M.G. (1998). Molecular mechanisms of interferon resistance mediated by viral-directed inhibition of PKR, the interferon-induced protein kinase. Pharmacol. Ther. *78,* 29-46.

Ganesh, S., Gonzalez-Edick, M., Gibbons, D., Van Roey, M., and Jooss, K. (2008). Intratumoral coadministration of hyaluronidase enzyme and oncolytic adenoviruses enhances virus potency in metastatic tumor models. Clin. Cancer Res. *14,* 3933-3941.

Gao, S., von der Malsburg, A., Dick, A., Faelber, K., Schroder, G.F., Haller, O., Kochs, G., and Daumke, O. (2011). Structure of myxovirus resistance protein a reveals intra- and intermolecular domain interactions required for the antiviral function. Immunity *35,* 514-525.

Gao, Y., Zhang, Y., Shinya, K., Deng, G., Jiang, Y., Li, Z., Guan, Y., Tian, G., Li, Y., Shi, J.*, et al.* (2009). Identification of amino acids in HA and PB2 critical for the transmission of H5N1 avian influenza viruses in a mammalian host. PLoS Pathog. *5,* e1000709.

Garber, K. (2006). China approves world's first oncolytic virus therapy for cancer treatment. J. Natl. Cancer Inst. *98,* 298-300.

Garcia, M., Crawford, J.M., Latimer, J.W., Rivera-Cruz, E., and Perdue, M.L. (1996). Heterogeneity in the haemagglutinin gene and emergence of the highly pathogenic phenotype among recent H5N2 avian influenza viruses from Mexico. J. Gen. Virol. *77 (Pt 7),* 1493-1504.

Garcia, M.A., Gil, J., Ventoso, I., Guerra, S., Domingo, E., Rivas, C., and Esteban, M. (2006). Impact of protein kinase PKR in cell biology: from antiviral to antiproliferative action. Microbiol. Mol. Biol. Rev. *70,* 1032-1060.

Garten, R.J., Davis, C.T., Russell, C.A., Shu, B., Lindstrom, S., Balish, A., Sessions, W.M., Xu, X., Skepner, E., Deyde, V.*, et al.* (2009). Antigenic and genetic characteristics of swine-origin 2009 A(H1N1) influenza viruses circulating in humans. Science *325,* 197-201.

Gatherer, D. (2010). Tempo and mode in the molecular evolution of influenza C. PLoS Curr. *2,* RRN1199.

Gaur, P., Ranjan, P., Sharma, S., Patel, J.R., Bowzard, J.B., Rahman, S.K., Kumari, R., Gangappa, S., Katz, J.M., Cox, N.J.*, et al.* (2012). Influenza A virus neuraminidase protein enhances cell survival through interaction with carcinoembryonic antigen-related cell adhesion molecule 6 (CEACAM6) protein. J. Biol. Chem. *287,* 15109-15117.

Geiss, G.K., Salvatore, M., Tumpey, T.M., Carter, V.S., Wang, X., Basler, C.F., Taubenberger, J.K., Bumgarner, R.E., Palese, P., Katze, M.G., and Garcia-Sastre, A. (2002). Cellular transcriptional profiling in influenza A virus-infected lung epithelial cells: the role of the nonstructural NS1 protein in the evasion of the host innate defense and its potential contribution to pandemic influenza. Proc. Natl. Acad. Sci. U. S. A. *99,* 10736-10741.

Genkinger, J.M., Spiegelman, D., Anderson, K.E., Bergkvist, L., Bernstein, L., van den Brandt, P.A., English, D.R., Freudenheim, J.L., Fuchs, C.S., Giles, G.G.*, et al.* (2009). Alcohol intake and pancreatic cancer risk: a pooled analysis of fourteen cohort studies. Cancer Epidemiol. Biomarkers Prev. *18,* 765-776.

Gerber, M., Isel, C., Moules, V., and Marquet, R. (2014). Selective packaging of the influenza A genome and consequences for genetic reassortment. Trends Microbiol. *22,* 446-455.

Ghadimi, B.M., Schrock, E., Walker, R.L., Wangsa, D., Jauho, A., Meltzer, P.S., and Ried, T. (1999). Specific chromosomal aberrations and amplification of the AIB1 nuclear receptor coactivator gene in pancreatic carcinomas. Am. J. Pathol. *154,* 525-536.

Ghosh, A., Sarkar, S.N., Rowe, T.M., and Sen, G.C. (2001). A specific isozyme of 2'-5' oligoadenylate synthetase is a dual function proapoptotic protein of the Bcl-2 family. J. Biol. Chem. *276,* 25447-25455.

Giannecchini, S., Campitelli, L., Calzoletti, L., De Marco, M.A., Azzi, A., and Donatelli, I. (2006). Comparison of in vitro replication features of H7N3 influenza viruses from wild ducks and turkeys: potential implications for interspecies transmission. J. Gen. Virol. *87,* 171-175.

Giardiello, F.M., Brensinger, J.D., Tersmette, A.C., Goodman, S.N., Petersen, G.M., Booker, S.V., Cruz-Correa, M., and Offerhaus, J.A. (2000). Very high risk of cancer in familial Peutz-Jeghers syndrome. Gastroenterology *119,* 1447-1453.

Gibbs, J.S., Malide, D., Hornung, F., Bennink, J.R., and Yewdell, J.W. (2003). The influenza A virus PB1-F2 protein targets the inner mitochondrial membrane via a predicted basic amphipathic helix that disrupts mitochondrial function. J. Virol. *77,* 7214-7224.

Githens, S. (1988). The pancreatic duct cell: proliferative capabilities, specific characteristics, metaplasia, isolation, and culture. J. Pediatr. Gastroenterol. Nutr. *7,* 486-506.

Goins, W.F., Huang, S., Cohen, J.B., and Glorioso, J.C. (2014). Engineering HSV-1 Vectors for Gene Therapy. Methods Mol. Biol. *1144,* 63-79.

Gorbalenya, A.E., Koonin, E.V., Donchenko, A.P., and Blinov, V.M. (1988). A novel superfamily of nucleoside triphosphate-binding motif containing proteins which are probably involved in duplex unwinding in DNA and RNA replication and recombination. FEBS Lett. *235,* 16-24.

Goto, H., Muramoto, Y., Noda, T., and Kawaoka, Y. (2013). The genome-packaging signal of the influenza A virus genome comprises a genome incorporation signal and a genome-bundling signal. J. Virol. *87,* 11316-11322.

Gottesman, M.M. (2002). Mechanisms of cancer drug resistance. Annu. Rev. Med. *53,* 615-627.

Grandi, P., Fernandez, J., Szentirmai, O., Carter, R., Gianni, D., Sena-Esteves, M., and Breakefield, X.O. (2010). Targeting HSV-1 virions for specific binding to epidermal growth factor receptor-vIII-bearing tumor cells. Cancer Gene Ther. *17,* 655-663.

Griffin, C.A., Hruban, R.H., Morsberger, L.A., Ellingham, T., Long, P.P., Jaffee, E.M., Hauda, K.M., Bohlander, S.K., and Yeo, C.J. (1995). Consistent chromosome abnormalities in adenocarcinoma of the pancreas. Cancer Res. *55,* 2394-2399.

Gros, A., Martinez-Quintanilla, J., Puig, C., Guedan, S., Mollevi, D.G., Alemany, R., and Cascallo, M. (2008). Bioselection of a gain of function mutation that enhances adenovirus 5 release and improves its antitumoral potency. Cancer Res. *68,* 8928-8937.

Grunewald, K., Lyons, J., Frohlich, A., Feichtinger, H., Weger, R.A., Schwab, G., Janssen, J.W., and Bartram, C.R. (1989). High frequency of Ki-ras codon 12 mutations in pancreatic adenocarcinomas. Int. J. Cancer *43,* 1037-1041.

Guedan, S., Rojas, J.J., Gros, A., Mercade, E., Cascallo, M., and Alemany, R. (2010). Hyaluronidase expression by an oncolytic adenovirus enhances its intratumoral spread and suppresses tumor growth. Mol. Ther. *18,* 1275-1283.

Guerrero, S., Casanova, I., Farre, L., Mazo, A., Capella, G., and Mangues, R. (2000). K-ras codon 12 mutation induces higher level of resistance to apoptosis and predisposition to anchorage-independent growth than codon 13 mutation or proto-oncogene overexpression. Cancer Res. *60,* 6750-6756.

Guilligay, D., Tarendeau, F., Resa-Infante, P., Coloma, R., Crepin, T., Sehr, P., Lewis, J., Ruigrok, R.W., Ortin, J., Hart, D.J., and Cusack, S. (2008). The structural basis for cap binding by influenza virus polymerase subunit PB2. Nat. Struct. Mol. Biol. *15,* 500-506.

Guo, Z.S., Thorne, S.H., and Bartlett, D.L. (2008). Oncolytic virotherapy: molecular targets in tumor-selective replication and carrier cell-mediated delivery of oncolytic viruses. Biochim. Biophys. Acta *1785,* 217-231.

Hagen, M., Chung, T.D., Butcher, J.A., and Krystal, M. (1994). Recombinant influenza virus polymerase: requirement of both 5' and 3' viral ends for endonuclease activity. J. Virol. *68,* 1509-1515.

Hahn, S.A., Greenhalf, B., Ellis, I., Sina-Frey, M., Rieder, H., Korte, B., Gerdes, B., Kress, R., Ziegler, A., Raeburn, J.A.*, et al.* (2003). BRCA2 germline mutations in familial pancreatic carcinoma. J. Natl. Cancer Inst. *95,* 214-221.

Halder, U.C., Bagchi, P., Chattopadhyay, S., Dutta, D., and Chawla-Sarkar, M. (2011). Cell death regulation during influenza A virus infection by matrix (M1) protein: a model of viral control over the cellular survival pathway. Cell. Death Dis. *2,* e197.

Hale, B.G. (2014). Conformational plasticity of the influenza A virus NS1 protein. J. Gen. Virol. *95,* 2099-2105.

Hale, B.G., Randall, R.E., Ortin, J., and Jackson, D. (2008). The multifunctional NS1 protein of influenza A viruses. J. Gen. Virol. *89,* 2359-2376.

Halfdanarson, T.R., Rabe, K.G., Rubin, J., and Petersen, G.M. (2008). Pancreatic neuroendocrine tumors (PNETs): incidence, prognosis and recent trend toward improved survival. Ann. Oncol. *19,* 1727-1733.

Haller, O., Acklin, M., and Staeheli, P. (1987). Influenza virus resistance of wild mice: wild-type and mutant Mx alleles occur at comparable frequencies. J. Interferon Res. *7,* 647-656.

Haller, O., Arnheiter, H., Lindenmann, J., and Gresser, I. (1980). Host gene influences sensitivity to interferon action selectively for influenza virus. Nature *283,* 660-662.

Haller, O., Gao, S., von der Malsburg, A., Daumke, O., and Kochs, G. (2010). Dynamin-like MxA GTPase: structural insights into oligomerization and implications for antiviral activity. J. Biol. Chem. *285,* 28419-28424.

Haller, O., and Kochs, G. (2011). Human MxA protein: an interferon-induced dynamin-like GTPase with broad antiviral activity. J. Interferon Cytokine Res. *31,* 79-87.

Haller, O., and Kochs, G. (2002). Interferon-induced mx proteins: dynamin-like GTPases with antiviral activity. Traffic *3,* 710-717.

Hamilton, J.A., and Anderson, G.P. (2004). GM-CSF Biology. Growth Factors *22,* 225-231.

Hansen, G., Hercus, T.R., McClure, B.J., Stomski, F.C., Dottore, M., Powell, J., Ramshaw, H., Woodcock, J.M., Xu, Y., Guthridge, M.*, et al.* (2008). The structure of the GM-CSF receptor complex reveals a distinct mode of cytokine receptor activation. Cell *134,* 496-507.

Hardcastle, J., Kurozumi, K., Chiocca, E.A., and Kaur, B. (2007). Oncolytic viruses driven by tumor-specific promoters. Curr. Cancer. Drug Targets *7,* 181-189.

Harris, P. (August 2006). Avian Influenza: An Animal Health Issue. Retrieved from the Food and Agriculture Organization (FAO), Agriculture Department Animal Production and Health Division

Hasegawa, K., Nakamura, T., Harvey, M., Ikeda, Y., Oberg, A., Figini, M., Canevari, S., Hartmann, L.C., and Peng, K.W. (2006). The use of a tropism-modified measles virus in folate receptor-targeted virotherapy of ovarian cancer. Clin. Cancer Res. *12,* 6170-6178.

Hay, A.J., Gregory, V., Douglas, A.R., and Lin, Y.P. (2001). The evolution of human influenza viruses. Philos. Trans. R. Soc. Lond. B. Biol. Sci. *356,* 1861-1870.

Hay, A.J., and Skehel, J.J. (1979). Characterization of influenza virus RNA transcripts synthesized in vitro. J. Gen. Virol. *44,* 599-608.

Hayman, A., Comely, S., Lackenby, A., Murphy, S., McCauley, J., Goodbourn, S., and Barclay, W. (2006). Variation in the ability of human influenza A viruses to induce and inhibit the IFN-beta pathway. Virology *347,* 52-64.

Heinemann, V., Quietzsch, D., Gieseler, F., Gonnermann, M., Schonekas, H., Rost, A., Neuhaus, H., Haag, C., Clemens, M., Heinrich, B.*, et al.* (2006). Randomized phase III trial of gemcitabine plus cisplatin compared with gemcitabine alone in advanced pancreatic cancer. J. Clin. Oncol. *24,* 3946-3952.

Helenius, A. (1992). Unpacking the incoming influenza virus. Cell *69,* 577-578.

Hellebrand, E., Mautner, J., Reisbach, G., Nimmerjahn, F., Hallek, M., Mocikat, R., and Hammerschmidt, W. (2006). Epstein-Barr virus vector-mediated gene transfer into human B cells: potential for antitumor vaccination. Gene Ther. *13,* 150-162.

Henkel, M., Mitzner, D., Henklein, P., Meyer-Almes, F.J., Moroni, A., Difrancesco, M.L., Henkes, L.M., Kreim, M., Kast, S.M., Schubert, U., and Thiel, G. (2010). The proapoptotic influenza A virus protein PB1-F2 forms a nonselective ion channel. PLoS One *5,* e11112.

Heo, J., Reid, T., Ruo, L., Breitbach, C.J., Rose, S., Bloomston, M., Cho, M., Lim, H.Y., Chung, H.C., Kim, C.W.*, et al.* (2013). Randomized dose-finding clinical trial of oncolytic immunotherapeutic vaccinia JX-594 in liver cancer. Nat. Med. *19,* 329-336.

Herceg, Z., and Wang, Z.Q. (1999). Failure of poly(ADP-ribose) polymerase cleavage by caspases leads to induction of necrosis and enhanced apoptosis. Mol. Cell. Biol. *19,* 5124-5133.

Herfst, S., Schrauwen, E.J., Linster, M., Chutinimitkul, S., de Wit, E., Munster, V.J., Sorrell, E.M., Bestebroer, T.M., Burke, D.F., Smith, D.J.*, et al.* (2012). Airborne transmission of influenza A/H5N1 virus between ferrets. Science *336,* 1534-1541.

Herskowitz, I. (1987). Functional inactivation of genes by dominant negative mutations. Nature *329,* 219-222.

Herz, C., Stavnezer, E., Krug, R., and Gurney, T.,Jr. (1981). Influenza virus, an RNA virus, synthesizes its messenger RNA in the nucleus of infected cells. Cell *26,* 391-400.

Hewison, M. (2011). Vitamin D and innate and adaptive immunity. Vitam. Horm. *86,* 23-62.

Higgins, C.F. (1994). Flip-flop: the transmembrane translocation of lipids. Cell *79,* 393-395.

Hikichi, M., Kidokoro, M., Haraguchi, T., Iba, H., Shida, H., Tahara, H., and Nakamura, T. (2011). MicroRNA regulation of glycoprotein B5R in oncolytic vaccinia virus reduces viral pathogenicity without impairing its antitumor efficacy. Mol. Ther. *19,* 1107-1115.

Hingorani, S.R., Wang, L., Multani, A.S., Combs, C., Deramaudt, T.B., Hruban, R.H., Rustgi, A.K., Chang, S., and Tuveson, D.A. (2005). Trp53R172H and KrasG12D cooperate to promote chromosomal instability and widely metastatic pancreatic ductal adenocarcinoma in mice. Cancer. Cell. *7,* 469-483.

Hinshaw, V.S., Olsen, C.W., Dybdahl-Sissoko, N., and Evans, D. (1994). Apoptosis: a mechanism of cell killing by influenza A and B viruses. J. Virol. *68,* 3667-3673.

Hoffmann, E., Neumann, G., Kawaoka, Y., Hobom, G., and Webster, R.G. (2000). A DNA transfection system for generation of influenza A virus from eight plasmids. Proc. Natl. Acad. Sci. U. S. A. *97,* 6108-6113.

Holmes, E.C., Ghedin, E., Miller, N., Taylor, J., Bao, Y., St George, K., Grenfell, B.T., Salzberg, S.L., Fraser, C.M., Lipman, D.J., and Taubenberger, J.K. (2005). Whole-genome analysis of human influenza A virus reveals multiple persistent lineages and reassortment among recent H3N2 viruses. PLoS Biol. *3,* e300.

Honeyman, M.C., Coulson, B.S., Stone, N.L., Gellert, S.A., Goldwater, P.N., Steele, C.E., Couper, J.J., Tait, B.D., Colman, P.G., and Harrison, L.C. (2000). Association between rotavirus infection and pancreatic islet autoimmunity in children at risk of developing type 1 diabetes. Diabetes *49,* 1319-1324.

Hopfner, K.P., and Michaelis, J. (2007). Mechanisms of nucleic acid translocases: lessons from structural biology and single-molecule biophysics. Curr. Opin. Struct. Biol. *17,* 87-95.

Hornung, V., Ellegast, J., Kim, S., Brzozka, K., Jung, A., Kato, H., Poeck, H., Akira, S., Conzelmann, K.K., Schlee, M., Endres, S., and Hartmann, G. (2006). 5'-Triphosphate RNA is the ligand for RIG-I. Science *314,* 994-997.

Hotte, S.J., Lorence, R.M., Hirte, H.W., Polawski, S.R., Bamat, M.K., O'Neil, J.D., Roberts, M.S., Groene, W.S., and Major, P.P. (2007). An optimized clinical regimen for the oncolytic virus PV701. Clin. Cancer Res. *13,* 977-985.

Hou, F., Sun, L., Zheng, H., Skaug, B., Jiang, Q.X., and Chen, Z.J. (2011). MAVS forms functional prion-like aggregates to activate and propagate antiviral innate immune response. Cell *146,* 448-461.

Hruban, R.H., Adsay, N.V., Albores-Saavedra, J., Compton, C., Garrett, E.S., Goodman, S.N., Kern, S.E., Klimstra, D.S., Kloppel, G., Longnecker, D.S., Luttges, J., and Offerhaus, G.J. (2001). Pancreatic intraepithelial neoplasia: a new nomenclature and classification system for pancreatic duct lesions. Am. J. Surg. Pathol. *25,* 579-586.

Hruban, R.H., Goggins, M., Parsons, J., and Kern, S.E. (2000a). Progression model for pancreatic cancer. Clin. Cancer Res. *6,* 2969-2972.

Hruban, R.H., Wilentz, R.E., and Kern, S.E. (2000b). Genetic progression in the pancreatic ducts. Am. J. Pathol. *156,* 1821-1825.

Hsiang, T.Y., Zhou, L., and Krug, R.M. (2012). Roles of the phosphorylation of specific serines and threonines in the NS1 protein of human influenza A viruses. J. Virol. *86,* 10370-10376.

Hsu, M.T., Parvin, J.D., Gupta, S., Krystal, M., and Palese, P. (1987). Genomic RNAs of influenza viruses are held in a circular conformation in virions and in infected cells by a terminal panhandle. Proc. Natl. Acad. Sci. U. S. A. *84,* 8140-8144.

Huang, A.Y., Golumbek, P., Ahmadzadeh, M., Jaffee, E., Pardoll, D., and Levitsky, H. (1994). Role of bone marrow-derived cells in presenting MHC class I-restricted tumor antigens. Science *264,* 961-965.

Huang, P., Chubb, S., Hertel, L.W., Grindey, G.B., and Plunkett, W. (1991). Action of 2',2'-difluorodeoxycytidine on DNA synthesis. Cancer Res. *51,* 6110-6117.

Huang, T.S., Palese, P., and Krystal, M. (1990). Determination of influenza virus proteins required for genome replication. J. Virol. *64,* 5669-5673.

Hutchinson, E.C., Charles, P.D., Hester, S.S., Thomas, B., Trudgian, D., Martinez-Alonso, M., and Fodor, E. (2014). Conserved and host-specific features of influenza virion architecture. Nat. Commun. *5,* 4816.

Hutchinson, E.C., and Fodor, E. (2013). Transport of the influenza virus genome from nucleus to nucleus. Viruses *5,* 2424-2446.

Hutchinson, E.C., von Kirchbach, J.C., Gog, J.R., and Digard, P. (2010). Genome packaging in influenza A virus. J. Gen. Virol. *91,* 313-328.

Hyoty, H., Hiltunen, M., Reunanen, A., Leinikki, P., Vesikari, T., Lounamaa, R., Tuomilehto, J., and Akerblom, H.K. (1993). Decline of mumps antibodies in type 1 (insulin-dependent) diabetic children and a plateau in the rising incidence of type

1 diabetes after introduction of the mumps-measles-rubella vaccine in Finland. Childhood Diabetes in Finland Study Group. Diabetologia *36,* 1303-1308.

Hyoty, H., and Taylor, K.W. (2002). The role of viruses in human diabetes. Diabetologia *45,* 1353-1361.

Iannolo, G., Conticello, C., Memeo, L., and De Maria, R. (2008). Apoptosis in normal and cancer stem cells. Crit. Rev. Oncol. Hematol. *66,* 42-51.

Ilett, E.J., Prestwich, R.J., Kottke, T., Errington, F., Thompson, J.M., Harrington, K.J., Pandha, H.S., Coffey, M., Selby, P.J., Vile, R.G., and Melcher, A.A. (2009). Dendritic cells and T cells deliver oncolytic reovirus for tumour killing despite pre-existing anti-viral immunity. Gene Ther. *16,* 689-699.

Imai, M., Watanabe, T., Hatta, M., Das, S.C., Ozawa, M., Shinya, K., Zhong, G., Hanson, A., Katsura, H., Watanabe, S.*, et al.* (2012). Experimental adaptation of an influenza H5 HA confers respiratory droplet transmission to a reassortant H5 HA/H1N1 virus in ferrets. Nature *486,* 420-428.

Indraccolo, S. (2010). Interferon-alpha as angiogenesis inhibitor: learning from tumor models. Autoimmunity *43,* 244-247.

Institute of Medicine (US) Forum on Microbial Threats. (2005).

International Committee on Taxonomy of Viruses (ICTV) EC 46, Montreal, Canada, July 2014.

Iodice, S., Gandini, S., Maisonneuve, P., and Lowenfels, A.B. (2008). Tobacco and the risk of pancreatic cancer: a review and meta-analysis. Langenbecks Arch. Surg. *393,* 535-545.

Isaacs, A., and Baron, S. (1960). Antiviral action of interferon in embryonic cells. Lancet *2,* 946-947.

Ito, T., Kobayashi, Y., Morita, T., Horimoto, T., and Kawaoka, Y. (2002). Virulent influenza A viruses induce apoptosis in chickens. Virus Res. *84,* 27-35.

Jacobs, J.L., and Coyne, C.B. (2013). Mechanisms of MAVS regulation at the mitochondrial membrane. J. Mol. Biol. *425,* 5009-5019.

Jagger, B.W., Wise, H.M., Kash, J.C., Walters, K.A., Wills, N.M., Xiao, Y.L., Dunfee, R.L., Schwartzman, L.M., Ozinsky, A., Bell, G.L.*, et al.* (2012). An overlapping protein-coding region in influenza A virus segment 3 modulates the host response. Science *337,* 199-204.

Jaidane, H., and Hober, D. (2008). Role of coxsackievirus B4 in the pathogenesis of type 1 diabetes. Diabetes Metab. *34,* 537-548.

Jaidane, H., Sane, F., Gharbi, J., Aouni, M., Romond, M.B., and Hober, D. (2009). Coxsackievirus B4 and type 1 diabetes pathogenesis: contribution of animal models. Diabetes Metab. Res. Rev. *25,* 591-603.

Jenne, D.E., Reimann, H., Nezu, J., Friedel, W., Loff, S., Jeschke, R., Muller, O., Back, W., and Zimmer, M. (1998). Peutz-Jeghers syndrome is caused by mutations in a novel serine threonine kinase. Nat. Genet. *18,* 38-43.

Jin, H., Leser, G.P., Zhang, J., and Lamb, R.A. (1997). Influenza virus hemagglutinin and neuraminidase cytoplasmic tails control particle shape. EMBO J. *16,* 1236-1247.

Jing, Y., Tong, C., Zhang, J., Nakamura, T., Iankov, I., Russell, S.J., and Merchan, J.R. (2009). Tumor and vascular targeting of a novel oncolytic measles virus retargeted against the urokinase receptor. Cancer Res. *69,* 1459-1468.

Johns, T.G., Mackay, I.R., Callister, K.A., Hertzog, P.J., Devenish, R.J., and Linnane, A.W. (1992). Antiproliferative potencies of interferons on melanoma cell lines and xenografts: higher efficacy of interferon beta. J. Natl. Cancer Inst. *84,* 1185-1190.

Johnson, G.R., Gonda, T.J., Metcalf, D., Hariharan, I.K., and Cory, S. (1989). A lethal myeloproliferative syndrome in mice transplanted with bone marrow cells infected with a retrovirus expressing granulocyte-macrophage colony stimulating factor. EMBO J. *8,* 441-448.

Jorba, N., Coloma, R., and Ortin, J. (2009). Genetic trans-complementation establishes a new model for influenza virus RNA transcription and replication. PLoS Pathog. *5,* e1000462.

K.G. Nicholson, R.G. Webster & A.J. Hay. (1998). Textbook of Influenza (Oxford, United Kingdom.: Blackwell Science Ltd).

Kambara, H., Okano, H., Chiocca, E.A., and Saeki, Y. (2005). An oncolytic HSV-1 mutant expressing ICP34.5 under control of a nestin promoter increases survival of animals even when symptomatic from a brain tumor. Cancer Res. *65,* 2832-2839.

Kantoff, P.W., Higano, C.S., Shore, N.D., Berger, E.R., Small, E.J., Penson, D.F., Redfern, C.H., Ferrari, A.C., Dreicer, R., Sims, R.B.*, et al.* (2010). Sipuleucel-T immunotherapy for castration-resistant prostate cancer. N. Engl. J. Med. *363,* 411-422.

Karlsson Hedestam, G.B., Fouchier, R.A., Phogat, S., Burton, D.R., Sodroski, J., and Wyatt, R.T. (2008). The challenges of eliciting neutralizing antibodies to HIV-1 and to influenza virus. Nat. Rev. Microbiol. *6,* 143-155.

Kasloff, S.B., Pizzuto, M.S., Silic-Benussi, M., Pavone, S., Ciminale, V., and Capua, I. (2014). Oncolytic activity of avian influenza virus in human pancreatic ductal adenocarcinoma cell lines. J. Virol. *88,* 9321-9334.

Kato, H., Takeuchi, O., Mikamo-Satoh, E., Hirai, R., Kawai, T., Matsushita, K., Hiiragi, A., Dermody, T.S., Fujita, T., and Akira, S. (2008). Length-dependent recognition of double-stranded ribonucleic acids by retinoic acid-inducible gene-I and melanoma differentiation-associated gene 5. J. Exp. Med. *205,* 1601-1610.

Kato, H., Takeuchi, O., Sato, S., Yoneyama, M., Yamamoto, M., Matsui, K., Uematsu, S., Jung, A., Kawai, T., Ishii, K.J.*, et al.* (2006). Differential roles of MDA5 and RIG-I helicases in the recognition of RNA viruses. Nature *441,* 101-105.

Katze, M.G., DeCorato, D., Safer, B., Galabru, J., and Hovanessian, A.G. (1987). Adenovirus VAI RNA complexes with the 68 000 Mr protein kinase to regulate its autophosphorylation and activity. EMBO J. *6,* 689-697.

Kaufmann, J.K., and Nettelbeck, D.M. (2012). Virus chimeras for gene therapy, vaccination, and oncolysis: adenoviruses and beyond. Trends Mol. Med. *18,* 365-376.

Kaur, B., Cripe, T.P., and Chiocca, E.A. (2009). "Buy one get one free": armed viruses for the treatment of cancer cells and their microenvironment. Curr. Gene Ther. *9,* 341-355.

Kaushansky, K., O'Hara, P.J., Hart, C.E., Forstrom, J.W., and Hagen, F.S. (1987). Role of carbohydrate in the function of human granulocyte-macrophage colony-stimulating factor. Biochemistry *26,* 4861-4867.

Kawai, T., and Akira, S. (2006). Innate immune recognition of viral infection. Nat. Immunol. *7,* 131-137.

Kawaoka, Y., Krauss, S., and Webster, R.G. (1989). Avian-to-human transmission of the PB1 gene of influenza A viruses in the 1957 and 1968 pandemics. J. Virol. *63,* 4603-4608.

Kearse, M., Moir, R., Wilson, A., Stones-Havas, S., Cheung, M., Sturrock, S., Buxton, S., Cooper, A., Markowitz, S., Duran, C.*, et al.* (2012). Geneious Basic: an integrated and extendable desktop software platform for the organization and analysis of sequence data. Bioinformatics *28,* 1647-1649.

Kelly, K., Nawrocki, S., Mita, A., Coffey, M., Giles, F.J., and Mita, M. (2009). Reovirus-based therapy for cancer. Expert Opin. Biol. Ther. *9,* 817-830.

Kerry, P.S., Ayllon, J., Taylor, M.A., Hass, C., Lewis, A., Garcia-Sastre, A., Randall, R.E., Hale, B.G., and Russell, R.J. (2011). A transient homotypic interaction model for the influenza A virus NS1 protein effector domain. PLoS One *6,* e17946.

KILBOURNE, E.D., and MURPHY, J.S. (1960). Genetic studies of influenza viruses. I. Viral morphology and growth capacity as exchangeable genetic traits. Rapid in ovo adaptation of early passage Asian strain isolates by combination with PR8. J. Exp. Med. *111,* 387-406.

Kim, J.H., Lee, S.R., Li, L.H., Park, H.J., Park, J.H., Lee, K.Y., Kim, M.K., Shin, B.A., and Choi, S.Y. (2011). High cleavage efficiency of a 2A peptide derived from porcine teschovirus-1 in human cell lines, zebrafish and mice. PLoS One *6,* e18556.

Kim, Y.S., Itzkowitz, S.H., Yuan, M., Chung, Y., Satake, K., Umeyama, K., and Hakomori, S. (1988). Lex and Ley antigen expression in human pancreatic cancer. Cancer Res. *48,* 475-482.

Kinoh, H., Inoue, M., Washizawa, K., Yamamoto, T., Fujikawa, S., Tokusumi, Y., Iida, A., Nagai, Y., and Hasegawa, M. (2004). Generation of a recombinant Sendai virus that is selectively activated and lyses human tumor cells expressing matrix metalloproteinases. Gene Ther. *11,* 1137-1145.

Kirn, D.H., Wang, Y., Le Boeuf, F., Bell, J., and Thorne, S.H. (2007). Targeting of interferon-beta to produce a specific, multi-mechanistic oncolytic vaccinia virus. PLoS Med. *4,* e353.

Kirn, D.H., Wang, Y., Liang, W., Contag, C.H., and Thorne, S.H. (2008). Enhancing poxvirus oncolytic effects through increased spread and immune evasion. Cancer Res. *68,* 2071-2075.

Kittel, C., Ferko, B., Kurz, M., Voglauer, R., Sereinig, S., Romanova, J., Stiegler, G., Katinger, H., and Egorov, A. (2005). Generation of an influenza A virus vector expressing biologically active human interleukin-2 from the NS gene segment. J. Virol. *79,* 10672-10677.

Klein, A.P., Brune, K.A., Petersen, G.M., Goggins, M., Tersmette, A.C., Offerhaus, G.J., Griffin, C., Cameron, J.L., Yeo, C.J., Kern, S., and Hruban, R.H. (2004). Prospective risk of pancreatic cancer in familial pancreatic cancer kindreds. Cancer Res. *64,* 2634-2638.

Klenk, H.D., and Garten, W. (1994). Host cell proteases controlling virus pathogenicity. Trends Microbiol. *2,* 39-43.

Klenk, H.D., Rott, R., Orlich, M., and Blodorn, J. (1975). Activation of influenza A viruses by trypsin treatment. Virology *68,* 426-439.

Kobayashi, K., and Hagiwara, K. (2013). Epidermal growth factor receptor (EGFR) mutation and personalized therapy in advanced nonsmall cell lung cancer (NSCLC). Target Oncol. *8,* 27-33.

Kochs, G., Garcia-Sastre, A., and Martinez-Sobrido, L. (2007). Multiple anti-interferon actions of the influenza A virus NS1 protein. J. Virol. *81,* 7011-7021.

Kolakofsky, D., Kowalinski, E., and Cusack, S. (2012). A structure-based model of RIG-I activation. RNA *18,* 2118-2127.

Koltai, T. (2014). Clusterin: a key player in cancer chemoresistance and its inhibition. Onco Targets Ther. *7,* 447-456.

Koshiba, T., Yasukawa, K., Yanagi, Y., and Kawabata, S. (2011). Mitochondrial membrane potential is required for MAVS-mediated antiviral signaling. Sci. Signal. *4,* ra7.

Krug, R.M., and Etkind, P.R. (1973). Cytoplasmic and nuclear virus-specific proteins in influenza virus-infected MDCK cells. Virology *56,* 334-348.

Kuhen, K.L., and Samuel, C.E. (1999). Mechanism of interferon action: functional characterization of positive and negative regulatory domains that modulate transcriptional activation of the human RNA-dependent protein kinase Pkr promoter. Virology *254,* 182-195.

Kundu, A., Avalos, R.T., Sanderson, C.M., and Nayak, D.P. (1996). Transmembrane domain of influenza virus neuraminidase, a type II protein, possesses an apical sorting signal in polarized MDCK cells. J. Virol. *70,* 6508-6515.

Kunitz, M. (1939). Formation of Trypsin from Crystalline Trypsinogen by Means of Enterokinase. J. Gen. Physiol. *22,* 429-446.

Kurokawa, M., Koyama, A.H., Yasuoka, S., and Adachi, A. (1999). Influenza virus overcomes apoptosis by rapid multiplication. Int. J. Mol. Med. *3,* 527-530.

Kwon, Y.K., Thomas, C., and Swayne, D.E. (2010). Variability in pathobiology of South Korean H5N1 high-pathogenicity avian influenza virus infection for 5 species of migratory waterfowl. Vet. Pathol. *47,* 495-506.

Laguesse, E. (1893). Sur la formation des ilots de Langerhans dans le panreas. . Comptes Rend SocBiol *5,* 819-820.

Lakdawala, S.S., Wu, Y., Wawrzusin, P., Kabat, J., Broadbent, A.J., Lamirande, E.W., Fodor, E., Altan-Bonnet, N., Shroff, H., and Subbarao, K. (2014). Influenza a virus assembly intermediates fuse in the cytoplasm. PLoS Pathog. *10,* e1003971.

Lam, W.Y., Tang, J.W., Yeung, A.C., Chiu, L.C., Sung, J.J., and Chan, P.K. (2008). Avian influenza virus A/HK/483/97(H5N1) NS1 protein induces apoptosis in human airway epithelial cells. J. Virol. *82,* 2741-2751.

Lamb, R.A., and Choppin, P.W. (1979). Segment 8 of the influenza virus genome is unique in coding for two polypeptides. Proc. Natl. Acad. Sci. U. S. A. *76,* 4908-4912.

Lamb, R.A., Choppin, P.W., Chanock, R.M., and Lai, C.J. (1980). Mapping of the two overlapping genes for polypeptides NS1 and NS2 on RNA segment 8 of influenza virus genome. Proc. Natl. Acad. Sci. U. S. A. *77,* 1857-1861.

Lamb, R.A., and Lai, C.J. (1980). Sequence of interrupted and uninterrupted mRNAs and cloned DNA coding for the two overlapping nonstructural proteins of influenza virus. Cell *21,* 475-485.

Lazarowitz, S.G., and Choppin, P.W. (1975). Enhancement of the infectivity of influenza A and B viruses by proteolytic cleavage of the hemagglutinin polypeptide. Virology *68,* 440-454.

Lazebnik, Y.A., Kaufmann, S.H., Desnoyers, S., Poirier, G.G., and Earnshaw, W.C. (1994). Cleavage of poly(ADP-ribose) polymerase by a proteinase with properties like ICE. Nature *371,* 346-347.

Le, D.T., Pardoll, D.M., and Jaffee, E.M. (2010). Cellular vaccine approaches. Cancer J. *16,* 304-310.

Lee, P., Strong, J., and Coffey, M. (Dec. 6, 2011). Reovirus for the treatment of cellular proliferative disorders. United States Patent No. US008071087B2.

Lee, C.Y., Bu, L.X., DeBenedetti, A., Williams, B.J., Rennie, P.S., and Jia, W.W. (2010). Transcriptional and translational dual-regulated oncolytic herpes simplex virus type 1 for targeting prostate tumors. Mol. Ther. *18,* 929-935.

Lee, M.T., Bishop, K., Medcalf, L., Elton, D., Digard, P., and Tiley, L. (2002). Definition of the minimal viral components required for the initiation of unprimed RNA synthesis by influenza virus RNA polymerase. Nucleic Acids Res. *30,* 429-438.

Lemaitre, M., and Carrat, F. (2010). Comparative age distribution of influenza morbidity and mortality during seasonal influenza epidemics and the 2009 H1N1 pandemic. BMC Infect. Dis. *10,* 162.

Li, B., Simmons, A., Du, T., Lin, C., Moskalenko, M., Gonzalez-Edick, M., VanRoey, M., and Jooss, K. (2009). Allogeneic GM-CSF-secreting tumor cell immunotherapies generate potent anti-tumor responses comparable to autologous tumor cell immunotherapies. Clin. Immunol. *133,* 184-197.

Li, D., Jiao, L., Li, Y., Doll, M.A., Hein, D.W., Bondy, M.L., Evans, D.B., Wolff, R.A., Lenzi, R., Pisters, P.W., Abbruzzese, J.L., and Hassan, M.M. (2006). Polymorphisms of cytochrome P4501A2 and N-acetyltransferase genes, smoking, and risk of pancreatic cancer. Carcinogenesis *27,* 103-111.

Li, D., Morris, J.S., Liu, J., Hassan, M.M., Day, R.S., Bondy, M.L., and Abbruzzese, J.L. (2009). Body mass index and risk, age of onset, and survival in patients with pancreatic cancer. JAMA *301,* 2553-2562.

Li, H., Peng, K.W., Dingli, D., Kratzke, R.A., and Russell, S.J. (2010). Oncolytic measles viruses encoding interferon beta and the thyroidal sodium iodide symporter gene for mesothelioma virotherapy. Cancer Gene Ther. *17,* 550-558.

Li, P., Nijhawan, D., Budihardjo, I., Srinivasula, S.M., Ahmad, M., Alnemri, E.S., and Wang, X. (1997). Cytochrome c and dATP-dependent formation of Apaf-1/caspase-9 complex initiates an apoptotic protease cascade. Cell *91,* 479-489.

Li, S., Min, J.Y., Krug, R.M., and Sen, G.C. (2006). Binding of the influenza A virus NS1 protein to PKR mediates the inhibition of its activation by either PACT or double-stranded RNA. Virology *349,* 13-21.

Li, S., Sieben, C., Ludwig, K., Hofer, C.T., Chiantia, S., Herrmann, A., Eghiaian, F., and Schaap, I.A. (2014). pH-Controlled two-step uncoating of influenza virus. Biophys. J. *106,* 1447-1456.

Li, X., and Palese, P. (1994). Characterization of the polyadenylation signal of influenza virus RNA. J. Virol. *68,* 1245-1249.

Lichty, B.D., Power, A.T., Stojdl, D.F., and Bell, J.C. (2004). Vesicular stomatitis virus: re-inventing the bullet. Trends Mol. Med. *10,* 210-216.

Lin, Y.P., Wharton, S.A., Martin, J., Skehel, J.J., Wiley, D.C., and Steinhauer, D.A. (1997). Adaptation of egg-grown and transfectant influenza viruses for growth in mammalian cells: selection of hemagglutinin mutants with elevated pH of membrane fusion. Virology *233,* 402-410.

Lindberg, B., Ahlfors, K., Carlsson, A., Ericsson, U.B., Landin-Olsson, M., Lernmark, A., Ludvigsson, J., Sundkvist, G., and Ivarsson, S.A. (1999). Previous exposure to measles, mumps, and rubella--but not vaccination during adolescence--correlates to the prevalence of pancreatic and thyroid autoantibodies. Pediatrics *104,* e12.

Lindner, D.J., Borden, E.C., and Kalvakolanu, D.V. (1997). Synergistic antitumor effects of a combination of interferons and retinoic acid on human tumor cells in vitro and in vivo. Clin. Cancer Res. *3,* 931-937.

Lipatov, A.S., Kwon, Y.K., Pantin-Jackwood, M.J., and Swayne, D.E. (2009). Pathogenesis of H5N1 influenza virus infections in mice and ferret models differs according to respiratory tract or digestive system exposure. J. Infect. Dis. *199,* 717-725.

Liu, C., Eichelberger, M.C., Compans, R.W., and Air, G.M. (1995). Influenza type A virus neuraminidase does not play a role in viral entry, replication, assembly, or budding. J. Virol. *69,* 1099-1106.

Liu, C., Hasegawa, K., Russell, S.J., Sadelain, M., and Peng, K.W. (2009). Prostate-specific membrane antigen retargeted measles virotherapy for the treatment of prostate cancer. Prostate *69,* 1128-1141.

Liu, H., Golebiewski, L., Dow, E.C., Krug, R.M., Javier, R.T., and Rice, A.P. (2010). The ESEV PDZ-binding motif of the avian influenza A virus NS1 protein protects infected cells from apoptosis by directly targeting Scribble. J. Virol. *84,* 11164-11174.

Lofgren, E., Fefferman, N.H., Naumov, Y.N., Gorski, J., and Naumova, E.N. (2007). Influenza seasonality: underlying causes and modeling theories. J. Virol. *81,* 5429-5436.

Logsdon, C.D., and Ji, B. (2013). The role of protein synthesis and digestive enzymes in acinar cell injury. Nat. Rev. Gastroenterol. Hepatol. *10,* 362-370.

Loison, F., Debure, L., Nizard, P., le Goff, P., Michel, D., and le Drean, Y. (2006). Up-regulation of the clusterin gene after proteotoxic stress: implication of HSF1-HSF2 heterocomplexes. Biochem. J. *395,* 223-231.

Lowen, A.C., and Steel, J. (2014). Roles of humidity and temperature in shaping influenza seasonality. J. Virol. *88,* 7692-7695.

Lowenfels, A.B., Maisonneuve, P., Cavallini, G., Ammann, R.W., Lankisch, P.G., Andersen, J.R., Dimagno, E.P., Andren-Sandberg, A., and Domellof, L. (1993). Pancreatitis and the risk of pancreatic cancer. International Pancreatitis Study Group. N. Engl. J. Med. *328,* 1433-1437.

Lowy, R.J. (2003). Influenza virus induction of apoptosis by intrinsic and extrinsic mechanisms. Int. Rev. Immunol. *22,* 425-449.

Luebeck, E.G. (2010). Cancer: Genomic evolution of metastasis. Nature *467,* 1053-1055.

Luft, R., Efendic, S., Hokfelt, T., Johansson, O., and Arimura, A. (1974). Immunohistochemical evidence for the localization of somatostatin--like immunoreactivity in a cell population of the pancreatic islets. Med. Biol. *52,* 428-430.

Luytjes, W., Krystal, M., Enami, M., Parvin, J.D., and Palese, P. (1989). Amplification, expression, and packaging of foreign gene by influenza virus. Cell *59,* 1107-1113.

Lynch, H.T., Fusaro, R.M., Lynch, J.F., and Brand, R. (2008). Pancreatic cancer and the FAMMM syndrome. Fam. Cancer. *7,* 103-112.

MacFarlane, M., and Williams, A.C. (2004). Apoptosis and disease: a life or death decision. EMBO Rep. *5,* 674-678.

Mackey, J.R., Mani, R.S., Selner, M., Mowles, D., Young, J.D., Belt, J.A., Crawford, C.R., and Cass, C.E. (1998). Functional nucleoside transporters are required for gemcitabine influx and manifestation of toxicity in cancer cell lines. Cancer Res. *58,* 4349-4357.

Maitra, A., Adsay, N.V., Argani, P., Iacobuzio-Donahue, C., De Marzo, A., Cameron, J.L., Yeo, C.J., and Hruban, R.H. (2003). Multicomponent analysis of the pancreatic adenocarcinoma progression model using a pancreatic intraepithelial neoplasia tissue microarray. Mod. Pathol. *16,* 902-912.

Maitra, A., Kern, S.E., and Hruban, R.H. (2006). Molecular pathogenesis of pancreatic cancer. Best Pract. Res. Clin. Gastroenterol. *20,* 211-226.

Malka, D., Hammel, P., Maire, F., Rufat, P., Madeira, I., Pessione, F., Levy, P., and Ruszniewski, P. (2002). Risk of pancreatic adenocarcinoma in chronic pancreatitis. Gut *51,* 849-852.

Manicassamy, B., Manicassamy, S., Belicha-Villanueva, A., Pisanelli, G., Pulendran, B., and Garcia-Sastre, A. (2010). Analysis of in vivo dynamics of influenza virus infection in mice using a GFP reporter virus. Proc. Natl. Acad. Sci. U. S. A. *107,* 11531-11536.

Manz, B., Brunotte, L., Reuther, P., and Schwemmle, M. (2012). Adaptive mutations in NEP compensate for defective H5N1 RNA replication in cultured human cells. Nat. Commun. *3,* 802.

Manz, B., Dornfeld, D., Gotz, V., Zell, R., Zimmermann, P., Haller, O., Kochs, G., and Schwemmle, M. (2013). Pandemic influenza A viruses escape from restriction by human MxA through adaptive mutations in the nucleoprotein. PLoS Pathog. *9,* e1003279.

Martin, K., and Helenius, A. (1991). Nuclear transport of influenza virus ribonucleoproteins: the viral matrix protein (M1) promotes export and inhibits import. Cell *67,* 117-130.

Mas, E., Pasqualini, E., Caillol, N., El Battari, A., Crotte, C., Lombardo, D., and Sadoulet, M.O. (1998). Fucosyltransferase activities in human pancreatic tissue: comparative study between cancer tissues and established tumoral cell lines. Glycobiology *8,* 605-613.

Massague, J., Blain, S.W., and Lo, R.S. (2000). TGFbeta signaling in growth control, cancer, and heritable disorders. Cell *103,* 295-309.

Matrosovich, M., Matrosovich, T., Garten, W., and Klenk, H.D. (2006). New low-viscosity overlay medium for viral plaque assays. Virol. J. *3,* 63.

Matrosovich, M., Stech, J., and Klenk, H.D. (2009). Influenza receptors, polymerase and host range. Rev. Sci. Tech. *28,* 203-217.

Matrosovich, M., Tuzikov, A., Bovin, N., Gambaryan, A., Klimov, A., Castrucci, M.R., Donatelli, I., and Kawaoka, Y. (2000). Early alterations of the receptor-binding properties of H1, H2, and H3 avian influenza virus hemagglutinins after their introduction into mammals. J. Virol. *74,* 8502-8512.

Matsumoto, M., Furihata, M., and Ohtsuki, Y. (2006). Posttranslational phosphorylation of mutant p53 protein in tumor development. Med. Mol. Morphol. *39,* 79-87.

Matzinger, S.R., Carroll, T.D., Dutra, J.C., Ma, Z.M., and Miller, C.J. (2013). Myxovirus resistance gene A (MxA) expression suppresses influenza A virus replication in alpha interferon-treated primate cells. J. Virol. *87,* 1150-1158.

Maurer-Stroh, S., Lee, R.T., Gunalan, V., and Eisenhaber, F. (2013). The highly pathogenic H7N3 avian influenza strain from July 2012 in Mexico acquired an extended cleavage site through recombination with host 28S rRNA. Virol. J. *10,* 139-422X-10-139.

Mazur, I., Anhlan, D., Mitzner, D., Wixler, L., Schubert, U., and Ludwig, S. (2008). The proapoptotic influenza A virus protein PB1-F2 regulates viral polymerase activity by interaction with the PB1 protein. Cell. Microbiol. *10,* 1140-1152.

McCart, J.A., Ward, J.M., Lee, J., Hu, Y., Alexander, H.R., Libutti, S.K., Moss, B., and Bartlett, D.L. (2001). Systemic cancer therapy with a tumor-selective vaccinia virus mutant lacking thymidine kinase and vaccinia growth factor genes. Cancer Res. *61,* 8751-8757.

McCarthy, D.M., Brat, D.J., Wilentz, R.E., Yeo, C.J., Cameron, J.L., Kern, S.E., and Hruban, R.H. (2001). Pancreatic intraepithelial neoplasia and infiltrating adenocarcinoma: analysis of progression and recurrence by DPC4 immunohistochemical labeling. Hum. Pathol. *32,* 638-642.

McLure, K.G., and Lee, P.W. (1998). How p53 binds DNA as a tetramer. EMBO J. *17,* 3342-3350.

Medina, R.A., and Garcia-Sastre, A. (2011). Influenza A viruses: new research developments. Nat. Rev. Microbiol. *9,* 590-603.

Mehle, A., and Doudna, J.A. (2009). Adaptive strategies of the influenza virus polymerase for replication in humans. Proc. Natl. Acad. Sci. U. S. A. *106,* 21312-21316.

Melcher, A., Parato, K., Rooney, C.M., and Bell, J.C. (2011). Thunder and lightning: immunotherapy and oncolytic viruses collide. Mol. Ther. *19,* 1008-1016.

Melin, J., Schulz, C., Wrobel, L., Bernhard, O., Chacinska, A., Jahn, O., Schmidt, B., and Rehling, P. (2014). Presequence recognition by the tom40 channel contributes to precursor translocation into the mitochondrial matrix. Mol. Cell. Biol. *34,* 3473-3485.

Menotti, L., Cerretani, A., and Campadelli-Fiume, G. (2006). A herpes simplex virus recombinant that exhibits a single-chain antibody to HER2/neu enters cells through the mammary tumor receptor, independently of the gD receptors. J. Virol. *80,* 5531-5539.

Metcalf, D., Begley, C.G., Johnson, G.R., Nicola, N.A., Vadas, M.A., Lopez, A.F., Williamson, D.J., Wong, G.G., Clark, S.C., and Wang, E.A. (1986). Biologic properties in vitro of a recombinant human granulocyte-macrophage colony-stimulating factor. Blood *67,* 37-45.

Meurs, E., Chong, K., Galabru, J., Thomas, N.S., Kerr, I.M., Williams, B.R., and Hovanessian, A.G. (1990). Molecular cloning and characterization of the human double-stranded RNA-activated protein kinase induced by interferon. Cell *62,* 379-390.

Michaud, D.S., Giovannucci, E., Willett, W.C., Colditz, G.A., Stampfer, M.J., and Fuchs, C.S. (2001). Physical activity, obesity, height, and the risk of pancreatic cancer. JAMA *286,* 921-929.

Miest, T.S., and Cattaneo, R. (2014). New viruses for cancer therapy: meeting clinical needs. Nat. Rev. Microbiol. *12,* 23-34.

Miest, T.S., Yaiw, K.C., Frenzke, M., Lampe, J., Hudacek, A.W., Springfeld, C., von Messling, V., Ungerechts, G., and Cattaneo, R. (2011). Envelope-chimeric entry-targeted measles virus escapes neutralization and achieves oncolysis. Mol. Ther. *19,* 1813-1820.

Min, J.Y., and Krug, R.M. (2006). The primary function of RNA binding by the influenza A virus NS1 protein in infected cells: Inhibiting the 2'-5' oligo (A) synthetase/RNase L pathway. Proc. Natl. Acad. Sci. U. S. A. *103,* 7100-7105.

Min, J.Y., Li, S., Sen, G.C., and Krug, R.M. (2007). A site on the influenza A virus NS1 protein mediates both inhibition of PKR activation and temporal regulation of viral RNA synthesis. Virology *363,* 236-243.

Minamoto, T., Buschmann, T., Habelhah, H., Matusevich, E., Tahara, H., Boerresen-Dale, A.L., Harris, C., Sidransky, D., and Ronai, Z. (2001). Distinct pattern of p53 phosphorylation in human tumors. Oncogene *20,* 3341-3347.

Miyashita, T., Krajewski, S., Krajewska, M., Wang, H.G., Lin, H.K., Liebermann, D.A., Hoffman, B., and Reed, J.C. (1994). Tumor suppressor p53 is a regulator of bcl-2 and bax gene expression in vitro and in vivo. Oncogene *9,* 1799-1805.

Miyashita, T., and Reed, J.C. (1995). Tumor suppressor p53 is a direct transcriptional activator of the human bax gene. Cell *80,* 293-299.

Moeller, A., Kirchdoerfer, R.N., Potter, C.S., Carragher, B., and Wilson, I.A. (2012). Organization of the influenza virus replication machinery. Science *338,* 1631-1634.

Moerdyk-Schauwecker, M., Shah, N.R., Murphy, A.M., Hastie, E., Mukherjee, P., and Grdzelishvili, V.Z. (2012). Resistance of pancreatic cancer cells to oncolytic vesicular stomatitis virus: Role of type I interferon signaling. Virology *436,* 221-234.

Mok, C.K., Lee, D.C., Cheung, C.Y., Peiris, M., and Lau, A.S. (2007). Differential onset of apoptosis in influenza A virus H5N1- and H1N1-infected human blood macrophages. J. Gen. Virol. *88,* 1275-1280.

Mollinedo, F., and Gajate, C. (2006). Fas/CD95 death receptor and lipid rafts: new targets for apoptosis-directed cancer therapy. Drug Resist Updat *9,* 51-73.

Momose, F., Sekimoto, T., Ohkura, T., Jo, S., Kawaguchi, A., Nagata, K., and Morikawa, Y. (2011). Apical transport of influenza A virus ribonucleoprotein requires Rab11-positive recycling endosome. PLoS One *6,* e21123.

Monne, I., Fusaro, A., Nelson, M.I., Bonfanti, L., Mulatti, P., Hughes, J., Murcia, P.R., Schivo, A., Valastro, V., Moreno, A., Holmes, E.C., and Cattoli, G. (2014). Emergence of a highly pathogenic avian influenza virus from a low-pathogenic progenitor. J. Virol. *88,* 4375-4388.

Morahan, P.S., and Grossberg, S.E. (1970). Age-related cellular resistance of the chicken embryo to viral infections. II. Inducible resistance produced by influenza virus and Escherichia coli. J. Infect. Dis. *121,* 624-633.

Mori, I., and Kimura, Y. (2000). Apoptotic neurodegeneration induced by influenza A virus infection in the mouse brain. Microbes Infect. *2,* 1329-1334.

Mori, I., Komatsu, T., Takeuchi, K., Nakakuki, K., Sudo, M., and Kimura, Y. (1995). In vivo induction of apoptosis by influenza virus. J. Gen. Virol. *76 (Pt 11),* 2869-2873.

Morrison, J., Briggs, S.S., Green, N., Fisher, K., Subr, V., Ulbrich, K., Kehoe, S., and Seymour, L.W. (2008). Virotherapy of ovarian cancer with polymer-cloaked adenovirus retargeted to the epidermal growth factor receptor. Mol. Ther. *16,* 244-251.

Morsy, J., Garten, W., and Rott, R. (1994). Activation of an influenza virus A/turkey/Oregon/71 HA insertion variant by the subtilisin-like endoprotease furin. Virology *202,* 988-991.

Muik, A., Kneiske, I., Werbizki, M., Wilflingseder, D., Giroglou, T., Ebert, O., Kraft, A., Dietrich, U., Zimmer, G., Momma, S., and von Laer, D. (2011). Pseudotyping vesicular stomatitis virus with lymphocytic choriomeningitis virus glycoproteins enhances infectivity for glioma cells and minimizes neurotropism. J. Virol. *85,* 5679-5684.

Muramoto, Y., Takada, A., Fujii, K., Noda, T., Iwatsuki-Horimoto, K., Watanabe, S., Horimoto, T., Kida, H., and Kawaoka, Y. (2006). Hierarchy among viral RNA (vRNA) segments in their role in vRNA incorporation into influenza A virions. J. Virol. *80,* 2318-2325.

Murphy, A.M., Besmer, D.M., Moerdyk-Schauwecker, M., Moestl, N., Ornelles, D., Mukherjee, P., and Grdzelishvili, V.Z. (2012). Vesicular Stomatitis Virus as an Oncolytic Agent Against Pancreatic Ductal Adenocarcinoma. J. Virol. *86,* 3073-3087.

Murphy, B.R., and Clements, M.L. (1989). The systemic and mucosal immune response of humans to influenza A virus. Curr. Top. Microbiol. Immunol. *146,* 107-116.

Murphy, J.A., Duerst, R.J., Smith, T.J., and Morrison, L.A. (2003). Herpes simplex virus type 2 virion host shutoff protein regulates alpha/beta interferon but not adaptive immune responses during primary infection in vivo. J. Virol. *77,* 9337-9345.

Muster, T., Rajtarova, J., Sachet, M., Unger, H., Fleischhacker, R., Romirer, I., Grassauer, A., Url, A., Garcia-Sastre, A., Wolff, K., Pehamberger, H., and Bergmann, M. (2004). Interferon resistance promotes oncolysis by influenza virus NS1-deletion mutants. Int. J. Cancer *110,* 15-21.

Mutinelli, F., Capua, I., Terregino, C., and Cattoli, G. (2003). Clinical, gross, and microscopic findings in different avian species naturally infected during the H7N1 low- and high-pathogenicity avian influenza epidemics in Italy during 1999 and 2000. Avian Dis. *47,* 844-848.

Myers, K.P., Olsen, C.W., and Gray, G.C. (2007). Cases of swine influenza in humans: a review of the literature. Clin. Infect. Dis. *44,* 1084-1088.

Naffakh, N., Tomoiu, A., Rameix-Welti, M.A., and van der Werf, S. (2008). Host restriction of avian influenza viruses at the level of the ribonucleoproteins. Annu. Rev. Microbiol. *62,* 403-424.

Naik, S., and Russell, S.J. (2009). Engineering oncolytic viruses to exploit tumor specific defects in innate immune signaling pathways. Expert Opin. Biol. Ther. *9,* 1163-1176.

Nakamura, T., Peng, K.W., Harvey, M., Greiner, S., Lorimer, I.A., James, C.D., and Russell, S.J. (2005). Rescue and propagation of fully retargeted oncolytic measles viruses. Nat. Biotechnol. *23,* 209-214.

Nelson, M.I., and Holmes, E.C. (2007). The evolution of epidemic influenza. Nat. Rev. Genet. *8,* 196-205.

Nemeroff, M.E., Barabino, S.M., Li, Y., Keller, W., and Krug, R.M. (1998). Influenza virus NS1 protein interacts with the cellular 30 kDa subunit of CPSF and inhibits 3'end formation of cellular pre-mRNAs. Mol. Cell *1,* 991-1000.

Nemeroff, M.E., Qian, X.Y., and Krug, R.M. (1995). The influenza virus NS1 protein forms multimers in vitro and in vivo. Virology *212,* 422-428.

Nenna, R., Papoff, P., Moretti, C., Pierangeli, A., Sabatino, G., Costantino, F., Soscia, F., Cangiano, G., Ferro, V., Mennini, M.*, et al.* (2011). Detection of respiratory viruses in the 2009 winter season in Rome: 2009 influenza A (H1N1) complications in children and concomitant type 1 diabetes onset. Int. J. Immunopathol. Pharmacol. *24,* 651-659.

Neumann, G., Hughes, M.T., and Kawaoka, Y. (2000). Influenza A virus NS2 protein mediates vRNP nuclear export through NES-independent interaction with hCRM1. EMBO J. *19,* 6751-6758.

Neumann, G., and Kawaoka, Y. (2004). Reverse genetics systems for the generation of segmented negative-sense RNA viruses entirely from cloned cDNA. Curr. Top. Microbiol. Immunol. *283,* 43-60.

Neumann, G., Noda, T., and Kawaoka, Y. (2009). Emergence and pandemic potential of swine-origin H1N1 influenza virus. Nature *459,* 931-939.

Neumann, G., Watanabe, T., Ito, H., Watanabe, S., Goto, H., Gao, P., Hughes, M., Perez, D.R., Donis, R., Hoffmann, E., Hobom, G., and Kawaoka, Y. (1999). Generation of influenza A viruses entirely from cloned cDNAs. Proc. Natl. Acad. Sci. U. S. A. *96,* 9345-9350.

Ngunjiri, J.M., Ali, A., Boyaka, P., Marcus, P.I., and Lee, C.W. (2015). In vivo assessment of NS1-truncated influenza virus with a novel SLSYSINWRH motif as a self-adjuvanting live attenuated vaccine. PLoS One *10,* e0118934.

Nicholls, J.M., Chan, R.W., Russell, R.J., Air, G.M., and Peiris, J.S. (2008). Evolving complexities of influenza virus and its receptors. Trends Microbiol. *16,* 149-157.

Nicholson, D.W., Ali, A., Thornberry, N.A., Vaillancourt, J.P., Ding, C.K., Gallant, M., Gareau, Y., Griffin, P.R., Labelle, M., and Lazebnik, Y.A. (1995). Identification and inhibition of the ICE/CED-3 protease necessary for mammalian apoptosis. Nature *376,* 37-43.

Nicotera, P., Leist, M., and Ferrando-May, E. (1998). Intracellular ATP, a switch in the decision between apoptosis and necrosis. Toxicol. Lett. *102-103,* 139-142.

Nimer, S.D., and Uchida, H. (1995). Regulation of granulocyte-macrophage colony-stimulating factor and interleukin 3 expression. Stem Cells *13,* 324-335.

Noah, D.L., Twu, K.Y., and Krug, R.M. (2003). Cellular antiviral responses against influenza A virus are countered at the posttranscriptional level by the viral NS1A protein via its binding to a cellular protein required for the 3' end processing of cellular pre-mRNAS. Virology *307,* 386-395.

Noda, T., Sagara, H., Yen, A., Takada, A., Kida, H., Cheng, R.H., and Kawaoka, Y. (2006). Architecture of ribonucleoprotein complexes in influenza A virus particles. Nature *439,* 490-492.

Normanno, N., Tejpar, S., Morgillo, F., De Luca, A., Van Cutsem, E., and Ciardiello, F. (2009). Implications for KRAS status and EGFR-targeted therapies in metastatic CRC. Nat. Rev. Clin. Oncol. *6,* 519-527.

Noteborn, M.H. (2009). Proteins selectively killing tumor cells. Eur. J. Pharmacol. *625,* 165-173.

Novel Swine-Origin Influenza A (H1N1) Virus Investigation Team, Dawood, F.S., Jain, S., Finelli, L., Shaw, M.W., Lindstrom, S., Garten, R.J., Gubareva, L.V., Xu, X., Bridges, C.B., and Uyeki, T.M. (2009). Emergence of a novel swine-origin influenza A (H1N1) virus in humans. N. Engl. J. Med. *360,* 2605-2615.

O'Callaghan, R.J., Gohd, R.S., and Labat, D.D. (1980). Human antibody to influenza C virus: its age-related distribution and distinction from receptor analogs. Infect. Immun. *30,* 500-505.

Office International des Epizooties (OIE). (May 2012). Avian Influenza. Manual of Diagnostic Tests and Vaccines for Terrestrial Animals Chapter 2.3.4.

Ohta, T., Tajima, H., Fushida, S., Kitagawa, H., Kayahara, M., Nagakawa, T., Miwa, K., Yamamoto, M., Numata, M., Nakanuma, Y., Kitamura, Y., and Terada, T. (1998). Cationic trypsinogen produced by human pancreatic ductal cancer has the characteristics of spontaneous activation and gelatinolytic activity in the presence of proton. Int. J. Mol. Med. *1,* 689-692.

Ohta, T., Terada, T., Nagakawa, T., Tajima, H., Itoh, H., Fonseca, L., and Miyazaki, I. (1994). Pancreatic trypsinogen and cathepsin B in human pancreatic carcinomas and associated metastatic lesions. Br. J. Cancer *69,* 152-156.

Oliver, L., and Vallette, F.M. (2005). The role of caspases in cell death and differentiation. Drug Resist Updat *8,* 163-170.

O'Neill, R.E., Jaskunas, R., Blobel, G., Palese, P., and Moroianu, J. (1995). Nuclear import of influenza virus RNA can be mediated by viral nucleoprotein and transport factors required for protein import. J. Biol. Chem. *270,* 22701-22704.

O'Neill, R.E., Talon, J., and Palese, P. (1998). The influenza virus NEP (NS2 protein) mediates the nuclear export of viral ribonucleoproteins. EMBO J. *17,* 288-296.

Ong, A.K., and Hayden, F.G. (2007). John F. Enders lecture 2006: antivirals for influenza. J. Infect. Dis. *196,* 181-190.

Onodera, T., Jenson, A.B., Yoon, J.W., and Notkins, A.L. (1978). Virus-induced diabetes mellitus: reovirus infection of pancreatic beta cells in mice. Science *201,* 529-531.

Orci, L. (1986). The insulin cell: its cellular environment and how it processes (pro)insulin. Diabetes Metab. Rev. *2,* 71-106.

Ortega, J., Martin-Benito, J., Zurcher, T., Valpuesta, J.M., Carrascosa, J.L., and Ortin, J. (2000). Ultrastructural and functional analyses of recombinant influenza virus ribonucleoproteins suggest dimerization of nucleoprotein during virus amplification. J. Virol. *74,* 156-163.

Oshiumi, H., Miyashita, M., Inoue, N., Okabe, M., Matsumoto, M., and Seya, T. (2010). The ubiquitin ligase Riplet is essential for RIG-I-dependent innate immune responses to RNA virus infection. Cell. Host Microbe *8,* 496-509.

Ouyang, H., Mou, L., Luk, C., Liu, N., Karaskova, J., Squire, J., and Tsao, M.S. (2000). Immortal human pancreatic duct epithelial cell lines with near normal genotype and phenotype. Am. J. Pathol. *157,* 1623-1631.

Palese, P. (2004). Influenza: old and new threats. Nat. Med. *10,* S82-7.

Palese, P., Tobita, K., Ueda, M., and Compans, R.W. (1974). Characterization of temperature sensitive influenza virus mutants defective in neuraminidase. Virology *61,* 397-410.

Pandol, S.J. (2010). The Exocrine Pancreas (San Rafael (CA): Morgan & Claypool Life Sciences).

Park, C.J., Bae, S.H., Lee, M.K., Varani, G., and Choi, B.S. (2003). Solution structure of the influenza A virus cRNA promoter: implications for differential recognition of viral promoter structures by RNA-dependent RNA polymerase. Nucleic Acids Res. *31,* 2824-2832.

Patel, B., Dey, A., Ghorani, E., Kumar, S., Malam, Y., Rai, L., Steele, A.J., Thomson, J., Wickremasinghe, R.G., Zhang, Y., Castleton, A.Z., and Fielding, A.K. (2011). Differential cytopathology and kinetics of measles oncolysis in two primary B-cell malignancies provides mechanistic insights. Mol. Ther. *19,* 1034-1040.

Paterson, D., and Fodor, E. (2012). Emerging roles for the influenza A virus nuclear export protein (NEP). PLoS Pathog. *8,* e1003019.

Pavlovic, J., Haller, O., and Staeheli, P. (1992). Human and mouse Mx proteins inhibit different steps of the influenza virus multiplication cycle. J. Virol. *66,* 2564-2569.

Pena, L., Sutton, T., Chockalingam, A., Kumar, S., Angel, M., Shao, H., Chen, H., Li, W., and Perez, D.R. (2013). Influenza viruses with rearranged genomes as live-attenuated vaccines. J. Virol. *87,* 5118-5127.

Peracaula, R., Tabares, G., Lopez-Ferrer, A., Brossmer, R., de Bolos, C., and de Llorens, R. (2005). Role of sialyltransferases involved in the biosynthesis of Lewis antigens in human pancreatic tumour cells. Glycoconj. J. *22,* 135-144.

Percy, N., Barclay, W.S., Garcia-Sastre, A., and Palese, P. (1994). Expression of a foreign protein by influenza A virus. J. Virol. *68,* 4486-4492.

Perdue, M.L., Garcia, M., Senne, D., and Fraire, M. (1997). Virulence-associated sequence duplication at the hemagglutinin cleavage site of avian influenza viruses. Virus Res. *49,* 173-186.

Perez, J.T., Varble, A., Sachidanandam, R., Zlatev, I., Manoharan, M., Garcia-Sastre, A., and tenOever, B.R. (2010). Influenza A virus-generated small RNAs regulate the switch from transcription to replication. Proc. Natl. Acad. Sci. U. S. A. *107,* 11525-11530.

Perez, J.T., Zlatev, I., Aggarwal, S., Subramanian, S., Sachidanandam, R., Kim, B., Manoharan, M., and tenOever, B.R. (2012). A small-RNA enhancer of viral polymerase activity. J. Virol. *86,* 13475-13485.

Perez-Garay, M., Arteta, B., Pages, L., de Llorens, R., de Bolos, C., Vidal-Vanaclocha, F., and Peracaula, R. (2010). alpha2,3-sialyltransferase ST3Gal III modulates pancreatic cancer cell motility and adhesion in vitro and enhances its metastatic potential in vivo. PLoS One *5,* 10.1371/journal.pone.0012524.

Permuth-Wey, J., and Egan, K.M. (2009). Family history is a significant risk factor for pancreatic cancer: results from a systematic review and meta-analysis. Fam. Cancer. *8,* 109-117.

Perroncito, E. (1878). Epizoozia tifoide nei gallinacei. . Ann. Acad. Agric. *21,* 87.

Pfanner, N. (2000). Protein sorting: recognizing mitochondrial presequences. Curr. Biol. *10,* R412-5.

Pica, N., Langlois, R.A., Krammer, F., Margine, I., and Palese, P. (2012). NS1-truncated live attenuated virus vaccine provides robust protection to aged mice from viral challenge. J. Virol. *86,* 10293-10301.

Pichlmair, A., Schulz, O., Tan, C.P., Naslund, T.I., Liljestrom, P., Weber, F., and Reis e Sousa, C. (2006). RIG-I-mediated antiviral responses to single-stranded RNA bearing 5'-phosphates. Science *314,* 997-1001.

Plotch, S.J., and Krug, R.M. (1977). Influenza virion transcriptase: synthesis in vitro of large, polyadenylic acid-containing complementary RNA. J. Virol. *21,* 24-34.

Portela, A., and Digard, P. (2002). The influenza virus nucleoprotein: a multifunctional RNA-binding protein pivotal to virus replication. J. Gen. Virol. *83,* 723-734.

Power, A.T., and Bell, J.C. (2008). Taming the Trojan horse: optimizing dynamic carrier cell/oncolytic virus systems for cancer biotherapy. Gene Ther. *15,* 772-779.

Prestwich, R.J., Ilett, E.J., Errington, F., Diaz, R.M., Steele, L.P., Kottke, T., Thompson, J., Galivo, F., Harrington, K.J., Pandha, H.S*., et al.* (2009). Immune-mediated antitumor activity of reovirus is required for therapy and is independent of direct viral oncolysis and replication. Clin. Cancer Res. *15,* 4374-4381.

Raff, M. (1998). Cell suicide for beginners. Nature *396,* 119-122.

Raimondi, S., Lowenfels, A.B., Morselli-Labate, A.M., Maisonneuve, P., and Pezzilli, R. (2010). Pancreatic cancer in chronic pancreatitis; aetiology, incidence, and early detection. Best Pract. Res. Clin. Gastroenterol. *24,* 349-358.

Rajsbaum, R., Albrecht, R.A., Wang, M.K., Maharaj, N.P., Versteeg, G.A., Nistal-Villan, E., Garcia-Sastre, A., and Gack, M.U. (2012). Species-specific inhibition of RIG-I ubiquitination and IFN induction by the influenza A virus NS1 protein. PLoS Pathog. *8,* e1003059.

Randall, R.E., and Goodbourn, S. (2008a). Interferons and viruses: an interplay between induction, signalling, antiviral responses and virus countermeasures. J. Gen. Virol. *89,* 1-47.

Randall, R.E., and Goodbourn, S. (2008b). Interferons and viruses: an interplay between induction, signalling, antiviral responses and virus countermeasures. J. Gen. Virol. *89,* 1-47.

Rapoport, T.A. (1992). Transport of proteins across the endoplasmic reticulum membrane. Science *258,* 931-936.

Raynal, P., and Pollard, H.B. (1994). Annexins: the problem of assessing the biological role for a gene family of multifunctional calcium- and phospholipid-binding proteins. Biochim. Biophys. Acta *1197,* 63-93.

Redondo, M., Tellez, T., and Roldan, M.J. (2009). The role of clusterin (CLU) in malignant transformation and drug resistance in breast carcinomas. Adv. Cancer Res. *105,* 21-43.

Redondo, M., Villar, E., Torres-Munoz, J., Tellez, T., Morell, M., and Petito, C.K. (2000). Overexpression of clusterin in human breast carcinoma. Am. J. Pathol. *157,* 393-399.

Redston, M.S., Caldas, C., Seymour, A.B., Hruban, R.H., da Costa, L., Yeo, C.J., and Kern, S.E. (1994). p53 mutations in pancreatic carcinoma and evidence of common involvement of homocopolymer tracts in DNA microdeletions. Cancer Res. *54,* 3025-3033.

Reed, M.L., Bridges, O.A., Seiler, P., Kim, J.K., Yen, H.L., Salomon, R., Govorkova, E.A., Webster, R.G., and Russell, C.J. (2010). The pH of activation of the hemagglutinin protein regulates H5N1 influenza virus pathogenicity and transmissibility in ducks. J. Virol. *84,* 1527-1535.

Reichard, K.W., Lorence, R.M., Cascino, C.J., Peeples, M.E., Walter, R.J., Fernando, M.B., Reyes, H.M., and Greager, J.A. (1992). Newcastle disease virus selectively kills human tumor cells. J. Surg. Res. *52,* 448-453.

Reid, A.H., Taubenberger, J.K., and Fanning, T.G. (2004). Evidence of an absence: the genetic origins of the 1918 pandemic influenza virus. Nat. Rev. Microbiol. *2,* 909-914.

Reperant, L.A., Rimmelzwaan, G.F., and Kuiken, T. (2009). Avian influenza viruses in mammals. Rev. Sci. Tech. *28,* 137-159.

Reutelingsperger, C.P., Hornstra, G., and Hemker, H.C. (1985). Isolation and partial purification of a novel anticoagulant from arteries of human umbilical cord. Eur. J. Biochem. *151,* 625-629.

Richer, M.J., and Horwitz, M.S. (2008). Viral infections in the pathogenesis of autoimmune diseases: focus on type 1 diabetes. Front. Biosci. *13,* 4241-4257.

Richt, J.A., and Garcia-Sastre, A. (2009). Attenuated influenza virus vaccines with modified NS1 proteins. Curr. Top. Microbiol. Immunol. *333,* 177-195.

Riegger, D., Hai, R., Dornfeld, D., Manz, B., Leyva-Grado, V., Sanchez-Aparicio, M.T., Albrecht, R.A., Palese, P., Haller, O., Schwemmle, M.*, et al.* (2015). The nucleoprotein of newly emerged H7N9 influenza A virus harbors a unique motif conferring resistance to antiviral human MxA. J. Virol. *89,* 2241-2252.

Rimmelzwaan, G.F., van Riel, D., Baars, M., Bestebroer, T.M., van Amerongen, G., Fouchier, R.A., Osterhaus, A.D., and Kuiken, T. (2006). Influenza A virus (H5N1) infection in cats causes systemic disease with potential novel routes of virus spread within and between hosts. Am. J. Pathol. *168,* 176-83; quiz 364.

Robb, N.C., Smith, M., Vreede, F.T., and Fodor, E. (2009). NS2/NEP protein regulates transcription and replication of the influenza virus RNA genome. J. Gen. Virol. *90,* 1398-1407.

Roberts, D.M., Nanda, A., Havenga, M.J., Abbink, P., Lynch, D.M., Ewald, B.A., Liu, J., Thorner, A.R., Swanson, P.E., Gorgone, D.A.*, et al.* (2006). Hexon-chimaeric adenovirus serotype 5 vectors circumvent pre-existing anti-vector immunity. Nature *441,* 239-243.

Roberts, K.L., Leser, G.P., Ma, C., and Lamb, R.A. (2013). The amphipathic helix of influenza A virus M2 protein is required for filamentous bud formation and scission of filamentous and spherical particles. J. Virol. *87,* 9973-9982.

Roberts, P.C., Lamb, R.A., and Compans, R.W. (1998). The M1 and M2 proteins of influenza A virus are important determinants in filamentous particle formation. Virology *240,* 127-137.

Robertson, J.S., Schubert, M., and Lazzarini, R.A. (1981). Polyadenylation sites for influenza virus mRNA. J. Virol. *38,* 157-163.

Robertson, K.D., and Jones, P.A. (1999). Tissue-specific alternative splicing in the human INK4a/ARF cell cycle regulatory locus. Oncogene *18,* 3810-3820.

Rogers, G.N., and Paulson, J.C. (1983). Receptor determinants of human and animal influenza virus isolates: differences in receptor specificity of the H3 hemagglutinin based on species of origin. Virology *127,* 361-373.

Roise, D., and Schatz, G. (1988). Mitochondrial presequences. J. Biol. Chem. *263,* 4509-4511.

Rosenblum, M.G., Yung, W.K., Kelleher, P.J., Ruzicka, F., Steck, P.A., and Borden, E.C. (1990). Growth inhibitory effects of interferon-beta but not interferon-alpha on human glioma cells: correlation of receptor binding, 2',5'-oligoadenylate synthetase and protein kinase activity. J. Interferon Res. *10,* 141-151.

Rossman, J.S., Jing, X., Leser, G.P., Balannik, V., Pinto, L.H., and Lamb, R.A. (2010a). Influenza virus m2 ion channel protein is necessary for filamentous virion formation. J. Virol. *84,* 5078-5088.

Rossman, J.S., Jing, X., Leser, G.P., and Lamb, R.A. (2010b). Influenza virus M2 protein mediates ESCRT-independent membrane scission. Cell *142,* 902-913.

Rossman, J.S., and Lamb, R.A. (2011). Influenza virus assembly and budding. Virology *411,* 229-236.

Rozenblum, E., Schutte, M., Goggins, M., Hahn, S.A., Panzer, S., Zahurak, M., Goodman, S.N., Sohn, T.A., Hruban, R.H., Yeo, C.J., and Kern, S.E. (1997). Tumor-suppressive pathways in pancreatic carcinoma. Cancer Res. *57,* 1731-1734.

Russell, S.J., Peng, K.W., and Bell, J.C. (2012). Oncolytic virotherapy. Nat. Biotechnol. *30,* 658-670.

Ryan, M.D., Luke, G., Hughes, L.E., Cowton, V.M., ten Dam, E., Li, X., Donnelly, M.L.L., Mehrotra, A., and Gani, D. (2002). The aphto- and cardiovirus "primary" 2A/2B polyprotein "cleavage". In Molecular Biology of Picornaviruses, Semler BL, Wimmer E. ed., (Washington, USA: ASM Press) pp. 213-223.

Ryan, M.D., and Drew, J. (1994). Foot-and-mouth disease virus 2A oligopeptide mediated cleavage of an artificial polyprotein. EMBO J. *13,* 928-933.

Sadler, A.J., and Williams, B.R. (2008). Interferon-inducible antiviral effectors. Nat. Rev. Immunol. *8,* 559-568.

Sakaguchi, K., Sakamoto, H., Lewis, M.S., Anderson, C.W., Erickson, J.W., Appella, E., and Xie, D. (1997). Phosphorylation of serine 392 stabilizes the tetramer formation of tumor suppressor protein p53. Biochemistry *36,* 10117-10124.

Samuel, C.E. (2001). Antiviral actions of interferons. Clin. Microbiol. Rev. *14,* 778-809, table of contents.

Samuel, C.E. (1993). The eIF-2 alpha protein kinases, regulators of translation in eukaryotes from yeasts to humans. J. Biol. Chem. *268,* 7603-7606.

Sano, H., Terasaki, J., Tsutsumi, C., Imagawa, A., and Hanafusa, T. (2008). A case of fulminant type 1 diabetes mellitus after influenza B infection. Diabetes Res. Clin. Pract. *79,* e8-9.

Santos, A., Pal, S., Chacon, J., Meraz, K., Gonzalez, J., Prieto, K., and Rosas-Acosta, G. (2013). SUMOylation affects the interferon blocking activity of the influenza A nonstructural protein NS1 without affecting its stability or cellular localization. J. Virol. *87,* 5602-5620.

Sarkioja, M., Pesonen, S., Raki, M., Hakkarainen, T., Salo, J., Ahonen, M.T., Kanerva, A., and Hemminki, A. (2008). Changing the adenovirus fiber for retaining gene delivery efficacy in the presence of neutralizing antibodies. Gene Ther. *15,* 921-929.

Sauthoff, H., Hu, J., Maca, C., Goldman, M., Heitner, S., Yee, H., Pipiya, T., Rom, W.N., and Hay, J.G. (2003). Intratumoral spread of wild-type adenovirus is limited after local injection of human xenograft tumors: virus persists and spreads systemically at late time points. Hum. Gene Ther. *14,* 425-433.

Scheiffele, P., Roth, M.G., and Simons, K. (1997). Interaction of influenza virus haemagglutinin with sphingolipid-cholesterol membrane domains via its transmembrane domain. EMBO J. *16,* 5501-5508.

Schlacher, K., Christ, N., Siaud, N., Egashira, A., Wu, H., and Jasin, M. (2011). Double-strand break repair-independent role for BRCA2 in blocking stalled replication fork degradation by MRE11. Cell *145,* 529-542.

Schlee, M. (2013). Master sensors of pathogenic RNA - RIG-I like receptors. Immunobiology *218,* 1322-1335.

Schlee, M., Roth, A., Hornung, V., Hagmann, C.A., Wimmenauer, V., Barchet, W., Coch, C., Janke, M., Mihailovic, A., Wardle, G.*, et al.* (2009). Recognition of 5' triphosphate by RIG-I helicase requires short blunt double-stranded RNA as contained in panhandle of negative-strand virus. Immunity *31,* 25-34.

Schmidt, A., Schwerd, T., Hamm, W., Hellmuth, J.C., Cui, S., Wenzel, M., Hoffmann, F.S., Michallet, M.C., Besch, R., Hopfner, K.P., Endres, S., and Rothenfusser, S. (2009). 5'-triphosphate RNA requires base-paired structures to activate antiviral signaling via RIG-I. Proc. Natl. Acad. Sci. U. S. A. *106,* 12067-12072.

Schmitt, A.P., and Lamb, R.A. (2005). Influenza virus assembly and budding at the viral budozone. Adv. Virus Res. *64,* 383-416.

Schmitt, A.P., and Lamb, R.A. (2004). Escaping from the cell: assembly and budding of negative-strand RNA viruses. Curr. Top. Microbiol. Immunol. *283,* 145-196.

Schmolke, M., Manicassamy, B., Pena, L., Sutton, T., Hai, R., Varga, Z.T., Hale, B.G., Steel, J., Perez, D.R., and Garcia-Sastre, A. (2011). Differential contribution of PB1-F2 to the virulence of highly pathogenic H5N1 influenza A virus in mammalian and avian species. PLoS Pathog. *7,* e1002186.

Schneider, R.M., Medvedovska, Y., Hartl, I., Voelker, B., Chadwick, M.P., Russell, S.J., Cichutek, K., and Buchholz, C.J. (2003). Directed evolution of retroviruses activatable by tumour-associated matrix metalloproteases. Gene Ther. *10,* 1370-1380.

Schnell, J.R., and Chou, J.J. (2008). Structure and mechanism of the M2 proton channel of influenza A virus. Nature *451,* 591-595.

Schnell, M.J., Mebatsion, T., and Conzelmann, K.K. (1994). Infectious rabies viruses from cloned cDNA. EMBO J. *13,* 4195-4203.

Scholtissek, C., Rohde, W., Von Hoyningen, V., and Rott, R. (1978). On the origin of the human influenza virus subtypes H2N2 and H3N2. Virology *87,* 13-20.

Schultz-Cherry, S., Dybdahl-Sissoko, N., Neumann, G., Kawaoka, Y., and Hinshaw, V.S. (2001). Influenza virus ns1 protein induces apoptosis in cultured cells. J. Virol. *75,* 7875-7881.

Schultze, H., Goilner, I., Heide, K., Schoenenberger, M., and Schwick, G. (1955). Zur Kenntnis der alpha-globulin des menschlichen nirmal serums. Naturforsch *10,* 463.

Schusser, B., Reuter, A., von der Malsburg, A., Penski, N., Weigend, S., Kaspers, B., Staeheli, P., and Hartle, S. (2011). Mx is dispensable for interferon-mediated resistance of chicken cells against influenza A virus. J. Virol. *85,* 8307-8315.

Schutte, M., Hruban, R.H., Geradts, J., Maynard, R., Hilgers, W., Rabindran, S.K., Moskaluk, C.A., Hahn, S.A., Schwarte-Waldhoff, I., Schmiegel, W.*, et al.* (1997). Abrogation of the Rb/p16 tumor-suppressive pathway in virtually all pancreatic carcinomas. Cancer Res. *57,* 3126-3130.

Schutte, M., Hruban, R.H., Hedrick, L., Cho, K.R., Nadasdy, G.M., Weinstein, C.L., Bova, G.S., Isaacs, W.B., Cairns, P., Nawroz, H.*, et al.* (1996). DPC4 gene in various tumor types. Cancer Res. *56,* 2527-2530.

Senne, D.A. (2007). Avian influenza in North and South America, 2002-2005. Avian Dis. *51,* 167-173.

Senne, D.A., Suarez, D.L., Stallnecht, D.E., Pedersen, J.C., and Panigrahy, B. (2006). Ecology and epidemiology of avian influenza in North and South America. Dev. Biol. (Basel) *124,* 37-44.

Seth, R.B., Sun, L., and Chen, Z.J. (2006). Antiviral innate immunity pathways. Cell Res. *16,* 141-147.

Shashkova, E.V., May, S.M., Doronin, K., and Barry, M.A. (2009). Expanded anticancer therapeutic window of hexon-modified oncolytic adenovirus. Mol. Ther. *17,* 2121-2130.

Shatkin, A.J., and Manley, J.L. (2000). The ends of the affair: capping and polyadenylation. Nat. Struct. Biol. *7,* 838-842.

Shi, X., Liu, S., Kleeff, J., Friess, H., and Buchler, M.W. (2002). Acquired resistance of pancreatic cancer cells towards 5-Fluorouracil and gemcitabine is associated with altered expression of apoptosis-regulating genes. Oncology *62,* 354-362.

Shi, Y., Liu, C.H., Roberts, A.I., Das, J., Xu, G., Ren, G., Zhang, Y., Zhang, L., Yuan, Z.R., Tan, H.S., Das, G., and Devadas, S. (2006). Granulocyte-macrophage colony-stimulating factor (GM-CSF) and T-cell responses: what we do and don't know. Cell Res. *16,* 126-133.

Shibata, D., Capella, G., and Perucho, M. (1990). Mutational activation of the c-K-ras gene in human pancreatic carcinoma. Baillieres Clin. Gastroenterol. *4,* 151-169.

Shimizu, T., Takizawa, N., Watanabe, K., Nagata, K., and Kobayashi, N. (2011). Crucial role of the influenza virus NS2 (NEP) C-terminal domain in M1 binding and nuclear export of vRNP. FEBS Lett. *585,* 41-46.

Shin, Y.K., Li, Y., Liu, Q., Anderson, D.H., Babiuk, L.A., and Zhou, Y. (2007a). SH3 binding motif 1 in influenza A virus NS1 protein is essential for PI3K/Akt signaling pathway activation. J. Virol. *81,* 12730-12739.

Shin, Y.K., Liu, Q., Tikoo, S.K., Babiuk, L.A., and Zhou, Y. (2007b). Influenza A virus NS1 protein activates the phosphatidylinositol 3-kinase (PI3K)/Akt pathway by direct interaction with the p85 subunit of PI3K. J. Gen. Virol. *88,* 13-18.

Shinya, K., Awakura, T., Shimada, A., Silvano, F.D., Umemura, T., and Otsuki, K. (1995). Pathogenesis of pancreatic atrophy by avian influenza a virus infection. Avian Pathol. *24,* 623-632.

Shinya, K., Fujii, Y., Ito, H., Ito, T., and Kawaoka, Y. (2004). Characterization of a neuraminidase-deficient influenza a virus as a potential gene delivery vector and a live vaccine. J. Virol. *78,* 3083-3088.

Shope, R.E. (1931). The Etiology of Swine Influenza. Science *73,* 214-215.

Shultz, L.D., Brehm, M.A., Garcia-Martinez, J.V., and Greiner, D.L. (2012). Humanized mice for immune system investigation: progress, promise and challenges. Nat. Rev. Immunol. *12,* 786-798.

Shultz, L.D., Ishikawa, F., and Greiner, D.L. (2007). Humanized mice in translational biomedical research. Nat. Rev. Immunol. *7,* 118-130.

Silverman, D.T., Hoover, R.N., Brown, L.M., Swanson, G.M., Schiffman, M., Greenberg, R.S., Hayes, R.B., Lillemoe, K.D., Schoenberg, J.B., Schwartz, A.G.*, et al.* (2003). Why do Black Americans have a higher risk of pancreatic cancer than White Americans? Epidemiology *14,* 45-54.

Silverman, R.H. (2007). Viral encounters with 2',5'-oligoadenylate synthetase and RNase L during the interferon antiviral response. J. Virol. *81,* 12720-12729.

Simons, K., and Ikonen, E. (1997). Functional rafts in cell membranes. Nature *387,* 569-572.

Singh, R., and Reddy, R. (1989). Gamma-monomethyl phosphate: a cap structure in spliceosomal U6 small nuclear RNA. Proc. Natl. Acad. Sci. U. S. A. *86,* 8280-8283.

Skalka, M., Matyasova, J., and Cejkova, M. (1976). Dna in chromatin of irradiated lymphoid tissues degrades in vivo into regular fragments. FEBS Lett. *72,* 271-274.

Skehel, J.J., and Wiley, D.C. (2000). Receptor binding and membrane fusion in virus entry: the influenza hemagglutinin. Annu. Rev. Biochem. *69,* 531-569.

Skountzou, I., Koutsonanos, D.G., Kim, J.H., Powers, R., Satyabhama, L., Masseoud, F., Weldon, W.C., Martin Mdel, P., Mittler, R.S., Compans, R., and Jacob, J. (2010). Immunity to pre-1950 H1N1 influenza viruses confers cross-protection against the pandemic swine-origin 2009 A (H1N1) influenza virus. J. Immunol. *185,* 1642-1649.

Smith, W., Andrewes CH, and Laidlaw PP. (1933). A virus obtained from influenza patients. The Lancet *222 (5732),* 66-68.

Smith, B.R. (1990). Regulation of hematopoiesis. Yale J. Biol. Med. *63,* 371-380.

Smith, D.J., Lapedes, A.S., de Jong, J.C., Bestebroer, T.M., Rimmelzwaan, G.F., Osterhaus, A.D., and Fouchier, R.A. (2004). Mapping the antigenic and genetic evolution of influenza virus. Science *305,* 371-376.

Smith, G.J., Vijaykrishna, D., Bahl, J., Lycett, S.J., Worobey, M., Pybus, O.G., Ma, S.K., Cheung, C.L., Raghwani, J., Bhatt, S.*, et al.* (2009). Origins and evolutionary genomics of the 2009 swine-origin H1N1 influenza A epidemic. Nature *459,* 1122-1125.

Smith, G.L., Levin, J.Z., Palese, P., and Moss, B. (1987). Synthesis and cellular location of the ten influenza polypeptides individually expressed by recombinant vaccinia viruses. Virology *160,* 336-345.

Spackman, E., Senne, D.A., Myers, T.J., Bulaga, L.L., Garber, L.P., Perdue, M.L., Lohman, K., Daum, L.T., and Suarez, D.L. (2002). Development of a real-time reverse transcriptase PCR assay for type A influenza virus and the avian H5 and H7 hemagglutinin subtypes. J. Clin. Microbiol. *40,* 3256-3260.

Spratlin, J., Sangha, R., Glubrecht, D., Dabbagh, L., Young, J.D., Dumontet, C., Cass, C., Lai, R., and Mackey, J.R. (2004). The absence of human equilibrative nucleoside transporter 1 is associated with reduced survival in patients with gemcitabine-treated pancreas adenocarcinoma. Clin. Cancer Res. *10,* 6956-6961.

Springate, C.M., Jackson, J.K., Gleave, M.E., and Burt, H.M. (2005). Efficacy of an intratumoral controlled release formulation of clusterin antisense oligonucleotide complexed with chitosan containing paclitaxel or docetaxel in prostate cancer xenograft models. Cancer Chemother. Pharmacol. *56,* 239-247.

Springfeld, C., von Messling, V., Frenzke, M., Ungerechts, G., Buchholz, C.J., and Cattaneo, R. (2006). Oncolytic efficacy and enhanced safety of measles virus activated by tumor-secreted matrix metalloproteinases. Cancer Res. *66,* 7694-7700.

Staeheli, P., Grob, R., Meier, E., Sutcliffe, J.G., and Haller, O. (1988). Influenza virus-susceptible mice carry Mx genes with a large deletion or a nonsense mutation. Mol. Cell. Biol. *8,* 4518-4523.

Starup-Linde, J., Karlstad, O., Eriksen, S.A., Vestergaard, P., Bronsveld, H.K., de Vries, F., Andersen, M., Auvinen, A., Haukka, J., Hjellvik, V.*, et al.* (2013). CARING (CAncer Risk and INsulin analoGues): the association of diabetes mellitus and cancer risk with focus on possible determinants - a systematic review and a meta-analysis. Curr. Drug Saf. *8,* 296-332.

Stasakova, J., Ferko, B., Kittel, C., Sereinig, S., Romanova, J., Katinger, H., and Egorov, A. (2005). Influenza A mutant viruses with altered NS1 protein function provoke caspase-1 activation in primary human macrophages, resulting in fast apoptosis and release of high levels of interleukins 1beta and 18. J. Gen. Virol. *86,* 185-195.

Stathis, A., and Moore, M.J. (2010). Advanced pancreatic carcinoma: current treatment and future challenges. Nat. Rev. Clin. Oncol. *7,* 163-172.

Stech, J., Garn, H., Wegmann, M., Wagner, R., and Klenk, H.D. (2005). A new approach to an influenza live vaccine: modification of the cleavage site of hemagglutinin. Nat. Med. *11,* 683-689.

Steel, J., Lowen, A.C., Mubareka, S., and Palese, P. (2009). Transmission of influenza virus in a mammalian host is increased by PB2 amino acids 627K or 627E/701N. PLoS Pathog. *5,* e1000252.

Steidle, S., Martinez-Sobrido, L., Mordstein, M., Lienenklaus, S., Garcia-Sastre, A., Staheli, P., and Kochs, G. (2010). Glycine 184 in nonstructural protein NS1 determines the virulence of influenza A virus strain PR8 without affecting the host interferon response. J. Virol. *84,* 12761-12770.

Steinhauer, D.A. (1999). Role of hemagglutinin cleavage for the pathogenicity of influenza virus. Virology *258,* 1-20.

Stencel-Baerenwald, J.E., Reiss, K., Reiter, D.M., Stehle, T., and Dermody, T.S. (2014). The sweet spot: defining virus-sialic acid interactions. Nat. Rev. Microbiol. *12,* 739-749.

Stevens, R.J., Roddam, A.W., and Beral, V. (2007). Pancreatic cancer in type 1 and young-onset diabetes: systematic review and meta-analysis. Br. J. Cancer *96,* 507-509.

Stieneke-Grober, A., Vey, M., Angliker, H., Shaw, E., Thomas, G., Roberts, C., Klenk, H.D., and Garten, W. (1992). Influenza virus hemagglutinin with multibasic cleavage site is activated by furin, a subtilisin-like endoprotease. EMBO J. *11,* 2407-2414.

Stray, S.J., and Air, G.M. (2001). Apoptosis by influenza viruses correlates with efficiency of viral mRNA synthesis. Virus Res. *77,* 3-17.

Strobel, I., Krumbholz, M., Menke, A., Hoffmann, E., Dunbar, P.R., Bender, A., Hobom, G., Steinkasserer, A., Schuler, G., and Grassmann, R. (2000). Efficient expression of the tumor-associated antigen MAGE-3 in human dendritic cells, using an avian influenza virus vector. Hum. Gene Ther. *11,* 2207-2218.

Sturlan, S., Stremitzer, S., Bauman, S., Sachet, M., Wolschek, M., Ruthsatz, T., Egorov, A., and Bergmann, M. (2010). Endogenous expression of proteases in colon cancer cells facilitate influenza A viruses mediated oncolysis. Cancer. Biol. Ther. *10,* 592-599.

Subbarao, E.K., London, W., and Murphy, B.R. (1993). A single amino acid in the PB2 gene of influenza A virus is a determinant of host range. J. Virol. *67,* 1761-1764.

Sugrue, R.J., and Hay, A.J. (1991). Structural characteristics of the M2 protein of influenza A viruses: evidence that it forms a tetrameric channel. Virology *180,* 617-624.

Szecsi, J., Drury, R., Josserand, V., Grange, M.P., Boson, B., Hartl, I., Schneider, R., Buchholz, C.J., Coll, J.L., Russell, S.J., Cosset, F.L., and Verhoeyen, E. (2006). Targeted retroviral vectors displaying a cleavage site-engineered hemagglutinin (HA) through HA-protease interactions. Mol. Ther. *14,* 735-744.

Taggart, A.J., DeSimone, A.M., Shih, J.S., Filloux, M.E., and Fairbrother, W.G. (2012). Large-scale mapping of branchpoints in human pre-mRNA transcripts in vivo. Nat. Struct. Mol. Biol. *19,* 719-721.

Takahasi, K., Yoneyama, M., Nishihori, T., Hirai, R., Kumeta, H., Narita, R., Gale, M.,Jr, Inagaki, F., and Fujita, T. (2008). Nonself RNA-sensing mechanism of RIG-I helicase and activation of antiviral immune responses. Mol. Cell *29,* 428-440.

Takeda, M., Leser, G.P., Russell, C.J., and Lamb, R.A. (2003). Influenza virus hemagglutinin concentrates in lipid raft microdomains for efficient viral fusion. Proc. Natl. Acad. Sci. U. S. A. *100,* 14610-14617.

Takizawa, T., Matsukawa, S., Higuchi, Y., Nakamura, S., Nakanishi, Y., and Fukuda, R. (1993). Induction of programmed cell death (apoptosis) by influenza virus infection in tissue culture cells. J. Gen. Virol. *74 (Pt 11),* 2347-2355.

Talimogene laherparepvec MOA. Wikimedia Commons.

Talon, J., Horvath, C.M., Polley, R., Basler, C.F., Muster, T., Palese, P., and Garcia-Sastre, A. (2000). Activation of interferon regulatory factor 3 is inhibited by the influenza A virus NS1 protein. J. Virol. *74,* 7989-7996.

Tamburrino, A., Piro, G., Carbone, C., Tortora, G., and Melisi, D. (2013). Mechanisms of resistance to chemotherapeutic and anti-angiogenic drugs as novel targets for pancreatic cancer therapy. Front. Pharmacol. *4,* 56-top-frame" src="./pubmed_files/top.

Tamerius, J., Nelson, M.I., Zhou, S.Z., Viboud, C., Miller, M.A., and Alonso, W.J. (2011). Global influenza seasonality: reconciling patterns across temperate and tropical regions. Environ. Health Perspect. *119,* 439-445.

Tamerius, J.D., Shaman, J., Alonso, W.J., Bloom-Feshbach, K., Uejio, C.K., Comrie, A., and Viboud, C. (2013). Environmental predictors of seasonal influenza epidemics across temperate and tropical climates. PLoS Pathog. *9,* e1003194.

Tamura, K., Stecher, G., Peterson, D., Filipski, A., and Kumar, S. (2013). MEGA6: Molecular Evolutionary Genetics Analysis version 6.0. Mol. Biol. Evol. *30,* 2725-2729.

Tang, H., Dong, X., Hassan, M., Abbruzzese, J.L., and Li, D. (2011). Body mass index and obesity- and diabetes-associated genotypes and risk for pancreatic cancer. Cancer Epidemiol. Biomarkers Prev. *20,* 779-792.

Tang, Y., Liu, F., Zheng, C., Sun, S., and Jiang, Y. (2012). Knockdown of clusterin sensitizes pancreatic cancer cells to gemcitabine chemotherapy by ERK1/2 inactivation. J. Exp. Clin. Cancer Res. *31,* 73.

Taniguchi, T., Palmieri, M., and Weissmann, C. (1978). QB DNA-containing hybrid plasmids giving rise to QB phage formation in the bacterial host. Nature *274,* 223-228.

Tarendeau, F., Crepin, T., Guilligay, D., Ruigrok, R.W., Cusack, S., and Hart, D.J. (2008). Host determinant residue lysine 627 lies on the surface of a discrete, folded domain of influenza virus polymerase PB2 subunit. PLoS Pathog. *4,* e1000136.

Taubenberger, J.K., and Kash, J.C. (2010). Influenza virus evolution, host adaptation, and pandemic formation. Cell. Host Microbe *7,* 440-451.

Taubenberger, J.K., Reid, A.H., Lourens, R.M., Wang, R., Jin, G., and Fanning, T.G. (2005). Characterization of the 1918 influenza virus polymerase genes. Nature *437,* 889-893.

Taylor, R.C., Cullen, S.P., and Martin, S.J. (2008). Apoptosis: controlled demolition at the cellular level. Nat. Rev. Mol. Cell Biol. *9,* 231-241.

Tchatalbachev, S., Flick, R., and Hobom, G. (2001). The packaging signal of influenza viral RNA molecules. RNA *7,* 979-989.

Tedcastle, A., Cawood, R., Di, Y., Fisher, K.D., and Seymour, L.W. (2012). Virotherapy--cancer targeted pharmacology. Drug Discov. Today *17,* 215-220.

Terui, Y., Furukawa, Y., Kikuchi, J., and Saito, M. (1995). Apoptosis during HL-60 cell differentiation is closely related to a G0/G1 cell cycle arrest. J. Cell. Physiol. *164,* 74-84.

Thaa, B., Herrmann, A., and Veit, M. (2010). Intrinsic cytoskeleton-dependent clustering of influenza virus M2 protein with hemagglutinin assessed by FLIM-FRET. J. Virol. *84,* 12445-12449.

Thaa, B., Levental, I., Herrmann, A., and Veit, M. (2011). Intrinsic membrane association of the cytoplasmic tail of influenza virus M2 protein and lateral membrane sorting regulated by cholesterol binding and palmitoylation. Biochem. J. *437,* 389-397.

The Human Protein Atlas. Pancreatic Cancer. http://www.proteinatlas.org.

Tomimaru, Y., Eguchi, H., Wada, H., Tomokuni, A., Kobayashi, S., Marubashi, S., Takeda, Y., Tanemura, M., Umeshita, K., Mori, M., Doki, Y., and Nagano, H. (2011). Synergistic antitumor effect of interferon-ss with gemcitabine in interferon-alpha-non-responsive pancreatic cancer cells. Int. J. Oncol. *38,* 1237-1243.

Tong, S., Zhu, X., Li, Y., Shi, M., Zhang, J., Bourgeois, M., Yang, H., Chen, X., Recuenco, S., Gomez, J., *et al.* (2013). New world bats harbor diverse influenza A viruses. PLoS Pathog. *9,* e1003657.

Tramacere, I., Scotti, L., Jenab, M., Bagnardi, V., Bellocco, R., Rota, M., Corrao, G., Bravi, F., Boffetta, P., and La Vecchia, C. (2010). Alcohol drinking and pancreatic cancer risk: a meta-analysis of the dose-risk relation. Int. J. Cancer *126,* 1474-1486.

Tripathi, S., Batra, J., Cao, W., Sharma, K., Patel, J.R., Ranjan, P., Kumar, A., Katz, J.M., Cox, N.J., Lal, R.B., Sambhara, S., and Lal, S.K. (2013). Influenza A virus nucleoprotein induces apoptosis in human airway epithelial cells: implications of a novel interaction between nucleoprotein and host protein Clusterin. Cell. Death Dis. *4,* e562-top-frame" src="./pubmed_files/top.

Tseng, W.W., Winer, D., Kenkel, J.A., Choi, O., Shain, A.H., Pollack, J.R., French, R., Lowy, A.M., and Engleman, E.G. (2010). Development of an orthotopic model of invasive pancreatic cancer in an immunocompetent murine host. Clin. Cancer Res. *16,* 3684-3695.

Turan, K., Mibayashi, M., Sugiyama, K., Saito, S., Numajiri, A., and Nagata, K. (2004). Nuclear MxA proteins form a complex with influenza virus NP and inhibit the transcription of the engineered influenza virus genome. Nucleic Acids Res. *32,* 643-652.

Twu, K.Y., Noah, D.L., Rao, P., Kuo, R.L., and Krug, R.M. (2006). The CPSF30 binding site on the NS1A protein of influenza A virus is a potential antiviral target. J. Virol. *80,* 3957-3965.

Ulmanen, I., Broni, B., and Krug, R.M. (1983). Influenza virus temperature-sensitive cap (m7GpppNm)-dependent endonuclease. J. Virol. *45,* 27-35.

Underhill, D.M., and Ozinsky, A. (2002). Phagocytosis of microbes: complexity in action. Annu. Rev. Immunol. *20,* 825-852.

van de Laar, L., Coffer, P.J., and Woltman, A.M. (2012). Regulation of dendritic cell development by GM-CSF: molecular control and implications for immune homeostasis and therapy. Blood *119,* 3383-3393.

van Engeland, M., Nieland, L.J., Ramaekers, F.C., Schutte, B., and Reutelingsperger, C.P. (1998). Annexin V-affinity assay: a review on an apoptosis detection system based on phosphatidylserine exposure. Cytometry *31,* 1-9.

Van Hoeven, N., Pappas, C., Belser, J.A., Maines, T.R., Zeng, H., Garcia-Sastre, A., Sasisekharan, R., Katz, J.M., and Tumpey, T.M. (2009). Human HA and polymerase subunit PB2 proteins confer transmission of an avian influenza virus through the air. Proc. Natl. Acad. Sci. U. S. A. *106,* 3366-3371.

van Ijzendoorn, S.C. (2006). Recycling endosomes. J. Cell. Sci. *119,* 1679-1681.

Van Reeth, K. (2007). Avian and swine influenza viruses: our current understanding of the zoonotic risk. Vet. Res. *38,* 243-260.

van Rikxoort, M., Michaelis, M., Wolschek, M., Muster, T., Egorov, A., Seipelt, J., Doerr, H.W., and Cinatl, J.,Jr. (2012). Oncolytic effects of a novel influenza A virus expressing interleukin-15 from the NS reading frame. PLoS One *7,* e36506.

Varga, Z.T., Grant, A., Manicassamy, B., and Palese, P. (2012). Influenza virus protein PB1-F2 inhibits the induction of type I interferon by binding to MAVS and decreasing mitochondrial membrane potential. J. Virol. *86,* 8359-8366.

Varga, Z.T., Ramos, I., Hai, R., Schmolke, M., Garcia-Sastre, A., Fernandez-Sesma, A., and Palese, P. (2011). The influenza virus protein PB1-F2 inhibits the induction of type I interferon at the level of the MAVS adaptor protein. PLoS Pathog. *7,* e1002067.

Vartak, D.G., and Gemeinhart, R.A. (2007). Matrix metalloproteases: underutilized targets for drug delivery. J. Drug Target. *15,* 1-20.

Veit, M., and Thaa, B. (2011). Association of influenza virus proteins with membrane rafts. Adv. Virol. *2011,* 370606.

Vermes, I., Haanen, C., Steffens-Nakken, H., and Reutelingsperger, C. (1995). A novel assay for apoptosis. Flow cytometric detection of phosphatidylserine expression on early apoptotic cells using fluorescein labelled Annexin V. J. Immunol. Methods *184,* 39-51.

Vesely, M.D., Kershaw, M.H., Schreiber, R.D., and Smyth, M.J. (2011). Natural innate and adaptive immunity to cancer. Annu. Rev. Immunol. *29,* 235-271.

Vidal, L., Pandha, H.S., Yap, T.A., White, C.L., Twigger, K., Vile, R.G., Melcher, A., Coffey, M., Harrington, K.J., and DeBono, J.S. (2008). A phase I study of intravenous oncolytic reovirus type 3 Dearing in patients with advanced cancer. Clin. Cancer Res. *14,* 7127-7137.

Vitale, G., de Herder, W.W., van Koetsveld, P.M., Waaijers, M., Schoordijk, W., Croze, E., Colao, A., Lamberts, S.W., and Hofland, L.J. (2006). IFN-beta is a highly potent inhibitor of gastroenteropancreatic neuroendocrine tumor cell growth in vitro. Cancer Res. *66,* 554-562.

Vitale, G., van Eijck, C.H., van Koetsveld Ing, P.M., Erdmann, J.I., Speel, E.J., van der Wansem Ing, K., Mooij, D.M., Colao, A., Lombardi, G., Croze, E., Lamberts, S.W., and Hofland, L.J. (2007). Type I interferons in the treatment of pancreatic cancer: mechanisms of action and role of related receptors. Ann. Surg. *246,* 259-268.

von Heijne, G., Steppuhn, J., and Herrmann, R.G. (1989). Domain structure of mitochondrial and chloroplast targeting peptides. Eur. J. Biochem. *180,* 535-545.

von Herrath, M.G., Holz, A., Homann, D., and Oldstone, M.B. (1998). Role of viruses in type I diabetes. Semin. Immunol. *10,* 87-100.

von Marschall, Z., Scholz, A., Cramer, T., Schafer, G., Schirner, M., Oberg, K., Wiedenmann, B., Hocker, M., and Rosewicz, S. (2003). Effects of interferon alpha on vascular endothelial growth factor gene transcription and tumor angiogenesis. J. Natl. Cancer Inst. *95,* 437-448.

Wacheck, V., Egorov, A., Groiss, F., Pfeiffer, A., Fuereder, T., Hoeflmayer, D., Kundi, M., Popow-Kraupp, T., Redlberger-Fritz, M., Mueller, C.A*., et al.* (2010). A novel type of influenza vaccine: safety and immunogenicity of replication-deficient influenza virus created by deletion of the interferon antagonist NS1. J. Infect. Dis. *201,* 354-362.

Walter, P., and Johnson, A.E. (1994). Signal sequence recognition and protein targeting to the endoplasmic reticulum membrane. Annu. Rev. Cell Biol. *10,* 87-119.

Walter, R.J., Attar, B.M., Rafiq, A., Tejaswi, S., and Delimata, M. (2012). Newcastle disease virus LaSota strain kills human pancreatic cancer cells in vitro with high selectivity. JOP *13,* 45-53.

Wang, B., Xiong, Q., Shi, Q., Le, X., Abbruzzese, J.L., and Xie, K. (2001). Intact nitric oxide synthase II gene is required for interferon-beta-mediated suppression of growth and metastasis of pancreatic adenocarcinoma. Cancer Res. *61,* 71-75.

Wang, D., Harmon, A., Jin, J., Francis, D.H., Christopher-Hennings, J., Nelson, E., Montelaro, R.C., and Li, F. (2010). The lack of an inherent membrane targeting signal is responsible for the failure of the matrix (M1) protein of influenza A virus to bud into virus-like particles. J. Virol. *84,* 4673-4681.

Wang, J.M., Colella, S., Allavena, P., and Mantovani, A. (1987). Chemotactic activity of human recombinant granulocyte-macrophage colony-stimulating factor. Immunology *60,* 439-444.

Wang, P., Palese, P., and O'Neill, R.E. (1997). The NPI-1/NPI-3 (karyopherin alpha) binding site on the influenza a virus nucleoprotein NP is a nonconventional nuclear localization signal. J. Virol. *71,* 1850-1856.

Wang, T.T., Tan, G.S., Hai, R., Pica, N., Ngai, L., Ekiert, D.C., Wilson, I.A., Garcia-Sastre, A., Moran, T.M., and Palese, P. (2010). Vaccination with a synthetic peptide from the influenza virus hemagglutinin provides protection against distinct viral subtypes. Proc. Natl. Acad. Sci. U. S. A. *107,* 18979-18984.

Watanabe, N. (2011). Conversion to type 1 diabetes after H1N1 influenza infection: a case report. J. Diabetes *3,* 103-0407.2010.00110.x.

Webster, R.G., Bean, W.J., Gorman, O.T., Chambers, T.M., and Kawaoka, Y. (1992). Evolution and ecology of influenza A viruses. Microbiol. Rev. *56,* 152-179.

Webster, R.G., and Rott, R. (1987). Influenza virus A pathogenicity: the pivotal role of hemagglutinin. Cell *50,* 665-666.

Wege, A.K., Ernst, W., Eckl, J., Frankenberger, B., Vollmann-Zwerenz, A., Mannel, D.N., Ortmann, O., Kroemer, A., and Brockhoff, G. (2011). Humanized tumor mice--a new model to study and manipulate the immune response in advanced cancer therapy. Int. J. Cancer *129,* 2194-2206.

Weis, W.I., Brunger, A.T., Skehel, J.J., and Wiley, D.C. (1990). Refinement of the influenza virus hemagglutinin by simulated annealing. J. Mol. Biol. *212,* 737-761.

Wennier, S., Li, S., and McFadden, G. (2011). Oncolytic virotherapy for pancreatic cancer. Expert Rev. Mol. Med. *13,* e18.

West, A.P., Shadel, G.S., and Ghosh, S. (2011). Mitochondria in innate immune responses. Nat. Rev. Immunol. *11,* 389-402.

Whitcomb, D.C., Gorry, M.C., Preston, R.A., Furey, W., Sossenheimer, M.J., Ulrich, C.D., Martin, S.P., Gates, L.K.,Jr, Amann, S.T., Toskes, P.P.*, et al.* (1996). Hereditary pancreatitis is caused by a mutation in the cationic trypsinogen gene. Nat. Genet. *14,* 141-145.

Wilden, H., Fournier, P., Zawatzky, R., and Schirrmacher, V. (2009). Expression of RIG-I, IRF3, IFN-beta and IRF7 determines resistance or susceptibility of cells to infection by Newcastle Disease Virus. Int. J. Oncol. *34,* 971-982.

Williams, J.A. (2001). Intracellular signaling mechanisms activated by cholecystokinin-regulating synthesis and secretion of digestive enzymes in pancreatic acinar cells. Annu. Rev. Physiol. *63,* 77-97.

Willmon, C.L., Saloura, V., Fridlender, Z.G., Wongthida, P., Diaz, R.M., Thompson, J., Kottke, T., Federspiel, M., Barber, G., Albelda, S.M., and Vile, R.G. (2009). Expression of IFN-beta enhances both efficacy and safety of oncolytic vesicular stomatitis virus for therapy of mesothelioma. Cancer Res. *69,* 7713-7720.

Wise, H.M., Foeglein, A., Sun, J., Dalton, R.M., Patel, S., Howard, W., Anderson, E.C., Barclay, W.S., and Digard, P. (2009). A complicated message: Identification of a novel PB1-related protein translated from influenza A virus segment 2 mRNA. J. Virol. *83,* 8021-8031.

Wollmann, G., Rogulin, V., Simon, I., Rose, J.K., and van den Pol, A.N. (2010). Some attenuated variants of vesicular stomatitis virus show enhanced oncolytic activity against human glioblastoma cells relative to normal brain cells. J. Virol. *84,* 1563-1573.

Wolschek, M., Samm, E., Seper, H., Sturlan, S., Kuznetsova, I., Schwager, C., Khassidov, A., Kittel, C., Muster, T., Egorov, A., and Bergmann, M. (2011). Establishment of a chimeric, replication-deficient influenza A virus vector by modulation of splicing efficiency. J. Virol. *85,* 2469-2473.

Wong, G.G., Witek, J.S., Temple, P.A., Wilkens, K.M., Leary, A.C., Luxenberg, D.P., Jones, S.S., Brown, E.L., Kay, R.M., and Orr, E.C. (1985). Human GM-CSF: molecular cloning of the complementary DNA and purification of the natural and recombinant proteins. Science *228,* 810-815.

World Health Organization (WHO). (March 2014). Influenza (Seasonal). Fact Sheet N°211 http://www.who.int/mediacentre/factsheets/fs211/en/.

World Health Organization (WHO). (20 February 2014). Recommended composition of influenza virus vaccines for use in the 2014-2015 northern hemisphere influenza season. WHO Recommendations on the Composition of Influenza Virus Vaccines.
http://www.who.int/influenza/vaccines/virus/recommendations/2014_15_north/en/

Wu, J., Lu, L.Y., and Yu, X. (2010). The role of BRCA1 in DNA damage response. Protein Cell. *1,* 117-123.

Wurzer, W.J., Ehrhardt, C., Pleschka, S., Berberich-Siebelt, F., Wolff, T., Walczak, H., Planz, O., and Ludwig, S. (2004). NF-kappaB-dependent induction of tumor necrosis factor-related apoptosis-inducing ligand (TRAIL) and Fas/FasL is crucial for efficient influenza virus propagation. J. Biol. Chem. *279,* 30931-30937.

Wurzer, W.J., Planz, O., Ehrhardt, C., Giner, M., Silberzahn, T., Pleschka, S., and Ludwig, S. (2003). Caspase 3 activation is essential for efficient influenza virus propagation. EMBO J. *22,* 2717-2728.

Wyllie, A.H. (1980). Glucocorticoid-induced thymocyte apoptosis is associated with endogenous endonuclease activation. Nature *284,* 555-556.

Wyllie, A.H., Kerr, J.F., and Currie, A.R. (1980). Cell death: the significance of apoptosis. Int. Rev. Cytol. *68,* 251-306.

Xiao, H., Killip, M.J., Staeheli, P., Randall, R.E., and Jackson, D. (2013). The human interferon-induced MxA protein inhibits early stages of influenza A virus infection by retaining the incoming viral genome in the cytoplasm. J. Virol. *87,* 13053-13058.

Xie, D., Lau, S.H., Sham, J.S., Wu, Q.L., Fang, Y., Liang, L.Z., Che, L.H., Zeng, Y.X., and Guan, X.Y. (2005). Up-regulated expression of cytoplasmic clusterin in human ovarian carcinoma. Cancer *103,* 277-283.

Xu, K., Klenk, C., Liu, B., Keiner, B., Cheng, J., Zheng, B.J., Li, L., Han, Q., Wang, C., Li, T.*, et al.* (2011). Modification of nonstructural protein 1 of influenza A virus by SUMO1. J. Virol. *85,* 1086-1098.

Yachida, S., and Iacobuzio-Donahue, C.A. (2013). Evolution and dynamics of pancreatic cancer progression. Oncogene *32,* 5253-5260.

Yachida, S., Jones, S., Bozic, I., Antal, T., Leary, R., Fu, B., Kamiyama, M., Hruban, R.H., Eshleman, J.R., Nowak, M.A.*, et al.* (2010). Distant metastasis occurs late during the genetic evolution of pancreatic cancer. Nature *467,* 1114-1117.

Yamada, S., Hatta, M., Staker, B.L., Watanabe, S., Imai, M., Shinya, K., Sakai-Tagawa, Y., Ito, M., Ozawa, M., Watanabe, T.*, et al.* (2010). Biological and structural characterization of a host-adapting amino acid in influenza virus. PLoS Pathog. *6,* e1001034.

Yang, L., Pang, Y., and Moses, H.L. (2010). TGF-beta and immune cells: an important regulatory axis in the tumor microenvironment and progression. Trends Immunol. *31,* 220-227.

Yao, J.C., Eisner, M.P., Leary, C., Dagohoy, C., Phan, A., Rashid, A., Hassan, M., and Evans, D.B. (2007). Population-based study of islet cell carcinoma. Ann. Surg. Oncol. *14,* 3492-3500.

Yao, L., Korteweg, C., Hsueh, W., and Gu, J. (2008). Avian influenza receptor expression in H5N1-infected and noninfected human tissues. FASEB J. *22,* 733-740.

Yap, D.B., Hsieh, J.K., Zhong, S., Heath, V., Gusterson, B., Crook, T., and Lu, X. (2004). Ser392 phosphorylation regulates the oncogenic function of mutant p53. Cancer Res. *64,* 4749-4754.

Yasuda, J., Nakada, S., Kato, A., Toyoda, T., and Ishihama, A. (1993). Molecular assembly of influenza virus: association of the NS2 protein with virion matrix. Virology *196,* 249-255.

Yin, H., Berg, A.K., Tuvemo, T., and Frisk, G. (2002). Enterovirus RNA is found in peripheral blood mononuclear cells in a majority of type 1 diabetic children at onset. Diabetes *51,* 1964-1971.

Yingst, S.L., Saad, M.D., and Felt, S.A. (2006). Qinghai-like H5N1 from domestic cats, northern Iraq. Emerg. Infect. Dis. *12,* 1295-1297.

Yip-Schneider, M.T., Lin, A., Barnard, D., Sweeney, C.J., and Marshall, M.S. (1999). Lack of elevated MAP kinase (Erk) activity in pancreatic carcinomas despite oncogenic K-ras expression. Int. J. Oncol. *15,* 271-279.

Ylosmaki, E., Hakkarainen, T., Hemminki, A., Visakorpi, T., Andino, R., and Saksela, K. (2008). Generation of a conditionally replicating adenovirus based on targeted destruction of E1A mRNA by a cell type-specific MicroRNA. J. Virol. *82,* 11009-11015.

York, A., and Fodor, E. (2013). Biogenesis, assembly, and export of viral messenger ribonucleoproteins in the influenza A virus infected cell. RNA Biol. *10,* 1274-1282.

Yoshizumi, T., Ichinohe, T., Sasaki, O., Otera, H., Kawabata, S., Mihara, K., and Koshiba, T. (2014). Influenza A virus protein PB1-F2 translocates into mitochondria via Tom40 channels and impairs innate immunity. Nat. Commun. *5,* 4713.

Yuan, P., Bartlam, M., Lou, Z., Chen, S., Zhou, J., He, X., Lv, Z., Ge, R., Li, X., Deng, T.*, et al.* (2009). Crystal structure of an avian influenza polymerase PA(N) reveals an endonuclease active site. Nature *458,* 909-913.

Yun, C.O. (2008). Overcoming the extracellular matrix barrier to improve intratumoral spread and therapeutic potential of oncolytic virotherapy. Curr. Opin. Mol. Ther. *10,* 356-361.

Zamarin, D., Garcia-Sastre, A., Xiao, X., Wang, R., and Palese, P. (2005). Influenza virus PB1-F2 protein induces cell death through mitochondrial ANT3 and VDAC1. PLoS Pathog. *1,* e4.

Zaraket, H., Bridges, O.A., and Russell, C.J. (2013). The pH of activation of the hemagglutinin protein regulates H5N1 influenza virus replication and pathogenesis in mice. J. Virol. *87,* 4826-4834.

Zellweger, T., Chi, K., Miyake, H., Adomat, H., Kiyama, S., Skov, K., and Gleave, M.E. (2002). Enhanced radiation sensitivity in prostate cancer by inhibition of the cell survival protein clusterin. Clin. Cancer Res. *8,* 3276-3284.

Zellweger, T., Miyake, H., July, L.V., Akbari, M., Kiyama, S., and Gleave, M.E. (2001). Chemosensitization of human renal cell cancer using antisense oligonucleotides targeting the antiapoptotic gene clusterin. Neoplasia *3,* 360-367.

Zhang, H., Kim, J.K., Edwards, C.A., Xu, Z., Taichman, R., and Wang, C.Y. (2005). Clusterin inhibits apoptosis by interacting with activated Bax. Nat. Cell Biol. *7,* 909-915.

Zhang, J., Francois, R., Iyer, R., Seshadri, M., Zajac-Kaye, M., and Hochwald, S.N. (2013). Current understanding of the molecular biology of pancreatic neuroendocrine tumors. J. Natl. Cancer Inst. *105,* 1005-1017.

Zhang, J., Pekosz, A., and Lamb, R.A. (2000). Influenza virus assembly and lipid raft microdomains: a role for the cytoplasmic tails of the spike glycoproteins. J. Virol. *74,* 4634-4644.

Zhirnov, O., and Klenk, H.D. (2003). Human influenza A viruses are proteolytically activated and do not induce apoptosis in CACO-2 cells. Virology *313,* 198-212.

Zhirnov, O.P., and Klenk, H.D. (2007). Control of apoptosis in influenza virus-infected cells by up-regulation of Akt and p53 signaling. Apoptosis *12,* 1419-1432.

Zhirnov, O.P., Konakova, T.E., Wolff, T., and Klenk, H.D. (2002). NS1 protein of influenza A virus down-regulates apoptosis. J. Virol. *76,* 1617-1625.

Zimmermann, P., Manz, B., Haller, O., Schwemmle, M., and Kochs, G. (2011). The viral nucleoprotein determines Mx sensitivity of influenza A viruses. J. Virol. *85,* 8133-8140.

Zitvogel, L., Tesniere, A., and Kroemer, G. (2006). Cancer despite immunosurveillance: immunoselection and immunosubversion. Nat. Rev. Immunol. *6,* 715-727.